

# Chapter 1: Assessment of the Walleye Pollock Stock in the Eastern Bering Sea

---

James Ianelli, Ben Fissel, Kirstin Holsman, Alex De Robertis, Taina Honkalehto,  
Stan Kotwicki, Cole Monnahan, Elizabeth Siddon, and James Thorson  
Alaska Fisheries Science Center, National Marine Fisheries Service  
National Oceanic and Atmospheric Administration  
7600 Sand Point Way NE., Seattle, WA 98115-6349  
October 21, 2021

---

## **Executive summary**

This chapter covers the Eastern Bering Sea (EBS) region—the Aleutian Islands region (Chapter 1A) and the Bogoslof Island area (Chapter 1B) are presented separately.

### *Summary of changes in assessment inputs*

Relative to last year's BSAI SAFE report, the following substantive changes have been made in the EBS pollock stock assessment. Notably, a number of surveys were cancelled including the 2020 NMFS bottom-trawl survey (BTS), the 2020 NMFS acoustic-trawl survey (ATS), and th 2020 opportunistic acoustic data from vessels (AVO).

### *Changes in the data*

1. Observer data for catch-at-age and average weight-at-age from the 2019 fishery were finalized and included.
2. Total catch as reported by NMFS Alaska Regional office was updated and included through 2020.
3. In summer 2020, the AFSC coordinated a survey conducted by three uncrewed surface vehicles (USVs) using acoustics.

### *Changes in the assessment methods*

There were some minor changes to data used for the assessment model this year. We continued to refine treatment of survey data via spatial-temporal models for creating an alternative index including the broader region of the northern Bering Sea, mainly by improving the documentation.

### ***Summary of EBS pollock results***

The following table applies for Model 20.0, the model used for last year's assessment but with data from the uncrewed surface vehicles (USVs) included as an extension of the acoustic trawl survey. An alternative table is provided for this model which excludes the USV data from 2020. As in past years, the ABC recommendation reflects the Tier 3 estimate.

Quantity	As estimated or specified last year for:		As estimated or recommended this year for:	
	2020	2021	2021	2022
M (natural mortality rate, ages 3+)	0.3	0.3	0.3	0.3
Tier	1a	1a	1a	1a
Projected total (age 3+) biomass (t)	9,128,000 t	8,494,000 t	8,145,000 t	7,641,000 t
Projected female spawning biomass (t)	2,991,000 t	2,674,000 t	2,602,000 t	2,406,000 t
$B_0$	5,777,000 t	5,777,000 t	5,792,000 t	5,792,000 t
$B_{msy}$	2,148,000 t	2,148,000 t	2,257,000 t	2,257,000 t
$F_{OFL}$	0.449	0.449	0.341	0.341
$maxF_{ABC}$	0.383	0.383	0.304	0.304
$F_{ABC}$	0.225	0.225	0.214	0.214
$OFL$	4,085,000 t	3,385,000 t	2,594,000 t	2,366,000 t
$maxABC$	3,485,000 t	2,888,000 t	2,307,000 t	2,105,000 t
ABC	2,043,000 t	1,767,000 t	1,626,000 t	1,484,000 t
Status	2018	2019	2019	2020
Overfishing	No	n/a	No	n/a
Overfished	n/a	No	n/a	No
Approaching overfished	n/a	No	n/a	No

### ***Response to SSC and Plan Team comments***

#### *General comments*

The SSC recommended that a detailed review of the support for retaining the EBS Pollock assessment in Tier 1 versus reclassifying it as Tier 3 be pursued in the 2020 assessment.

- *We evaluated factors affecting the Tier classification.*

#### **The SSC had a number of recommendations for additional research supporting this assessment:**

The SSC encourages further investigation of the apparent shift between a clear 2012 year-class to mixed 2012-2013 year classes in the data, suggestive of potentially variable ageing bias.

- *The newly available 2019 fishery age data shows a similar relative proportion of these two year classes; this suggests (based on earlier inquiries with the age-determination experts) that this pattern is reasonable.*

Noting the work in deriving an external estimate of temporal variability in catchability for the bottom trawl survey (relative to the acoustic survey) due to vertical availability, the SSC noted that

catchability would logically also vary for the acoustic survey. The SSC encourages further work to develop the simultaneous modelling of these two surveys, accounting for vertical and distributional shifts (including into the northern Bering Sea survey area; NBS). When sufficiently explored, the SSC looks forward to assessment model configurations that explore the use of a time-series from this method.

- *Work on this topic stalled as analysts focused their efforts on methods to incorporate the uncrewed surface vessels (USVs) to collect acoustic data.*

The SSC supports ongoing genetic studies to determine the relationship between pollock in the NBS and EBS, as well as other surrounding regions (AI, GOA).

- *A post doctoral researcher has begun this work but progress has been limited due to lab access and other factors related to the pandemic.*

The SSC supports the continued use of a formal decision table to illustrate risks of alternative harvest strategies.

- *This was included in this year's assessment report.*

The SSC supports the GPT's recommendation to revisit the treatment of all variance parameters in the next assessment, particularly those that are set at fixed values (e.g., the value of 0.2 for the acoustic survey).

- *This planned activity is only partially underway. More work is planned on estimating process error parameters.*

The SSC also looks forward to estimates of movement and abundance along the US-Russia EEZ boundary based on echosounders fixed to moorings in this area.

- *The moored sounders have been recovered in September 2020 but the data have yet to be processed.*

#### **From previous requests:**

Re-examine the geographic subset of data currently used to develop the AVO index, specifically to see if including Bristol Bay data improves the correlation.

- *Work on this continues but was given lower priority given that the AVO was not part of this year's assessment.*

Explore “A” season trends in mean weight-at-length with a GAM or similar technique, to determine if the trends are either predominantly environmental or predominantly fishery-driven, Regarding  $\sigma_R$ , explore alternative fixed values or estimation methods.

- *Trends in mean weight given length are again presented. The extent that fishery affects this pattern was shown to be related to timing. Further work is needed to establish a mean baseline (in time and space) to try to sort out environmental effects hypotheses. Values of  $\sigma_R$  were explored in previous years, no further work was done on this in 2020.*

## **Introduction**

### ***General***

Walleye pollock (*Gadus chalcogrammus*; hereafter referred to as pollock) are broadly distributed throughout the North Pacific with the largest concentrations found in the Eastern Bering Sea. Also known as Alaska pollock, this species continues to play important roles ecologically and economically.

### ***Review of Life History***

In the EBS pollock spawn generally in the period March-May and in relatively localized regions during specific periods (Bailey 2000). Generally spawning begins nearshore north of Unimak Island in March and April and later near the Pribilof Islands (Jung et al. 2006, Bacheler et al. 2010). Females are batch spawners with up to 10 batches of eggs per female per year. Eggs and larvae of EBS pollock are planktonic for a period of about 90 days and appear to be sensitive to environmental conditions. These conditions likely affect their dispersal into favorable areas (for subsequent separation from predators) and also affect general food requirements for over-wintering survival (Gann et al. 2015, Heintz et al., 2013, Hunt et al. 2011, Ciannelli et al. 2004). Duffy-Anderson et al. (2015) provide a review of the early life history of EBS pollock.

Throughout their range juvenile pollock feed on a variety of planktonic crustaceans, including calanoid copepods and euphausiids. In the EBS shelf region, one-year-old pollock are found throughout the water column, but also commonly occur in the NMFS bottom trawl survey. Ages 2 and 3 year old pollock are rarely caught in summer bottom trawl survey gear and are more common in the midwater zone as detected by mid-water acoustic trawl surveys. Younger pollock are generally found in the more northern parts of the survey area and appear to move to the southeast as they age (Buckley et al. 2009). Euphausiids, principally *Thysanoessa inermis* and *T. raschii*, are among the most important prey items for pollock in the Bering Sea (Livingston, 1991; Lang et al., 2000; Brodeur et al., 2002; Cianelli et al., 2004; Lang et al., 2005). Pollock diets become more piscivorous with age, and cannibalism has been commonly observed in this region. However, Buckley et al. (2016) showed spatial patterns of pollock foraging by size of predators. For example, the northern part of the shelf region between the 100 and 200 m isobaths (closest to the shelf break) tends to be more piscivorous than counterparts in other areas.

### ***Stock structure***

Genetic samples were taken from pollock and collections have continued from sources including observers and AFSC research surveys. A large study using whole genome sequencing is currently underway for samples of walleye pollock from Zhemchug Canyon, Japan, Prince William Sound, Bogoslof, Shelikof, and the Northern Bering Sea. This project is a collaboration between the Joint Institute for the Study of Atmosphere and Oceans (currently CICOES, the Cooperative Institute for Climate, Ocean, and Ecosystem Science) and the Alaska Fisheries Science Center Cooperative Research Program. The goals of the project include investigating whether genetic stock structure exists in walleye pollock, if these patterns are temporally stable, and if distributional shifts under climate change are detectable using genomic data. Whole genome sequencing is a new approach to the study of pollock stock structure that is expected to yield higher statistical power than previous

results using microsatellite DNA markers. This planned study should help improve stock structure evaluation (last done in Ianelli et al. 2015).

## Fishery

### *Description of the directed fishery*

Historically, EBS pollock catches were low until directed foreign fisheries began in 1964. Catches increased rapidly during the late 1960s and reached a peak in 1970–75 when they ranged from 1.3 to 1.9 million t annually. Following the peak catch in 1972, bilateral agreements with Japan and the USSR resulted in reductions. During a 10-year period, catches by foreign vessels operating in the “Donut Hole” region of the Aleutian Basin were substantial totaling nearly 7 million t (Table 1). A fishing moratorium for this area was enacted in 1993 and only trace amounts of pollock have been harvested from the Aleutian Basin region since then. Since the late 1970s, the average EBS pollock catch has been about 1.2 million t, ranging from 0.810 million t in 2009 to nearly 1.5 million t during 2003–2006 (Table 1). United States vessels began fishing for pollock in 1980 and by 1987 they were able to take 99% of the quota. Since 1988, U.S. flagged vessels have been operating in this fishery. The current observer program for the domestic fishery formally began in 1991 and prior to that, observers were deployed aboard the foreign vessels since the late 1970s. From the period 1991 to 2011 about 80% of the catch was observed at sea or during dockside offloading. Since 2011, regulations require that all vessels participating in the pollock fishery carry at least one observer so nearly 100% of the pollock fishing operations are monitored by scientifically trained observers. Historical catch estimates used in the assessment, along with management measures (i.e., ABCs and TACs) are shown in Table 2.

### *Catch patterns*

The "A-season" for directed EBS pollock fishing opens on January 20th and fishing typically extends into early-mid April. During this season the fishery targets pre-spawning pollock and produces pollock roe that, under optimal conditions, can comprise over 4% of the catch in weight. The summer, or "B-season" presently opens on June 10th and fishing extends through noon on November 1st. The A-season fishery concentrates primarily north and west of Unimak Island depending on ice conditions and fish distribution. There has also been effort along the 100m depth contour (and deeper) between Unimak Island and the Pribilof Islands. The general pattern by season (and area) has varied over time with recent B-season catches occurring in the southeast portion of the shelf (east of 170°W longitude; Fig. 1). Since 2011, regulations and industry-based measures to reduce Chinook salmon bycatch have affected the spatial distribution of the fishery and to some degree, the way individual vessel operators fish (Stram and Ianelli, 2014). In 2020, the fishing fleet encountered higher than normal bycatch of herring and this has further constrained the fishing grounds due to area closures. Additionally, sablefish appear to be highly abundant in the region and have comprised a significant proportion of the incidental catches in the pollock fishery (proportionally still less than 1% of the total landings). Comparing encounters of bycatch and pollock relative to the effort (total duration of all tows) the pollock fleet the Chinook salmon bycatch rate was relatively flat whereas the encounters with sablefish were markedly higher (Fig. 2).

The catch estimates by sex for the seasons indicate that over time, the number of males and females has been fairly equal but in the period 2017-2019 the A-season catch of females has been slightly

higher and conversely, in the B-season there has been a slightly higher number of males taken (Fig. 3). The 2020 A-season fishery spatial pattern had relatively high concentrations of fishing on the shelf north of Unimak Island and extended along the 200m depth contour similar to 2019 but with a more dispersed distribution (Fig. 4). The 2020 A-season nominal catch rates were high similar to the good conditions observed in other recent A seasons (Fig. 5). Beginning in 2017, due to a regulatory change, up to 45% of the TAC could be taken in the A-season (previously only 40% of the TAC could be taken). This conservation measure was made to allow greater flexibility to avoid Chinook salmon in the B-season. To date, it appears that the pollock fleet as a whole took advantage of this added flexibility (Fig. 6). While an important product from the winter fishery is the sale of pollock roe, production during the B-season is consistently about 10% of the annual commercial products produced (Fig. 7).

The fishing in summer-fall 2020 was characterized as having low nominal catch rates (Fig. 5). The number of hours the fleet required to catch the same tonnage of pollock was much higher than in recent years.

Catches in the northwestern area continued to increase over the past three years (Fig. 8). Also, the approach presented in 2019 to compute the fleet dispersion (the relative distance or spread of the fishery in space) indicated that the A-season in 2019 and 2020 was relatively more concentrated compared to other years since 2000. Conversely, the B-season indicated the most dispersed fishing activity over the same period (Fig 9).

In addition to logistic issues related to ensuring crew and observer safety due to the COVID19 pandemic, there were reports of unusually small pollock in the catch. Consequently, we investigated whether the amount of small fish has occurred in the past. The NMFS observer collections, in addition to containing value length and weight data, also include a large number of observations for the observed tows that provide a direct mean somatic mass for pollock within that tow. This is based on the sampled total weight (e.g., of a basket of pollock) divided by the enumerated number of fish in that sample. Such records exist for each tow. Summing these by extrapolated weight of the pollock catch within that tow, and binning by weight increments (here by 50 gram intervals), allows us to obtain some additional fine-scale information on the size trends in the pollock fishery. The annual patterns of these data show that overall, 2020 was different, particularly for the B-season (Fig. 10). To look more closely at the B-season fishery, we compiled these data by week over recent years and found that there were very smaller fish predominated in the catch (Fig. 11).

The catch of EBS pollock has averaged 1.21 million t in the period since 1979. The lowest catches occurred in 2009 and 2010 when the limits were set to 0.81 million t due to stock declines (Table 2). The recent 5-year average (2016–2020) catch has been 1.365 million t. Pollock catches that are retained or discarded (based on NMFS observer estimates) in the Eastern Bering Sea and Aleutian Islands for 1991–2020 are shown in Table 3. Since 1991, estimates of discarded pollock have ranged from a high of 9.1% of total pollock catch in 1992 to recent lows of around 0.6%. These low values reflect the implementation of the NMFS' Improved Retention /Improved Utilization program. Prior to the implementation of the American Fisheries Act (AFA) in 1999, higher discards may have occurred under the “race for fish” and pollock marketable sizes were caught incidentally. Since implementation of the AFA, the vessel operators have more time to pursue optimal sizes of pollock for market since the quota is allocated to vessels (via cooperative arrangements). In addition, several vessels have made gear modifications to avoid retention of smaller pollock. In all cases, the magnitude of discards counts as part of the total catch for management (to ensure the TAC is not exceeded) and within the assessment. Bycatch of other non-target, target, and prohibited species is presented in the section titled Ecosystem Considerations below. In that section it is noted that the

bycatch of pollock in other target fisheries is more than double the bycatch of other target species (e.g., Pacific cod) in the pollock fishery.

### ***Management measures***

The EBS pollock stock is managed by NMFS regulations that provide limits on seasonal catch. The NMFS observer program data provide near real-time statistics during the season and vessels operate within well-defined limits. In most years, the TACs have been set well below the ABC value and catches have stayed within these constraints (Table 2). Allocations of the TAC split first with 10% to western Alaska communities as part of the Community Development Quota (CDQ) program and the remainder between at-sea processors and shore-based sectors. For a characterization of the CDQ program see Haynie (2014). Seung and Ianelli (2016) combined a fish population dynamics model with an economic model to evaluate regional impacts.

Due to concerns that groundfish fisheries may impact the rebuilding of the Steller sea lion population, a number of management measures have been implemented over the years. Some measures were designed to reduce the possibility of competitive interactions between fisheries and Steller sea lions. For the pollock fisheries, seasonal fishery catch and pollock biomass distributions (from surveys) indicated that the apparent disproportionately high seasonal harvest rates within Steller sea lion critical habitat could lead to reduced sea lion prey densities. Consequently, management measures redistributed the fishery both temporally and spatially according to pollock biomass distributions. This was intended to disperse fishing so that localized harvest rates were more consistent with estimated annual exploitation rates. The measures include establishing: 1) pollock fishery exclusion zones around sea lion rookery or haulout sites; 2) phased-in reductions in the seasonal proportions of TAC that can be taken from critical habitat; and 3) additional seasonal TAC releases to disperse the fishery in time.

Prior to adoption of the above management measures, the pollock fishery occurred in each of the three major NMFS management regions of the North Pacific Ocean: the Aleutian Islands (1,001,780 km<sup>2</sup> inside the EEZ), the Eastern Bering Sea (968,600 km<sup>2</sup>), and the Gulf of Alaska (1,156,100 km<sup>2</sup>). The marine portion of Steller sea lion critical habitat in Alaska west of 150°W encompasses 386,770 km<sup>2</sup> of ocean surface, or 12% of the fishery management regions.

From 1995–1999 84,100 km<sup>2</sup>, or 22% of the Steller sea lion critical habitat was closed to the pollock fishery. Most of this closure consisted of the 10 and 20 nm radius all-trawl fishery exclusion zones around sea lion rookeries (48,920 km<sup>2</sup>, or 13% of critical habitat). The remainder was largely management area 518 (35,180 km<sup>2</sup>, or 9% of critical habitat) that was closed pursuant to an international agreement to protect spawning stocks of central Bering Sea pollock. In 1999, an additional 83,080 km<sup>2</sup> (21%) of critical habitat in the Aleutian Islands was closed to pollock fishing along with 43,170 km<sup>2</sup> (11%) around sea lion haulouts in the GOA and Eastern Bering Sea. In 1998, over 22,000 t of pollock were caught in the Aleutian Island region, with over 17,000 t taken within critical habitat region. Between 1999 and 2004 a directed fishery for pollock was prohibited in this region. Subsequently, 210,350 km<sup>2</sup> (54%) of critical habitat was closed to the pollock fishery. In 2000 the remaining phased-in reductions in the proportions of seasonal TAC that could be caught within the BSAI Steller sea lion Conservation Area (SCA) were implemented.

On the EBS shelf, an estimate (based on observer at-sea data) of the proportion of pollock caught in the SCA has averaged about 44% annually. During the A-season, the average is also about 44%. Nonetheless, the proportion of pollock caught within the SCA varies considerably, presumably due to temperature regimes and the relative population age structure. The annual proportion of catch

within the SCA varies and has ranged from an annual low of 11% in 2010 to high of 60% in 1998—the 2019 annual value was 58% but quite high again in the A-season (68%; Table 4). The higher values in recent years were likely due to good fishing conditions close to the main port.

The AFA reduced the capacity of the catcher/processor fleet and permitted the formation of cooperatives in each industry sector by the year 2000. Because of some of its provisions, the AFA gave the industry the ability to respond efficiently to changes mandated for sea lion conservation and salmon bycatch measures. Without such a catch-share program, these additional measures would likely have been less effective and less economical (Strong and Criddle 2014).

An additional strategy to minimize potential adverse effects on sea lion populations is to disperse the fishery throughout more of the pollock range on the Eastern Bering Sea shelf. While the distribution of fishing during the A-season is limited due to ice and weather conditions, there appears to be some dispersion to the northwest area (Fig. 4).

The majority (about 56%) of Chinook salmon caught as bycatch in the pollock fishery originate from western Alaskan rivers. An Environmental Impact Statement (EIS) was completed in 2009 in conjunction with the Council's recommended bycatch management approach. This EIS evaluated the relative impacts of different bycatch management approaches as well as estimated the impact of bycatch levels on adult equivalent salmon (AEQ) returning to river systems (NMFS/NPFMC 2009). As a result, revised Chinook salmon bycatch management measures went into effect in 2011 which imposed new prohibited species catch (PSC) limits. These limits, when reached, close the fishery by sector and season (Amendment 91 to the BSAI Groundfish Fishery Management Plan (FMP) resulting from the NPFMC's 2009 action). Previously, all measures for salmon bycatch imposed seasonal area closures when PSC levels reached the limit (fishing could continue outside of the closed areas). The current program imposes a dual cap system by fishing sector and season. A goal of this system was to maintain incentives to avoid bycatch at a broad range of relative salmon abundance (and encounter rates). Participants are also required to take part in an incentive program agreement (IPA). These IPAs are approved and reviewed annually by NMFS to ensure individual vessel accountability. The fishery has been operating under rules to implement this program since January 2011.

Further measures to reduce salmon bycatch in the pollock fishery were developed and the Council took action on Amendment 110 to the BSAI Groundfish FMP in April 2015. These additional measures were designed to add protection for Chinook salmon by imposing more restrictive PSC limits in times of low western Alaskan Chinook salmon abundance. This included provisions within the IPAs that reduce fishing in months of higher bycatch encounters and mandate the use of salmon excluders in trawl nets. These provisions were also included to provide more flexible management measures for chum salmon bycatch within the IPAs rather than through regulatory provisions implemented by Amendment 84 to the FMP. The new measure also included additional seasonal flexibility in pollock fishing so that more pollock (proportionally) could be caught during seasons when salmon bycatch rates were low. Specifically, an additional 5% of the pollock can be caught in the A-season (effectively changing the seasonal allocation from 40% to 45% (as noted above in Fig. 6)). These measures are all part of Amendment 110 and a summary of this and other key management measures is provided in Table 5.

There are three time/area closures in regulation to minimize herring PSC impacts: *Summer Herring Savings Area 1* an area south of 57°N latitude and between 162°W and 164°W longitude from June 15 through July 1st. *Summer Herring Savings Area 2* an area south of 56° 30' N latitude and between 164°W and 167°W longitude from July 1 through August 15. *Winter Herring Savings Area* an area between 58° and 60°N latitude and between 172°W and 175°W longitude from September

1st through March 1st of the next fishing year.

The pollock fishery exceeded the herring PSC limit late in the 2020 A season which invoked two directed pollock fishing closures: the Summer Herring Savings Area 1 and the Winter Herring Savings Area (closed since September 1, 2020 through March 1, 2021). Voluntary closures by the CV fleet for directed fishing for pollock. 2nd closure for trawl CVs for herring. Additionally, voluntary closure areas were announced throughout the B-season 2020 and intended to minimize herring bycatch in areas where herring occurred.

### ***Economic conditions as of 2019***

Alaska pollock is the dominant species in terms of catch in the Bering Sea & Aleutian Island (BSAI) region. In 2019 pollock accounted for 73% of the BSAI's FMP groundfish harvest and 92% of the total pollock harvest in Alaska. Retained catch of pollock increased 2.2% to 1.41 million t in 2019 (Table 6). BSAI pollock first-wholesale value was \$1.55 billion 2019, which was 12% increase from 2018 and above the 2010–2014 average of \$1.26 billion (Table 7). The higher revenues in recent years is the combined effect of strong catch and production levels and a steady increase in the average first-wholesale price since 2016. The increases in the average first-wholesale price of pollock products in 2016 and 2017 were largely due to increases the price of surimi products while the price increase in 2018 was largely due to an increase in the price of fillets. Price increases in 2019 were the combined effect of price increases in both fillets and surimi.

Pollock is targeted exclusively with pelagic trawl gear. The catch of pollock in the BSAI was rationalized with the passage of the AFA in 1998,<sup>1</sup> which, among other things, established a proportional allocation of the total allowable catch (TAC) among vessels in sectors which were allowed to form into cooperatives.<sup>2</sup>

Prior to 2008 pollock catches were high at approximately 1.4 million t in the BSAI for an extended period (Table 6). The U.S. accounted for over 50% of the global pollock catch (Table 8). Between 2008–2010 conservation reductions in the pollock total allowable catch (TAC) trimmed catches to an average 867 kt. The supply reduction resulted in price increases for most pollock products, which mitigated the short-term revenue loss (Table 8). Over this same period, the pollock catch in Russia increased from an average of 1 million t in 2005–2007 to 1.4 million t in 2008–2010 and Russia's share of global catch increased to over 50% and the U.S. share decreased to 35%. Russia lacks the primary processing capacity of the U.S. and much of their catch is exported to China and is re-processed as twice-frozen fillets. Around the mid- to late- 2000s, buyers in Europe, an important segment of the fillet market, started to source fish products with the MSC sustainability certification, and retailers in the U.S. later began to follow suit. Asian markets, an important export destination for a number of pollock products, have shown less interest in requiring MSC certification. The U.S. was the only producer of MSC certified pollock until 2013 when roughly 50% of the Russian catch became MSC certified.<sup>3</sup> Since 2010 the U.S. pollock stock rebounded with catches in the BSAI ranging from 1.2–1.3 million t and Russia's catch has stabilized at 1.5 to 1.6 million t. The majority of pollock is exported; consequently exchange rates can have a significant

<sup>1</sup>The AFA was implemented in 1999 for catcher/processors, and in 2000 for catcher vessel and motherships.

<sup>2</sup>The BSAI pollock TAC is divided between Community Development Program (10% off the top), with the remaining amount split among shore-based catcher vessels (50%), at-sea catcher/processors (40%) and motherships (10%).

<sup>3</sup>Alaska caught pollock in the BSAI became certified by the Marine Stewardship Council (MSC) in 2005, an NGO based third-party sustainability certification, which some buyers seek.

impact on market dynamics, particularly the Dollar-Yen and Dollar-Euro.<sup>4</sup> In 2015 the official U.S. market name changed from “Alaska pollock” to “pollock” enabling U.S. retailers to differentiate between pollock caught in Alaska and Russia. Additionally, pollock more broadly competes with other whitefish that, to varying degrees, can serve as substitutes depending on the product. The pollock industry has avoided U.S. tariffs that would have a significant negative impact on them in the U.S.-China trade war. However, Chinese tariffs on U.S. products could inhibit growth in that market.

This market environment accounts for some of the major trends in prices and production across product types. Fillet prices peaked in 2008–2010 but declined afterwards because of the greater supply from U.S. and Russia. The 2013 MSC certification of Russian-caught pollock enabled access to segments of European and U.S. fillet markets, which has put continued downward pressure on prices. Pollock roe prices and production have declined steadily over the last decade as international demand has waned with changing consumer preferences in Asia. Additionally, the supply of pollock roe from Russia has increased with catch. The net effect has been not only a reduction in the supply of roe from the U.S. industry, but also a significant reduction in roe prices which are roughly half pre-2008 levels. Prior to 2008, roe comprised 23% of the U.S. wholesale value share, and since 2011 it has been roughly 10% (Table 7). With the U.S. supply reduction in 2008–2010, surimi production from pollock came under increased pressure as U.S. pollock prices rose and markets sought cheaper sources of raw materials (see Guenneugues and Ianelli 2013 for a global review of surimi resources and market). This contributed to a growth in surimi from warm-water fish of southeast Asia. Surimi prices spiked in 2008–2010 and have since tapered off as production from warm-water species increased (as has pollock). A relatively small fraction of pollock caught in Russian waters is processed as surimi. Surimi is consumed globally, but Asian markets dominate the demand for surimi and demand has remained strong.

The catch of pollock can be broadly divided between the shore-based sector where catcher vessels make deliveries to inshore processors, and the at-sea sector where catch is processed at-sea by catcher/processors and motherships before going directly to the wholesale markets. The retained catch of the shore-based sector increased 1% to 710 kt. The value of these deliveries (shore-based ex-vessel value) totaled \$259.8 million in 2019, which was up 10% from the ex-vessel value in 2018 driven mostly by a 7% increase in the ex-vessel price which is above the 2010-2014 average (Table 6). The first-wholesale value of pollock products was \$920 million for the at-sea sector and \$630 million for the shore-based sector (Table 7). The higher revenue in recent years is combined effect of increased catch levels and price increases of pollock products of fillet and surimi products. The average price of pollock products in 2019 increased 9% for the at-sea sector to \$1.38 and increased 5% for the shore-based sector to \$1.12. Surimi prices increased 8% and fillet prices increased 11% in 2019. Roe prices decreased 26% while production increased 36%—the highest level observed in the last decade.

The portfolios of products shore-based and at-sea processors produce are similar. In both sectors the primary products processed from pollock are fillets, surimi and roe, with each accounting for approximately 40%, 40%, and 10% of first-wholesale value (Table 7). The price of products produced at-sea tend to be higher than comparable products produced by the shore-based because of the shorter time span between catch, processing and freezing. Since 2014 the price of fillets produced at-sea tend to be about 10% higher, surimi prices tend to be about 30% higher and the price of roe about 50% higher. Average prices for fillets produced at-sea also tend to be higher

<sup>4</sup>Aggregate exports in Table 8 may not fully account for all pollock exports as products such as meal, minced fish and other ancillary product may be coded as generic fish type for export purposes.

because they produce proportionally more higher-priced fillet types (like deep-skin fillets). The at-sea price first wholesale premium averaged roughly \$0.21 per pound between 2010–2014 and has increased to an average of \$0.27 per pound between 2015–2019.<sup>5</sup>

#### *Pollock fillets*

A variety of different fillets are produced from pollock, with pin-bone-out (PBO) and deep-skin fillets typically accounting for approximately 70% and 30% of production in the BSAI, respectively. Deep-skin fillet's share of fillet production was 33% in 2019. Total fillet production increased 11.5% to 187 kt in 2019, and since 2010 has increased with aggregate production and catch and was higher than the 2010–2014 average (Table 7). The average price of fillet products in the BSAI increased 11% to \$1.52 per pound and is below the inflation adjusted average price of fillets in 2010–2014 of \$1.69 per pound (2019 dollars). Media reports indicate that fillet prices tended to be strong throughout much of 2019. Pollock fillets sourced from Russia are the direct competitor to Alaska sourced pollock fillets. Fillets were a relatively small portion of Russian primary production however, they are increasing their fillet production capacity. Much of the Russian catch goes to China for secondary processing into fillets so this would do little to increase the overall volume, however, increased primary fillet processing in Russia could increase competition with U.S. produced single-frozen fillet products. Approximately 30% of the fillets produced in Alaska are estimated to remain in the domestic market, which accounts for roughly 45% of domestic pollock fillet consumption (AFSC 2016).<sup>6</sup> The U.S. industry has tried to maintain value by increasing domestic marketing for fillet based product and creating product types that are better suited to the American palette, in addition to increased utilization of by-products. Reductions in global pollock supplies in 2020 reported by the Groundfish Forum may upward pressure on pollock fillet prices.

#### *Surimi seafood*

Surimi production in 2019 was 192.2 kt, which was down 2.2% and was above the 2010–2014 average. Prices have generally increased since 2013 and resumed their upward progress in 2019 increasing 8% to \$1.37 (Table 7). Because surimi and fillets are both made from pollock meat, activity in the fillet market can influence the decision of processors to produce surimi as smaller average size of fish can incentivize surimi production, particularly if it yields a higher value than fillets. Additionally, strong demand for surimi has put upward pressure on prices.

#### *Pollock roe*

Roe is a high priced product that is the focus of the A season catch destined primarily for Asian markets. Roe production in the BSAI tapered off in the late–2000s and since has generally fluctuated at under or near 20 kt annually. Roe production increased to 28 kt in 2019 Production averaged 27 kt in 2005–2007 and was 20.6 kt in 2018, which was up 12% from 2017 (Fig. 7). Prices peaked in the mid-2000s and have followed a decreasing trend over the last decade which

<sup>5</sup>The at-sea price premium is the difference between the average price of first-wholesale products at-sea and the average price of first-wholesale products shore-based.

<sup>6</sup>Additionally, roughly 10% of the at-sea BSAI production is processed as H&G which is mostly exported, primarily to China, where is reprocessed as fillets and some share of which returns to the U.S.. China also processes H&G from Russia into fillets which are also imported into the domestic market. Current data collection does not allow us to estimate the share of U.S. returning imports.

continued until 2015, after which prices increased to \$2.89 per pound in 2018. The Yen to U.S. Dollar exchange rate can influence prices and weakened against the Yen in 2019. The average roe price in the BSAI was down 26% in 2019 to \$2.15 per pound, but value rose 1% with the increase in production to \$132.2 million (Table 7).

### *Fish oil*

Using oil production per 100 tons as a basic index (tons of oil per ton retained catch) shows increases for the at-sea sector. In 2005–2007 it was 0.3% and starting in 2008 it increased and leveled off after 2010 with over 1.5% of the catch being converted to fish oil (Table 9). This represents about a 5-fold increase in recorded oil production during this period. Oil production from the shore-based fleet was somewhat higher than the at-sea processors prior to 2008 but has been relatively stable. Oil production estimates from the shore-based fleet may be biased low because some production occurs at secondary processors (fishmeal plants) in Alaska. The increased production of oil beginning in 2008 can be attributed to the steady trend to add more value per ton of fish landed. The oil production index increased 15% in 2019 and was at levels not seen since before 2015.

## **Data**

The following lists the data used in this assessment:

Source	Type	Years
Fishery	Catch biomass	1964–2020
Fishery	Catch age composition	1964–2019
Fishery	Japanese trawl CPUE	1965–1976
EBS bottom trawl	Area-swept biomass and age-specific proportions	1982–2019
Acoustic trawl survey	Biomass index and age-specific proportions	1994, 1996, 1997, 1999, 2000, 2002, 2004, 2006–2010, 2012, 2014, 2016, 2018, 2020
Acoustic vessels of opportunity (AVO)	Biomass index	2006–2019

*Note the 2020 acoustic survey data based on unmanned surface vessel (USV) transects*

### ***Fishery***

#### *Catch*

The catch-at-age composition was estimated using the methods described by Kimura (1989) and modified by Dorn (1992). Length-stratified age data are used to construct age-length keys for each stratum and sex. These keys are then applied to randomly sampled catch length frequency data. The stratum-specific age composition estimates are then weighted by the catch within each stratum to arrive at an overall age composition for each year. Data were collected through shore-side sampling and at-sea observers. The three strata for the EBS were: i) January–June (all areas, but mainly east of 170°W); ii) INPFC area 51 (east of 170°W) from July–December; and iii) INPFC area 52 (west of 170°W) from July–December. This method was used to derive the age compositions

from 1991–2019 (the period for which all the necessary information is readily available). Prior to 1991, we used the same catch-at-age composition estimates as presented in Wespestad et al. (1996).

The catch-at-age estimation method uses a two-stage bootstrap re-sampling of the data. Observed tows were first selected with replacement, followed by re-sampling actual lengths and age specimens given that set of tows. This method allows an objective way to specify the effective sample size for fitting fishery age composition data within the assessment model. In addition, estimates of stratum-specific fishery mean weights-at-age (and variances) are provided which are useful for evaluating general patterns in growth and growth variability. For example, Ianelli et al. (2007) showed that seasonal aspects of pollock condition factor could affect estimates of mean weight-at-age. They showed that within a year, the condition factor for pollock varies by more than 15%, with the heaviest pollock caught late in the year from October–December (although most fishing occurs during other times of the year) and the thinnest fish at length tending to occur in late winter. They also showed that spatial patterns in the fishery affect mean weights, particularly when the fishery is shifted more towards the northwest where pollock tend to be smaller at age. In 2011 the winter fishery catch consisted primarily of age 5 pollock (the 2006 year class) and later in that year age 3 pollock (the 2008 year class) were present. In 2012–2016 the 2008 year class was prominent in the catches with 2015 showing the first signs of the 2012 year-class as three year-olds in the catch (Fig. 12; Table 10). The sampling effort for age determinations, weight-length measurements, and length frequencies is shown in Tables 11, 12, and 13. Sampling for pollock lengths and ages by area has been shown to be relatively proportional to catches (e.g., Fig. 1.8 in Ianelli et al. 2004). The precision of total pollock catch biomass is considered high with estimated CVs to be on the order of 1% (Miller 2005).

Scientific research catches are reported to fulfill requirements of the Magnuson-Stevens Fisheries Conservation and Management Act. The annual estimated research catches (1963–2018) from NMFS surveys in the Bering Sea and Aleutian Islands Region are given in (Table 14). Since these values represent extremely small fractions of the total removals (about 0.02%) they are ignored for assessment purposes.

## ***Surveys***

### ***Bottom trawl survey (BTS)***

Trawl surveys have been conducted annually by the AFSC to assess the abundance of crab and groundfish in the Eastern Bering Sea since 1979 and since 1982 using standardized gear and methods. For pollock, this survey has been instrumental in providing an abundance index and information on the population age structure. This survey is complemented by the acoustic trawl (AT) surveys that sample mid-water components of the pollock stock. Between 1991 and 2019 the BTS biomass estimates ranged from 2.28 to 8.39 million t (Table 15; Fig. 13). In the mid-1980s and early 1990s several years resulted in above-average biomass estimates. The stock appeared to be at lower levels during 1996–1999 then increased moderately until about 2003 and since then has averaged just over 4 million t. These surveys also provide consistent measurements of environmental conditions, such as the sea surface and bottom temperatures. Large-scale zoogeographic shifts in the EBS shelf documented during a warming trend in the early 2000s were attributed to temperature changes (e.g., Mueter and Litzow 2008). However, after the period of relatively warm conditions ended in 2005, the next eight years were mainly below average, indicating that the zoogeographic responses may be less temperature-dependent than they initially appeared (Kotwicki and Lauth 2013). Bottom temperatures increased in 2011 to about average from the low value in 2010 but

declined again in 2012–2013. However, in the period 2014–2016, bottom temperatures increased and reached a new high in 2016. In 2018 bottom temperatures were nearly as warm (after 2017 was slightly above average) but was highly unusual due to the complete lack of “cold pool” (i.e., a defined area where water near bottom was less than zero degrees. In 2019, the mean bottom temperature was the warmest during the period the survey has occurred (since 1982; Fig. 14). In 2020 the survey was canceled and detailed data were unavailable. The 2020 Ecosystem report (Siddon 2020) contains model estimates of temperature distributions for the region and indicates that the bottom temperatures and cold pool extent were about average in 2020.

The AFSC has expanded the area covered by the bottom trawl survey over time. In 1987 the “standard survey area” comprising 6 main strata was increased farther to the northwest and covered in all subsequent years. These two northern strata have varied in estimated pollock abundance. In 2019 about 9% of the pollock biomass was found in these strata compared to a long term average of 5% (Table 15). Importantly, this region is contiguous with the Russian border and the NBS region, and measures to increase consideration of those regions relative to the exploited pollock stock continues (e.g., O’leary et al. Submitted).

As noted last year, the 2019 bottom-trawl survey biomass estimate (design-based, area swept) was 5.48 million t, above the average for this survey (4.7 million t). This was a substantial increase over the 3.11 million t estimated from the 2018 estimates. Both years were unusual in that there was a near-complete lack of cold water on the bottom throughout the survey area (Fig. 15). Pollock appeared to be distributed more broadly over the shelf in 2019, different than in 2017 and 2018 where fish were more concentrated (Fig. 16).

The BTS abundance-at-age estimates show variability in year-class strengths with substantial consistency over time (Fig. 17). Pollock above 40 cm in length generally appear to be fully selected and in some years many 1-year olds occur on or near the bottom (with modal lengths around 10–19 cm). Age 2 or 3 pollock (lengths around 20–29 cm and 30–39 cm, respectively) are relatively rare in this survey presumably because they are more pelagic as juveniles. Observed fluctuations in survey estimates may be attributed to a variety of sources including unaccounted-for variability in natural mortality, survey catchability, and migrations. As an example, some strong year classes appear in the surveys over several ages (e.g., the 1989 year class) while others appear only at older ages (e.g., the 1992 and 2008 year class). Sometimes initially strong year classes appear to wane in successive assessments (e.g., the 1996 year class estimate (at age 1) dropped from 43 billion fish in 2003 to 32 billion in 2007 (Ianelli et al. 2007). Retrospective analyses (e.g., Parma 1993) have also highlighted these patterns, as presented in Ianelli et al. (2006, 2011). Kotwicki et al. (2013) also found that the catchability of either the BTS or AT survey for pollock is variable in space and time because it depends on environmental variables, and is density-dependent in the case of the BTS survey.

The 2019 survey age compositions were developed from age-structures collected during the survey (June-July) and processed at the AFSC labs within a few weeks after the survey was completed. The level of sampling for lengths and ages in the BTS is shown in (Table 16). The estimated numbers-at- age from the BTS for strata (1–9 except for 1982–84 and 1986, when only strata 1–6 were surveyed) are presented in Table 17 (based on the method in Kotwicki et al. 2014). Mean body mass at ages from the survey are shown in (Table 18) and the different alternative time series of BTS survey indices is shown in Table 19.

The NBS survey area was sampled in 2010, 2017, 2018 (limited to 49 stations), and in 2019. Given that the pollock abundance was quite high in 2017 and 2018, a method for incorporating this information as part of the standard survey was desired. One approach for constructing a full time series that included the NBS area is to use observed spatial and temporal correlations. We used the

vector-autoregressive spatial temporal (VAST) model of Thorson (2018b) together with the density-dependent corrected CPUE values from each station (including stations where pollock were absent; Table 19). Please refer to the appendix for further details on the implementation. The appendix also shows results that indicate the VAST model diagnostics are reasonable and provide consistent interpretations relative to the observations. Notably, results indicate increased uncertainty in years and areas when stations were missing. As noted in past assessments, application of this index within the stock assessment model required accounting for the temporal covariation.

#### *Acoustic trawl (AT) surveys*

Acoustic trawl (AT) surveys The AT surveys are typically conducted every other year and are designed to estimate the off-bottom component of the pollock stock (compared to the BTS which are conducted annually and provide an abundance index of the near-bottom pollock). The number of trawl hauls, lengths, and ages sampled from the AT survey are presented in (Table 19). Estimated pollock biomass (to 0.5m from bottom) for the EBS shelf was above 4 million tons in the early years of the time series (prior to 1998 Table 19). Biomass dipped below 2 million t in 1991. Since 1994, the years for which AT survey estimates are available to within 0.5 m of bottom, the biomass increased and remained between about 3 and 4.5 million t for a decade (1994–2004). The early 2000s (a relatively ‘warm’ period) were characterized by low pollock recruitment, which was subsequently reflected in lower pollock biomass estimates between 2006 and 2012 (a ‘cold’ period; Honkalehto and McCarthy 2015). In 2014 and 2016 (another ‘warm’ period) with the growth of the strong 2012 year class, AT biomass estimates increased to over 4 million t, exceeding levels observed in 1994–2004 (Tables 19).

Relative estimation errors for the total biomass were derived from a one-dimensional (1D) geostatistical method, which accounts for observed spatial structure for sampling along transects (Table 21; Petitgas 1993, Walline 2007, Williamson and Traynor 1996). As in previous assessments, the other sources of error (e.g., target strength, trawl selectivity) were accounted for by inflating the annual error estimates to have an overall average CV of 20% for application within the assessment model. The age composition data from the ATS sampling are provided in Table 22.

*Uncrewed surface vehicle (USV) deployment and data processing* NOAA’s fisheries research vessel was unable to perform the planned 2020 acoustic-trawl survey due to the COVID-19 pandemic. Instead, three chartered Saildrone<sup>(TM)</sup> uncrewed surface vehicles (USVs) were deployed from Alameda, CA, to the Bering Sea to perform this task. AFSC scientists acted quickly with support from NOAA’s office of science and technology in the late spring to organize this as an option given the potential for surveys to be canceled or curtailed. This contingency plan was possible due to AFSC’s previous experience working closely as part of a private-public partnership between Saildrone, Simrad, and NOAA Research’s Pacific Marine Environmental Laboratory (PMEL). Saildrone has collaborated with the AFSC and PMEL on several missions in the Arctic since 2016 to develop the vehicle’s capabilities and refine the sensors (Meinig et al., 2019).

The USVs were equipped with Simrad EK80 mini split-beam echo sounders equivalent to those used on NOAA surveys (De Robertis et al., 2019).

In addition, they are equipped with a suite of instruments to collect oceanographic and meteorological data above and below the sea surface including air and sea temperatures, wind speed and direction, relative humidity, barometric pressure, photosynthetically active radiation, salinity, dissolved oxygen, chlorophyll fluorescence, and wave height and period (Mordy et al., 2017). Data

summaries are transmitted to shore via a satellite link, and the vehicles are controlled over this link.

Missions include studying the impacts of climate variability and other environmental aspects on northern fur seals and other marine mammal populations, measuring carbon dioxide and the abundance of Arctic cod, collecting observations for sea ice prediction and satellite algorithm development, and tracking Alaska red king crab (e.g. Mordy et al., 2017, De Robertis et al. 2019, Levine et al., in press). Comparisons of backscatter recorded from saildrone USVs and ‘follow the leader’ vessel comparisons conducted during the 2016 EBS survey have confirmed that the USVs and the NOAA ship Oscar Dyson produce equivalent measurements of pollock backscatter under survey conditions (De Robertis et al., 2019).

The three USVs reached the Bering Sea on July 4 and conducted a survey until August 20. Each vehicle covered about one third of the total survey area normally covered by research vessel, with each USV proceeding from south to north. The timing of the survey was within the window of other acoustic surveys in the EBS (Fig. 18). The USVs were equipped with Simrad EK80 mini split-beam echo sounders equipped with 38/200 kHz combi-split transducers which were calibrated before and after the survey. The instruments were similar to those used on previous ship-based AT surveys. One important difference is that the USVs were equipped with smaller transducers which transmit an 18 degree beam—larger than the 7 degree beam emitted from the larger transducers carried by NOAA survey vessels.

Given the larger beamwidth, the so-called ‘acoustic dead zone’ differs. This zone refers to a near seafloor area within the beam where fish may go undetected (and this varies with beamwidth angle). To correct for this difference, we applied the method of Ona and Mitson (1996) and found that, given the physical differences from the equipment and the degree to which fish aggregate near the seafloor, the adjustment to the data meant a 6.7% increase in total backscatter.

The ship-based AT surveys use trawls to sample fish aggregations observed acoustically. One drawback of using the USVs is the inability to confirm the species, size, and biological characteristics of the acoustic backscatter. The lack of biological samples affects the ability to convert the areal measures of acoustic backscatter ( $sA$ ,  $m^2 \text{ nmi}^{-2}$ ) into pollock biomass. The conversion depends on the species composition and size distribution of the backscattering organisms. Also, biological samples help determine the age composition of the pollock that are within the backscatter. Fortunately, midwater fish in the survey area are predominately pollock (Fig. 19). This simplifies the interpretation of acoustic measurements since fish aggregations are most likely to be pollock (e.g. as is assumed in the AVO backscatter index derived from the bottom trawl charter vessels (Honkalehto et al., 2011)). Nonetheless, retrospective analysis indicates that there is a strong relationship between total backscatter and biomass estimates from the research ships (Fig. 20). As a result, linear regressions of these relationships (Fig. 21) were used to convert the acoustic backscatter to biomass for the USV data collected in 2020. As in previous surveys, the midwater component ( $>3\text{m}$  above bottom), and the demersal component ( $0.5$  to  $3\text{m}$  above bottom) were converted to biomass using separate relationships and then combined as demersal community composition is more diverse than in midwater (Lauffenburger et al., 2017). A sensitivity analysis in which the biomass in each year was predicted based on the trawl samples in other years rather than the trawl observations in that year suggests that this conversion does not alter the primary trends in the time series (Fig. 22).

Another component of uncertainty for the USV data was the fact that due to time constraints, the transect spacing to cover the area of the EBS had to be doubled (this survey design was a contingency plan in case the Dyson was delayed but available for the survey). To evaluate the

impact of this, we compared past surveys and computed biomass and uncertainty estimates as if the even number (20-mile transects) were dropped or alternatively the odd numbered transects. Results from this showed that the estimates were consistent with the “full” survey (at 20-mile transects) but that the uncertainty increased (Fig. 23). Similar comparisons using the 1-D geostatistical technique are ongoing and have produced similar initial results (i.e. the coefficient of variation (CV) increases approximately two fold for 40 nmi spacing compared to 20 nmi spacing). The uncertainty of the survey was characterized by increasing the observed 1-D CV based on the prediction intervals based on a Monte-Carlo which accounts for the additional variance introduced by the unit conversion from backscatter to biomass.

In 2020 the acoustic backscatter index increased by 45.2% relative to the last survey in 2018 (Fig. 20). Converting to biomass, the estimate increased by 44.5% to 3.6 million t (the 2018 estimate was 2.5 million t; Fig. 24). The CV based on the 1-D geostatistical estimate for backscatter measurements 2020 was 6.9%, which increased to 9.7% when the additional uncertainty of the backscatter to biomass conversion was added (Fig. 24). This CV is 2.6 times the average CV of the 1994–2020 time series (3.8%, see (Fig. 24)). The backscatter data show that the density of pollock was highest in the northwest portion of the survey area (Fig. 25). The proportion of backscatter in the lower three meters was consistent with observations in previous years (Fig. 26), which suggests that the difference in beamwidth between the USV and the research vessels used for previous surveys did not introduce a major bias. Finally, a VAST-spatio-temporal model based on backscatter data which expanded the survey grid to the area covered by the BTS survey (see appendix for details) was used to enabled visualization of past surveys, and to computing an alternate index extrapolated over a larger survey area than that occupied by the survey (Fig. 27). The VAST and design based survey estimates were considered as inputs to the assessment model.

### ***Other time series used in the assessment***

#### ***Japanese fishery CPUE index***

An available time series relating the abundance of pollock during the period 1965–1976 was included. This series is based on Japanese fishery catch rates which used the same size class of trawl vessels as presented in Low and Ikeda (1980). A coefficient of variation of 20% was applied.

#### ***Biomass index from Acoustic-Vessels-of-Opportunity (AVO)***

The details of how acoustic backscatter data from the two commercial fishing vessels chartered for the eastern Bering Sea bottom trawl survey (BTS) were used to compute a midwater abundance index for pollock can be found in Honkalehto et al. (2011). Since the BTS was canceled this year, the AVO data are only available through to 2019 (Table 23).

## **Analytic approach**

### ***General model structure***

A statistical age-structured assessment model conceptually outlined in Fournier and Archibald (1982) and like Methot’s (1990) stock synthesis model was applied over the period 1964–2020. A technical description is presented in the Model Details section attached. The analysis was first

introduced in the 1996 SAFE report and compared to the cohort analyses that had been used previously and was later documented in Ianelli and Fournier (1998). The model was written in “ADMB”—a library for non-linear estimation and statistical applications (Fournier et al. 2012). The data updated from last year’s analyses include:

- The 2019 fishery age composition data were added
- The catch biomass estimates were updated through to the current year
- The USV backscatter data collected in 2020 was converted to biomass and applied as an extension of the ATS time series

A simplified version of the assessment (with mainly the same data and likelihood-fitting method) is included as a supplemental multi-species assessment model. As presented since 2016, it allows for trophic interactions among key prey and predator species and for pollock, and it can be used to evaluate age and time-varying natural mortality estimates in addition to alternative catch scenarios and management targets (see this volume: [EBS multi-species model](#)).

### ***Description of alternative models***

In the 2019 assessment, the spatio-temporal model fit to BTS CPUE data *including stations from the NBS* was expanded using the VAST methods detailed in Thorson (2018). This data treatment was included as a model alternative and adopted for ABC/OFL specifications by the SSC. This application also included a spatio-temporal treatment of the age composition data which showed minor differences compared to the standard design-based expansion of ages. Using the SSC convention for model numbering, we designated it as “Model 16.2”. Given that this year we present a new data type, we examined the following models:

- Model 16.2 (identical to 2019 model selected by the SSC but includes updated fishery catch-at-age and catch biomass data)
- Model 20.0, a model which includes the 2020 USV data extending the time series of ATS biomass estimates
- Model 20.1, a model which includes the 2020 USV data but applies a spatio-temporal model (VAST) to the backscatter data from 1994-2018 (RV Oscar Dyson) in addition to the USV backscatter data from 2020.

### ***Tier 1 considerations***

For the latter set of evaluations (Model 20.0), we examined the factors affecting Tier 1 classifications including the reliable pdf of  $F_{MSY}$ , i.e., the influence of assumptions related to the uncertainties on the stock recruitment relationship, body mass-at-age, maturation, and fishery selectivity. For a number of years the Tier 1 ABC and OFL specifications for EBS pollock have been very high, in excess of the 2 million t OY for combined groundfish stocks managed within this FMP area. This has been because the spawning stock estimates have been well above target and mean levels. To add precaution to these estimates, ABC recommendations have been below the maximum permissible under Tier 1 but the rationale for such an adjustment could be improved. As such, the SSC

requested an examination of the issues related to classifying this stock in Tier 1 versus Tier 3. The FMP (under amendment 56) guides this classification. It notes that a reliable estimate of  $F_{MSY}$  and its uncertainty (as expressed through a probability distribution or PDF) is required. Since these values depend primarily on the stock-recruitment relationship (SRR), the following sensitivities were pursued relative to the status quo (Model 20.0) configuration:

- a) As status quo but ignore influence of the 1978 year class on SRR
- b) As in sensitivity a) but with a less informative prior on steepness
- c) As in status quo but the SRR conditioned such that  $F_{MSY} = F_{35\%}$
- d) As in status quo but the SRR conditioned such that  $F_{MSY} = F_{45\%}$

The first option is intended to reflect that the high value observed of the 1978 year-class occurred under an estimated low level of spawning biomass (designated Model 20.0a). The rationale for excluding this influential value would be that the stock structure and environmental conditions may differ now. This could be an aspect of non-stationarity in the relationship that is worth considering. Also, it is unknown if spawning from other adjacent regions (e.g., the spawning biomass that contributed to the Aleutian Basin fishery throughout the 1980s) contributed to the success of this year-class. Sensitivity test b) is intended to illustrate the role of the prior mean and variance on the steepness estimate. Finally sensitivities c) and d) were considered as how the SRR may translate an implicit assumption under Tier 3 since  $F_{35\%}$  is a proxy for  $F_{MSY}$  and  $F_{45\%}$  is closer to the recent mean SPR rate.

#### *Input sample size*

Sample sizes for age-composition data were re-evaluated in 2016 against the trade-off with flexibility in time and age varying selectivity. This resulted in tuning the recent era (1991-present year) to average sample sizes of 350 for the fishery and then using estimated values for the intermediate and earliest period (Table 24).

We assumed average values of 100 and 50 for the BTS and ATS data, respectively with inter-annual variability reflecting the variability in the number of hauls sampled for ages. The tuning aspects for these effective sample size weights were estimated following Francis 2011 (equation TA1.8, hereafter referred to as Francis weights).

#### ***Parameters estimated outside of the assessment model***

##### *Natural mortality and maturity at age*

The baseline 16.1 (and 16.2) model specification has been to use constant natural mortality rates at age (M=0.9, 0.45, and 0.3 for ages 1, 2, and 3+ respectively (Wespestad and Terry 1984). When predation was explicitly considered estimates tend to be higher and more variable (Holsman et al. *this volume*; Holsman et al. 2015; Livingston and Methot 1998; Hollowed et al. 2000). Clark (1999) found that specifying a conservative (lower) natural mortality rate may be advisable when natural mortality rates are uncertain. More recent studies confirm this (e.g., Johnson et al. 2015).

In the supplemental multi-species assessment model alternative values of age and time-varying natural mortality are presented. As in past years the estimates indicate higher values than used

here. In the 2018 assessment we evaluated natural mortality it was noted that the survey age compositions favored lower values of  $M$  while the fishery age composition favored higher values. This is consistent with the patterns seen in the BTS survey data as they show increased abundances of “fully selected” cohorts. Hence, given the model specification (asymptotic selectivity for the BTS age composition data), lower natural mortality rates would be consistent with those data. Given these trade-offs, structural model assumptions were held to be the same as previous years for consistency (i.e., the mortality schedule presented below).

Maturity-at-age values used for the EBS pollock assessment were originally based on Smith (1981) and were reevaluated (e.g., Stahl 2004; Stahl and Kruse 2008a; and Ianelli et al. 2005). These studies found inter-annual variability but general consistency with the current assumed schedule of proportion mature at age.

The values assumed for pollock natural mortality-at-age and maturity-at-age (for all models; Smith 1981) were kept the same as in previous assessments:

Age	1	2	3	4	5	6	7	8	9	10	11	12	13	14	15
$M$	0.90	0.45	0.30	0.30	0.30	0.30	0.30	0.30	0.30	0.30	0.30	0.30	0.30	0.30	0.30
$P_{mat}$	0.00	0.008	0.29	0.64	0.84	0.90	0.95	0.96	0.97	1.00	1.00	1.00	1.00	1.00	1.00

### *Length and weight-at-age*

Age determination methods have been validated for pollock (Kimura et al. 1992; Kimura et al. 2006, and Kastelle and Kimura 2006). EBS pollock size-at-age show important differences in growth with differences by area, year, and year class. Pollock in the northwest area are typically smaller at age than pollock in the southeast area. The differences in average weight-at-age are taken into account by stratifying estimates of catch-at-age by year, area, season, and weighting estimates proportional to catch.

The assessment model for EBS pollock accounts for numbers of individuals in the population. As noted above, management recommendations are based on allowable catch levels expressed as tons of fish. While estimates of pollock catch-at-age are based on large data sets, the data are only available up until the most recent completed calendar year of fishing (e.g., 2019 for this year). Consequently, estimates of weight-at-age in the current year are required to map total catch biomass (typically equal to the quota) to numbers of fish caught (in the current year). Therefore, if there are errors (or poorly accounted uncertainty) in the current and future mean weight-at-age, this can translate directly into errors between the expected fishing mortality and what mortality occurs. For example, if the mean weight at age is biased high, then an ABC (and OFL) value will result in greater numbers of fish being caught (and fishing mortality being higher due to more fish fitting within the ABC).

To explore patterns in size-at-age and fish condition, we applied the extensive fishery observer data weight given length. We began by standardizing for length over all available years and areas (1991–2019) as follows:

1. extract all data where non-zero measurements of pollock length and weight were available between the lengths of 35 and 60 cm for the EBS region
2. compute the mean value of body mass (weight) for each cm length bin over all areas and time
3. divide each weight measurement by that mean cm-specific value (the “standardization” step)

4. plot these standardized values by different areas, years, months etc. to evaluate condition differences (pooling over ages is effective as there were no size-specific biases apparent)

In the first instance, the overarching seasonal pattern in body mass relative to the mean shows that as the winter progresses prior to peak spawning, pollock are generally skinnier than average whereas in July, the median is about average (Fig. 28). As the summer/fall progresses, fish were at their heaviest given length (Fig. 28). This is also apparent when the data are aggregated by A- and B-seasons (and by east and west of 170°W; referred to as SE and NW respectively) when plotted over time (Fig. 30). Combining across seasons, the fishery data show that the 2020 fish were well below average weight given length (Fig. 29).

Examining the weight-at-age, there are also consistent patterns of variability that vary due to environmental conditions in addition to spatial and temporal patterns of the fishery. Based on the bootstrap distributions and large sample sizes, the within-year sampling variability for pollock is small. However, the between-year variability in mean weights-at-age is relatively high (Table 26). The coefficients of variation between years are on the order of 6% to 9% (for the ages that are targeted) whereas the sampling variability is generally around 1% or 2%. The approach to account for the identified mean weight-at-age having clear year and cohort effects was continued (e.g., Fig. 31). Details were provided in appendix 1A of Ianelli et al. (2016). The results from this method showed the relative variability between years and cohorts and provide estimates (and uncertainty) for 2020–2022 (Table 26).

In the 2019 fishery, the average weight-at-age for the two most important year classes (2012 and 2013) appeared to be average whereas in 2018, those year-classes appeared to be below average body weight (Fig. 31). To examine this more closely, we split the bootstrap results into area-season strata and were able to get an overall picture of the pattern by strata (Fig. 32) and Fig. 33). This showed that the mean weight-at-age is higher in the the B-season in the area east of 170°W compared to the A-season and B-season in the area west 170°W.

### ***Parameters estimated within the assessment model***

For the selected model, 979 parameters were estimated conditioned on data and model assumptions. Initial age composition, subsequent recruitment, and stock- recruitment parameters account for 79 parameters. This includes vectors describing the initial age composition (and deviation from the equilibrium expectation) in the first year (as ages 2–15 in 1964) and the recruitment mean and deviations (at age 1) from 1964–2019 and projected recruitment variability (using the variance of past recruitments) for five years (2021–2026). The two- parameter stock-recruitment curve is included in addition to a term that allows the average recruitment before 1964 (that comprises the initial age composition in that year) to have a mean value different from subsequent years. Note that the stock-recruit relationship is fit only to stock and recruitment estimates from 1978 year-class through to the 2018 year-class.

Fishing mortality is parameterized to be semi-separable with year and age (selectivity) components. The age component is allowed to vary over time; changes are allowed in each year. The mean value of the age component is constrained to equal one and the last 5 age groups (ages 11–15) are specified to be equal. This latter specification feature is intended to reduce the number of parameters while acknowledging that pollock in this age-range are likely to exhibit similar life-history characteristics (i.e., unlikely to change their relative availability to the fishery with age). The annual components of fishing mortality result in 57 parameters and the age-time selectivity schedule forms a 10x57

matrix of 570 parameters bringing the total fishing mortality parameters to 627. The rationale for including time-varying selectivity has recently been supported as a means to improve retrospective patterns (Szuwalski, Ianelli, and Punt 2017) and as best practice (Martell and Stewart, 2013).

For surveys and indices, the treatment of the catchability coefficient, and interactions with age-specific selectivity require consideration. For the BTS index, selectivity-at-age is estimated with a logistic curve in which year specific deviations in the parameters is allowed. Such time-varying survey selectivity is estimated to account for changes in the availability of pollock to the survey gear and is constrained by pre-specified variance terms. For the AT survey, which originally began in 1979 (the current series including data down to 0.5 m from bottom begins in 1994), optional parameters to allow for age and time-varying patterns exist but for this assessment and other recent assessments, ATS selectivity is constant over time. Overall, five catchability coefficients were estimated: one each for the early fishery catch-per-unit effort (CPUE) data (from Low and Ikeda, 1980), the early bottom trawl survey data (where only 6 strata were surveyed), the main bottom trawl survey data (including all strata surveyed), the AT survey data, and the AVO data. An uninformative prior distribution is used for all of the indices. The selectivity parameters for the 2 main indices total 135 (the CPUE and AVO data mirror the fishery and AT survey selectivities, respectively).

Additional fishing mortality rates used for recommending harvest levels are estimated conditionally on other outputs from the model. For example, the values corresponding to the  $F_{40\%}$ ,  $F_{35\%}$  and  $F_{MSY}$  harvest rates are found by satisfying the constraint that, given age-specific population parameters (e.g., selectivity, maturity, mortality, weight-at-age), unique values exist that correspond to these fishing mortality rates. The likelihood components that are used to fit the model can be categorized as:

- Total catch biomass (log-normal,  $\sigma = 0.05$ )
- Log-normal indices of pollock biomass; bottom trawl surveys assume annual estimates of sampling error, as represented in Fig. 13 along with the covariance matrices (for the density-dependent and VAST index series); for the AT index the annual errors were specified to have a mean of 0.20; while for the AVO data, a value relative to the AT index was estimated and gave a mean of about 0.25).
- Fishery and survey proportions-at-age estimates (multinomial with effective sample sizes presented Table 24).
- Age 1 index from the AT survey (CV set equal to 30% as in prior assessments).
- Selectivity constraints: penalties/priors on age-age variability, time changes, and decreasing (with age) patterns.
- Stock-recruitment: penalties/priors involved with fitting a stochastic stock-recruitment relationship within the integrated model.
- “Fixed effects” terms accounting for cohort and year sources of variability in fishery mean weights-at-age estimated based on available data from 1991-2019 from the fishery (and 1982-2020 for the bottom-trawl survey data) and externally estimated variance terms as described in Appendix 1A of Ianelli et al. (2016).

Work evaluating temperature and predation-dependent effects on the stock-recruitment estimates continues (Spencer et al. 2016). This approach modified the estimation of the stock-recruitment

relationship by including the effect of temperature and predation mortality. A relationship between recruitment residuals and temperature was noted (similar to that found in Mueter et al., 2011) and lower pollock recruitment during warmer conditions might be expected. Similar results relating summer temperature conditions to subsequent pollock recruitment for recent years were also found by Yasumiishi et al. (2015).

## Results

### *Model evaluation*

A sequential sensitivity of available new data showed that adding the 2020 fishery catch-at-age data and the 2020 catch biomass information was relatively uninformative with respect to spawning biomass estimates (Fig. 34). As the new design-based biomass estimate from the USV data were added to the model (named Model 20.0), the biomass estimate changed slightly (Fig. 34). Subsequently, we were able to apply a VAST model configuration to the acoustic backscatter from the survey vessels (prior to 2020) and from the USV for 2020. Historically the CVs for the ATS data have been scaled to have a mean of 20% while allowing for inter-annual variation the CVs. An alternative we tested was to simply apply the sampling errors as they are computed for the design-based method and for the VAST application. Results from this show that the assumption for specified CVs from the design-based method had a relatively large impact on the results compared to doing the same thing with the VAST index data. The relative trends in survey were less smooth when the original sampling variability was used (Fig. 35). The impact on the spawning biomass resulted in similar trends but definitely narrower error bands compared with the base model assumption (CV averaged 20%; Fig. 36). Diagnostics of model fits between the set evaluated are given in Table ?? and comparisons of management quantities are given in Table 27). For setting advice, we selected Model 20.0 as the baseline as we feel the USV data extend the time series of historical biomass in way that makes the best use of past and new data. The VAST application to the backscatter information (Model 20.1) provided similar trends and has some advantages over Model 20.0 (e.g., the area included is constant for all years). However, we selected Model 20.0 because 20.1 is based on backscatter data only. Model 20.1 excludes the corrections (which are minor it seems) to species and size composition of the fish observed by echo sounders and sampled by trawl gear.

The SRR evaluations related to Tier 1 classification showed that dropping the influence of the 1978 year-class in the estimation lowered the steepness of the curve (Fig. 37). When the influence of the prior distribution was removed, the left-most “data” were all below the curve (Fig. 38). This reiterates how the prior was selected in the past—namely to fit the slope at the origin better. Finally, conditioning the SRR to fit the condition of having the “actual”  $F_{MSY}$  equal some  $F_{MSY}$  proxies (e.g., equal  $F_{35\%}$ ) shows that the resulting curve, while being more conservative (shallow initial slopes), fit the observations reasonably (Fig. 39). One conclusion from this exercise could be that the SPR proxy for  $F_{MSY}$  implies a reasonable “shape” to the SRR. Another is that dropping the 1978 year-class influence on the fit could provide some added precaution. Finally, as noted in past assessments, fitting the apparent low year-classes that occurred during periods of high spawning biomass results in very high steepness values near the origin (and misses the data in region of lower spawning biomass).

The fit to the early Japanese fishery CPUE data (Low and Ikeda 1980) was consistent with the estimated population trends for this period (Fig. 41). The model fits the fishery- independent

index from the 2006–2019 AVO data well indicating a downward trend since 2015 but stabilizing compared to 2018 values (Fig. 42). The fits to the bottom-trawl survey biomass (the density-dependent corrected series) were reasonable (Fig. 43). Similarly, the fits to the acoustic-trawl survey biomass series was consistent with the specified observation uncertainty (Fig. 40).

The estimated parameters and standard errors are provided [online](#). The code for the model (with dimensions and links to parameter names) and input files are available on request.

The input sample size (as tuned in 2016 using “Francis Weights”) can be evaluated visually for consistency with expectations of mean annual age for the different gear types (Fig. 44; Francis 2011). The estimated selectivity pattern changes over time and reflects to some degree the extent to which the fishery is focused on particularly prominent year- classes (Fig. 45). The model fits the fishery age- composition data quite well under this form of selectivity (Fig. 46).

Bottom-trawl survey selectivity (Fig. 47) and fits to the pollock biomass index indicate that the model predicts fewer pollock than observed in the 2014 and 2015 survey but slightly more than observed in the years since then (Fig. 43). The pattern of bottom trawl survey age composition data in recent years shows a decline in the abundance of older pollock since 2011. The 2006 year-class observations are below model expectations in 2012 and 2013. This is partly due to the fact that in 2010 the survey estimates are greater than the model predictions (Fig. 48). The model predicted much higher proportions of age 6 (2012 year class) than observed in the 2018 survey data whereas the expectations of 5-year old pollock were much lower than observations (both surveys indicated that the 2013 year class was more abundant than the 2012 year-class).

The fit to the ATS biomass index survey generally falls within the confidence bounds of the survey sampling distributions (here assumed to have an average CV of 20%) with a reasonable pattern of residuals (Fig. 40). The AT age compositions consistently track large year classes through the population and the model fits these patterns reasonably well (Fig. 49).

As in past assessments, an evaluation of the multivariate posterior distribution was performed by running a chain of 3 million Monte-Carlo Markov chain (MCMC) simulations and saving every 600th iteration (final posterior draws totaled 5,000). A pairwise comparison for some key parameters could be evaluated (along with their marginal distributions; Fig. 50). To compare the point estimates (highest posterior density) with the mean of the posterior marginal distribution, overplotting the former on the latter for the 2020 spawning biomass estimate were similar (Fig. 51).

### ***Time series results***

The time series of begin-year biomass estimates (ages 3 and older) suggests that the abundance of Eastern Bering Sea pollock remained at a high level from 1982–88, with estimates ranging from 8 to 11 million t (Table 28). Historically, biomass levels increased from 1979 to the mid-1980s due to the strong 1978 and relatively strong 1982 and 1984 year classes recruiting to the fishable population. The stock is characterized by peaks in the mid-1980s, the mid-1990s and again appears to be increasing to new highs over 13 million t in 2016 following the low in 2008 of 4.7 million t. The estimate for 2020 is trending downward and at 8.69 million t. with 2021 estimated at 8.15 million t.

The level of fishing relative to biomass estimates show that the spawning exploitation rate (SER, defined as the percent removal of egg production in each spawning year) has been mostly below 20% since 1980 (Fig. 52). During 2006 and 2007 the rate averaged more than 20% and the average fishing mortality for ages 3–8 increased during the period of stock decline. The estimate for 2009

through 2019 was below 20% due to the reductions in TACs relative to the maximum permissible ABC values and increases in the spawning biomass. The average  $F$  (ages 3–8) increased in 2011 to above 0.25 when the TAC increased but has dropped since then and in 2020 is estimated at about 17%. Age specific fishing mortality rates reflect these patterns and show some increases in the oldest ages from 2011–2013 but also indicate a decline in recent years (Fig. 53). The estimates of age 3+ pollock biomass are generally similar over different years of assessments (Fig. 54, Table 28).

Estimated numbers-at-age are presented in (Table 29) and estimated catch-at-age values are presented in (Table 30). Estimated summary biomass (age 3+), female spawning biomass, and age-1 recruitment are given in (Table 31).

To evaluate past management and assessment performance it can be useful to examine estimated fishing mortality relative to reference values. For EBS pollock, we computed the reference fishing mortality from Tier 1 (unadjusted) and recalculated the historical values for  $F_{MSY}$  (since selectivity has changed over time). Since 1977 the current estimates of fishing mortality suggest that during the early period, harvest rates were above  $F_{MSY}$  until about 1980. Since that time, the levels of fishing mortality have averaged about 35% of the  $F_{MSY}$  level (Fig. 55). Projections of spawning stock biomass given the 2021 estimate of fishing mortality rate given catches equal to the 2020 values shows a decline through 2021 and then an increase after; albeit with considerable uncertainty due to uncertainty in recruitment (Fig. 56).

### ***Recruitment***

Model estimates indicate that the 2008, 2012, and 2013 year classes are above average (Fig. 57). The stock-recruitment curve as fit within the integrated model shows a fair amount of variability both in the estimated recruitments and in the uncertainty of the curve (Fig. 58). Note that the 2015 and 2016 year classes (as age 1 recruits in 2016 and 2017) are excluded from the stock-recruitment curve estimation. Separate from fitting the stock- recruit relationship within the model, examining the estimated recruits-per-spawning biomass shows variability over time but seems to lack trend and also is consistent with the Ricker stock- recruit relationship used within the model (Fig. 59).

Environmental factors affecting recruitment are considered important and contribute to the variability. Previous studies linked strong Bering Sea pollock recruitment to years with warm sea temperatures and northward transport of pollock eggs and larvae (Wespestad et al. 2000; Mueter et al. 2006). As part of the Bering-Aleutian Salmon International Survey (BASIS) project research has also been directed toward the relative density and quality (in terms of condition for survival) of young-of-year pollock. For example, Moss et al. (2009) found age-0 pollock were very abundant and widely distributed to the north and east on the Bering Sea shelf during 2004 and 2005 (warm sea temperature; high water column stratification) indicating high northern transport of pollock eggs and larvae during those years. Mueter et al. (2011) found that warmer conditions tended to result in lower pollock recruitment in the EBS. This is consistent with the hypothesis that when sea temperatures on the eastern Bering Sea shelf are warm and the water column is highly stratified during summer, age-0 pollock appear to allocate more energy to growth than to lipid storage (presumably due to a higher metabolic rate), leading to low energy density prior to winter. This then may result in increased over-winter mortality (Swartzman et al. 2005, Winter et al. 2005). Ianelli et al. (2011) evaluated the consequences of current harvest policies in the face of warmer conditions with the link to potentially lower pollock recruitment and noted that the current management system is likely to face higher chances of ABCs below the historical average catches.

### ***Retrospective analysis***

Running the assessment model over a grid with progressively fewer years included (going back to 20 years, i.e., assuming the data extent ended in 2000) results in a fair amount of variability in both spawning biomass and recruitment (Fig. 60) Although the variability is high, the average bias appears to be low with Mohns  $\rho$  equal to 0.008 for the 10 year retrospective and 0.086 if extended back 20-years.

### **Harvest recommendations**

#### ***Status summary***

The estimate of  $B_{MSY}$  is 2,257 kt (with a CV of 24%) which is less than the projected 2021 spawning biomass of 2,600 kt; (Table 32). For 2020, the Tier 1 levels of yield are 2,307,000 t from a fishable biomass estimated at around 7,597 kt (Table 33; about 115% of the  $B_{MSY}$  level). A diagnostic (see section below on model details) on the impact of fishing shows that the 2020 spawning stock size is about 58% of the predicted value had no fishing occurred since 1978 (Table 32). This compares with the 48% of  $B_{100\%}$  (based on the SPR expansion using mean recruitment from 1978–2017) and 131% of  $B_{MSY}$  (based on the estimated stock-recruitment curve). The latter two values are based on expected recruitment from the mean value since 1978 or from the estimated stock recruitment relationship.

Relative to Tier 3 indicators, the model indicates that spawning biomass will be above  $B_{40\%}$  (2,600 kt) in 2021. The probability that the current stock size is below 20% of  $B_0$  (a level important for additional management measures related to Steller sea lion recovery) is <0.1% for 2021 and 2022.

#### ***Amendment 56 Reference Points***

Amendment 56 to the BSAI Groundfish Fishery Management Plan (FMP) defines overfishing level (OFL), the fishing mortality rate used to set OFL (FOFL), the maximum permissible ABC, and the fishing mortality rate used to set the maximum permissible ABC. The fishing mortality rate used to set ABC ( $F_{ABC}$ ) may be less than this maximum permissible level, but not greater. Estimates of reference points related to maximum sustainable yield (MSY) are currently available. However, their reliability is questionable. We therefore present both reference points for pollock in the BSAI to retain the option for classification in either Tier 1 or Tier 3 of Amendment 56. These Tiers require reference point estimates for biomass level determinations. Consistent with other groundfish stocks, the following values are based on recruitment estimates from post-1976 spawning events:

$B_{MSY}$	= 2,257 kt female spawning biomass
$B_0$	= 5,792 kt female spawning biomass
$B_{100\%}$	= 6,142 kt female spawning biomass
$B_{40\%}$	= 2,457 kt female spawning biomass
$B_{35\%}$	= 2,150 kt female spawning biomass

### ***Specification of OFL and Maximum Permissible ABC***

Assuming the stock-recruit relationship the 2021 spawning biomass is estimated to be 2,602,000 t (at the time of spawning, assuming the stock is fished at about recent catch levels). This is above the  $B_{MSY}$  value of 2,257,000 t. Under Amendment 56, this stock has qualified under Tier 1 and the harmonic mean value is considered a risk-averse policy since reliable estimates of  $F_{MSY}$  and its pdf are available (Thompson 1996). The exploitation- rate type value that corresponds to the  $F_{MSY}$  level was applied to the fishable biomass for computing ABC levels. For a future year, the fishable biomass is defined as the sum over ages of predicted begin-year numbers multiplied by age specific fishery selectivity (normalized to the value at age 6) and mean body mass. The uncertainty in the average weights-at-age projected for the fishery and “future selectivity” has been demonstrated to affect the buffer between ABC and OFL (computed as 1-ABC/OFL) for Tier 1 maximum permissible ABC (Ianelli et al. 2015). The uncertainty in future mean weights-at-age had a relatively large impact as did the selectivity estimation.

Since the 2021 female spawning biomass is estimated to be above the  $B_{MSY}$  level (2,257 kt) and the  $B_{40\%}$  value (2,457 kt) in 2021 and if the 2020 catch is as specified above, then the OFL and maximum permissible ABC values by the different Tiers would be:

Tier	Year	MaxABC	OFL
1a	2021	2,307,000	2,594,000
1a	2022	2,105,000	2,366,000
3a	2021	1,626,000	1,986,000
3a	2022	1,484,000	1,788,000

### ***Standard Harvest Scenarios and Projection Methodology***

A standard set of projections is required for each stock managed under Tiers 1, 2, or 3 of Amendment 56 to the FMP. This set of projections encompasses seven harvest scenarios designed to satisfy the requirements of Amendment 56, the National Environmental Policy Act, and the Magnuson-Stevens Fishery Conservation and Management Act (MSFCMA). While EBS pollock is generally considered to fall within Tier 1, the standard projection model requires knowledge of future uncertainty in  $F_{MSY}$ . Since this would require a number of additional assumptions that presume future knowledge about stock-recruit uncertainty, the projections in this subsection are based on Tier 3.

For each scenario, the projections begin with the vector of 2020 numbers at age estimated in the assessment. This vector is then projected forward to the beginning of 2021 using the schedules of natural mortality and selectivity described in the assessment and the best available estimate of total (year- end) catch assumed for 2020. In each subsequent year, the fishing mortality rate is prescribed on the basis of the spawning biomass in that year and the respective harvest scenario. Annual recruits are simulated from an inverse Gaussian distribution whose parameters consist of maximum likelihood estimates determined from the estimated age-1 recruits. Spawning biomass is computed in each year based on the time of peak spawning and the maturity and weight schedules described in the assessment. Total catch is assumed to equal the catch associated with the respective harvest scenario in all years. This projection scheme is run 1,000 times to obtain distributions of possible future stock sizes and catches under alternative fishing mortality rate scenarios.

Five of the seven standard scenarios will be used in an Environmental Assessment prepared in conjunction with the final SAFE. These five scenarios, which are designed to provide a range of

harvest alternatives that are likely to bracket the final TAC for 2021, are as follows (“ $\max F_{ABC}$ ” refers to the maximum permissible value of FABC under Amendment 56):

**Scenario 1:** In all future years,  $F$  is set equal to  $\max F_{ABC}$ . (Rationale: Historically, TAC has been constrained by ABC, so this scenario provides a likely upper limit on future TACs).

**Scenario 2:** In 2021 and 2022 the catch is set equal to 1.35 million t and in future years  $F$  is set equal to the Tier 3 estimate (Rationale: this has been about equal to the catch level in recent years).

**Scenario 3:** In all future years,  $F$  is set equal to the 2019 average  $F$ . (Rationale: For some stocks, TAC can be well below ABC, and recent average  $F$  may provide a better indicator of  $F_{TAC}$  than  $F_{ABC}$ .)

**Scenario 4:** Scenario 4: In all future years,  $F$  is set equal to  $F_{60\%}$ . (Rationale: This scenario provides a likely lower bound on  $F_{ABC}$  that still allows future harvest rates to be adjusted downward when stocks fall below reference levels.

**Scenario 5:** Scenario 5: In all future years,  $F$  is set equal to zero. (Rationale: In extreme cases, TAC may be set at a level close to zero.)

**Scenario 6:** In all future years,  $F$  is set equal to  $F_{OFL}$ . (Rationale: This scenario determines whether a stock is overfished. If the stock is expected to be 1) below its MSY level in 2020 or 2) below half of its MSY level in 2020 or below its MSY level in 2030 under this scenario, then the stock is overfished.)

**Scenario 7:** In 2021 and 2022,  $F$  is set equal to  $\max F_{ABC}$ , and in all subsequent years,  $F$  is set equal to  $F_{OFL}$ . (Rationale: This scenario determines whether a stock is approaching an overfished condition. If the stock is 1) below its MSY level in 2022 or 2) below 1/2 of its MSY level in 2022 and expected to be below its MSY level in 2032 under this scenario, then the stock is approaching an overfished condition).

The latter two scenarios are needed to satisfy the MSFCMA’s requirement to determine whether a stock is currently in an overfished condition or is approaching an overfished condition (for Tier 3 stocks, the MSY level is defined as  $B_{35\%}$ ).

### ***Projections and status determination***

For the purposes of these projections, we present results based on selecting the  $F_{40\%}$  harvest rate as the  $F_{ABC}$  value and use  $F_{35\%}$  as a proxy for  $F_{MSY}$ . Scenarios 1 through 7 were projected 14 years from 2020 (Tables 35 through 41 for Model 16.1 and for 16.2—the configuration that uses the NBS VAST data set). Under the catch set to Tier 3 ABC estimates, the expected spawning biomass will decline until 2020 and stabilize slightly above  $B_{40\%}$  (in expectation, Fig. 61).

Any stock that is below its minimum stock size threshold (MSST) is defined to be overfished. Any stock that is expected to fall below its MSST in the next two years is defined to be approaching an overfished condition. Harvest scenarios 6 and 7 are used in these determinations as follows:

Is the stock overfished? This depends on the stock’s estimated spawning biomass in 2020:

- If spawning biomass for 2020 is estimated to be below 1/2  $B_{35\%}$  the stock is below its MSST.

- If spawning biomass for 2020 is estimated to be above  $B_{35\%}$ , the stock is above its MSST.
- If spawning biomass for 2020 is estimated to be above  $1/2 B_{35\%}$  but below  $B_{35\%}$ , the stock's status relative to MSST is determined by referring to harvest scenario 6 ((Tables 38 through 41)). If the mean spawning biomass for 2030 is below  $B_{35\%}$ , the stock is below its MSST. Otherwise, the stock is above its MSST.

Is the stock approaching an overfished condition? This is determined by referring to harvest Scenario 7:

- If the mean spawning biomass for 2018 is below  $1/2 B_{35\%}$ , the stock is approaching an overfished condition.
- If the mean spawning biomass for 2018 is above  $B_{35\%}$ , the stock is not approaching an overfished condition.
- If the mean spawning biomass for 2022 is above  $1/2 B_{35\%}$  but below  $B_{35\%}$ , the determination depends on the mean spawning biomass for 2028. If the mean spawning biomass for 2032 is below  $B_{35\%}$ , the stock is approaching an overfished condition. Otherwise, the stock is not approaching an overfished condition.

For scenarios 6 and 7, we conclude that pollock is above MSST for the year 2020, and it is expected to be above the “overfished condition” based on Scenario 7 (the mean spawning biomass in 2020 is above the  $B_{35\%}$  estimate; (Table 41)). Based on this, the EBS pollock stock is being fished below the overfishing level and the stock size is estimated to be above, and stay above the overfished level.

To fulfill reporting requirements for the Species Information System, each model was used to reverse-engineer the fishing mortality rate corresponding to the specified OFL for the last complete year (2019). This reverse-engineered  $F_{OFL}$  values ( $REF_{OFL}$ ) is 0.508.

### ***ABC Recommendation***

ABC levels are affected by estimates of  $F_{MSY}$  which depends principally on the estimated stock-recruitment steepness parameter, demographic schedules such as selectivity-at-age, maturity, and growth. The current stock size (both spawning and fishable) is estimated to be at above-average levels and projections indicate declines. Updated data and analysis result in an estimate of 2020 spawning biomass (2,960 kt) which is about 131% of  $B_{MSY}$  (2,257 kt). This follows a period of increases from 2008–2017. The extent that the stock will decline further depends on recruitment, which given the available information, is uncertain. Given the same estimated aggregate fishing effort in 2020, the estimated stock trend is downwards except at low catch levels. Furthermore, the ability to catch roughly the same amount as in 2020 through to 2023 will require more effort (effectively) and will result in further declines in spawning biomass.

#### *Should the ABC be reduced below the maximum permissible ABC?*

The SSC in its September 2018 minutes recommended that assessment authors and Plan Teams use the risk matrix table below when determining whether to recommend an ABC lower than the maximum permissible.

Considerations				
	Assessment-related	Population dynamics	Environmental & ecosystem	Fishery performance
Level 1 Normal	Typical to moderately increased uncertainty & minor unresolved issues in assessment	Stock trends are typical for the stock; recent recruitment is within normal range.	No apparent environmental & ecosystem concerns	No apparent fishery/resource-use performance and/or behavior concerns
Level 2 Substantially increased concerns	Substantially increased assessment uncertainty unresolved issues.	Stock trends are unusual; abundance increasing or decreasing faster than has been seen recently, or recruitment pattern is atypical.	Some indicators showing an adverse signals but the pattern is inconsistent across all indicators.	Some indicators showing adverse signals but the pattern is inconsistent across all indicators.
Level 3 Major Concern	Major problems with the stock assessment, very poor fits to data, high level of uncertainty, strong retrospective bias.	Stock trends are highly unusual; very rapid changes in stock abundance, or highly atypical recruitment patterns.	Multiple indicators showing consistent adverse signals a) across the same trophic level, and/or b) up or down trophic levels (i.e., predators and prey of stock)	Multiple indicators showing consistent adverse signals a) across different sectors, and/or b) different gear types
Level 4 Extreme concern	Severe problems with the stock assessment, severe retrospective bias. Assessment considered unreliable.	Stock trends are unprecedented. More rapid changes in stock abundance than have ever been seen previously, or a very long stretch of poor recruitment compared to previous patterns.	Extreme anomalies in multiple ecosystem indicators that are highly likely to impact the stock. Potential for cascading effects on other ecosystem components	Extreme anomalies in multiple performance indicators that are highly likely to impact the stock.

The table is applied by evaluating the severity of four types of considerations that could be used to support a scientific recommendation to reduce the ABC from the maximum permissible. Examples of the types of concerns that might be relevant include the following (as identified by the work-group):

### 1. Assessment considerations

- *Data-inputs*: biased ages, skipped surveys, lack of fishery-independent trend data
- *Model fits*: poor fits to fits to fishery or survey data, inability to simultaneously fit multiple data inputs.
- *Model performance*: poor model convergence, multiple minima in the likelihood surface, parameters hitting bounds.
- *Estimation uncertainty*: poorly-estimated but influential year classes.
- Retrospective bias in biomass estimates.

### 2. Population dynamics considerations—decreasing biomass trend, poor recent recruitment, inability of the stock to rebuild, abrupt increase or decrease in stock abundance.

### 3. Environmental/ecosystem considerations—trends in environmental/ecosystem indicators, ecosystem model results, decreases in ecosystem productivity, decreases in prey abundance or availability, increases or increases in predator abundance or productivity.

4. Fisheries considerations—fishery CPUE is showing a contrasting pattern from the stock biomass trend, unusual spatial pattern of fishing, changes in the percent of TAC taken, changes in the duration of fishery openings.”

*Assessment considerations* The EBS pollock assessment model appears to track the stock from year based on retrospective analysis (the pattern lacks tendency to over or under estimate the stock trend. The model tracks the available data well including multiple abundance indices. Of minor concern (presently) is the fact that the model estimate of declining abundance is somewhat less than that suggested by the survey data. The data and model appear to be consistent without big surprises relative to the ability to fit the information and provide a trade-off between process and observation errors (which combined, provide relatively high estimates of uncertainty). The lack of two summer surveys in 2020 (and 3 updated biomass indices) might be a consideration. However, the addition of the USV data and general consistency from the spatial pattern of pollock abundance and what the fishery was catching seems consistent. **We therefore rated the assessment-related concern as level 1, normal.**

*Population dynamics considerations* The age structure of EBS pollock has exhibited some peculiarities over time. On the positive side, some strong year-classes appear to have increased in abundance based on the bottom-trawl survey data (e.g., the 1992, 2012 and 2013 year classes). Conversely, the period from 2000–2007 had relatively poor year-class strengths which resulted in declines in stock below  $B_{msy}$  and reduced TACs due to lower ABC values. There also are clear density-dependent effects on growth, in particular, the 2012 year class. The stock is estimated to be well above  $B_{msy}$  at present, but projections indicate a decline given recent catch levels and future trends will depend on pollock survival at egg, larval, and juvenile stages which may be compromised given the lack of a cold pool and a considerable redistribution into the northern part of the Bering Sea. Recruitment in the near term could be below average yet projections assume average recruitment (with uncertainty). Additional age-specific aspects of the spawning population indicates that the stock has recovered somewhat from a low diversity of ages (for both the population and the mean age of the spawning stock weighted by spawning output Fig. 62). **We therefore rated the population-dynamics concern as level 1, normal.**

*Environmental/Ecosystem considerations*<sup>7</sup> *Environmental processes* Following two years of physical oceanographic perturbations, the eastern Bering Sea experienced a return to near-normal climatic conditions in 2020. Residual warmth delayed sea ice formation until late 2019. Considerable cooling then allowed for rapid build-up of sea ice, even exceeding median ice extent in parts of February and March 2020. The 2019-2020 daily mean extent was within 1 SD of the long-term mean. However, ice thickness was low, and retreated quickly in spring. Summer bottom temperatures and spatial extent of the cold pool were average based on

the ROMS hindcast model and observations from the 2020 Dyson cruise. However, summer sea surface temperatures through August were above average in the southeastern and northern Bering Sea, similar to those observed in 2019. In fact, both the southeastern and northern Bering Sea are experiencing a persistent warm stanza, greater in both magnitude and duration than that of the early 2000s. The winters of 2017/2018 and 2018/2019 had strong south winds, which contributed to low sea ice extent in those years. These anomalous winds from the south are hypothesized to have bolstered productivity over the shelf, sustained metabolic demands, and subsidized overwinter survival of the 2018 year class of pollock. The most recent winter (2019/2020) had an average wind speed direction (north/south) near the long-term average. Similarly, based on the OSCURS model,

---

<sup>7</sup>Provided by: Elizabeth Siddon, NOAA/AFSC

the 2020 springtime drift pattern was mixed, with an early period of eastward drift followed by a period of westward drift that may have retained larvae over the middle shelf. These environmental indicators are presented in the new Physical Oceanography Summary section of the 2020 EBS Ecosystem Status Report (Siddon, 2020).

Age-0 fish experiencing warm temperatures during late summer followed by relatively cooler temperatures in spring of age-1 are thought to have below average survival (Yasumiishi, 2020). Based on this Temperature Change index, the 2016 and 2019 year classes are predicted to have below-average recruitment to age-4 in 2020 and 2023.

*Prey:* The spring bloom over the south inner and middle domains occurred about a week earlier than the long-term mean; in comparison, 2017 was among the earliest spring blooms while 2018 was among the latest (Nielsen et al., 2020). Chlorophyll concentrations in this region have been below the long-term mean since 2016. Depending on the spatial and temporal overlap of productivity, this can result in a match or mismatch with favorable feeding conditions for larval pollock. Small copepods form the prey base for larval to early juvenile pollock during spring. Late juvenile pollock feed on a variety of planktonic crustaceans, including calanoid copepods and euphausiids. Pollock diets become more piscivorous with age and cannibalism is commonly observed. No direct measurements of zooplankton community composition are available for 2020 due to survey cancellations. The abundance of large copepods during late-summer is correlated with recruitment to age-3 pollock; low abundance of large copepods during late-summer 2017 and 2018 indicate poor overwinter survival and recruitment to age-3 in 2020 and 2021 (Yasumiishi et al., 2020). In 2019, over the southern middle shelf, small copepods were abundant in spring while large copepod abundance was quite low in late-summer (Kimmel et al., 2020). This indicates good foraging conditions for larval and juvenile pollock early in the year, however, large, lipid-rich copepods may have again limited energy storage for age-0 pollock entering their first winter. Fish condition (as measured by weighted length-weight residuals [updated method]) patterns over the southeastern and northern shelves differed for juvenile (100-250 mm total length) and adult (>250 mm TL) pollock in 2019 (no 2020 survey data available) (Rohan and Laman, 2020). Within both regions, juvenile condition was at the long-term mean while adult condition was positive. This indicates juvenile fish may not be finding adequate prey resources, while adult fish are finding adequate prey (including cannibalism on juvenile pollock). Spatially, adult pollock showed negative residuals while juvenile pollock showed positive residuals over the inner shelf from 2015-2019 (warm years).

*Predators:* Pollock are cannibalistic and rates of cannibalism might be expected to increase as the biomass of older, larger fish increases. In 2019, over the southern shelf, biomass increased 75% indicating movement of adult fish over the southern shelf. In the northern Bering Sea, abundance increased, but biomass decreased, indicating successful recruitment over the northern shelf (L. Britt, pers comm). In 2020, with an average cold pool extent over the shelf, predation pressure from cannibalism may have been mitigated by this thermal barrier as adult pollock tend to avoid the cold bottom waters. Fur seal consumption of adult pollock generally increases in years when juvenile pollock are less abundant (Kuhn et al., 2019). However, no information on 2020 population trends for fur seals is available. Other potential predators of juvenile pollock include jellyfish and chum salmon; no direct measurements of predation pressure exist at this time.

*Competitors:* While historical recruitment trends between Pacific cod and pollock have mirrored each other, the timeseries appear to decouple between 2008 and 2009. This may indicate broad-scale transitions in the southeastern Bering Sea ecosystem (e.g., from pelagic- to benthic-dominated production). The mechanisms driving early life history survival versus recruitment success of Pacific cod and pollock may differ based on pelagic versus benthic habitat associations (e.g., prey

availability). The decoupling of abundance timeseries suggests a shift (or greater disparity) between drivers of survival in these two populations. The widespread die-off event of short-tailed shearwaters slowed in 2020 (Siddon, 2020). Shearwaters are planktivorous birds and feed on euphausiids in the Bering Sea in summer. The die-off event is thought to reflect poor foraging conditions for birds during summer 2018 as most sampled birds showed signs of emaciation; lower mortality in 2020 may reflects (i) better feeding conditions in 2019 or (ii) lower overall population levels for shearwaters.

### **Summary for Environmental/Ecosystem considerations**

- The eastern Bering Sea returned to near-normal climatic conditions in 2020;
- Sea ice extent exceeded the historical median in parts of February and March 2020;
- Ice thickness was low and retreated quickly in spring 2020;
- The spatial extent of the cold pool was average;
- The eastern Bering Sea is experiencing a persistent warm stanza, greater in both magnitude and duration than that of the early 2000s;
- The 2019 year class experienced unfavorable temperature conditions from age-0 to age-1 and is predicted to have below-average recruitment to age-4 in 2023.
- Winter 2019/2020 had an average wind speed direction (north/south) near the long-term average;
- The 2020 springtime drift pattern was mixed indicating larvae may have been retained over the southern middle shelf;
- The spring bloom over the southern shelf occurred about a week earlier than the long-term mean;
- Chlorophyll concentrations over the southern shelf have been below the long-term mean since 2016;
- Low abundance of large copepods during late-summer in 2017-2019 indicate poor overwinter survival and recruitment to age-3 in 2020-2022;
- Condition (weighted length-weight residuals) of juvenile pollock (100-250 mm TL) in 2019 was at the long-term mean indicating moderate foraging conditions;
- Condition of adult pollock (>250 mm TL) in 2019 was above-average indicating good foraging conditions (including cannibalism of juvenile pollock);
- Predation pressure from cannibalism may have been mitigated by the average spatial extent of the cold pool (i.e., thermal barrier);
- The decoupling of abundance timeseries for Pacific cod and pollock suggests a shift in drivers of survival in these two populations and may indicate broad-scale transitions in the ecosystem (e.g., from pelagic- to benthic-dominated production);
- The widespread die-off event of short-tailed shearwaters slowed in 2020 and may reflect better feeding conditions (i.e., euphausiids) over the shelf in 2019.

**We therefore rated the Ecosystem concern as Level 2, substantially increased concern.** Some indicators showing adverse signals relevant to the stock but the pattern was inconsistent across indicators.

*Fishery performance* As noted above, the 2020 B-season fishery was more dispersed and experienced relatively low catch rates compared to recent years. Also, an approach to computing fleet dispersion (the relative distance or spread of the fishery in space) was developed and indicated that while the A-season was intensely concentrated in 2019, in 2020 it was more dispersed and this metric also increased for the fleet during the B-season (Fig 9).

The pollock fishery faced a number of PSC issues with very high CPUE increases for sablefish and for herring (Fig 2). species. Chinook salmon encounters were relatively high again in 2020 as with 2019 and overall mortality slightly higher than last year. Sectors were operating under a higher annual threshold in 2020 as compared with 2019 due to the index of Chinook salmon abundance from three key western Alaska rivers remaining above the specified threshold (it was below the threshold for the 3-River Index in 2019 resulting in lowered PSC limits). Mortality has reduced slightly in A season compared to 2019 but moderately higher in B season. Encounter rates may have been higher in 2020 as a result of more salmon returning. The fleet was also balancing measures to avoid herring in the A season and increased sablefish incidental catch particularly in the B season. In 2020, the overall numbers of chum salmonPSC were slightly lower than recent years as the fleet continued to avoid chum salmon bycatch hot spots.

The fact that the pollock fleet experienced poor fishing conditions throughout most of the 2020 B-season, pollock being skinny given their length, and the catch comprised of fish unusually small, **We scored fishery performance a value of 2, substantially increased concerns.**

These results are summarized as:

Considerations			
Assessment-related	Population dynamics	Environmental or ecosystem	Fisheries
Level 1: No concern	Level 1: No concern	Level 2: Substantially increased concerns	Level 2: Substantially increased concerns

Having two out of four scores at level 2 suggests that setting an ABC below the maximum permissible may be warranted. The SSC recommended against using a table that showed example alternatives to select buffers based on that risk level. Thompson (unpublished Sept 2018 plan team document) tabulated the magnitude of buffers applied by the Plan Teams for the period 2003–2017, and found that the mode of the buffers recommended was 10–20%. Using this as a guideline, a buffer of 15% would give an ABC as  $0.85 \times ABC_{max} = 1,960 \text{ kt}$ ). In the past, the SSC has considered factors similar to those presented above and selected an ABC based on Tier 3 estimates. We recommend this added precaution again this year, (i.e.,  $ABC = 1,626 \text{ kt}$ ) which implies a buffer of 30%. The SSC requested “an explicit set of concerns that explain the ABC adjustment.” In response, we direct attention to the decision table 48) and the fact that the biological basis for the continued stock productivity has most to do with the OY constraint which has effectively maintained fishery production at around 1.3 million t since 1990. Demonstrations that would allow fishing to near  $F_{MSY}$  catch quantities would show that catch variability would be extremely high (and unrealistic give current capacity and OY limits for combined BSAI groundfish; Ianelli 2005). Furthermore, the frequency of being at much lower spawning stock sizes would be much higher, and would likely be riskier and fishing effort would need to be much higher. While the biological basis for ABC setting is founded in sound conservation of spawning biomass, the history of the current fishery productivity should inform desirable biomass. In only 5 of the 38 years since

1981 has the stock been below the  $B_{MSY}$  level (13% of the years). The mean spawning biomass over this period has averaged about 30% higher than the estimated  $B_{MSY}$ . In terms of an actual “management target”, Punt et al. (2013) developed some robust estimators for  $B_{MEY}$  (Maximum Economic Yield) noting that a typical target would be  $1.2 \times B_{MSY}$ . In this case that would make the female spawning biomass target at 2.708 million t. It therefore seems worth considering making an explicit harvest control rule that achieves the productivity and ecosystem stability given the catches and biomass estimates observed over the past 30 years.

Recognizing that the actual catch will be constrained by other factors (the 2 million t BSAI ground-fish catch limit and bycatch avoidance measures), applying the maximum permissible Tier 1a ABC seems clearly risky. Such high catches would result in unprecedented variability and removals from the stock (and require considerably more capacity and effort). Less variability in catch would also result in less spawning stock variability (and reduce risks to the fishery should another period of poor recruitments occur). To more fully evaluate these considerations performance indicators as modified from Ianelli et al. (2012) were developed to evaluate some near-term risks given alternative 2021 catch values. These indicators and rationale for including them are summarized in Table 47). Model 16.1 results for these indicators are provided in Table 48. Each column of this table uses a fixed 2021 catch and assumes the same effort for the four additional projection years (2022–2025). Given this specification , there is a low probability that any of the catches shown in the first row would exceed the  $F_{MSY}$  level. Also, in the near term it appears unlikely that the spawning stock will be below  $B_{MSY}$  (rows 3 and 4). Relative to the historical mean spawning biomass, by 2021 it is more likely than not that the spawning biomass will be lower than the historical mean (fifth row). The range of catches examined have relatively small or no impact on the age diversity indicators. However, for catch to equal the 2020 value, more fishing effort will likely be required and there is a good chance that the proportion of the stock less than age 6 will be greater than the historical average. In terms of catch advice, the results presented in the decision table indicates that catches above 1.0 million t will very likely result in 2022 spawning stock estimates being below the long term mean (but above  $B_{MSY}$ ).

Another approach/rationale would be to stabilize effort from the 2020 levels and recommend that 2021 fishing mortality is set equal to the 2020 estimate. This gives an ABC of 1,300,000 kt. The Plan Teams and SSC may wish to consider this as an added measure of precaution for ABC considerations.

## **Additional ecosystem considerations**

In general, a number of key issues for ecosystem conservation and management can be highlighted. These include:

- Preventing overfishing;
- Avoiding habitat degradation;
- Minimizing incidental bycatch;
- Monitoring bycatch and the level of discards; and
- Considering multi-species trophic interactions relative to harvest policies.

For the case of pollock in the Eastern Bering Sea, the NPFMC and NMFS continue to manage the fishery on the basis of these issues in addition to the single- species harvest approach (Hollowed et al. 2011). The prevention of overfishing is clearly set out as the main guideline for management. Habitat degradation has been minimized in the pollock fishery by converting the industry to pelagic-gear only. Bycatch in the pollock fleet is closely monitored by the NMFS observer program and managed on that basis. Discard rates of many species have been reduced in this fishery and efforts to minimize bycatch continue.

In comparisons of the Western Bering Sea (WBS) with the Eastern Bering Sea using mass-balance food-web models based on 1980–85 summer diet data, Aydin et al. (2002) found that the production in these two systems is quite different. On a per-unit-area measure, the western Bering Sea has higher productivity than the EBS. Also, the pathways of this productivity are different with much of the energy flowing through epifaunal species (e.g., sea urchins and brittlestars) in the WBS whereas for the EBS, crab and flatfish species play a similar role. In both regions, the keystone species in 1980–85 were pollock and Pacific cod. This study showed that the food web estimated for the EBS ecosystem appears to be relatively mature due to the large number of interconnections among species. In a more recent study based on 1990–93 diet data (see Appendix 1 of the Ecosystem Considerations chapter for methods), pollock remain in a central role in the ecosystem. The diet of pollock is similar between adults and juveniles with the exception that adults become more piscivorous (with consumption of pollock by adult pollock representing their third largest prey item).

Regarding specific small-scale ecosystems of the EBS, Ciannelli et al. (2004a, 2004b) presented an application of an ecosystem model scaled to data available around the Pribilof Islands region. They applied bioenergetics and foraging theory to characterize the spatial extent of this ecosystem. They compared energy balance, from a food web model relevant to the foraging range of northern fur seals and found that a range of 100 nautical mile radius encloses the area of highest energy balance representing about 50% of the observed foraging range for lactating fur seals. This has led to a hypothesis that fur seals depend on areas outside the energetic balance region. This study develops a method for evaluating the shape and extent of a key ecosystem in the EBS (i.e., the Pribilof Islands). Furthermore, the overlap of the pollock fishery and northern fur seal foraging habitat (see Sterling and Ream 2004, Zeppelin and Ream 2006).

A brief summary of these two perspectives (ecosystem effects on pollock stock and pollock fishery effects on ecosystem) is given in (Table 45). Unlike the food-web models discussed above, examining predators and prey in isolation may overly simplify relationships. This table serves to highlight the main connections and the status of our understanding or lack thereof.

### ***Ecosystem effects on the EBS pollock stock***

The pollock stock condition appears to have benefited substantially from the recent conditions in the EBS. The conditions on the shelf during 2008 apparently affected age-0 northern rock sole due to cold conditions and apparently unfavorable currents that retain them into the over- summer nursery areas (Cooper et al. 2014). It may be that such conditions favor pollock recruitment. Hollowed et al. (2012) provided an extensive review of habitat and density for age-0 and age-1 pollock based on survey data. They noted that during cold years, age-0 pollock were distributed primarily in the outer domain in waters greater than 1°C and during warm years, age-0 pollock were distributed mostly in the middle domain. This temperature relationship, along with interactions with available food in early-life stages, appears to have important implications for pollock recruitment success

(Coyle et al. 2011).

A separate section presented again this year updates a multispecies model with more recent data and is presented as a supplement to the BSAI SAFE report. In this approach, a number of simplifications for the individual species data and fisheries processes (e.g., constant fishery selectivity and the use of design-based survey indices for biomass). However, that model mimics the biomass levels and trends with the single species reasonably well. It also allows specific questions to be addressed regarding pollock TACs. For example, since predation (and cannibalism) is explicitly modeled, the impact of relative stock sizes on subsequent recruitment to the fishery can be now be directly estimated and evaluated (in the model presented here, cannibalism is explicitly accounted for in the assumed Ricker stock-recruit relationship).

### ***EBS pollock fishery effects on the ecosystem.***

Since the pollock fishery is primarily pelagic in nature, the bycatch of non-target species is small relative to the magnitude of the fishery (Table 44). Jellyfish represent the largest component of the bycatch of non-target species and had averaged around 5–6 kt per year but more than doubled in 2014 but has dropped in 2015. The 2018 value was relatively high again. The data on non-target species shows a high degree of inter-annual variability, which reflects the spatial variability of the fishery and high observation error. This variability may reduce the ability to detect significant trends for bycatch species.

The catch of other target species in the pollock fishery (defined as any trawl set where the catch represents more than 80% of the catch) represents less than 1% of the total pollock catch. Incidental catch of Pacific cod has varied but in the past three years it is about half of the 2011 and 2012 levels (Table 42). There has been a marked increase in the incidental catch of Pacific ocean perch, sablefish, and Atka mackerel and a decrease in flatfish species. Proportionately, the incidental catch decreased since the overall levels of pollock catch have increased since 2008. In fact, the bycatch of pollock in other target fisheries is more than double the bycatch of target species in the pollock fishery (Table 43).

The number of non-Chinook salmon (nearly all made up of chum salmon) taken incidentally has steadily increased since 2014 with 2017 number in excess of 465 thousand fish but the 2018 level was slightly more than the 2003–2017 average of 227 thousand fish; Table 45). Chinook salmon bycatch has also increased steadily since 2012 with the 2017 counts at just below 30,000 (which was 18% below the 2003–2017 mean value). In 2018–2020 the bycatch dropped back down to 13.5 thousand fish (Table 45). Ianelli and Stram (2014) provided estimates of the bycatch impact on Chinook salmon runs to the coastal west Alaska region and found that the peak bycatch levels exceeded 7% of the total run return. Since 2011, the impact has been estimated to be below 2%. Updated estimates given new genetic information and these levels of PSC as provided to the Council continues to suggest that the impact is low.

### **Data gaps and research priorities**

The available data for EBS pollock are extensive yet many processes behind the observed patterns continue to be poorly understood.

The recent patterns of abundance observed in the northern Bering Sea provide an example. As such, we recommend the following research priorities:

- Continue to investigate using spatial processes for estimation purposes (e.g., combining acoustic and bottom trawl survey data). The application of the geostatistical methods (presented for comparative purposes in this assessment) seems like a reasonable approach to statistically model disparate data sources for generating better abundance indices. Also, examine the potential to use pelagic samples from the BASIS survey to inform recruitment and subsequent spatial patterns.
- Develop methods to use spatio-temporal models to estimate composition information (i.e., length and age).
- Study the relationship between climate and recruitment and trophic interactions of pollock within the ecosystem. This would be useful for improving ways to evaluate the current and alternative fishery management system. In particular, studies investigating the processes affecting recruitment of pollock in the different regions of the EBS (including potential for influx from the GOA) should be pursued.
- Apply new technologies (e.g., bottom-moored echosounders) to evaluate pollock movement between regions and supplement this work with analytical approaches.
- Expand genetic sample collections for pollock (and process available samples) and apply high resolution genetic tools for stock structure analyses.

## Acknowledgments

We thank the survey staff who always collect samples diligently, especially this year when extra effort was required to process data due to unforeseen problems with survey cancellations. The AFSC age-and-growth department is thanked for their continued excellence in promptly processing the samples used in this assessment. Finally, thanks to the many colleagues who provided edits and suggestions to improve this document.

## References

- Alaska Fisheries Science Center (AFSC). 2016. Wholesale market profiles for Alaska groundfish and crab fisheries. 134 p. Alaska Fish. Sci. Cent., NOAA, Natl. Mar. Fish. Serv., 7600 San Point Way NE, Seattle WA 98115.
- Aydin, K. Y., et al. 2002. A comparison of the Eastern Bering and western Bering Sea shelf and slope ecosystems through the use of mass-balance food web models. U.S. Department of Commerce, Seattle, WA. (NOAA Technical Memorandum NMFS-AFSC-130) 78p.
- Bacheler, N.M., L. Ciannelli, K.M. Bailey, and J.T. Duffy-Anderson. 2010. Spatial and temporal patterns of walleye pollock (*Theragra chalcogramma*) spawning in the eastern Bering Sea inferred from egg and larval distributions. *Fish. Oceanogr.* 19:2. 107-120.
- Bailey, K.M., T.J. Quinn, P. Bentzen, and W.S. Grant. 1999. Population structure and dynamics of walleye pollock, *Theragra chalcogramma*. *Advances in Mar. Biol.* 37:179-255.
- Bailey, K. M. 2000. Shifting control of recruitment of walleye pollock *Theragra chalcogramma* after a major climatic and ecosystem change. *Mar. Ecol. Prog. Ser.*, 198, 215–224. [link](#)
- Barbeaux, S. J., S. Gaichas, J. N. Ianelli, and M. W. Dorn. 2005. Evaluation of biological sampling protocols for at-sea groundfish observers in Alaska. *Alaska Fisheries Research Bulletin* 11(2):82-101.
- Barbeaux, S.J., Horne, J., Ianelli, J. 2014. A novel approach for estimating location and scale specific fishing exploitation rate of eastern Bering Sea walleye pollock (*Theragra chalcogramma*). *Fish. Res.* 153 p. 69 – 82.
- Brodeur, R.D.; Wilson, M.T.; Ciannelli, L.; Doyle, M. and Napp, J.M. (2002). Interannual and regional variability in distribution and ecology of juvenile pollock and their prey in frontal structures of the Bering Sea. *Deep-Sea Research II*. 49: 6051-6067.
- Butterworth, D.S., J.N. Ianelli, and R. Hilborn. 2003. A statistical model for stock assessment of southern bluefin tuna with temporal changes in selectivity. *Afr. J. mar. Sci.* 25: 331-361.
- Buckley, T.W., Greig, A., Boldt, J.L., 2009. Describing summer pelagic habitat over the continental shelf in the eastern Bering Sea, 1982–2006. United States Department of Commerce, NOAA Technical Memorandum. NMFS-AFSC-196. pp. 49.
- Buckley, T. W., Ortiz, I., Kotwicki, S., & Aydin, K. (2015). Summer diet composition of walleye pollock and predator-prey relationships with copepods and euphausiids in the eastern Bering Sea, 1987-2011. *Deep-Sea Research Part II: Topical Studies in Oceanography*, 134, 302–311. [link](#).
- Canino, M.F., P.T. O'Reilly, L. Hauser, and P. Bentzen. 2005. Genetic differentiation in walleye pollock (*Theragra chalcogramma*) in response to selection at the pantophysin (Pan I) locus. *Can. J. Fish. Aquat. Sci.* 62:2519-2529.
- Ciannelli, L., B.W. Robson, R.C. Francis, K. Aydin, and R.D. Brodeur 2004a. Boundaries of open marine ecosystems: an application to the Pribilof Archipelago, southeast Bering Sea. *Ecological Applications*, Volume 14, No. 3. pp. 942-953.
- Ciannelli, L.; Brodeur, R.D., and Napp, J.M. 2004b. Foraging impact on zooplankton by age-0 walleye pollock (*Theragra chalcogramma*) around a front in the southeast Bering Sea. *Marine Biology*. 144: 515-525.
- Clark, W.G. 1999. Effects of an erroneous natural mortality rate on a simple age-structured model. *Can. J. Fish. Aquat. Sci.* 56:1721-1731.

- Cooper, D. W., Duffy-Anderson, J. T., Norcross, B. L., Holladay, B. A., & Stabeno, P. J. (2014). Nursery areas of juvenile northern rock sole (*Lepidopsetta polyxystra*) in the eastern Bering Sea in relation to hydrography and thermal regimes. *ICES Journal of Marine Science*, 71(7), 1683–1695. doi:10.1093/icesjms/fst210
- Cotter, A.J.R., L. Burt, C.G.M Paxton, C. Fernandez, S.T. Buckland, and J.X Pan. 2004. Are stock assessment methods too complicated? *Fish and Fisheries*, 5:235-254.
- Cotter, A. J. R., Mesnil, B., and Piet, G. J. 2007. Estimating stock parameters from trawl cpue-at-age series using year-class curves. – *ICES Journal of Marine Science*, 64: 234–247.
- Coyle, K. O., Eisner, L. B., Mueter, F. J., Pinchuk, A. I., Janout, M. A., Cieciel, K. D., ... Andrews, A. G. (2011). Climate change in the southeastern Bering Sea: impacts on pollock stocks and implications for the oscillating control hypothesis. *Fisheries Oceanography*, 20(2), 139–156. doi:10.1111/j.1365-2419.2011.00574.x
- De Robertis, A., and K. Williams. 2008. Weight-length relationships in fisheries studies: the standard allometric model should be applied with caution. *Trans. Am. Fish. Soc.* 137:707-719.
- De Robertis, A., McKelvey, D. R., and Ressler, P. H. 2010. Development and application of an empirical multifrequency method for backscatter classification. *Canadian Journal of Fisheries and Aquatic Sciences*, 67: 1459-1474.
- De Robertis, A., Taylor, K., Wilson, C., and Farley, E. 2017. Abundance and Distribution of Arctic cod (*Boreogadus saida*) and other Pelagic Fishes over the U.S. Continental Shelf of the Northern Bering and Chukchi Seas Deep-Sea Research II, 135: 51-65.
- De Robertis, A., N. Lawrence-Slavas, R. Jenkins, I. Wangen, C.W. Mordy, C. Meinig, M. Levine, D. Peacock, H. Tabisola, and O. Rune Godø. 2019. “Long-Term Measurements of Fish Backscatter from Saildrone Unmanned Surface Vehicles and Comparison with Observations from a Noise-Reduced Research Vessel.” *ICES Journal of Marine Science* 76 (7): 2459–70. https://doi.org/10.1093/icesjms/fsz030
- Dorn, M.W. 1992. Detecting environmental covariates of Pacific whiting *Merluccius productus* growth using a growth-increment regression model. *Fish. Bull.* 90:260-275.
- Duffy-Anderson, J. T., Barbeaux, S. J., Farley, E., Heintz, R., Horne, J. K., Parker-Stetter, S. L., ... Smart, T. I. (2016). The critical first year of life of walleye pollock (*Gadus chalcogrammus*) in the eastern Bering Sea: Implications for recruitment and future research. *Deep-Sea Research Part II: Topical Studies in Oceanography*, 134, 283–301. [link](#).
- Eisner, L., J. Gann, K. Cieciel. 2019. “Variations in Temperature and Salinity During Late Summer/ Early Fall 2002-2018 in the Eastern Bering Sea - BASIS.” In Siddon, E., and Zador, S., 2019. *Ecosystem Status Report 2019: Eastern Bering Sea, Stock Assessment and Fishery Evaluation Report*, North Pacific Fishery Management Council, 605 W 4th Ave, Suite 306, Anchorage, AK 99501.
- Fissel, B., M. Dalton, R. Felthoven, B. Garber-Yonts, A. Haynie, A. Himes-Cornell, S. Kasperski, J. Lee, D. Lew, and C. Seung. 2014. Stock assessment and fishery evaluation report for the Groundfish fisheries of the Gulf of Alaska and Bering Sea/Aleutian Islands area: Economic status of the groundfish fisheries off Alaska, 2013.
- Fournier, D.A. and C.P. Archibald. 1982. A general theory for analyzing catch-at-age data. *Can. J. Fish. Aquat. Sci.* 39:1195-1207.
- Fournier, D.A., J.R. Sibert, J. Majkowski, and J. Hampton. 1990. MULTIFAN a likelihood-based method for estimating growth parameters and age composition from multiple length frequency samples with an application to southern bluefin tuna (*Thunnus maccoyii*). *Can. J. Fish. Aquat. Sci.* 47:301-317.

- Francis, R.I.C.C., and Shotton, R. 1997. Risk in fisheries management: a review. *Can. J. Fish. Aquat. Sci.* 54: 1699–1715.
- Francis, R.I.C.C. 1992. Use of risk analysis to assess fishery management strategies: a case study using orange roughy (*Hoplostethus atlanticus*) on the Chatham Rise, New Zealand. *Can. J. Fish. Aquat. Sci.* 49: 922-930.
- Francis, R I C C 2011. Data weighting in statistical fisheries stock assessment models. *Can. Journ. Fish. Aquat. Sci.* 1138: 1124-1138.
- Gann, J. C., Eisner, L. B., Porter, S., Watson, J. T., Cieciel, K. D., Mordy, C. W., Farley, E. V. (2015). Possible mechanism linking ocean conditions to low body weight and poor recruitment of age-0 walleye pollock (*Gadus chalcogrammus*) in the southeast Bering Sea during 2007. *Deep Sea Research Part II: Topical Studies in Oceanography*, 134, 1–13. [link](#).
- Gislason, H., Daan, N., Rice, J. C., & Pope, J. G. (2010). Size, growth, temperature and the natural mortality of marine fish. *Fish and Fisheries*, 11(2), 149–158. doi:10.1111/j.1467-2979.2009.00350.
- Grant, W. S., Spies, I., and Canino, M. F. 2010. Shifting-balance stock structure in North Pacific walleye pollock (*Gadus chalcogrammus*). – *ICES Journal of Marine Science*, 67:1686-1696.
- Griewank, A., and G.F. Corliss (eds.) 1991. Automatic differentiation of algorithms: theory, implementation and application. Proceedings of the SIAM Workshop on the Automatic Differentiation of Algorithms, held Jan. 6-8, Breckenridge, CO. Soc. Indust. And Applied Mathematics, Philadelphia.
- Guenneugues, P., & Ianelli, J. (2013). Surimi Resources and Market. In Surimi and Surimi Seafood, Third Edition (pp. 25–54). CRC Press. [link](#).
- Haynie, A. C. (2014). Changing usage and value in the Western Alaska Community Development Quota (CDQ) program. *Fisheries Science*, 80(2), 181–191. [link](#).
- Heintz, R. a., Siddon, E. C., Farley, E. V., & Napp, J. M. (2013). Correlation between recruitment and fall condition of age-0 pollock (*Theragra chalcogramma*) from the eastern Bering Sea under varying climate conditions. *Deep Sea Research Part II: Topical Studies in Oceanography*, 94, 150–156. [link](#).
- Hinckley, S. 1987. The reproductive biology of walleye pollock, *Theragra chalcogramma*, in the Bering Sea, with reference to spawning stock structure. *Fish. Bull.* 85:481-498.
- Hollowed, A. B., J. N. Ianelli, and P. A. Livingston. 2000. Including predation mortality in stock assessments: A case study involving Gulf of Alaska walleye pollock. *ICES Journal of Marine Science*, 57, pp. 279-293.
- Hollowed, A. B., Aydin, K. Y., Essington, T. E., Ianelli, J. N., Megrey, B. a, Punt, A. E., & Smith, A. D. M. (2011). Experience with quantitative ecosystem assessment tools in the northeast Pacific. *Fish and Fisheries*, 12(2), 189–208. doi:10.1111/j.1467-2979.2011.00413.
- Hollowed, A. B., Barbeaux, S. J., Cokelet, E. D., Farley, E., Kotwicki, S., Ressler, P. H., ... Wilson, C. D. 2012. Effects of climate variations on pelagic ocean habitats and their role in structuring forage fish distributions in the Bering Sea. *Deep Sea Research Part II: Topical Studies in Oceanography*, 65-70, 230–250. doi:10.1016/j.dsr2.2012.02.008
- Honkalehto, T., Ressler, P. H., Towler, R., and Wilson, C. D. 2011. Using acoustic data from fishing vessels to estimate walleye pollock abundance in the eastern Bering Sea. *Can J. Fish. Aquat. Sci.*, 68: 1231-1242.
- Honkalehto, T., D. McKelvey, and N. Williamson. 2005. Results of the echo integration-trawl

- survey of walleye pollock (*Theragra chalcogramma*) on the U.S. and Russian Bering Sea shelf in June and July 2004. AFSC Processed Rep. 2005-02, 43 p.
- Honkalehto, T., A. McCarthy, P. Ressler, K. Williams, and D. Jones. 2012. Results of the Acoustic-Trawl Survey of Walleye Pollock (*Theragra chalcogramma*) on the U.S. and Russian Bering Sea Shelf in June - August 2010. AFSC Processed Rep. 2012-01, 57 p. Alaska Fish. Sci. Cent., NOAA, Natl. Mar. Fish. Serv., 7600 Sand Point Way NE, Seattle WA 98115.
- Honkalehto, T., A. McCarthy, P. Ressler, and D. Jones, 2013. Results of the acoustic-trawl survey of walleye pollock (*Theragra chalcogramma*) on the U.S., and Russian Bering Sea shelf in June–August 2012 (DY1207). AFSC Processed Rep. 2013-02, 60 p. Alaska Fish. Sci. Cent. NOAA, Natl. Mar. Fish. Serv., 7600 Sand Point Way NE, Seattle WA 98115. [Available](#)
- Honkalehto, T, P. H. Ressler, S. C. Stienessen, Z. Berkowitz, R. H. Towler, a. L. McCarthy, and R. R. Lauth. 2014. Acoustic Vessel-of-Opportunity (AVO) index for midwater Bering Sea walleye pollock, 2012-2013. AFSC Processed Rep. 2014-04, 19 p. Alaska Fish. Sci. Cent., NOAA, Natl. Mar. Fish. Serv., 7600 Sand Point Way NE, Seattle WA 98115. [Available](#)
- Honkalehto, T, and A. McCarthy. 2015. Results of the Acoustic-Trawl Survey of Walleye Pollock (*Gaddus chalcogrammus*) on the U.S. and Russian Bering Sea Shelf in June - August 2014. AFSC Processed Rep. 2015-07, 62 p. Alaska Fish. Sci. Cent., NOAA, Natl. Mar. Fish. Serv., 7600 Sand Point Way NE, Seattle WA 98115. [Available](#)
- Hulson, P.-J.F., Miller, S.E., Ianelli, J.N., and Quinn, T.J., II. 2011. Including mark-recapture data into a spatial age-structured model: walleye pollock (*Theragra chalcogramma*) in the eastern Bering Sea. Can. J. Fish. Aquat. Sci. 68(9): 1625–1634. doi:10.1139/f2011-060.
- Hulson, P. F., Quinn, T. J., Hanselman, D. H., Ianelli, J. N. (2013). Spatial modeling of Bering Sea walleye pollock with integrated age-structured assessment models in a changing environment. Canadian Journal of Fisheries & Aquatic Sciences, 70(9), 1402-1416. doi:10.1139/cjfas-2013-0020.
- Hunt Jr., G.L., Coyle, K.O., Eisner, L.B., Farley, E.V., Heintz, R.A., Mueter, F., Napp, J.M., Overland, J.E., Ressler, P.H., Salo, S., Stabeno, P.J., 2011. Climate impacts on eastern Bering Sea foodwebs: a synthesis of new data and an assessment of the Oscillating Control Hypothesis. ICES J. Mar. Sci. 68 (6), 1230–1243. [link](#).
- Ianelli, J.N. 2005. Assessment and Fisheries Management of Eastern Bering Sea Walleye Pollock: is Sustainability Luck Bulletin of Marine Science, Volume 76, Number 2, April 2005 , pp. 321-336(16)
- Ianelli, J.N. and D.A. Fournier. 1998. Alternative age-structured analyses of the NRC simulated stock assessment data. In Restrepo, V.R. [ed.]. Analyses of simulated data sets in support of the NRC study on stock assessment methods. NOAA Tech. Memo. NMFS-F/SPO-30. 96 p.
- Ianelli, J.N., L. Fritz, T. Honkalehto, N. Williamson and G. Walters 1998. Bering Sea-Aleutian Islands Walleye Pollock Assessment for 1999. In: Stock assessment and fishery evaluation report for the groundfish resources of the Bering Sea/Aleutian Islands regions. North Pac. Fish. Mgmt. Council, Anchorage, AK, section 1:1-79.
- Ianelli, J.N., S. Barbeaux, T. Honkalehto, N. Williamson and G. Walters. 2003. Bering Sea-Aleutian Islands Walleye Pollock Assessment for 2003. In: Stock assessment and fishery evaluation report for the groundfish resources of the Bering Sea/Aleutian Islands regions. North Pac. Fish. Mgmt. Council, Anchorage, AK, section 1:1-101.
- Ianelli, J.N., S. Barbeaux, T. Honkalehto, S. Kotwicki, K. Aydin and N. Williamson. 2011. Assessment of the walleye pollock stock in the Eastern Bering Sea. In Stock assessment and fishery

- evaluation report for the groundfish resources of the Bering Sea/Aleutian Islands regions. North Pac. Fish. Mgmt. Council, Anchorage, AK, section 1:58-157.
- Ianelli, J.N., T. Honkalehto, S. Barbeaux, S. Kotwicki, K. Aydin, and N. Williamson, 2013. Assessment of the walleye pollock stock in the Eastern Bering Sea, pp. 51-156. In Stock assessment and fishery evaluation report for the groundfish resources of the Bering Sea/Aleutian Islands regions for 2014. North Pacific Fishery Management Council, Anchorage, AK. [Available](#)
- Ianelli, J.N., T. Honkalehto, S. Barbeaux, S. Kotwicki, B. Fissel, and K. Holsman, 2016. Assessment of the walleye pollock stock in the Eastern Bering Sea, pp. 51-156. In Stock assessment and fishery evaluation report for the groundfish resources of the Bering Sea/Aleutian Islands regions for 2017. North Pacific Fishery Management Council, Anchorage, AK. [Available](#)
- Ianelli, J.N., A.B. Hollowed, A.C. Haynie, F.J. Mueter, and N.A. Bond. 2011. Evaluating management strategies for eastern Bering Sea walleye pollock (*Theragra chalcogramma*) in a changing environment. ICES Journal of Marine Science, doi:10.1093/icesjms/fsr010.
- Ianelli, J.N. and D.L. Stram. 2014. Estimating impacts of the pollock fishery bycatch on western Alaska Chinook salmon. ICES Journal of Marine Science. doi:10.1093/icesjms/fsu173
- Jensen, A. 1996. Beverton and Holt life history invariants result from optimal trade-off of reproduction and survival. Canadian Journal of Fisheries and Aquatic Sciences 53, 820–822.
- Johnson, K. F., Monnahan, C. C., McGilliard, C. R., Vert-pre, K. A., Anderson, S. C., Cunningham, C. J., ... Punt, A. E. (2015). Time-varying natural mortality in fisheries stock assessment models: identifying a default approach. ICES Journal of Marine Science, 72(1), 137–150. [link](#).
- Jurado-Molina J., P. A. Livingston and J. N. Ianelli. 2005. Incorporating predation interactions to a statistical catch-at-age model for a predator-prey system in the eastern Bering Sea. Canadian Journal of Fisheries and Aquatic Sciences. 62(8): 1865-1873.
- Kastelle, C. R., and Kimura, D. K. 2006. Age validation of walleye pollock (*Theragra chalcogramma*) from the Gulf of Alaska using the disequilibrium of Pb-210 and Ra-226. e ICES Journal of Marine Science, 63: 1520e1529.
- Kimmel, D., Eisner, L., Harpold, C., and Crouser, D. 2020. Current and Historical Trends for Zooplankton in the Bering Sea. In: E.C. Siddon, 2020. Ecosystem Status Report 2020: Eastern Bering Sea, Stock Assessment and Fishery Evaluation Report, North Pacific Fishery Management Council, 1007 West Third, Suite 400, Anchorage, Alaska 99501.
- Kimura, D.K. 1989. Variability in estimating catch-in-numbers-at-age and its impact on cohort analysis. In R.J. Beamish and G.A. McFarlane (eds.), Effects on ocean variability on recruitment and an evaluation of parameters used in stock assessment models. Can. Spec. Publ. Fish. Aq. Sci. 108:57-66.
- Kimura, D.K., J.J. Lyons, S.E. MacLellan, and B.J. Goetz. 1992. Effects of year-class strength on age determination. Aust. J. Mar. Freshwater Res. 43:1221-8.
- Kimura, D.K., C.R. Kastelle , B.J. Goetz, C.M. Gburski, and A.V. Buslov. 2006. Corroborating ages of walleye pollock (*Theragra chalcogramma*), Australian J. of Marine and Freshwater Research 57:323-332.
- Kotenev, B.N. and A.I. Glubokov. 2007. Walleye pollock *Theragra chalcogramma* from the Navarin Region and adjacent waters of the Bering Sea: ecology, biology, and stock structure. Moscow VNIRO publishing. 180p.
- Kotwicki, S., T.W. Buckley, T. Honkalehto, and G. Walters. 2004. Comparison of walleye pollock data collected on the Eastern Bering Sea shelf by bottom trawl and echo integration trawl

- surveys. (poster presentation available at: <ftp://ftp.afsc.noaa.gov/posters/pKotwicki01 pollock.pdf>).
- Kotwicki, S., T.W. Buckley, T. Honkalehto, and G. Walters. 2005. Variation in the distribution of walleye pollock (*Theragra chalcogramma*) with temperature and implications for seasonal migration. Fish. Bull. 103:574–587.
- Kotwicki, S., A. DeRobertis, P. vonSzalay, and R. Towler. 2009. The effect of light intensity on the availability of walleye pollock (*Theragra chalcogramma*) to bottom trawl and acoustic surveys. Can. J. Fisheries and Aquatic Science. 66(6): 983–994.
- Kotwicki, S. and Lauth R.R. 2013. Detecting temporal trends and environmentally-driven changes in the spatial distribution of groundfishes and crabs on the eastern Bering Sea shelf. Deep-Sea Research Part II: Topical Studies in Oceanography. 94:231-243.
- Kotwicki, S., Ianelli, J. N., & Punt, A. E. 2014. Correcting density-dependent effects in abundance estimates from bottom-trawl surveys. ICES Journal of Marine Science, 71(5), 1107–1116.
- Kuhn, C., Sterling, J., and McHuron, E. 2019. Contrasting Trends in Northern Fur Seal Foraging Effort Between St. Paul and Bogoslof Islands: 2019 Preliminary Results. In: Siddon, E., and Zador, S., 2019. Ecosystem Status Report 2019: Eastern Bering Sea, Stock Assessment and Fishery Evaluation Report, North Pacific Fishery Management Council, 605 W 4th Ave, Suite 306, Anchorage, AK 99501.
- Laman, N. 2019. “Eastern and Northern Bering Sea Ground  
sh Condition.” In Siddon, E., and Zador, S., 2019. Ecosystem Status Report 2019: Eastern Bering Sea, Stock Assessment and Fishery Evaluation Report, North Pacific Fishery Management Council, 605 W 4th Ave, Suite 306, Anchorage, AK 99501.
- Lang, G.M., Livingston, P.A., Dodd, K.A., 2005. Groundfish food habits and predation on commercially important prey species in the eastern Bering Sea from 1997 through 2001. U.S. Dep. Commer., NOAA Tech. Memo. NMFS-AFSC-158, 230p. [URL](#)
- Lang, G.M., R.D. Brodeur, J.M. Napp, and R. Schabetsberger. (2000). Variation in groundfish predation on juvenile walleye pollock relative to hydrographic structure near the Pribilof Islands, Alaska. ICES Journal of Marine Science. 57:265-271.
- Lauffenberger, N., De Robertis, A., and Kotwicki, S. 2017. Combining bottom trawls and acoustics in a diverse semipelagic environment: What is the contribution of walleye pollock (*Gadus chalcogrammus*) to near-bottom acoustic backscatter? Can J. Fish. Aquat. Sci., 74: 256-264.
- Lauth, R.R., J.N. Ianelli, and W.W. Wakefield. 2004. Estimating the size selectivity and catching efficiency of a survey bottom trawl for thornyheads, *Sebastolobus* spp. using a towed video camera sled. Fisheries Research. 70:39-48.
- Lehodey, P., I. Senina, and R. Murtugudde. 2008. A spatial ecosystem and populations dynamics model (SEAPODYM) – Modeling of tuna and tuna-like populations. Progress in Oceanography 78: 304–318.
- Livingston, P. A., and Methot, R. D. (1998). Incorporation of predation into a population assessment model of Eastern Bering Sea walleye pollock. In Fishery Stock Assessment Models. NOAA Technical Report 126, NMFS F/NWC-54, Alaska Sea Grant Program, 304 Eielson Building, University of Alaska Fairbanks, Fairbanks, AK 99775. pp. 663-678.
- Livingston, P.A. (1991). Walleye pollock. Pages 9-30 in: P.A. Livingston (ed.). Groundfish food habits and predation on commercially important prey species in the eastern Bering Sea, 1984-1986. U.S. Dep. Commer., NOAA Tech. Memo. NMFS-F/NWC-207, 240 p.

- Lorenzen, K. 1996. The relationship between body weight and natural mortality in juvenile and adult fish: a comparison of natural ecosystems and aquaculture. *J. Fish. Biol.* 49:627-647.
- Lorenzen, K. 2000. Allometry of natural mortality as a basis for assessing optimal release size in fish-stocking programmes. *Canadian Journal of Fisheries and Aquatic Sciences* 57, 2374-2381.
- Low, L.L., and Ikeda. 1980. Average density index of walleye pollock in the Bering Sea. NOAA Tech. Memo. SFRF743.
- Mace, P., L. Botsford, J. Collie, W. Gabriel, P. Goodyear J. Powers, V. Restrepo, A. Rosenberg, M. Sissenwine, G. Thompson, J. Witzig. 1996. Scientific review of definitions of overfishing in U.S. Fishery Management Plans. NOAA Tech. Memo. NMFS-F/SPO-21. 20 p.
- MacLennan, D. N., Fernandes, P. G., and Dalen, J. 2002. A consistent approach to definitions and symbols in fisheries acoustics. *ICES J. Mar Sci*, 59: 365-369.
- Martell, S., & Stewart, I. (2013). Towards defining good practices for modeling time-varying selectivity. *Fisheries Research*, 1–12. [URL][\(link\)](#)
- Martinson, E.C., H.H. Stokes and D.L. Scarneccchia. 2012. Use of juvenile salmon growth and temperature change indices to predict groundfish post age-0 yr class strengths in the Gulf of Alaska and eastern Bering Sea. *Fisheries Oceanography* 21:307-319.
- McAllister, M.K. and Ianelli, J.N. 1997. Bayesian stock assessment using catch-age data and the sampling-importance resampling algorithm. *Can. J. Fish. Aquat. Sci.* 54:284-300.
- Meinig, C., Burger, E. F., Cohen, N., Cokelet, E. D., Cronin, M. F., Cross, J. N., de Halleux, S., et al. 2019. Public–Private Partnerships to Advance Regional Ocean-Observing Capabilities: A Saildrone and NOAA-PMEL Case Study and Future Considerations to Expand to Global Scale Observing. *Frontiers in Marine Science*, 6. doi: 10.3389/fmars.2019.00448.
- Merritt, M.F. and T.J. Quinn II. 2000. Using perceptions of data accuracy and empirical weighting of information: assessment of a recreational fish population. *Canadian Journal of Fisheries and Aquatic Sciences*. 57: 1459-1469.
- Methot, R.D. 1990. Synthesis model: an adaptable framework for analysis of diverse stock assessment data. In Proceedings of the symposium on applications of stock assessment techniques to Gadids. L. Low [ed.]. *Int. North Pac. Fish. Comm. Bull.* 50: 259-277.
- Miller, T.J. 2005. Estimation of catch parameters from a fishery observer program with multiple objectives. PhD Dissertation. Univ. of Washington. 419p.
- Mohn, R. 1999. The retrospective problem in sequential population analysis: An investigation using cod fishery and simulated data. *Ices J. Mar Sci.* 56, 473-488.
- Moss, J.H., E.V. Farley, Jr., A.M. Feldmann, and J.N. Ianelli. 2009. Spatial distribution, energetic status, and food habits of eastern Bering Sea age-0 walleye pollock. *Transactions of the American Fisheries Society*.
- Mueter, F. J., and M. Litzow. 2008. Sea ice retreat alters the biogeography of the Bering Sea continental shelf. *Ecological Applications* 18:309–320.
- Mueter, F. J., C. Ladd, M. C. Palmer, and B. L. Norcross. 2006. Bottom-up and top-down controls of walleye pollock (*Theragra chalcogramma*) on the Eastern Bering Sea shelf. *Progress in Oceanography* 68:152-183.
- Mueter, F. J., N.A. Bond, J.N. Ianelli, and A.B. Hollowed. 2011. Expected declines in recruitment of walleye pollock (*Theragra chalcogramma*) in the eastern Bering Sea under future climate change. *ICES Journal of Marine Science*.
- Nielsen, J.M., Eisner, L., Watson, J., Gann, J.C., Mordy, C.W., Bell, S.W., Harpold, C., Crouser,

- D., and Stabeno, P. (2020). Spring satellite chlorophyll-a concentrations in the Eastern Bering Sea. In: E.C. Siddon, 2020. Ecosystem Status Report 2020: Eastern Bering Sea, Stock Assessment and Fishery Evaluation Report, North Pacific Fishery Management Council, 1007 West Third, Suite 400, Anchorage, Alaska 99501.
- O'Leary, C.A., J.T. Thorson, J.N. Ianelli, and S. Kotwicki. 2020. Adapting to Climate-Driven Distribution Shifts Using Model-Based Indices and Age Composition from Multiple Surveys in the Walleye Pollock (*Gadus Chalcogrammus*) Stock Assessment. *Fisheries Oceanography* 29 (6): 541–57. <https://doi.org/10.1111/fog.12494>.
- O'Leary, C.A., J.T. Thorson, J.N. Ianelli, S. Kotwicki, G.R. Hoff, V.V. Kulik, R.R. Lauth, D.G. Nichol, J. Conner, and A.E. Punt (*submitted*). Estimating spatiotemporal availability of trans-boundary fishes to fishery-independent surveys. *Journal of Applied Ecology*
- O'Reilly, P.T., M.F. Canino, K.M. Bailey and P. Bentzen. 2004. Inverse relationship between FST and microsatellite polymorphism in the marine fish, walleye pollock (*Theragra chalcogramma*): implications for resolving weak population structure. *Molecular Ecology* (2004) 13, 1799–1814
- Parma, A.M. 1993. Retrospective catch-at-age analysis of Pacific halibut: implications on assessment of harvesting policies. In Proceedings of the International Symposium on Management Strategies of Exploited Fish Populations. Alaska Sea Grant Rep. No. 93-02. Univ. Alaska Fairbanks.
- Petitgas, P. 1993. Geostatistics for fish stock assessments: a review and an acoustic application. *ICES J. Mar. Sci.* 50: 285–298.
- Petrik, C. M., Duffy-Anderson, J. T., Mueter, F., Hedstrom, K., & Curchitser, E. N. 2014. Biophysical transport model suggests climate variability determines distribution of Walleye Pollock early life stages in the eastern Bering Sea through effects on spawning. *Progress in Oceanography*, 138, 459–474. [link](#).
- Powers, J. E. 2014. Age-specific natural mortality rates in stock assessments: size-based vs. density-dependent. *ICES Journal of Marine Science*, 71(7), 1629–1637.
- Press, W.H., S.A. Teukolsky, W.T. Vetterling, B.P. Flannery. 1992. Numerical Recipes in C. Second Ed. Cambridge University Press. 994 p.
- Punt, E, Anthony D M Smith, David C Smith, Geoffrey N Tuck, and Neil L Klaer. 2014. Selecting Relative Abundance Proxies for BMSY and BMEY. *ICES Journal of Marine Science* 71: 469–83. <https://doi.org/10.1093/icesjms/fst162>.
- Punt, A.E., Smith, D.C., KrusicGolub, K. and Robertson, S. 2008. Quantifying age-reading error for use in fisheries stock assessments, with application to species in Australia's Southern and Eastern Scalefish and Shark Fishery. *Can. J. Fish. Aquat. Sci.* 65:1991-2005.
- Ressler, P.H., De Robertis, A., Warren, J.D., Smith, J.N., and Kotwicki, S. (2012). Using an acoustic index of euphausiid abundance to understand trophic interactions in the Bering Sea ecosystem. *Deep-Sea Res. II*. 0967-0645,
- Restrepo, V.R., G.G. Thompson, P.M Mace, W.L Gabriel, L.L. Low, A.D. MacCall, R.D. Methot, J.E. Powers, B.L. Taylor, P.R. Wade, and J.F. Witzig. 1998. Technical guidance on the use of precautionary approaches to implementing National Standard 1 of the Magnuson-Stevens Fishery Conservation and Management Act. NOAA Tech. Memo. NMFS-F/SPO-31. 54 p.
- Rohan, S., and Laman, N., 2020. Eastern and Northern Bering Sea Groundfish Condition. In Siddon, E.C., 2020. Ecosystem Status Report 2020: Eastern Bering Sea, Stock Assessment and Fishery Evaluation Report, North Pacific Fishery Management Council, 1007 West Third, Suite 400, Anchorage, Alaska 99501.

- Schnute, J.T. 1994. A general framework for developing sequential fisheries models. *Can. J. Fish. Aquat. Sci.* 51:1676-1688.
- Schnute, J.T. and Richards, L.J. 1995. The influence of error on population estimates from catch-age models. *Can. J. Fish. Aquat. Sci.* 52:2063-2077.
- Seung, C., & Ianelli, J. (2016). Regional economic impacts of climate change: a computable general equilibrium analysis for an Alaskan fishery. *Natural Resource Modeling*, 29(2), 289–333. [link](#).
- Sewall, F., K. Cieciel, T. Jarvis, J. Murphy, H. Schultz, J. Watson. 2019. “Total Energy Trends Among Juvenile Fishes in the Northern Bering Sea.” In Siddon, E., and Zador, S., 2019. *Ecosystem Status Report 2019: Eastern Bering Sea, Stock Assessment and Fishery Evaluation Report*, North Pacific Fishery Management Council, 605 W 4th Ave, Suite 306, Anchorage, AK 99501.
- Siddon, E. C., Heintz, R. a., & Mueter, F. J. (2013). Conceptual model of energy allocation in walleye pollock (*Theragra chalcogramma*) from age-0 to age-1 in the southeastern Bering Sea. *Deep Sea Research Part II: Topical Studies in Oceanography*, 94, 140–149. [link](#).
- Siddon, E.C., T. Jarvis, R. Heintz, E. Farley, B. Cormack. 2019. “Condition of Age-0 Walleye Pollock and Pacific Cod.” In Siddon, E., and Zador, S., 2019. *Ecosystem Status Report 2019: Eastern Bering Sea, Stock Assessment and Fishery Evaluation Report*, North Pacific Fishery Management Council, 605 W 4th Ave, Suite 306, Anchorage, AK 99501.
- Siddon, E.C., 2020. *Ecosystem Status Report 2020: Eastern Bering Sea, Stock Assessment and Fishery Evaluation Report*, North Pacific Fishery Management Council, 1007 West Third, Suite 400, Anchorage, Alaska 99501.
- Smart, T. I., Siddon, E. C., & Duffy-Anderson, J. T. (2013). Vertical distributions of the early life stages of walleye pollock (*Theragra chalcogramma*) in the Southeastern Bering Sea. *Deep Sea Research Part II: Topical Studies in Oceanography*, 94, 201–210. [link](#).
- Smith, G.B. 1981. The biology of walleye pollock. In Hood, D.W. and J.A. Calder, *The Eastern Bering Sea Shelf: Oceanography and Resources*. Vol. I. U.S. Dep. Comm., NOAA/OMP 527-551.
- Stahl, J. 2004. Maturation of walleye pollock, *Theragra chalcogramma*, in the Eastern Bering Sea in relation to temporal and spatial factors. Masters thesis. School of Fisheries and Ocean Sciences, Univ. Alaska Fairbanks, Juneau. 000p.
- Stahl, J., and G. Kruse. 2008a. Spatial and temporal variability in size at maturity of walleye pollock in the eastern Bering Sea. *Transactions of the American Fisheries Society* 137:1543–1557.
- Stahl, J., and G. Kruse. 2008b. Classification of Ovarian Stages of Walleye Pollock (*Theragra chalcogramma*). In *Resiliency of Gadid Stocks to Fishing and Climate Change*. Alaska Sea Grant College Program, AK-SG-08-01.
- Sterling, J. T. and R. R. Ream 2004. At-sea behavior of juvenile male northern fur seals (*Callorhinus ursinus*). *Canadian Journal of Zoology* 82: 1621-1637.
- Stewart, I. J., & Martell, S. J. D. (2015). Reconciling stock assessment paradigms to better inform fisheries management. *ICES Journal of Marine Science: Journal Du Conseil*, 72(8), 2187–2196. [link](#).
- Strong, J. W., & Criddle, K. R. (2014). A Market Model of Eastern Bering Sea Alaska Pollock: Sensitivity to Fluctuations in Catch and Some Consequences of the American Fisheries Act. *North American Journal of Fisheries Management*, 34(6), 1078–1094. [link](#).
- Stram, D. L., and Ianelli, J. N. 2014. Evaluating the efficacy of salmon bycatch measures using

- fishery-dependent data. ICES Journal of Marine Science, 3(2). doi:10.1093/icesjms/fsu168
- Szuwalski, C.S., Ianelli, J.N., and Punt, A.E. 2018. Reducing retrospective patterns in stock assessment and impacts on management performance, ICES Journal of Marine Science, Volume 75, Issue 2, 1 March 2018, Pages 596–609, <https://doi.org/10.1093/icesjms/fsx159>
- Swartzman, G.L., A.G. Winter, K.O. Coyle, R.D. Brodeur, T. Buckley, L. Ciannelli, G.L. Hunt, Jr., J. Ianelli, and S.A. Macklin (2005). Relationship of age-0 pollock abundance and distribution around the Pribilof Islands with other shelf regions of the Eastern Bering Sea. Fisheries Research, Vol. 74, pp. 273-287.
- Takahashi, Y., and Yamaguchi, H. 1972. Stock of the Alaska pollock in the eastern Bering Sea. Bull. Jpn. Soc. Sci. Fish. 38:418-419.
- Thoman, R.L. 2019. “Sea Ice Metrics for the Bering Sea.” In Siddon, E., and Zador, S., 2019. Ecosystem Status Report 2019: Eastern Bering Sea, Stock Assessment and Fishery Evaluation Report, North Pacific Fishery Management Council, 605 W 4th Ave, Suite 306, Anchorage, AK 99501.
- Thompson, G.G. 1996. Risk-averse optimal harvesting in a biomass dynamic model. Unpubl. Manusc., 54 p. Alaska Fisheries Science Center, 7600 Sand Pt. Way NE, Seattle WA, 98115. Distributed as Appendix B to the Environmental Analysis Regulatory Impact Review of Amendments 44/44 to the Fishery Management Plans for the Groundfish Fisheries of the Bering Sea and Aleutian Islands Area and the Gulf of Alaska.
- Thorson, J. T., & Taylor, I. G. (2014). A comparison of parametric, semi-parametric, and non-parametric approaches to selectivity in age-structured assessment models. *Fisheries Research*, 158, 74–83. [link](#).
- Thorson, J.T., Ianelli, J.N., Larsen, E., Ries, L., Scheuerell, M.D., Szuwalski, C., and Zipkin, E. 2016. Joint dynamic species distribution models: a tool for community ordination and spatiotemporal monitoring. *Glob.Ecol. Biogeogr.* 25(9): 1144-1158. doi:10.1111/geb.12464. url: <http://onlinelibrary.wiley.com/doi/10.1111/geb.12464/abstract>
- Thorson, J.T., Shelton, A.O., Ward, E.J., Skaug, H.J., 2015. Geostatistical delta-generalized linear mixed models improve precision for estimated abundance indices for West Coast ground-fishes. *ICES J. Mar. Sci. J.Cons.* 72(5), 1297-1310. doi:10.1093/icesjms/fsu243. URL: <http://icesjms.oxfordjournals.org/content/72/5/1297>
- Thorson, J.T., Kristensen, K., 2016. Implementing a generic method for bias correction in statistical models using random effects, with spatial and population dynamics examples. *Fish. Res.* 175, 66–74. <https://doi.org/10.1016/j.fishres.2015.11.016>
- Thorson, J.T., Rindorf, A., Gao, J., Hanselman, D.H., and Winker, H. 2016. Density-dependent changes in effective area occupied for sea-bottom-associated marine fishes. *Proc R Soc B* 283(1840): 20161853.doi:10.1098/rspb.2016.1853. URL: <http://rspb.royalsocietypublishing.org/content/283/1840/20161853>. see these entries in BibTeX format, use ‘print(, bibtex=TRUE)’, ‘toBibtex(.)’, or set ‘options(citation.bibtex.max=999)’.
- Thorson, J.T., 2018. Three problems with the conventional delta-model for biomass sampling data, and a computationally efficient alternative. *Can. J. Fish. Aquat. Sci.* 75, 1369–1382. <https://doi.org/10.1139/cjfas-2017-0266>
- Thorson, J.T. 2018a, *In Press*. Predicting recruitment density dependence and intrinsic growth rate for all fishes worldwide using a data-integrated life-history model. *Fish and Fisheries*.
- Thorson, J..T. 2018b. Guidance for decisions using the Vector Autoregressive Spatio-Temporal (VAST) package in stock, ecosystem, habitat and climate assessments, *Fisheries Research*, Vol-

- ume 210, 2019, Pages 143-161, ISSN 0165-7836, <https://doi.org/10.1016/j.fishres.2018.10.013>. (<http://www.sciencedirect.com/science/article/pii/S016578361830303X>)
- Thorson, J.T., 2019. Measuring the impact of oceanographic indices on species distribution shifts: The spatially varying effect of cold-pool extent in the eastern Bering Sea. Limnol. Oceanogr. 64, 2632–2645. <https://doi.org/10.1002/limo.1238>
- von Szalay PG, Somerton DA, Kotwicki S. 2007. Correlating trawl and acoustic data in the Eastern Bering Sea: A first step toward improving biomass estimates of walleye pollock (*Theragra chalcogramma*) and Pacific cod (*Gadus macrocephalus*)? Fisheries Research 86(1) 77-83.
- Walline, P. D. 2007. Geostatistical simulations of eastern Bering Sea walleye pollock spatial distributions, to estimate sampling precision. ICES J. Mar. Sci. 64:559-569.
- Walters, C. J., and J. F. Kitchell. 2001. Cultivation/depensation effects on juvenile survival and recruitment. Can. J. Fish. Aquat. Sci. 58:39-50.
- Wespestad, V. G. and J. M. Terry. 1984. Biological and economic yields for Eastern Bering Sea walleye pollock under differing fishing regimes. N. Amer. J. Fish. Manage., 4:204-215.
- Wespestad, V. G., J. Ianelli, L. Fritz, T. Honkalehto, G. Walters. 1996. Bering Sea-Aleutian Islands Walleye Pollock Assessment for 1997. In: Stock assessment and fishery evaluation report for the groundfish resources of the Bering Sea/Aleutian Islands regions. North Pac. Fish. Mgmt. Council, Anchorage, AK, section 1:1-73.
- Wespestad, V. G., L. W. Fritz, W. J. Ingraham, and B. A. Megrey. 2000. On relationships between cannibalism, climate variability, physical transport, and recruitment success of Bering Sea walleye pollock (*Theragra chalcogramma*). ICES Journal of Marine Science 57:272-278.
- Whitehouse, A., G. Lang. 2019.“Mean Length of the Fish Community.” In Siddon, E., and Zador, S., 2019. Ecosystem Status Report 2019: Eastern Bering Sea, Stock Assessment and Fishery Evaluation Report, North Pacific Fishery Management Council, 605 W 4th Ave, Suite 306, Anchorage, AK 99501.
- Williamson, N., and J. Traynor. 1996. Application of a one-dimensional geostatistical procedure to fisheries acoustic surveys of Alaskan pollock. ICES J. Mar. Sci. 53:423-428.
- Winter, A.G., G.L. Swartzman, and L. Ciannelli (2005). Early- to late-summer population growth and prey consumption by age-0 pollock (*Theragra chalcogramma*), in two years of contrasting pollock abundance near the Pribilof Islands, Bering Sea. /Fisheries Oceanography/, Vol. 14, No. 4, pp. 307-320.
- Yasumiishi, E. 2019. “ Pre- and Post-Winter Temperature Change Index and the Recruitment of Bering Sea Pollock.” In Siddon, E., and Zador, S., 2019. Ecosystem Status Report 2019: Eastern Bering Sea, Stock Assessment and Fishery Evaluation Report, North Pacific Fishery Management Council, 605 W 4th Ave, Suite 306, Anchorage, AK 99501.
- Yasumiishi, E., Eisner, L., and Kimmel, D. 2020. Large Copepod Abundance (Sample-Based and Modeled) as an Indicator of Pollock Recruitment to Age-3 in the Southeastern Bering Sea. In: E.C. Siddon, 2020. Ecosystem Status Report 2020: Eastern Bering Sea, Stock Assessment and Fishery Evaluation Report, North Pacific Fishery Management Council, 1007 West Third, Suite 400, Anchorage, Alaska 99501.
- Yasumiishi, E. M., K. R. Criddle, N. Hillgruber, F. J. Mueter, and J. H. Helle. 2015. Chum salmon (*Oncorhynchus keta*) growth and temperature indices as indicators of the year-class strength of age-1 walleye pollock (*Gadus chalcogrammus*) in the eastern Bering Sea. Fish. Oceanogr. 24:242-256.
- Yasumiishi, E., 2020. Temperature Change Index and the Recruitment of Bering Sea Pollock. In:

E.C. Siddon, 2020. Ecosystem Status Report 2020: Eastern Bering Sea, Stock Assessment and Fishery Evaluation Report, North Pacific Fishery Management Council, 1007 West Third, Suite 400, Anchorage, Alaska 99501.

Zeppelin, T. K. and R.R. Ream. 2006. Foraging habitats based on the diet of female northern fur seals (*Callorhinus ursinus*) on the Pribilof Islands, Alaska. *Journal of Zoology* 270(4): 565-576.

## Tables

Table 1: Catch from the Eastern Bering Sea by area, the Aleutian Islands, the Donut Hole, and the Bogoslof Island area, 1979–2020 (2020 values through October 25th 2020). The southeast area refers to the EBS region east of 170W; the Northwest is west of 170W. Note: 1979–1989 data are from Pacfin, 1990–2020 data are from NMFS Alaska Regional Office, and include discards. The 2020 EBS catch estimates are preliminary.

Eastern Bering Sea						
Year	Southeast	Northwest	Total	Aleutians	Donut Hole	Bogoslof I.
1979	368,848	566,866	935,714	9,446		
1980	437,253	521,027	958,280	58,157		
1981	714,584	258,918	973,502	55,517		
1982	713,912	242,052	955,964	57,753		
1983	687,504	293,946	981,450	59,021		
1984	442,733	649,322	1,092,055	77,595	181,200	
1985	604,465	535,211	1,139,676	58,147	363,400	
1986	594,997	546,996	1,141,993	45,439	1,039,800	
1987	529,461	329,955	859,416	28,471	1,326,300	377,436
1988	931,812	296,909	1,228,721	41,203	1,395,900	87,813
1989	904,201	325,399	1,229,600	10,569	1,447,600	36,073
1990	640,511	814,682	1,455,193	79,025	917,400	151,672
1991	653,555	542,109	1,195,664	98,604	293,400	316,038
1992	830,559	559,741	1,390,299	52,352	10,000	241
1993	1,094,429	232,173	1,326,602	57,132	1,957	886
1994	1,152,575	176,777	1,329,352	58,659		556
1995	1,172,306	91,941	1,264,247	64,925		334
1996	1,086,843	105,939	1,192,781	29,062		499
1997	819,889	304,544	1,124,433	25,940		163
1998	969,644	132,515	1,102,159	23,798		8
1999	782,983	206,698	989,680	1,010		29
2000	839,177	293,532	1,132,710	1,244		29
2001	961,977	425,220	1,387,197	825		258
2002	1,160,334	320,442	1,480,776	1,177		1,042
2003	933,191	557,588	1,490,779	1,649		24
2004	1,090,008	390,544	1,480,552	1,158		0
2005	802,154	680,868	1,483,022	1,621		0
2006	827,207	660,824	1,488,031	1,745		0
2007	728,249	626,253	1,354,502	2,519		0
2008	482,698	507,880	990,578	1,278		9
2009	358,252	452,532	810,784	1,662		73
2010	255,114	555,072	810,186	1,289		176
2011	747,891	451,150	1,199,041	1,208		173
2012	618,872	586,350	1,205,222	975		71
2013	695,673	575,098	1,270,770	2,964		57
2014	858,243	439,180	1,297,422	2,375		427
2015	696,253	625,331	1,321,584	913		733
2016	1,167,072	185,609	1,352,681	1,257		1,005
2017	1,178,021	181,161	1,359,182	1,507		185
2018	1,048,693	330,595	1,379,287	1,860		14
2019	1,102,049	307,177	1,409,227	1,663		8
2020	829,704	496,080	1,325,784	2,870		8
Avg.	797,950	413,862	1,211,812	24,419	697,696	28,707

Table 2: Time series of 1964–1976 catch (left) and ABC, TAC, and catch for EBS pollock, 1977–2020 in t. Source: compiled from NMFS Regional office web site and various NPFMC reports. Note that the 2020 value is based on catch reported to October 25th 2020 plus an added component due to bycatch of pollock in other fisheries.

Year	Catch	Year	ABC	TAC	Catch
1964	174,792	1977	950,000	950,000	978,370
1965	230,551	1978	950,000	950,000	979,431
1966	261,678	1979	1,100,000	950,000	935,714
1967	550,362	1980	1,300,000	1,000,000	958,280
1968	702,181	1981	1,300,000	1,000,000	973,502
1969	862,789	1982	1,300,000	1,000,000	955,964
1970	1,256,565	1983	1,300,000	1,000,000	981,450
1971	1,743,763	1984	1,300,000	1,200,000	1,092,055
1972	1,874,534	1985	1,300,000	1,200,000	1,139,676
1973	1,758,919	1986	1,300,000	1,200,000	1,141,993
1974	1,588,390	1987	1,300,000	1,200,000	859,416
1975	1,356,736	1988	1,500,000	1,300,000	1,228,721
1976	1,177,822	1989	1,340,000	1,340,000	1,229,600
		1990	1,450,000	1,280,000	1,455,193
		1991	1,676,000	1,300,000	1,195,664
		1992	1,490,000	1,300,000	1,390,299
		1993	1,340,000	1,300,000	1,326,602
		1994	1,330,000	1,330,000	1,329,352
		1995	1,250,000	1,250,000	1,264,247
		1996	1,190,000	1,190,000	1,192,781
		1997	1,130,000	1,130,000	1,124,433
		1998	1,110,000	1,110,000	1,102,159
		1999	992,000	992,000	989,680
		2000	1,139,000	1,139,000	1,132,710
		2001	1,842,000	1,400,000	1,387,197
		2002	2,110,000	1,485,000	1,480,776
		2003	2,330,000	1,491,760	1,490,779
		2004	2,560,000	1,492,000	1,480,552
		2005	1,960,000	1,478,500	1,483,022
		2006	1,930,000	1,485,000	1,488,031
		2007	1,394,000	1,394,000	1,354,502
		2008	1,000,000	1,000,000	990,578
		2009	815,000	815,000	810,784
		2010	813,000	813,000	810,206
		2011	1,270,000	1,252,000	1,199,041
		2012	1,220,000	1,200,000	1,205,293
		2013	1,375,000	1,247,000	1,270,827
		2014	1,369,000	1,267,000	1,297,849
		2015	1,637,000	1,310,000	1,322,317
		2016	2,090,000	1,340,000	1,353,686
		2017	2,800,000	1,345,000	1,359,367
		2018	2,592,000	1,364,341	1,379,301
		2019	2,163,000	1,397,000	1,409,235
		2020	2,043,000	1,425,000	1,325,792
1977–2020 mean			1,492,045	1,218,468	1,201,282

Table 3: Estimates of discarded pollock (t), percent of total (in parentheses) and total catch for the Aleutians, Bogoslof, Northwest and Southeastern Bering Sea, 1991–2020. SE represents the EBS east of 170W, NW is the EBS west of 170W, source: NMFS Blend and catch-accounting system database. 2020 data are preliminary. Note that the higher discard rates in the Aleutian Islands and Bogoslof region reflect the lack of directed pollock fishing.

Aleut. Is.	Bog.	Discarded pollock			Total	Total (retained plus discard)					
		NW	SE	Total		Aleut. Is.	Bog.	NW	SE	Total	
Discarded pollock						Total (retained plus discard)					
Aleut. Is.	Bog.	NW	SE	Total	Aleut. Is.	Bog.	NW	SE	Total		
1991	5,231 (5%)	20,327 (6%)	48,257 (9%)	66,792 (10%)	140,607 (9%)	98,604	316,038	542,109	653,555	1,610,306	
1992	2,986 (6%)	240 (100%)	57,581 (10%)	71,194 (9%)	132,002 (9%)	52,362	241	559,750	830,559	1,442,912	
1993	1,740 (3%)	308 (35%)	26,107 (11%)	83,986 (8%)	112,141 (8%)	57,138	886	232,180	1,094,429	1,384,633	
1994	1,373 (2%)	11 (2%)	16,084 (9%)	88,098 (8%)	105,566 (8%)	58,659	556	176,777	1,152,575	1,388,567	
1995	1,380 (2%)	267 (80%)	9,715 (11%)	87,492 (7%)	98,855 (7%)	64,925	334	91,941	1,172,306	1,329,506	
1996	994 (3%)	7 (1%)	4,838 (5%)	71,368 (7%)	77,208 (6%)	29,062	499	105,939	1,086,843	1,222,342	
1997	618 (2%)	13 (8%)	22,557 (7%)	71,032 (9%)	94,220 (8%)	25,940	163	304,544	819,889	1,150,536	
1998	162 (1%)	3 (39%)	1,581 (1%)	14,291 (1%)	16,037 (1%)	22,054	8	132,515	969,644	1,124,221	
1999	480 (48%)	11 (39%)	1,912 (1%)	26,912 (3%)	29,315 (3%)	1,010	29	206,698	782,983	990,719	
2000	790 (64%)	20 (67%)	1,942 (1%)	19,678 (2%)	22,429 (2%)	1,244	10	293,532	819,499	1,133,984	
2001	380 (46%)	28 (11%)	2,450 (1%)	14,874 (2%)	17,732 (1%)	825	231	425,220	947,103	1,388,280	
2002	779 (66%)	12 (1%)	1,441 (tr)	19,430 (2%)	21,661 (1%)	1,177	1,031	320,442	1,140,904	1,482,995	
2003	468 (28%)	19 (79%)	2,959 (1%)	13,795 (1%)	17,242 (1%)	1,649	5	557,588	919,397	1,492,452	
2004	287 (25%)	0 (100%)	2,781 (1%)	20,380 (2%)	23,448 (2%)	1,158	-	390,544	1,069,628	1,481,710	
2005	324 (20%)	0 (89%)	2,586 (tr)	14,838 (2%)	17,747 (1%)	1,621	0	680,868	787,316	1,484,643	
2006	311 (18%)	0 (50%)	3,677 (1%)	11,877 (1%)	15,865 (1%)	1,745	0	660,824	815,330	1,489,776	
2007	425 (17%)	- (%)	3,769 (1%)	12,334 (2%)	16,529 (1%)	2,519	0	626,253	715,915	1,357,021	
2008	81 (6%)	0 (%)	1,643 (tr)	5,968 (1%)	7,692 (1%)	1,278	9	507,880	476,730	991,865	
2009	395 (24%)	6 (8%)	1,936 (tr)	4,014 (1%)	6,351 (1%)	1,662	67	452,532	354,238	812,520	
2010	146 (12%)	53 (30%)	1,270 (tr)	2,490 (1%)	3,959 (tr)	1,289	124	555,072	252,623	811,651	
2011	75 (6%)	23 (13%)	1,377 (tr)	3,446 (tr)	4,919 (tr)	1,208	150	451,150	744,445	1,200,421	
2012	95 (10%)	0 (%)	1,191 (tr)	4,080 (1%)	5,366 (tr)	975	71	586,350	614,792	1,206,268	
2013	107 (4%)	0 (1%)	1,226 (tr)	4,085 (1%)	5,418 (tr)	2,964	56	575,098	691,588	1,273,791	
2014	138 (6%)	54 (13%)	1,787 (tr)	12,556 (1%)	14,534 (1%)	2,375	373	439,180	845,687	1,300,224	
2015	19 (2%)	138 (19%)	2,419 (tr)	7,056 (1%)	9,632 (1%)	913	595	625,331	689,197	1,323,230	
2016	59 (5%)	7 (1%)	1,035 (1%)	8,124 (1%)	9,226 (1%)	1,257	997	185,609	1,158,948	1,354,942	
2017	18 (1%)	1 (1%)	1,356 (1%)	6,848 (1%)	8,224 (1%)	1,507	184	181,161	1,171,173	1,360,874	
2018	216 (12%)	2 (1%)	2,005 (1%)	9,170 (1%)	11,393 (1%)	1,860	11	330,595	1,039,523	1,381,161	
2019	65 (4%)	0 (1%)	1,979 (1%)	7,118 (1%)	9,162 (1%)	1,663	8	307,177	1,094,931	1,410,897	
2020	231 (8%)	2 (28%)	2,467 (0%)	9,138 (1%)	11,838 (1%)	2,828	6	496,080	820,566	1,328,620	

Table 4: Total EBS shelf pollock catch recorded by observers (rounded to nearest 100 t) by year and season with percentages indicating the proportion of the catch that came from within the Steller sea lion conservation area (SCA), 1998–2019.

Year	A season	B-season	Total
1998	385,000 t (82%)	403,000 t (38%)	788,000 t (60%)
1999	339,000 t (54%)	468,000 t (23%)	807,000 t (36%)
2000	375,000 t (36%)	572,000 t (44%)	947,000 t (16%)
2001	490,000 t (27%)	674,000 t (46%)	1,164,000 t (38%)
2002	512,200 t (56%)	689,100 t (42%)	1,201,200 t (48%)
2003	532,400 t (47%)	737,400 t (40%)	1,269,800 t (43%)
2004	532,600 t (45%)	710,800 t (34%)	1,243,300 t (38%)
2005	530,300 t (45%)	673,200 t (17%)	1,203,500 t (29%)
2006	533,400 t (51%)	764,300 t (14%)	1,297,700 t (29%)
2007	479,500 t (57%)	663,200 t (11%)	1,142,700 t (30%)
2008	341,700 t (46%)	498,800 t (12%)	840,500 t (26%)
2009	282,700 t (39%)	388,800 t (13%)	671,500 t (24%)
2010	269,800 t (15%)	403,100 t (9%)	672,900 t (11%)
2011	477,600 t (54%)	666,600 t (32%)	1,144,200 t (41%)
2012	457,100 t (52%)	687,500 t (17%)	1,144,600 t (31%)
2013	472,200 t (22%)	708,100 t (19%)	1,180,300 t (20%)
2014	482,800 t (38%)	741,200 t (37%)	1,224,000 t (37%)
2015	490,400 t (15%)	765,900 t (45%)	1,256,300 t (33%)
2016	510,700 t (35%)	784,000 t (62%)	1,294,700 t (51%)
2017	555,300 t (51%)	750,800 t (54%)	1,306,100 t (53%)
2018	573,000 t (63%)	746,500 t (46%)	1,319,500 t (53%)
2019	573,400 t (68%)	762,800 t (51%)	1,336,200 t (58%)

Table 5: Highlights of some management measures affecting the pollock fishery.

Year	Management
1977	Preliminary BSAI FMP implemented with several closure areas
1982	FMP implement for the BSAI
1982	Chinook salmon bycatch limits established for foreign trawlers
1984	2 million t groundfish OY limit established
1984	Limits on Chinook salmon bycatch reduced
1990	New observer program established along with data reporting
1992	Pollock CDQ program commences
1994	NMFS adopts minimum mesh size requirements for trawl codends
1994	Voluntary retention of salmon for foodbank donations
1994	NMFS publishes individual vessel bycatch rates on internet
1995	Trawl closures areas and trigger limits established for chum and Chinook salmon
1998	Improved utilization and retention in effect (reduced discarded pollock)
1998	American Fisheries Act (AFA) passed
1999	The AFA was implemented for catcher/processors
1999	Additional critical habitat areas around sea lion haulouts in the GOA and Eastern Bering Sea are closed.
2000	AFA implemented for remaining sectors (catcher vessel and motherships)
2001	Pollock industry adopts voluntary rolling hotspot program for chum salmon
2002	Pollock industry adopts voluntary rolling hotspot program for Chinook salmon
2005	Rolling hotspot program adopted in regulations to exempt fleet from triggered time/area closures for Chinook and chum salmon
2011	Amendment 91 enacted, Chinook salmon management under hard limits
2015	Amendment 110 (BSAI) Salmon prohibited species catch management in the Bering Sea pollock fishery (additional measures that change limits depending on Chinook salmon run-strength indices) and includes additional provisions for reporting requirements (see <a href="https://alaskafisheries.noaa.gov/fisheries/chinook-salmon-bycatch-management">https://alaskafisheries.noaa.gov/fisheries/chinook-salmon-bycatch-management</a> for update and general information)
2016	Measures of amendment 110 go into effect for 2017 fishing season; Chinook salmon runs above the 3-run index value so bycatch limits stay the same
2017	Due to amendment 110 about 45% of the TAC is taken in the A-season (traditionally only 40% was allowed).
2018	In-river estimates of Chinook salmon (three river index) fell below the threshold and therefore a lower PSC limit applies (from a performance standard of 47,491 to 33,318 and a PSC limit from 60,000 to 45,000 Chinook salmon overall). Additionally, squid have been recategorized as an ecosystem component.
2019	Some pollock sectors experienced high bycatch levels for chum and Chinook salmon and also for sablefish.
2020	Bycatch rates unusually high again for sablefish. Herring PSC occurred in the A season and triggered area closures that will persist into 2021. Salmon bycatch rates (relative to hours fished) was lower than last year for both chum and Chinook.

Table 6: BSAI pollock catch and ex-vessel data showing the total and retained catch (in kt), the number of vessels for all sectors and for trawl catcher vessels including ex-vessel value (million US\$), price (US\$ per pound), and catcher vessel shares. Years covered include the 2010-2014 average, and annual from 2015-2019.

	Avg 10-14	2015	2016	2017	2018	2019
All sectors						
Catch	1,158	1,323	1,355	1,361	1,381	1,411
Retained catch	1,151	1,314	1,346	1,353	1,370	1,402
Vessels #	120.2	120	122	118	112	114
Catcher vessels						
Retained catch	603	687	704	710	718	736
Ex-vessel value	211.7	227.4	209.4	205.5	236.7	259.8
Ex-vessel price	0.159	0.154	0.139	0.137	0.156	0.167
CV share of catch	0.52	0.52	0.52	0.53	0.52	0.52
Vessels #	88	87	89	87	85	84

Source: NMFS Alaska Region Blend and Catch-accounting System estimates; and ADF&G Commercial Operators Annual Reports (COAR). Data compiled and provided by the Alaska Fisheries Information Network (AKFIN).

Table 7: BSAI pollock first-wholesale market data including production (kt), value (million US\$), price (US\$ per pound) for all products and then separately for other categories (head and gut, fillet, surimi, and roe production). Years covered include the 2010-2014 average, and annual from 2015-2019.

	Avg 10-14	2015	2016	2017	2018	2019
All Products volume	468.5	520.9	534.9	523.9	532.4	557.9
All Products value	\$1,263	\$1,275	\$1,352	\$1,338	\$1,383	\$1,551
All Products price	\$1.22	\$1.11	\$1.15	\$1.16	\$1.18	\$1.26
At-sea value share	58%	60%	60%	62%	59%	59%
Fillets volume	152.2	167	161.3	157	167.6	186.8
Fillets value share	40%	39%	37%	33%	36%	40%
Fillets price	\$1.51	\$1.36	\$1.41	\$1.29	\$1.37	\$1.52
Surimi volume	145.6	187.7	190.8	196.7	196.5	192.2
Surimi value share	32%	37%	37%	43%	40%	38%
Surimi price	\$1.25	\$1.14	\$1.19	\$1.33	\$1.27	\$1.37
Roe volume	16.9	18.8	14.3	18.4	20.6	28
Roe value share	10%	7%	7%	9%	10%	9%
Roe price	\$3.38	\$2.29	\$2.84	\$2.88	\$2.89	\$2.15
At-sea price premium	\$0.21	\$0.25	\$0.25	\$0.37	\$0.20	\$0.26

Source: NMFS Alaska Region Blend and Catch-accounting System estimates; NMFS Alaska Region At-sea Production Reports; and ADF&G Commercial Operators Annual Reports (COAR). Data compiled and provided by the Alaska Fisheries Information Network (AKFIN).

Table 8: Alaska pollock U.S. trade and global market data showing global production (in kt) and the U.S. and Russian shares followed by U.S. export volumes (kt), values (million US\$), export prices (US\$ per pound), import values (million US\$), and net exports (million US\$). Subsequent rows show the breakout of export shares (of U.S. pollock) by country (Japan, China and Europe) and the share of U.S. export volume and value of fish (i.e., H&G and fillets), and other product categories (surimi and roe). Years covered include the 2010-2014 average, and annual from 2015-2019.

	Avg 10-14	2015	2016	2017	2018	2019
Global pollock catch	3,255	3,373	3,476	3,489	3,397	-
U.S. share	42%	44%	44%	44%	45%	-
Russian share	48%	48%	50%	50%	49%	-
BSAI share	36%	39%	39%	39%	41%	-
Export volume	315.5	377.8	379.6	397.9	415.2	380.2
Export value	\$916	\$1,038	\$991	\$1,008	\$1,130	\$1,122
Export price	\$1.32	\$1.25	\$1.18	\$1.15	\$1.23	\$1.34
Import value	\$169	\$131	\$91	\$75	\$78	\$123
Net exports	\$747	\$908	\$899	\$933	\$1,051	\$998
Japan volume share	22%	25%	20%	22%	22%	23%
Japan value share	21%	26%	20%	23%	26%	24%
China volume share	14%	13%	12%	15%	14%	10%
China value share	11%	10%	10%	13%	10%	7%
Europe volume share	38%	36%	35%	32%	33%	35%
Europe value share	38%	36%	35%	33%	33%	37%
Meat volume share	51%	49%	49%	49%	50%	47%
Meat value share	49%	46%	46%	47%	45%	44%
Surimi volume share	44%	45%	47%	47%	45%	46%
Surimi value share	37%	39%	42%	42%	42%	43%
Roe Volume share	5%	5%	4%	5%	5%	7%
Roe Value share	14%	15%	11%	11%	13%	13%

Notes: 2019 data thru June; Exports are from the US and are note specific to the BSAI region. 'Meat' includes fillets, H&G, minced and other non-surimi meat based products. Europe refers to Austria, Belgium, Denmark, France, Germany, Greece, Ireland, Italy, Netherlands, Norway, Portugal, Spain, Sweden, Switzerland, and United Kingdom.

Source: FAO Fisheries & Aquaculture Dept. Statistics <http://www.fao.org/fishery/statistics/en>. NOAA Fisheries, Fisheries Statistics Division, Foreign Trade Division of the U.S. Census Bureau, <http://www.st.nmfs.noaa.gov/commercial-fisheries/foreign-trade/index>. U.S. Department of Agriculture <http://www.ers.usda.gov/data-products/agricultural-exchange-rate-data-set.aspx>.

Table 9: BSAI pollock fish oil production index (tons of oil per 100 tons of retained catch); 2010-2014 average, and annual from 2015-2019.

Sector	Avg 10-14	2015	2016	2017	2018	2019
All Sectors	1.96	1.84	2.06	1.92	1.93	2.21
Shoreside	2.22	1.94	2.28	2.09	2.07	2.32
At Sea	1.68	1.72	1.82	1.74	1.77	2.10

Source: NMFS Alaska Region Blend and Catch-accounting System estimates; NMFS Alaska Region At-sea Production Reports; and ADF&G Commercial Operators Annual Reports (COAR). Data compiled and provided by the Alaska Fisheries Information Network (AKFIN).



Table 11: Numbers of pollock NMFS observer samples measured for fishery catch length frequency (by sex and strata), 1977–2019.

Year	Length Frequency samples						
	A Season		B Season SE		B Season NW		
	Males	Females	Males	Females	Males	Females	Total
1977	26,411	25,923	4,301	4,511	29,075	31,219	121,440
1978	25,110	31,653	9,829	9,524	46,349	46,072	168,537
1979	59,782	62,512	3,461	3,113	62,298	61,402	252,568
1980	42,726	42,577	3,380	3,464	47,030	49,037	188,214
1981	64,718	57,936	2,401	2,147	53,161	53,570	233,933
1982	74,172	70,073	16,265	14,885	181,606	163,272	520,273
1983	94,118	90,778	16,604	16,826	193,031	174,589	585,946
1984	158,329	161,876	106,654	105,234	243,877	217,362	993,332
1985	119,384	109,230	96,684	97,841	284,850	256,091	964,080
1986	186,505	189,497	135,444	123,413	164,546	131,322	930,727
1987	373,163	399,072	14,170	21,162	24,038	22,117	853,722
1991	160,491	148,236	166,117	150,261	141,085	139,852	906,042
1992	158,405	153,866	163,045	164,227	101,036	102,667	843,244
1993	143,296	133,711	148,299	140,402	27,262	28,522	621,490
1994	139,332	147,204	159,341	153,526	28,015	27,953	655,370
1995	131,287	128,389	179,312	154,520	16,170	16,356	626,032
1996	149,111	140,981	200,482	156,804	18,165	18,348	683,890
1997	124,953	104,115	116,448	107,630	60,192	53,191	566,527
1998	136,605	110,620	208,659	178,012	32,819	40,307	707,019
1999	36,258	32,630	38,840	35,695	16,282	18,339	178,044
2000	64,575	58,162	63,832	41,120	40,868	39,134	307,689
2001	79,333	75,633	54,119	51,268	44,295	45,836	350,483
2002	71,776	69,743	65,432	64,373	37,701	39,322	348,347
2003	74,995	77,612	49,469	53,053	51,799	53,463	360,390
2004	75,426	76,018	63,204	62,005	47,289	44,246	368,188
2005	76,627	69,543	43,205	33,886	68,878	63,088	355,225
2006	72,353	63,108	28,799	22,363	75,180	65,209	327,010
2007	62,827	60,522	32,945	25,518	75,128	69,116	326,054
2008	46,125	51,027	20,493	23,503	61,149	64,598	266,894
2009	46,051	44,080	19,877	18,579	50,451	53,344	232,379
2010	39,495	41,054	19,194	20,591	40,449	41,323	202,106
2011	58,822	62,617	60,254	65,057	51,137	48,084	345,971
2012	53,641	57,966	45,044	46,940	50,167	53,224	306,982
2013	52,303	62,336	37,434	44,709	49,484	49,903	296,168
2014	55,954	58,097	46,568	51,950	46,643	46,202	305,414
2015	55,646	56,507	45,074	41,218	46,237	43,084	287,766
2016	57,478	59,000	10,264	9,016	72,973	69,669	278,400
2017	55,965	64,728	15,871	14,136	70,285	66,026	287,011
2018	57,156	64,639	35,811	32,842	56,243	49,671	296,362
2019	57,156	64,639	35,811	32,842	56,243	49,671	296,362

Table 12: Number of EBS pollock measured for weight and length by sex and strata as collected by the NMFS observer program, 1977-2019

	Weight-length samples						
	A Season		B Season SE		B Season NW		
	Males	Females	Males	Females	Males	Females	Total
1977	1,222	1,338	137	166	1,461	1,664	5,988
1978	1,991	2,686	409	516	2,200	2,623	10,425
1979	2,709	3,151	152	209	1,469	1,566	9,256
1980	1,849	2,156	99	144	612	681	5,541
1981	1,821	2,045	51	52	1,623	1,810	7,402
1982	2,030	2,208	181	176	2,852	3,043	10,490
1983	1,199	1,200	144	122	3,268	3,447	9,380
1984	980	1,046	117	136	1,273	1,378	4,930
1985	520	499	46	55	426	488	2,034
1986	689	794	518	501	286	286	3,074
1987	1,351	1,466	25	33	72	63	3,010
1991	2,712	2,781	2,339	2,496	1,065	1,169	12,562
1992	1,517	1,582	1,911	1,970	588	566	8,134
1993	1,201	1,270	1,448	1,406	435	450	6,210
1994	1,552	1,630	1,569	1,577	162	171	6,661
1995	1,215	1,259	1,320	1,343	223	232	5,592
1996	2,094	2,135	1,409	1,384	1	1	7,024
1997	628	627	616	665	511	523	3,570
1998	1,852	1,946	959	923	327	350	6,357
1999	5,318	4,798	7,797	7,054	3,532	3,768	32,267
2000	11,346	12,457	7,736	7,991	7,800	12,463	59,793
2001	14,411	14,965	9,064	8,803	10,460	10,871	68,574
2002	13,564	14,098	7,648	7,213	13,004	12,988	68,515
2003	15,535	14,857	10,272	10,031	10,111	9,437	70,243
2004	7,924	7,742	4,318	4,617	6,868	6,850	38,319
2005	7,039	7,428	6,426	6,947	4,114	5,139	37,093
2006	6,566	7,381	6,442	7,406	3,045	4,006	34,846
2007	6,640	6,695	7,081	7,798	3,202	4,305	35,721
2008	4,501	4,865	5,855	6,264	2,236	2,624	26,345
2009	4,033	4,382	4,655	4,511	1,723	1,934	21,238
2010	4,258	4,536	3,883	4,125	2,012	2,261	21,075
2011	5,845	6,388	4,954	4,647	5,929	6,456	34,219
2012	5,494	5,979	4,923	5,346	4,507	4,774	31,023
2013	5,689	6,525	4,844	4,920	3,599	4,313	29,890
2014	5,675	5,871	4,785	4,652	4,753	5,180	30,916
2015	5,310	5,323	4,648	4,194	4,365	4,064	27,904
2016	5,312	5,725	1,077	909	6,872	6,635	26,530
2017	5,238	6,047	1,586	1,343	6,575	6,254	27,043
2018	5,583	6,174	3,430	3,172	5,506	4,850	28,715
2019	6,098	4,520	2,953	3,594	5,501	5,822	28,488

Table 13: Numbers of pollock fishery samples used for age determination estimates by sex and strata, 1977–2019, as sampled by the NMFS observer program.

	A Season		B Season SE		B Season NW		Total
	Males	Females	Males	Females	Males	Females	
1977	1,229	1,344	137	166	1,415	1,613	5,904
1978	1,992	2,686	407	514	2,188	2,611	10,398
1979	2,647	3,088	152	209	1,464	1,561	9,121
1980	1,854	2,158	93	138	606	675	5,524
1981	1,819	2,042	51	52	1,620	1,807	7,391
1982	2,030	2,210	181	176	2,865	3,062	10,524
1983	1,200	1,200	144	122	3,249	3,420	9,335
1984	980	1,046	117	136	1,272	1,379	4,930
1985	520	499	46	55	426	488	2,034
1986	689	794	518	501	286	286	3,074
1987	1,351	1,466	25	33	72	63	3,010
1991	420	423	272	265	320	341	2,041
1992	392	392	371	386	178	177	1,896
1993	444	473	503	493	124	122	2,159
1994	201	202	570	573	131	141	1,818
1995	298	316	436	417	123	131	1,721
1996	468	449	442	433	1	1	1,794
1997	433	436	284	311	326	326	2,116
1998	592	659	307	307	216	232	2,313
1999	540	500	730	727	306	298	3,100
2000	629	667	293	254	596	847	3,286
2001	563	603	205	178	697	736	2,982
2002	672	663	247	202	890	839	3,513
2003	653	588	274	262	701	671	3,149
2004	547	561	221	245	698	600	2,872
2005	599	617	420	422	490	614	3,162
2006	528	609	507	568	367	459	3,038
2007	627	642	552	568	485	594	3,468
2008	513	497	538	650	342	368	2,908
2009	404	484	440	432	240	299	2,299
2010	545	624	413	466	418	505	2,971
2011	581	808	404	396	582	660	3,431
2012	517	571	485	579	480	533	3,165
2013	666	703	525	568	401	518	3,381
2014	609	629	413	407	475	553	3,086
2015	653	642	511	493	508	513	3,320
2016	488	599	157	125	929	969	3,267
2017	604	778	179	163	777	753	3,254
2018	569	662	366	358	621	591	3,167
2019	778	552	332	387	531	558	3,138

Table 14: NMFS total pollock research catch by year in t, 1964–2019.

Year	Bering Sea	Year	Bering Sea	Year	Bering Sea
1964	0	1982	682	2000	313
1965	18	1983	508	2001	241
1966	17	1984	208	2002	440
1967	21	1985	435	2003	285
1968	7	1986	163	2004	363
1969	14	1987	174	2005	87
1970	9	1988	467	2006	251
1971	16	1989	393	2007	333
1972	11	1990	369	2008	168
1973	69	1991	465	2009	156
1974	83	1992	156	2010	226
1975	197	1993	221	2011	1322
1976	122	1994	267	2012	219
1977	35	1995	249	2013	183
1978	94	1996	206	2014	308
1979	458	1997	262	2015	256
1980	139	1998	121	2016	198
1981	466	1999	299	2017	226
				2018	177
				2019	230

Table 15: Survey biomass estimates (age 1+, t) of Eastern Bering Sea pollock based on design-based area-swept expansion methods from NMFS bottom trawl surveys 1982–2019.

Year	Survey biomass			
	Strata 1-6	Strata 8-9	Total	%NW
1982	2,858,400	54,469	2,912,869	2%
1983	5,921,380	-	5,921,380	-
1984	4,542,405	-	4,542,405	-
1985	4,560,122	637,881	5,198,003	12%
1986	4,835,722	-	4,835,722	-
1987	5,111,645	386,788	5,498,433	7%
1988	7,003,983	179,980	7,183,963	3%
1989	5,906,477	643,938	6,550,415	10%
1990	7,107,218	189,435	7,296,653	3%
1991	5,067,092	62,446	5,129,538	1%
1992	4,316,660	209,493	4,526,153	5%
1993	5,196,453	98,363	5,294,816	2%
1994	4,977,639	49,686	5,027,325	1%
1995	5,409,297	68,541	5,477,838	1%
1996	2,981,680	143,573	3,125,253	5%
1997	2,868,734	693,429	3,562,163	19%
1998	2,137,049	550,706	2,687,755	20%
1999	3,598,688	199,786	3,798,474	5%
2000	4,985,064	118,565	5,103,629	2%
2001	4,145,746	51,108	4,196,854	1%
2002	4,755,668	197,770	4,953,438	4%
2003	8,106,358	285,902	8,392,261	3%
2004	3,744,501	118,473	3,862,974	3%
2005	4,731,068	137,548	4,868,616	3%
2006	2,845,553	199,827	3,045,380	7%
2007	4,158,234	179,986	4,338,220	4%
2008	2,834,093	189,174	3,023,267	6%
2009	2,231,225	51,185	2,282,410	2%
2010	3,550,981	186,898	3,737,878	5%
2011	2,945,641	166,672	3,112,312	5%
2012	3,281,223	206,005	3,487,229	6%
2013	4,297,970	277,433	4,575,403	6%
2014	6,552,849	877,104	7,429,952	12%
2015	5,944,325	450,034	6,394,359	7%
2016	4,698,430	211,650	4,910,080	4%
2017	4,688,500	125,873	4,814,373	3%
2018	3,015,612	97,185	3,112,797	3%
2019	4,973,872	484,494	5,458,366	9%
Average	4,489,986	245,123	4,735,108	5%

Table 16: Sampling effort for pollock in the EBS from the NMFS bottom trawl survey 1982–2019.

Year	Number of Hauls	Lengths	Aged	Year	Number of Hauls	Lengths	Aged
1982	329	40,001	1,611	1999	373	32,532	1,385
1983	354	78,033	1,931	2000	372	41,762	1,545
1984	355	40,530	1,806	2001	375	47,335	1,641
1985	434	48,642	1,913	2002	375	43,361	1,695
1986	354	41,101	1,344	2003	376	46,480	1,638
1987	356	40,144	1,607	2004	375	44,102	1,660
1988	373	40,408	1,173	2005	373	35,976	1,676
1989	373	38,926	1,227	2006	376	39,211	1,573
1990	371	34,814	1,257	2007	376	29,679	1,484
1991	371	43,406	1,083	2008	375	24,635	1,251
1992	356	34,024	1,263	2009	375	24,819	1,342
1993	375	43,278	1,385	2010	376	23,142	1,385
1994	375	38,901	1,141	2011	376	36,227	1,734
1995	376	25,673	1,156	2012	376	35,782	1,785
1996	375	40,789	1,387	2013	376	35,908	1,847
1997	376	35,536	1,193	2014	376	43,042	2,099
1998	375	37,673	1,261	2015	376	54,241	2,320
				2016	376	50,857	1,766
				2017	376	47,873	1,623
				2018	376	48,673	1,486
				2019	376	42,382	1,519





Table 19: Biomass (age 1+) of Eastern Bering Sea pollock as estimated by surveys 1979–2019 (millions of t). Note that the bottom-trawl survey data only represent biomass from the survey strata (1–6) areas in 1982–1984, and 1986. For all other years the estimates include strata 8–9. DDC indicates the values obtained from the Kotwicki et al. Density-Dependence Correction method and the VAST columns are for the standard survey area including the Northern Bering Sea (NBS) extension. BTS=Bottom trawl survey, DB=Design-based, CPE=cold pool extent, ATS=Acoustic trawl survey.

Year	DB.BTS	DDC	VAST.NBS	VAST.NBS.CPE	ATS	VAST.ATS
1982	2,912	4,069	3,916	3,946	NA	NA
1983	5,921	8,409	10,303	9,398	NA	NA
1984	4,542	6,408	7,791	6,886	NA	NA
1985	5,198	7,189	9,070	7,993	NA	NA
1986	4,835	6,825	7,658	7,276	NA	NA
1987	5,498	7,892	7,967	7,694	NA	NA
1988	7,183	11,088	11,561	11,784	NA	NA
1989	6,550	9,795	10,450	10,745	NA	NA
1990	7,296	11,899	12,964	11,815	NA	NA
1991	5,129	7,389	7,772	7,476	NA	NA
1992	4,526	6,210	7,121	6,628	NA	NA
1993	5,294	7,089	8,319	7,967	NA	NA
1994	5,027	7,100	7,952	7,513	3,629	3,703
1995	5,477	9,107	7,885	7,258	NA	NA
1996	3,125	4,079	4,387	4,268	2,945	2,870
1997	3,562	5,019	5,108	4,849	3,591	3,525
1998	2,687	3,509	3,731	3,586	NA	NA
1999	3,798	5,454	5,532	5,932	4,141	3,665
2000	5,103	7,355	8,255	7,747	3,626	3,292
2001	4,196	5,439	6,282	6,168	NA	NA
2002	4,953	6,770	7,392	6,878	4,306	4,477
2003	8,392	13,508	12,305	12,159	NA	NA
2004	3,862	5,105	5,866	5,866	4,010	3,611
2005	4,868	6,696	7,608	7,272	NA	NA
2006	3,045	3,886	4,582	4,251	1,873	1,727
2007	4,338	6,145	7,653	6,835	NA	NA
2008	3,023	3,994	4,751	4,830	2,278	2,072
2009	2,282	2,989	3,617	2,888	1,406	1,428
2010	3,737	5,131	5,829	5,328	1,325	1,377
2011	3,112	3,948	4,533	4,485	2,642	2,585
2012	3,487	4,613	5,186	5,076	2,296	2,375
2013	4,575	6,114	6,668	6,475	NA	NA
2014	7,429	10,331	12,172	12,007	4,730	5,122
2015	6,394	8,587	10,589	10,857	NA	NA
2016	4,910	6,607	9,128	9,539	4,829	5,381
2017	4,814	6,256	9,011	8,968	NA	NA
2018	3,112	4,187	5,826	5,823	2,499	2,819
2019	5,458	7,380	9,732	9,511	NA	NA
2020	NA	NA	NA	NA	3,605	3,694
Avg.	4,728	6,673	7,539	7,263	3,161	3,161

Table 20: Number of (age 1+) hauls and sample sizes for EBS pollock collected by the AT surveys. Sub-headings E and W represent collections east and west of 170W (within the US EEZ) and US represents the US sub-total and RU represents the collections from the Russian side of the surveyed region.

Year	Hauls				Lengths				Otoliths				Number aged			
	E	W	US	RU	E	W	US	RU	E	W	US	RU	E	W	US	RU
1979			25			7,722				0					2,610	
1982	13	31	48		1,725	6,689	8,687		840	2,324	3,164		783	1,958	2,741	
1985			73			19,872					2,739				2,739	
1988			25			6,619					1,471				1,471	
1991			62			16,343					2,062				1,663	
1994	25	51	76	19	4,553	21,011	25,564	8,930	1,560	3,694	4,966	1,270	612	932	1,770	455
1996	15	42	57		3,551	13,273	16,824		669	1,280	1,949		815	1,111	1,926	
1997	25	61	86		6,493	23,043	29,536		966	2,669	3,635		936	1,349	2,285	
1999	41	77	118		13,841	28,521	42,362		1,945	3,001	4,946		946	1,500	2,446	
2000	29	95	124		7,721	36,008	43,729		850	2,609	3,459		850	1,403	2,253	
2002	47	79	126		14,601	25,633	40,234		1,424	1,883	3,307		1,000	1,200	2,200	
2004	33	57	90	15	8,896	18,262	27,158	5,893	1,167	2,002	3,169	461	798	1,192	2,351	461
2006	27	56	83		4,939	19,326	24,265		822	1,871	2,693		822	1,870	2,692	
2007	23	46	69	4	5,492	14,863	20,355	1,407	871	1,961	2,832	319	823	1,737	2,560	315
2008	9	53	62	6	2,394	15,354	17,748	1,754	341	1,698	2,039	177	338	1,381	1,719	176
2009	13	33	46	3	1,576	9,257	10,833	282	308	1,210	1,518	54	306	1,205	1,511	54
2010	11	48	59	9	2,432	20,263	22,695	3,502	653	1,868	2,521	381	652	1,598	2,250	379
2012	17	60	77	14	4,422	23,929	28,351	5,620	650	2,045	2,695	418	646	1,483	2,129	416
2014	52	87	139	3	28,857	8,645	37,502	747	1,739	849	2,588	72	845	1,735	2,580	72
2016	37	71	108		10,912	24,134	35,046		880	1,514	2,394		876	1,513	2,388	
2018	36	55	91		11,031	18,654	29,685		1,105	1,515	2,620		1,071	1,632	2,703	

Table 21: Mid-water pollock biomass (near surface down to 0.5m from the bottom) by area as estimated from summer acoustic-trawl surveys on the U.S. EEZ portion of the Bering Sea shelf, 1994–2018 (Honkalehto et al. 2015). CVs for biomass estimates were assumed to average 20 percent with the 1994–2018 inter-annual variability arising from the 1-dimensional variance estimation method. Note the last column reflects biomass index values based on a VAST model application applied to acoustic backscatter was rescaled to have the same mean as the total biomass to 0.5m.

Year	Date	Area		Biomass			
		(nmi) <sup>2</sup>	SCA	E170-SCA	W170	0.5m total	VAST ( <i>sA</i> )
1994	9 Jul - 19 Aug	78,251	0.378	0.656	2.595	3.629	3.704
1996	20 Jul - 30 Aug	93,810	0.272	0.490	2.182	2.944	2.870
1997	17 Jul - 4 Sept	102,770	0.274	0.853	2.463	3.59	3.526
1999	7 Jun - 5 Aug	103,670	0.323	0.758	3.060	4.141	3.665
2000	7 Jun - 2 Aug	106,140	0.457	0.717	2.452	3.626	3.292
2002	4 Jun - 30 Jul	99,526	0.755	0.946	2.605	4.306	4.477
2004	4 Jun - 29 Jul	99,659	0.546	0.920	2.543	4.009	3.612
2006	3 Jun - 25 Jul	89,550	0.144	0.342	1.387	1.873	1.728
2007	2 Jun - 30 Jul	92,944	0.136	0.244	1.898	2.278	2.073
2008	2 Jun - 31 Jul	95,374	0.122	0.087	1.197	1.406	1.429
2009	9 Jun - 7 Aug	91,414	0.153	0.057	1.115	1.325	1.378
2010	5 Jun - 7 Aug	92,849	0.098	0.193	2.351	2.642	2.585
2012	7 Jun - 10 Aug	96,852	0.195	0.320	1.782	2.297	2.375
2014	12 Jun - 13 Aug	94,361	0.561	1.462	2.707	4.73	5.122
2016	12 Jun - 17 Aug	100,674	0.540	1.267	3.022	4.829	5.381
2018	12 Jun - 22 Aug	92,283	0.231	0.513	1.755	2.499	2.819
2020	4 Jul - 20 Aug	102320	-	0.462	-	3.605	3.695

Table 22: AT survey estimates of EBS pollock abundance-at-age (millions), 1979–2018. Age-1s were modeled as a separate index, ages 2+ modeled as proportions at age.

Year	Age										Age	
	1	2	3	4	5	6	7	8	9	10+	2+	Total
1979	69,110	41,132	3,884	413	534	128	30	4	28	161	46,314	115,424
1982	108	3,401	4,108	7,637	1,790	283	141	178	90	177	17,805	17,913
1985	2,076	929	8,149	898	2,186	1,510	1,127	130	21	15	14,965	17,041
1988	11	1,112	3,586	3,864	739	1,882	403	151	130	414	12,280	12,292
1991	639	5,942	967	215	224	133	120	39	37	53	7,730	8,369
1994	1,140	4,969	1,424	1,819	2,252	389	109	96	56	221	11,335	12,475
1996	1,800	567	552	2,741	915	634	585	142	39	165	6,338	8,139
1997	13,227	2,881	440	536	2,330	546	313	290	75	220	7,633	20,860
1999	607	1,780	3,717	1,810	652	398	1,548	526	180	249	10,859	11,466
2000	460	1,322	1,230	2,588	1,012	327	308	950	278	252	8,266	8,726
2002	796	4,944	3,385	1,295	661	935	538	140	162	493	12,554	13,351
2004	83	313	1,217	3,123	1,634	567	288	283	121	265	7,811	7,894
2006	525	217	291	654	783	659	390	145	75	171	3,386	3,910
2007	5,775	1,041	345	478	794	729	407	241	98	135	4,267	10,042
2008	71	2,915	1,047	166	161	288	235	136	102	120	5,169	5,240
2009	5,197	816	1,734	281	77	94	129	111	77	114	3,433	8,630
2010	2,568	6,404	984	2,295	446	73	33	37	38	91	10,400	12,968
2012	177	1,989	1,693	2,710	280	367	113	36	25	103	7,315	7,492
2014	4,751	8,655	969	1,161	1,119	1,770	740	170	79	99	14,762	19,513
2016	174	1,038	4,496	4,476	715	348	392	420	96	64	12,046	12,220
2018	450	517	249	621	2,268	944	198	112	107	104	5,120	5,570
Mean	5,226	4,423	2,118	1,894	1,027	619	388	206	91	176	10,942	16,168
Median	639	1,780	1,230	1,295	783	398	308	142	79	161	8,266	11,466

Table 23: An abundance index derived from acoustic data collected opportunistically aboard bottom-trawl survey vessels (AVO index; Honkalehto et al. 2014). Note values in parentheses are the coefficients of variation from using 1-D geostatistical estimates of sampling variability (Petitgas, 1993). See Honkalehto et al. (2011) for the derivation of these estimates. The column “ $CV_{AVO}$ ” was assumed to have a mean value of 0.30 for model fitting purposes (scaling relative to the AT and BTS indices).

Year	AT scaled biomass index	AVO index	$CV_{AVO}$
2006	1.8729 (4%)	0.555 9%	25%
2007	2.2779 (4%)	0.638 14%	37%
2008	1.4056 (8%)	0.316 20%	56%
2009	1.3248 (9%)	0.285 42%	116%
2010	2.6423 (6%)	0.679 13%	35%
2011	—no survey—	0.543 11%	29%
2012	2.2958 (4%)	0.661 9%	26%
2013	—no survey—	0.694 6%	16%
2014	4.7300 (5%)	0.897 5%	13%
2015	—no survey—	0.953 5%	13%
2016	4.8290 (2%)	0.776 5%	13%
2017	—no survey—	0.73 5%	13%
2018	2.4994 (2%)	0.672 5%	14%
2019	—no survey—	0.68 5%	13%
2020		-NA-	13%

Table 24: Pollock sample sizes assumed for the age-composition data likelihoods from the fishery, bottom-trawl survey, and AT surveys, 1964–2020. Note fishery sample size for 1964–1977 was fixed at 10.

Year	Fishery	BTS	ATS
1978	39	0	
1979	39	0	
1980	39	0	
1981	39	0	
1982	39	105	
1983	39	126	
1984	39	118	
1985	39	125	
1986	39	88	
1987	39	105	
1988	39	76	
1989	39	80	
1990	39	82	
1991	401	71	
1992	453	82	
1993	569	90	
1994	338	74	43
1995	572	75	
1996	254	90	32
1997	582	78	49
1998	426	82	
1999	519	90	67
2000	526	101	70
2001	390	107	
2002	513	110	72
2003	453	107	
2004	457	108	51
2005	482	109	
2006	469	102	47
2007	529	97	39
2008	464	82	35
2009	362	87	26
2010	602	90	34
2011	561	113	
2012	541	116	44
2013	625	120	
2014	513	137	79
2015	668	151	
2016	588	115	61
2017	587	105	
2018	545	100	50
2019	500	100	



```
## Error in round(x$cope_like, 2): non-numeric argument to mathematical function  
## Error in 'align<-.xtable`(*tmp*, value = switch(1 + is.null(align), : "align" must have l
```



Table 27: Summary of different model results and the stock condition for EBS pollock. Biomass units are thousands of t.

Component	16.2 last year	20.0 USV	20.1 USVast	20.0a base
$B_{2021}$	3,000	2,600	2,800	2,600
$CV_{B_{2021}}$	0.12	0.13	0.15	0.13
$B_{MSY}$	2,148	2,154	2,174	2,257
$CV_{B_{MSY}}$	0.24	0.22	0.22	0.24
$B_{2021}/B_{MSY}$	139%	121%	131%	115%
$B_0$	5,777	5,611	5,665	5,792
$B_{35\%}$	2,190	2,149	2,172	2,150
SPR rate at $F_{MSY}$	27%	28%	28%	30%
Steepness	0.66	0.67	0.67	0.64
Est. $B_{2020}/B_{2020, no fishing}$	0.64	0.6	0.63	0.58
$B_{2020}/B_{MSY}$	161%	138%	148%	131%









Table 32: Summary of model results and the stock condition for EBS pollock. Biomass units are thousands of t.

Component	16.2 last year	20.0 USV
$B_{2021}$	3,000	2,600
$CV_{B_{2021}}$	0.12	0.13
$B_{MSY}$	2,148	2,154
$CV_{B_{MSY}}$	0.24	0.22
$B_{2021}/B_{MSY}$	139%	121%
$B_0$	5,777	5,611
$B_{35\%}$	2,190	2,149
SPR rate at $F_{MSY}$	27%	28%
Steepness	0.66	0.67
Est. $B_{2020}/B_{2020,no fishing}$	0.64	0.6
$B_{2020}/B_{MSY}$	161%	138%

Table 33: Summary results of Tier 1 2021 yield projections for EBS pollock.

Component	16.2 last year	20.0 USV
2021 fishable biomass (GM)	9,094,000	7,609,000
Equilibrium fishable biomass at MSY	5,749,000	6,503,000
MSY R (HM)	0.383	0.339
2021 Tier 1 ABC	3,485,000	2,582,000
2021 Tier 1 $FOFL$	0.449	0.381
2021 Tier 1 OFL	4,085,000	2,896,000
MSY R (HM)	0.326	0.288
Recommended ABC	1,767,000	1,788,000

Table 34: For the configuration named 20.0a base, Tier 3 projections of EBS pollock catch for the 7 scenarios.

Catch	Scenario.1	Scenario.2	Scenario.3	Scenario.4	Scenario.5	Scenario.6	Scenario.7
2020	1,400	1,400	1,400	1,400	1,400	1,400	1,400
2021	1,625	1,300	1,404	760	0	1,986	1,625
2022	1,342	1,300	1,292	779	0	1,447	1,342
2023	1,274	1,399	1,263	816	0	1,353	1,543
2024	1,317	1,365	1,292	866	0	1,418	1,482
2025	1,451	1,468	1,395	950	0	1,573	1,594
2026	1,539	1,542	1,470	1,019	0	1,658	1,665
2027	1,578	1,579	1,509	1,062	0	1,689	1,691
2028	1,600	1,601	1,536	1,092	0	1,703	1,704
2029	1,604	1,600	1,547	1,110	0	1,700	1,700
2030	1,588	1,587	1,534	1,110	0	1,678	1,678
2031	1,580	1,583	1,529	1,111	0	1,668	1,668
2032	1,571	1,572	1,522	1,110	0	1,659	1,659
2033	1,570	1,568	1,521	1,111	0	1,659	1,659

Table 35: For the configuration named 20.0a base, Tier 3 projections of EBS pollock ABC for the 7 scenarios. Note: scenario 2 results for 2021 and 2022 are conditioned on catches in that scenario listed in Table 38).

ABC	Scenario.1	Scenario.2	Scenario.3	Scenario.4	Scenario.5	Scenario.6	Scenario.7
2020	1,992	1,992	1,724	939	0	2,425	2,425
2021	1,625	1,625	1,404	760	0	1,986	1,986
2022	1,342	1,483	1,292	779	0	1,447	1,622
2023	1,274	1,399	1,263	816	0	1,353	1,543
2024	1,317	1,365	1,292	866	0	1,418	1,482
2025	1,451	1,470	1,395	950	0	1,573	1,594
2026	1,539	1,547	1,470	1,019	0	1,658	1,665
2027	1,578	1,584	1,509	1,062	0	1,689	1,691
2028	1,600	1,604	1,536	1,092	0	1,703	1,704
2029	1,604	1,608	1,547	1,110	0	1,700	1,700
2030	1,588	1,592	1,534	1,110	0	1,678	1,678
2031	1,580	1,583	1,529	1,111	0	1,668	1,668
2032	1,571	1,573	1,522	1,110	0	1,659	1,659
2033	1,570	1,571	1,521	1,111	0	1,659	1,659



Table 39: For the configuration named 20.0 USV, Tier 3 projections of EBS pollock ABC for the 7 scenarios. Note: scenario 2 results for 2021 and 2022 are conditioned on catches in that scenario listed in Table 38).

ABC	Scenario.1	Scenario.2	Scenario.3	Scenario.4	Scenario.5	Scenario.6	Scenario.7
2020	2,316	2,316	1,661	1,021	0	2,878	2,878
2021	1,788	1,788	1,278	783	0	2,187	2,187
2022	1,285	1,517	1,133	761	0	1,385	1,599
2023	1,267	1,442	1,138	805	0	1,351	1,580
2024	1,310	1,369	1,169	854	0	1,413	1,478
2025	1,451	1,471	1,266	937	0	1,582	1,599
2026	1,567	1,574	1,364	1,020	0	1,696	1,700
2027	1,613	1,619	1,416	1,071	0	1,730	1,731
2028	1,635	1,641	1,450	1,107	0	1,742	1,742
2029	1,648	1,653	1,473	1,133	0	1,749	1,749
2030	1,632	1,638	1,466	1,137	0	1,724	1,724
2031	1,617	1,624	1,459	1,137	0	1,708	1,708
2032	1,610	1,615	1,455	1,138	0	1,702	1,702
2033	1,601	1,604	1,448	1,134	0	1,693	1,693

Table 40: For the configuration named 20.0 USV, Tier 3 projections of EBS pollock fishing mortality for the 7 scenarios.

F	Scenario.1	Scenario.2	Scenario.3	Scenario.4	Scenario.5	Scenario.6	Scenario.7
2020	0.197	0.197	0.197	0.197	0.197	0.197	0.197
2021	0.361	0.246	0.241	0.139	0.000	0.470	0.361
2022	0.317	0.284	0.241	0.139	0.000	0.390	0.317
2023	0.316	0.333	0.241	0.139	0.000	0.387	0.414
2024	0.319	0.324	0.241	0.139	0.000	0.398	0.405
2025	0.323	0.325	0.241	0.139	0.000	0.407	0.409
2026	0.327	0.327	0.241	0.139	0.000	0.413	0.414
2027	0.329	0.329	0.241	0.139	0.000	0.416	0.416
2028	0.329	0.329	0.241	0.139	0.000	0.415	0.415
2029	0.328	0.327	0.241	0.139	0.000	0.413	0.413
2030	0.328	0.327	0.241	0.139	0.000	0.412	0.412
2031	0.327	0.327	0.241	0.139	0.000	0.411	0.411
2032	0.327	0.327	0.241	0.139	0.000	0.411	0.411
2033	0.327	0.326	0.241	0.139	0.000	0.410	0.410

Table 41: For the configuration named 20.0 USV, Tier 3 projections of EBS pollock spawning biomass (kt) for the 7 scenarios.

SSB	Scenario.1	Scenario.2	Scenario.3	Scenario.4	Scenario.5	Scenario.6	Scenario.7
2020	2,856	2,856	2,856	2,856	2,856	2,856	2,856
2021	2,449	2,524	2,527	2,595	2,692	2,382	2,449
2022	2,167	2,355	2,386	2,628	3,027	1,998	2,167
2023	2,173	2,301	2,414	2,763	3,413	1,993	2,127
2024	2,292	2,342	2,548	2,975	3,856	2,104	2,147
2025	2,434	2,454	2,714	3,204	4,307	2,227	2,241
2026	2,514	2,524	2,828	3,377	4,692	2,284	2,288
2027	2,560	2,568	2,909	3,508	5,024	2,313	2,315
2028	2,578	2,585	2,952	3,593	5,287	2,321	2,321
2029	2,569	2,576	2,959	3,631	5,475	2,307	2,307
2030	2,552	2,559	2,950	3,644	5,619	2,289	2,289
2031	2,538	2,545	2,939	3,649	5,733	2,276	2,276
2032	2,535	2,540	2,937	3,655	5,826	2,275	2,275
2033	2,545	2,548	2,945	3,668	5,905	2,287	2,287

Table 42: Bycatch estimates ( $t$ ) of other target species caught in the BSAI directed pollock fishery, 1997–2020 based on then NMFS Alaska Regional Office reports from observers (2020 data are preliminary).

Year	Pacific.Cod	Rock.Sole	Flathead.Sole	Arrowtooth.Flounder	Pacific.Ocean.Perch	Yellowfin.Sole	Sablefish	Sharks	Sculpin	Other
1991	24,310	5,120	0	5,719	418	417	9	0	0	10,722
1992	24,005	7,233	2	4,311	173	892	7	0	0	14,716
1993	20,930	8,713	0	1,222	282	1,102	1	0	0	7,548
1994	14,409	3,009	0	2,010	170	1,207	1	0	0	4,171
1995	19,776	2,179	2,175	1,177	142	675	12	0	0	1,021
1996	15,174	2,042	3,207	1,844	303	1,797	7	0	0	1,638
1997	8,262	1,522	2,350	984	428	605	2	0	0	1,026
1998	6,255	770	2,047	1,712	616	1,744	2	0	0	885
1999	3,220	1,058	1,885	272	120	349	7	0	0	610
2000	3,432	2,687	2,510	978	21	1,465	12	0	0	987
2001	3,879	1,672	2,199	529	574	594	21	0	0	1,312
2002	5,886	1,885	1,844	607	543	768	34	0	0	1,272
2003	5,968	1,418	1,501	617	935	209	48	0	0	1,861
2004	6,436	2,553	2,104	556	393	841	16	0	0	1,328
2005	7,413	1,125	2,351	651	652	63	11	0	0	1,234
2006	7,291	1,360	2,862	1,088	735	256	8	0	0	2,219
2007	5,629	510	4,225	2,795	624	85	11	0	0	2,028
2008	6,971	2,149	4,315	1,715	335	552	4	0	0	3,373
2009	7,875	7,591	4,665	2,202	114	270	2	0	0	4,495
2010	6,964	2,241	4,357	1,466	230	1,056	2	0	0	2,338
2011	10,040	8,480	4,885	1,599	659	1,082	1	65	315	310
2012	10,061	6,701	3,968	748	705	1,496	0	54	286	356
2013	8,957	6,319	3,146	965	610	2,087	0	43	219	339
2014	5,213	4,359	2,553	757	1,300	1,953	1	75	190	724
2015	8,302	1,709	2,259	402	2,516	863	0	51	186	412
2016	4,980	1,141	1,629	297	3,273	895	18	58	124	470
2017	5,955	1,825	956	208	4,818	623	101	92	81	324
2018	4,270	1,077	973	270	3,803	743	396	60	52	1,494
2019	6,213	1,116	1,087	421	7,968	443	1,236	100	58	1,580
2020	9,166	835	1,969	685	5,980	1,204	3,459	130	131	2,712

Table 43: Bycatch estimates (t) of pollock caught in the other non-pollock EBS directed fisheries, 1997–2020 based on then NMFS Alaska Regional Office reports from observers.

Year	Pacific.Cod	Yellowfin.Sole	Rock.Sole	Flathead.Sole	Other.flatfish	Other.fisheries	Total
1991	10,695	0	9,711	0	7,992	755	29,154
1992	20,778	13,100	9,824	0	1,371	628	45,704
1993	31,299	15,253	18,582	0	2,581	623	68,339
1994	26,594	33,200	15,784	0	6,770	89	82,438
1995	25,691	27,041	7,766	1,851	3,359	63	65,773
1996	22,382	22,254	7,698	4,082	1,373	805	58,597
1997	33,658	24,100	9,123	2,983	496	14	70,376
1998	10,468	15,339	3,960	2,369	641	941	33,720
1999	21,131	8,701	5,207	4,040	731	1,197	41,009
2000	14,508	13,425	5,480	6,467	600	520	41,003
2001	11,570	16,502	4,577	4,337	402	488	37,879
2002	15,255	14,489	9,942	1,934	286	51	41,959
2003	15,926	11,578	4,924	2,983	688	260	36,362
2004	18,650	10,383	8,975	5,162	1,233	194	44,599
2005	14,109	10,312	7,235	3,662	1,394	201	36,917
2006	15,168	5,966	6,986	2,663	1,162	143	32,090
2007	20,319	4,020	3,245	3,417	935	276	32,214
2008	9,533	9,827	4,930	4,102	719	17	29,131
2009	7,875	7,036	6,171	3,160	344	13	24,602
2010	6,575	5,179	6,074	2,996	320	85	21,231
2011	8,990	8,673	6,931	1,473	828	301	27,198
2012	8,383	11,197	6,703	903	849	413	28,450
2013	9,811	20,171	7,326	2,010	2,037	238	41,596
2014	11,507	24,712	11,258	4,106	2,297	202	54,085
2015	9,072	21,281	9,386	2,632	2,361	429	45,163
2016	9,071	22,306	11,850	1,662	2,024	450	47,364
2017	8,320	23,414	5,616	1,956	1,656	508	41,472
2018	8,007	28,235	5,182	2,833	691	957	45,907
2019	7,592	23,051	3,183	7,045	914	1,364	43,152
2020	4,352	29,370	6,411	1,459	894	110	42,599

Table 44: Bycatch estimates (t) of non-target species caught in the BSAI directed pollock fishery, 2003–2020, based on observer data as processed through the catch accounting system (NMFS Regional Office, Juneau, Alaska).

Year	Scypho.jellies	Misc.fish	Sea.star	Eulachon.Osmerid	Eelpouts	Grenadier	Sea.pen	Sea.anemone.unidentified	urchins.dollars.cucumbers	All.other
2003	5,643	101	89	9	7	20	0	0	0	2
2004	6,590	89	7	21	0	14	1	0	0	1
2005	5,197	158	9	12	1	14	1	0	0	9
2006	2,717	154	11	99	21	15	1	0	0	16
2007	2,403	204	5	138	118	27	3	0	0	12
2008	4,184	121	19	4	8	27	1	0	0	10
2009	8,117	135	9	5	4	4	2	1	0	5
2010	2,517	150	12	0	0	4	2	2	0	11
2011	8,232	277	27	1	1	1	2	1	0	9
2012	3,521	142	7	1	1	2	3	1	0	4
2013	5,294	121	15	0	1	1	2	2	0	10
2014	12,767	44	29	1	7	10	3	1	0	9
2015	4,950	90	41	24	10	4	2	2	0	5
2016	2,203	75	54	5	22	4	1	0	0	3
2017	6,152	48	12	3	18	2	0	1	0	2
2018	8,252	52	24	0	4	9	0	0	0	4
2019	3,889	73	50	0	2	8	0	0	1	4
2020	3,164	94	60	1	6	42	1	5	20	6



Table 46: Ecosystem considerations for BSAI pollock and the pollock fishery.

Indicator	Observation	Interpretation	Evaluation
<b>Ecosystem effects on EBS pollock</b>			
<i>Prey availability or abundance trends</i>			
Zooplankton	Stomach contents, AT and ichthyoplankton surveys, changes mean wt-at-age	Data improving, indication of increases from 2004–2009 and subsequent decreases (for euphausiids in 2012 and 2014)	Variable abundance indicates important recruitment (for prey)
<i>Predator population trends</i>			
Marine mammals	Fur seals declining, Steller sea lions increasing slightly	Possibly lower mortality on pollock	Probably no concern
Birds	Stable, some increasing some decreasing	Affects young-of-year mortality	Probably no concern
Fish (Pollock, Pacific cod, halibut)	Stable to increasing	Possible increases to pollock mortality	
<i>Changes in habitat quality</i>			
Temperature regime	Cold years pollock distribution towards NW on average	Likely to affect surveyed stock	Some concern, the distribution of pollock availability to different surveys may change systematically
Winter-spring environmental conditions	Affects pre-recruit survival	Probably a number of factors	Causes natural variability
Production	Fairly stable nutrient flow from upwelled BS Basin	Inter-annual variability low	No concern
<b>Fishery effects on ecosystem</b>			
<i>Fishery contribution to bycatch</i>			
Prohibited species	Stable, heavily monitored	Likely to be safe	No concern
Forage (including herring, Atka mackerel, cod, and pollock)	Stable, heavily monitored	Likely to be safe	No concern
HAPC biota	Likely minor impact	Likely to be safe	No concern
Marine mammals and birds	Very minor direct-take	Safe	No concern
Sensitive non-target species	Likely minor impact	Data limited, likely to be safe	No concern
Fishery concentration in space and time	Generally more diffuse	Mixed potential impact (fur seals vs Steller sea lions)	Possible concern
Fishery effects on amount of large size target fish	Depends on highly variable year-class strength	Natural fluctuation	Probably no concern
Fishery contribution to discards and offal production	Decreasing	Improving, but data limited	Possible concern
Fishery effects on age-at-maturity and fecundity	Maturity study (gonad collection) continues	NA	Possible concern

Table 47: Details and explanation of the decision table factors selected in response to the Plan Team requests (as originally proposed in the 2012 assessment).

Term	Description	Rationale
$P [F_{2021} > F_{MSY}]$	Probability that the fishing mortality in 2021 exceeds $F_{MSY}$	OFL definition is based on $F_{MSY}$
$P [B_{2022} < B_{MSY}]$	Probability that the spawning biomass in 2022 is less than $B_{MSY}$	$B_{MSY}$ is a reference point target and biomass in 2021 provides an indication of the impact of 2021 fishing
$P [B_{2023} < B_{MSY}]$	Probability that the spawning biomass in 2023 is less than $B_{MSY}$	$B_{MSY}$ is a reference point target and biomass in 2023 provides an indication of the impact of fishing in 2021 and 2022
$P [B_{2023} < \bar{B}]$	Probability that the spawning biomass in 2022 is less than the 1978–2020 mean	To provide some perspective of what the stock condition might be relative to historical estimates after fishing in 2021.
$P [B_{2025} < \bar{B}]$	Probability that the spawning biomass in 2025 is less than the long term mean	To provide some perspective of what the stock condition might be relative to historical estimates after fishing in 2021.
$P [B_{2025} < B_{2021}]$	Probability that the spawning biomass in 2025 is less than that estimated for 2021	To provide a medium term expectation of stock status relative to 2021 levels
$P [B_{2023} < B_{20\%}]$	Probability that the spawning biomass in 2023 is less than $B_{20\%}$	$B_{20\%}$ had been selected as a Steller Sea Lion lower limit for allowing directed fishing
$P [p_{a_5,2023} > \bar{p}_{a_5}]$	Probability that in 2023 the proportion of age 1–5 pollock in the population exceeds the long-term mean	To provide some relative indication of the age composition of the population relative to the long term mean.
$P [D_{2022} < D_{1994}]$	Probability that the diversity of ages represented in the spawning biomass (by weight) in 2022 is less than the value estimated for 1994	To provide a relative index on the abundance of different age classes in the 2022 population relative to 1994 (a year identified as having low age composition diversity)
$P [D_{2025} < D_{1994}]$	Probability that the diversity of ages represented in the spawning biomass (by weight) in 2025 is less than the value estimated for 1994	To provide a medium-term relative index on the abundance of different age classes in the population relative to 1994 (a year identified as having low age composition diversity)
$P [E_{2021} > E_{2020}]$	Probability that the theoretical fishing effort in 2021 will be greater than that estimated in 2020.	To provide the relative effort that is expected (and hence some idea of costs).

Table 48: Outcomes of decision (expressed as chances out of 100) given different 2021 catches (first row, in kt). Note that for the 2018 and later year-classes average values were assumed. Constant Fs based on the 2021 catches were used for subsequent years.

	10	850	1000	1150	1350	1300	1450	1600
$P[F_{2021} > F_{MSY}]$	0	1	5	13	29	25	36	47
$P[B_{2022} < B_{MSY}]$	14	28	32	35	41	39	44	48
$P[B_{2023} < B_{MSY}]$	8	23	27	32	39	37	43	49
$P[B_{2022} < \bar{B}]$	34	84	89	93	96	96	97	98
$P[B_{2025} < \bar{B}]$	4	28	35	41	50	48	54	60
$P[B_{2025} < B_{2021}]$	3	19	23	28	34	33	38	42
$P[B_{2023} < B_{20\%}]$	0	1	1	1	2	2	2	3
$P[p_{a_5,2023} > \bar{p}_{a_5}]$	20	66	72	76	81	80	83	85
$P[D_{2022} < D_{1994}]$	0	0	0	0	0	0	0	0
$P[D_{2025} < D_{1994}]$	0	4	5	8	12	11	14	19
$P[E_{2021} > E_{2020}]$	0	4	22	47	74	69	82	90

## Figures

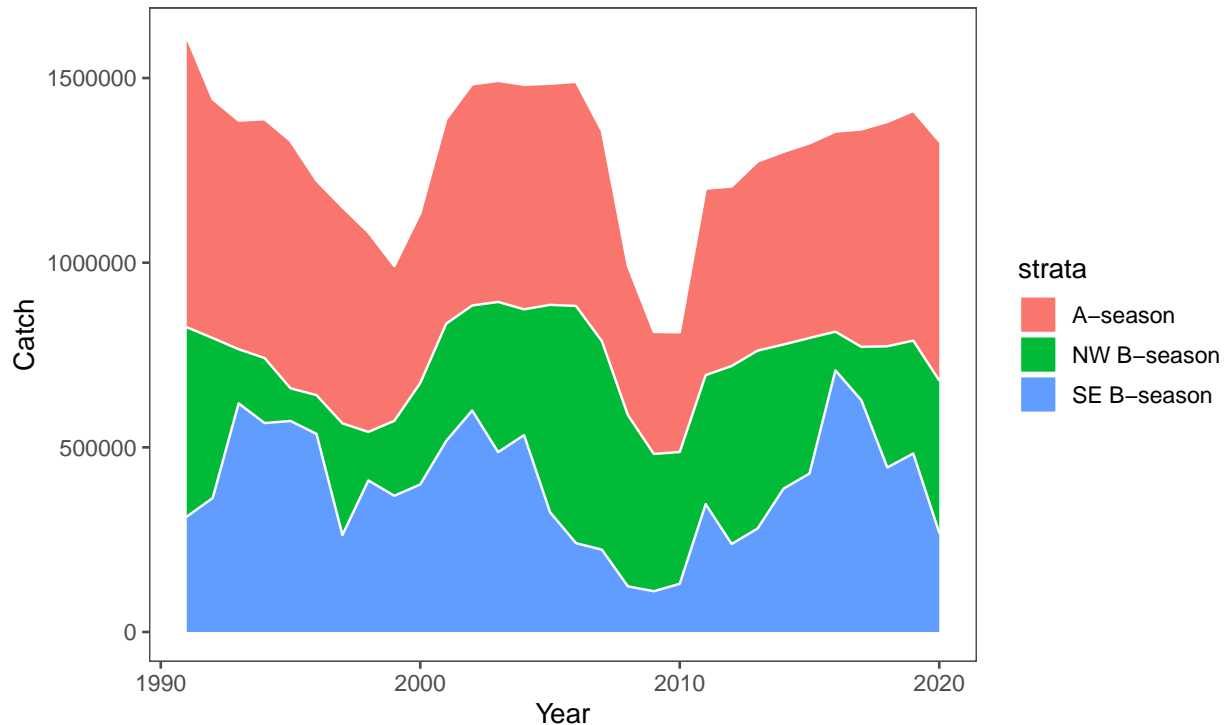


Figure 1: Pollock catch estimates ( $t$ ) from the Eastern Bering Sea by season and region. The A-season is defined as from Jan-May and B-season from June-October.

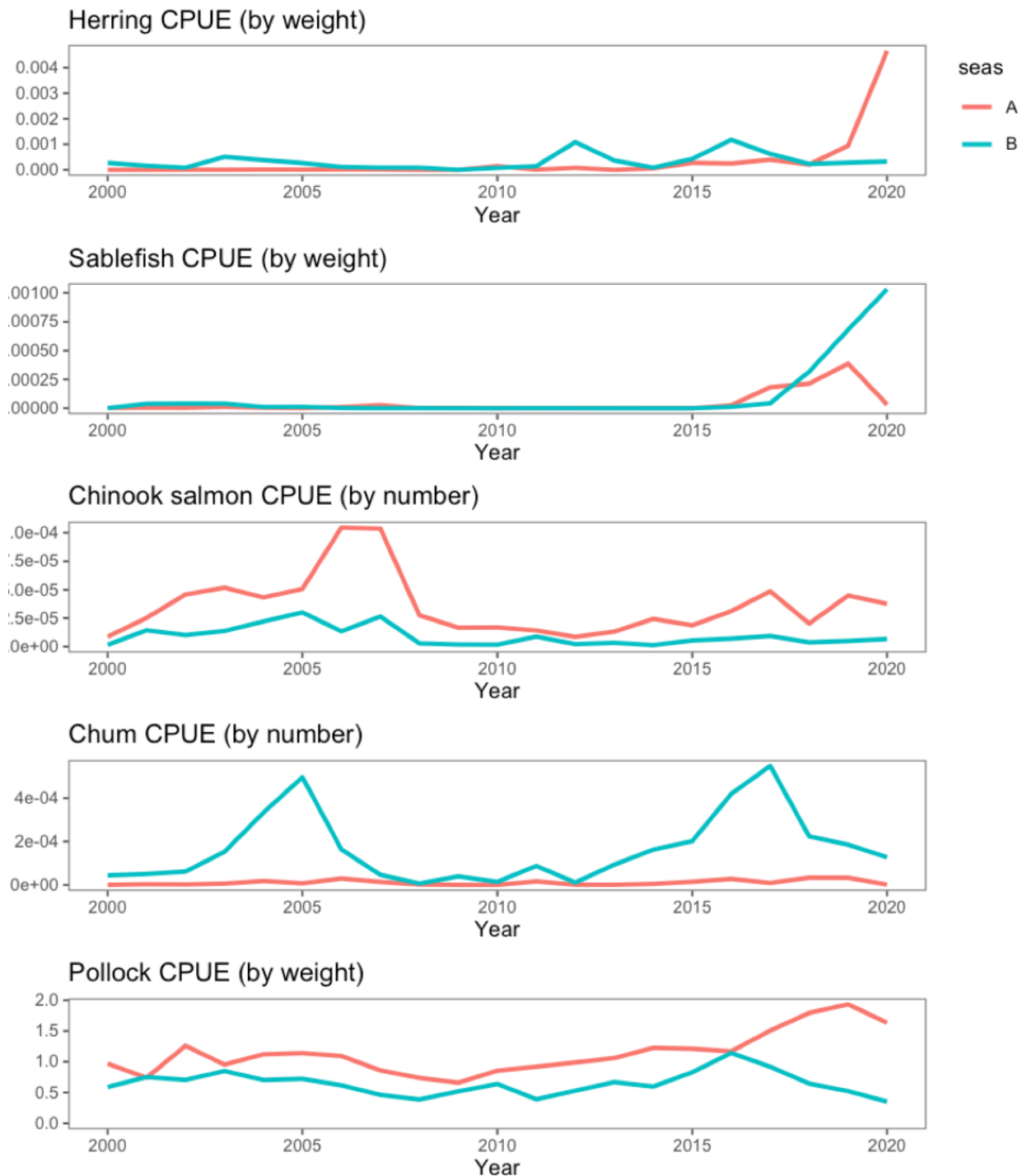


Figure 2: Nominal catch divided by effort (hours towed) for some bycatch species and pollock for the EBS pollock fleet (sectors combined), 2000-2020.

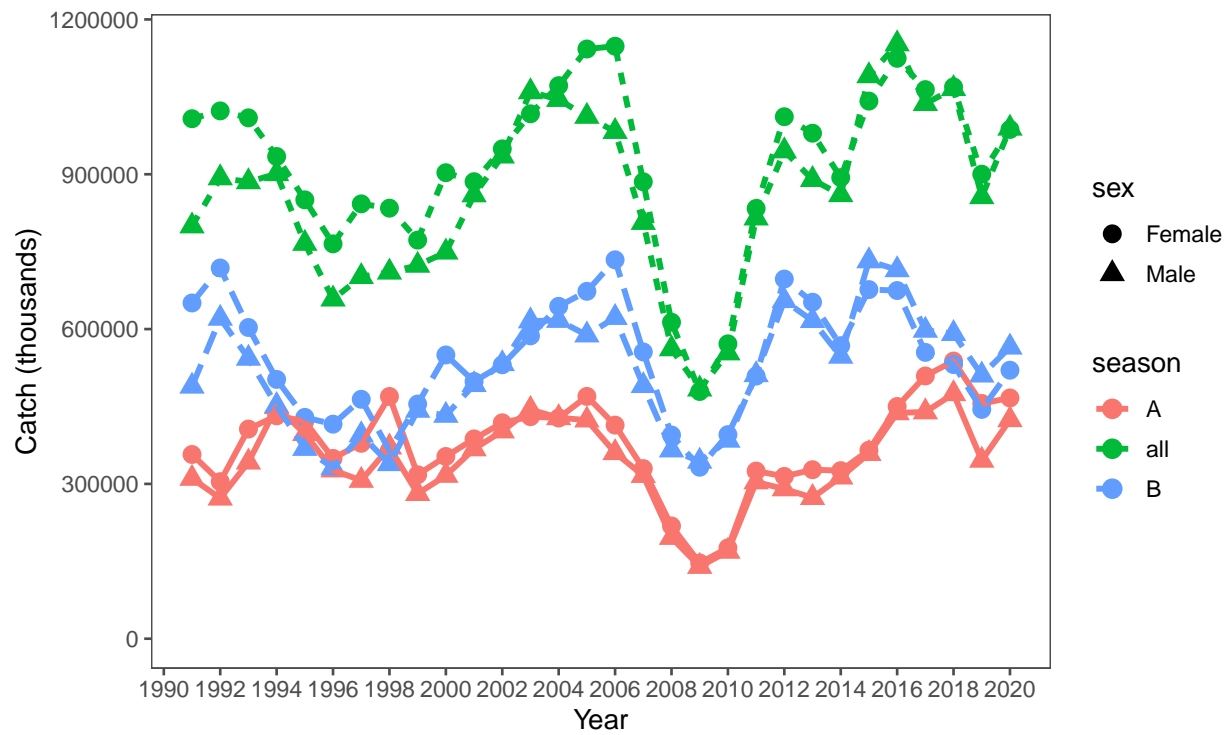


Figure 3: Estimate of EBS pollock catch numbers by sex for the A season (January-May) and B seasons (June-October) and total.

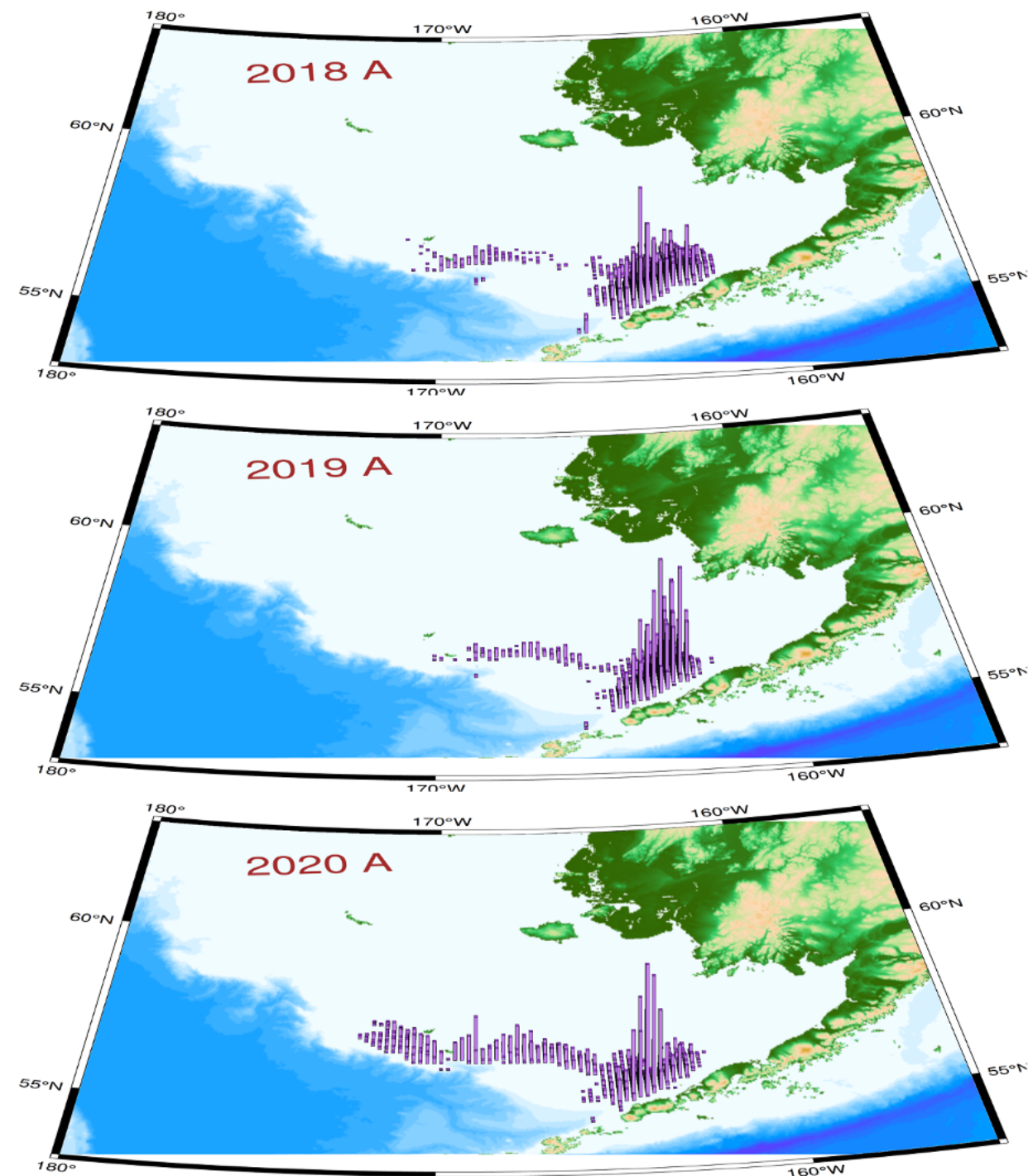


Figure 4: EBS pollock catch distribution during A-season, 2018–2020. Column height is proportional to total catch.

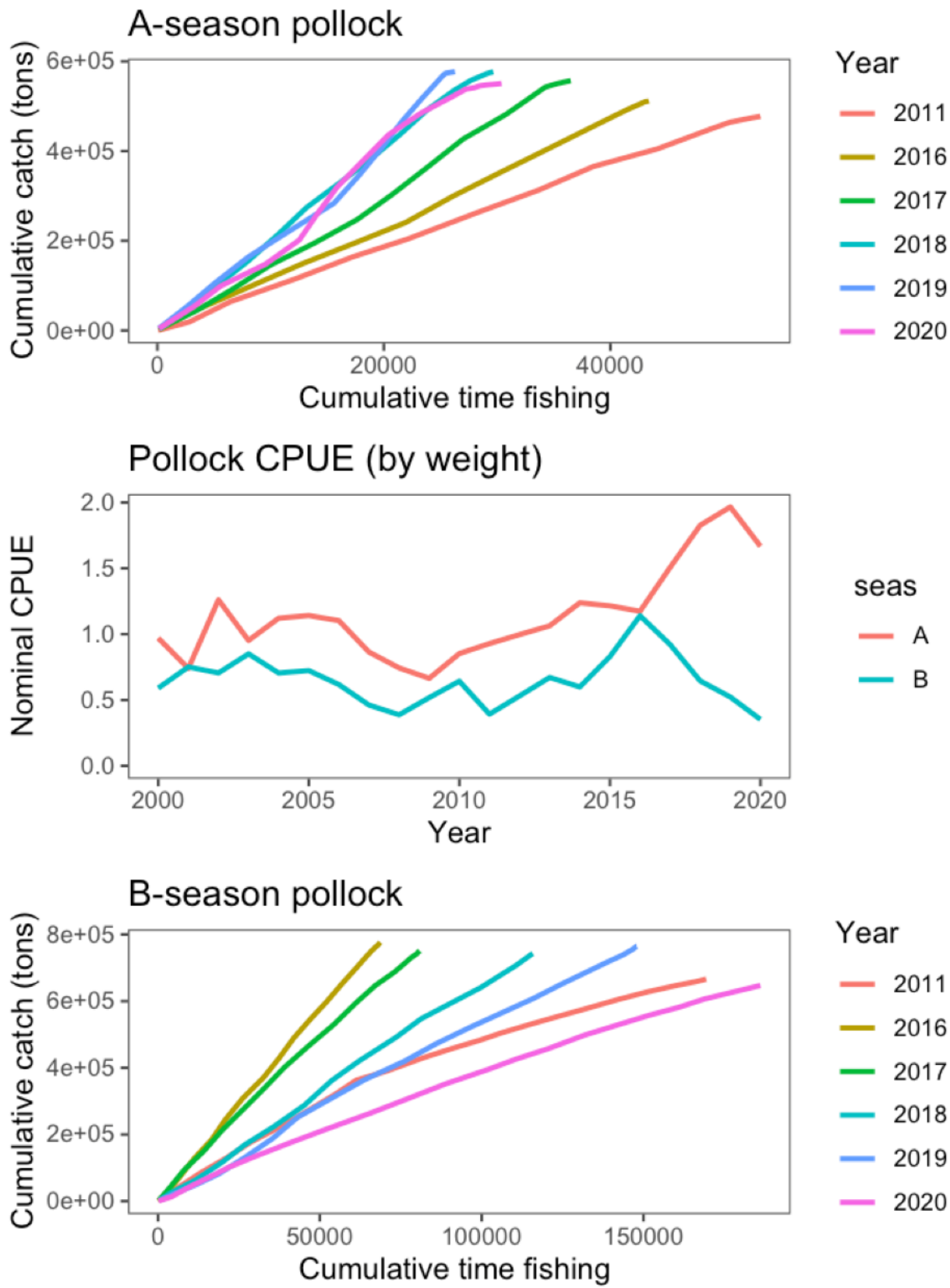


Figure 5: A-season (top) and B-season (bottom) EBS fleet-wide nominal pollock catch (kg) per hour of fishing recorded by NMFS scientific observers along with the catch divided by effort (hours) by season since 2000 (middle panel).

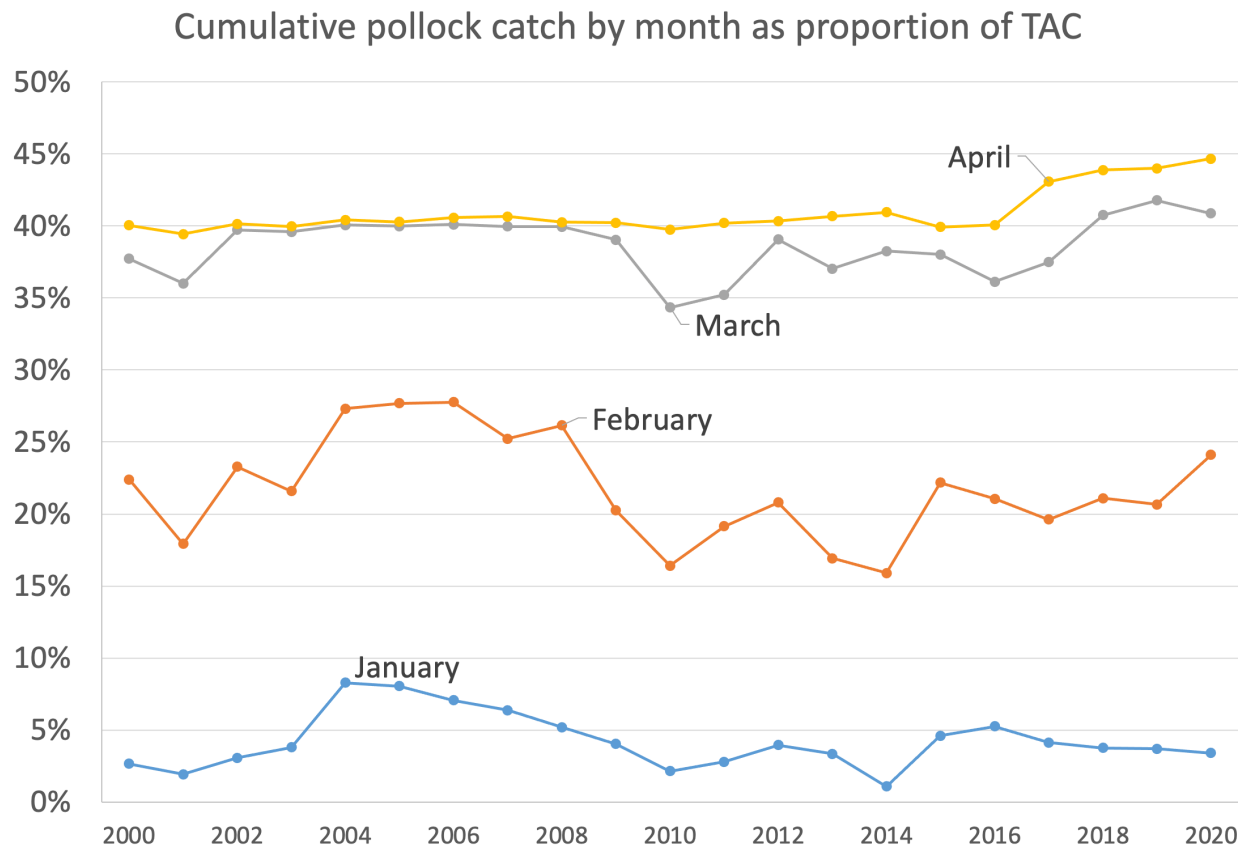


Figure 6: Proportion of the annual EBS pollock TAC by month during the A-season, 2000–2020. The higher value observed since 2017 was due to Amendment 110 of the FMP to allow greater flexibility to avoid Chinook salmon.

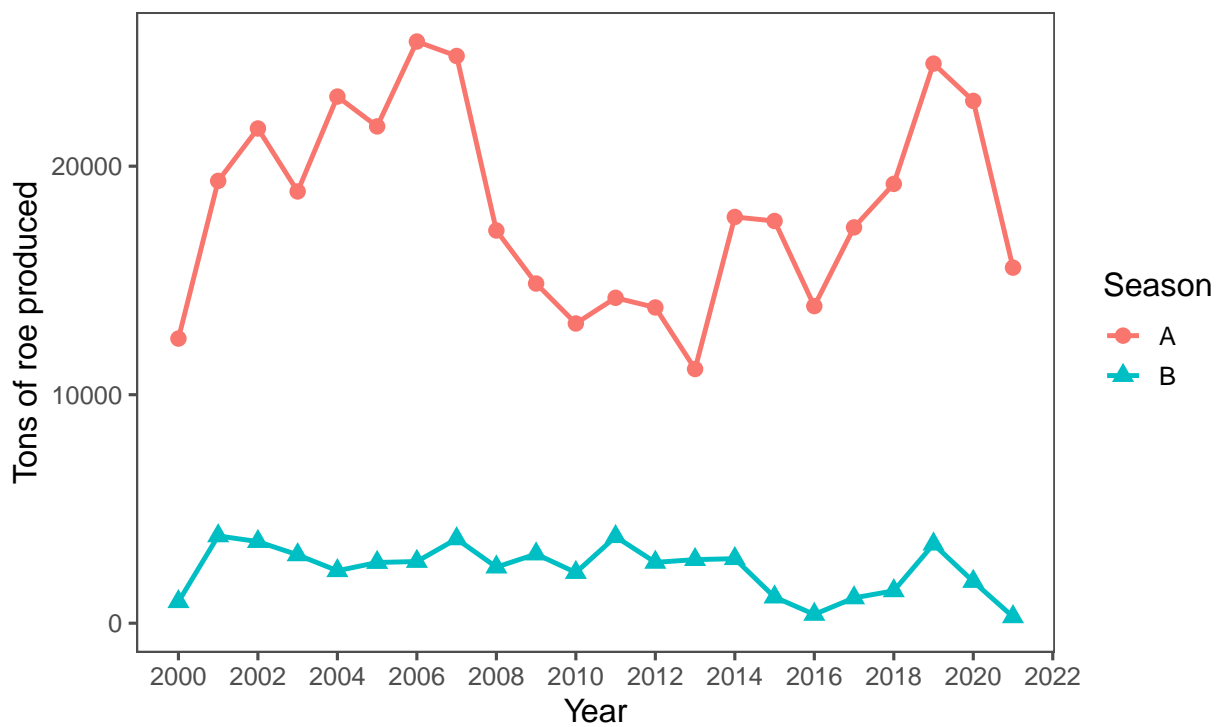


Figure 7: EBS pollock roe production in A and B seasons , 2000-2020.

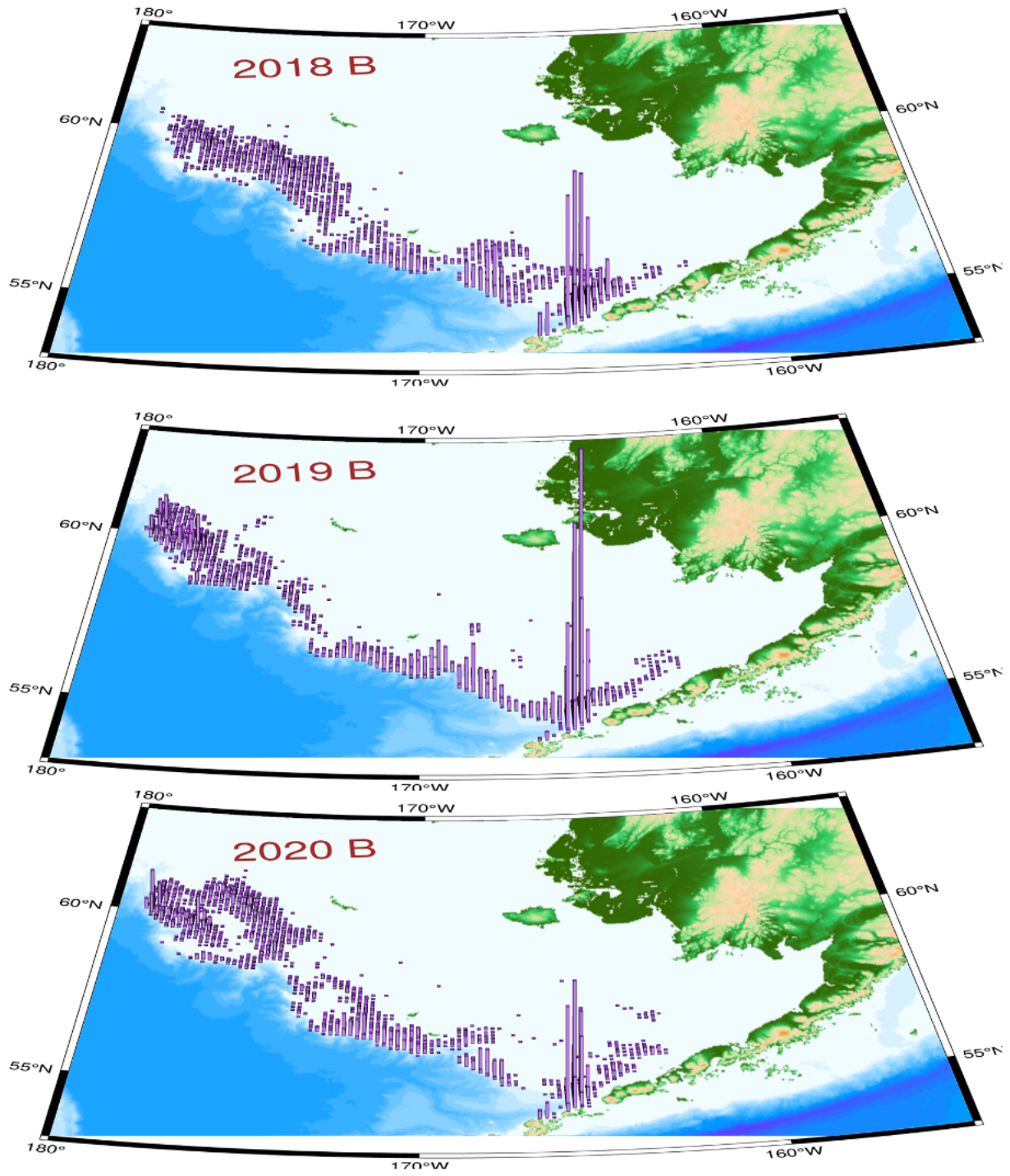


Figure 8: EBS pollock catch distribution during B-season, 2018–2020. Column height is proportional to total catch. Note that directed fishery for pollock generally is finished prior to October; the labels are indicative full-year catches.

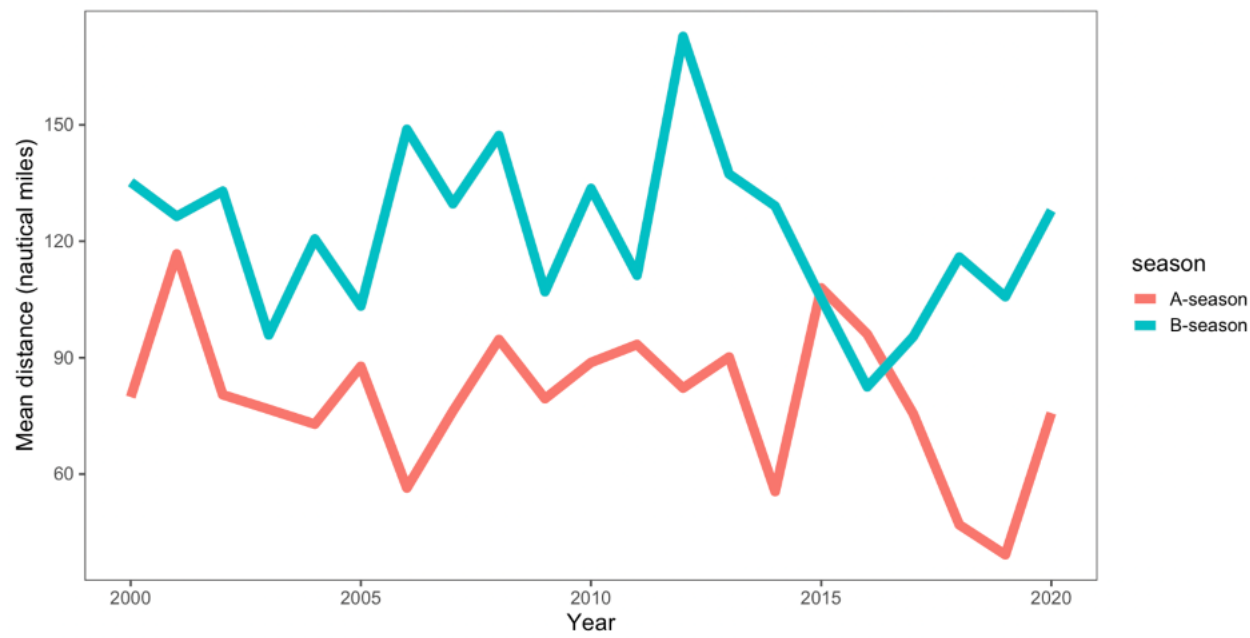


Figure 9: Estimated mean daily distance between operations, 2000-2020.

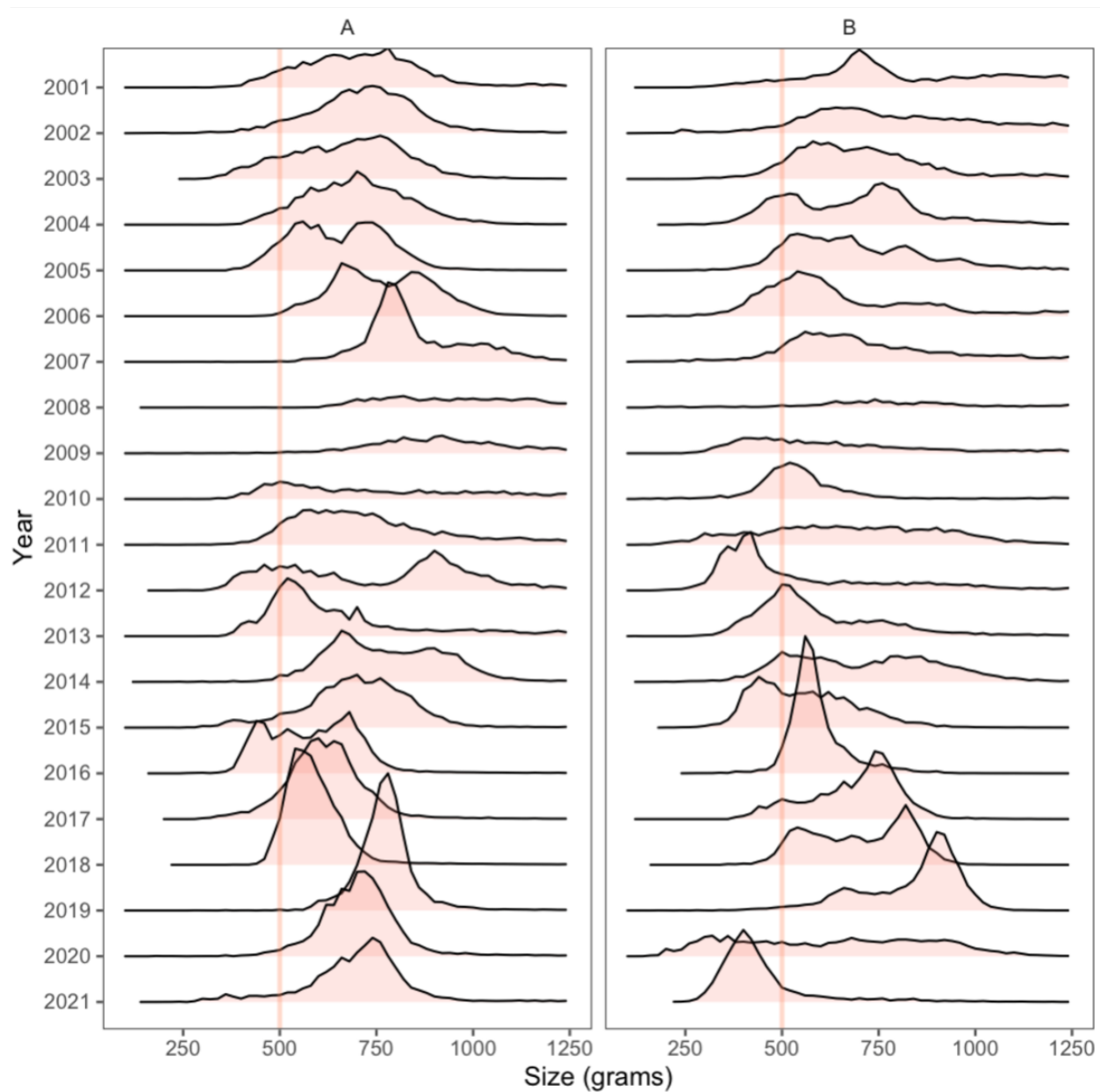


Figure 10: Pollock fishery data showing the weight-frequency (50 g increments) by year and season.

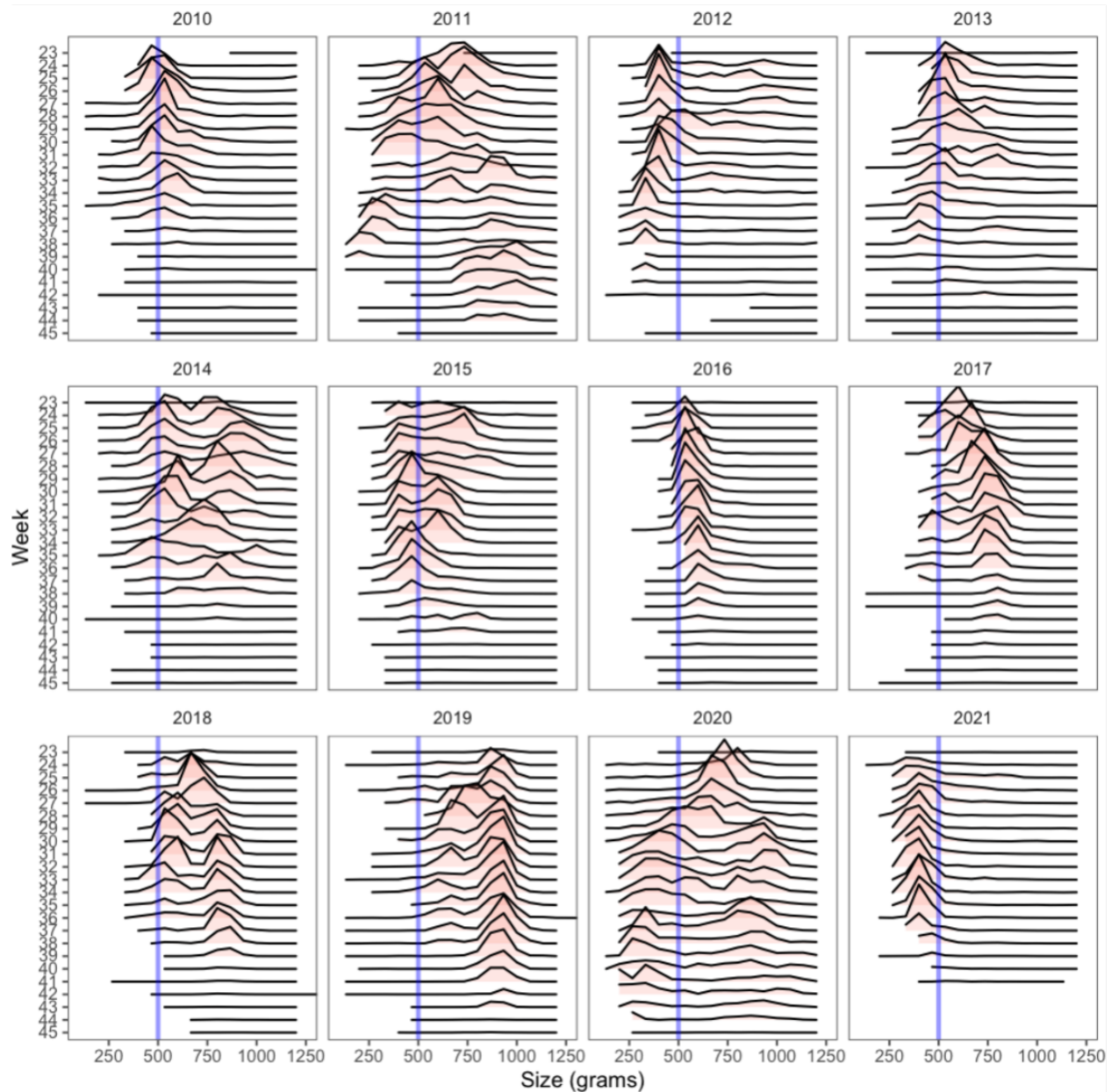


Figure 11: Pollock fishery data showing the weight-frequency (50 g increments) by recent years and weeks of the B-season.

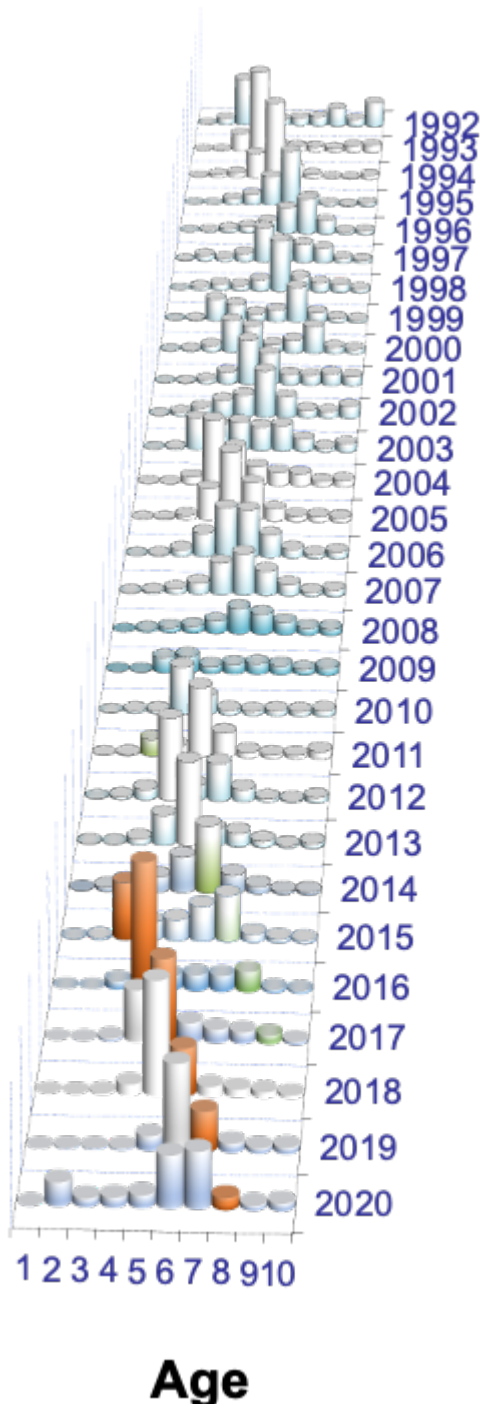


Figure 12: EBS pollock fishery estimated catch-at-age data (in number) for 1992–2019. Age 10 represents pollock age 10 and older. The 2012 year-class is shaded in orange.

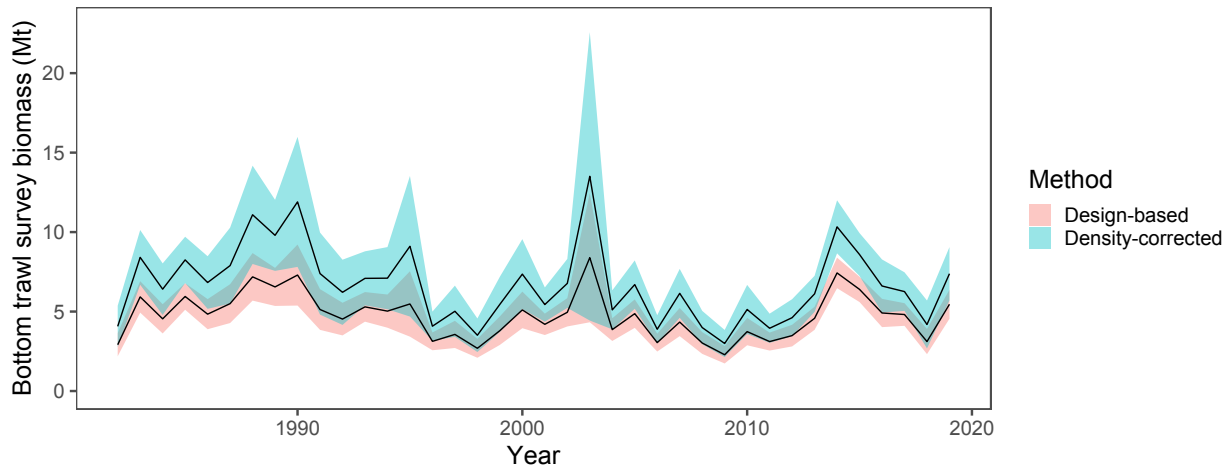


Figure 13: Bottom-trawl survey biomass estimates with error bars representing 1 standard deviation (for design-based and density-dependent correction method) for EBS pollock.

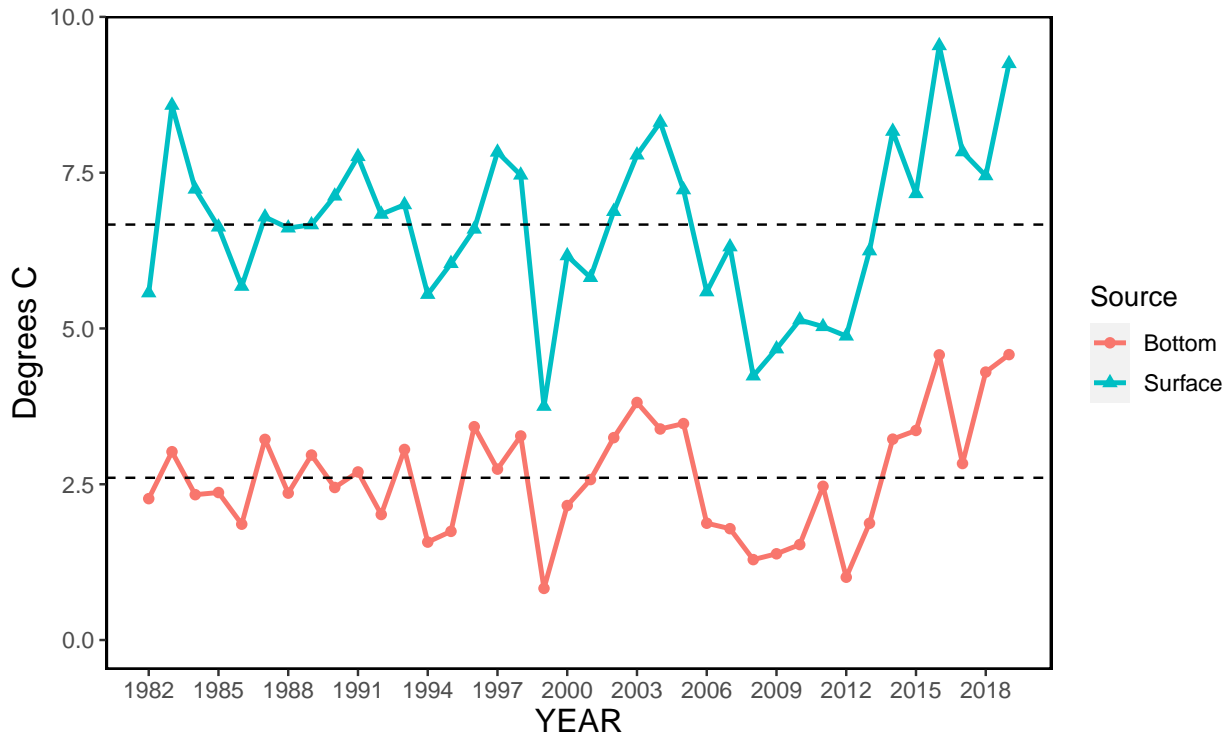


Figure 14: Bottom and surface temperatures for the Bering Sea from the NMFS summer bottom-trawl surveys (1982–2019). Dashed lines represent mean values.

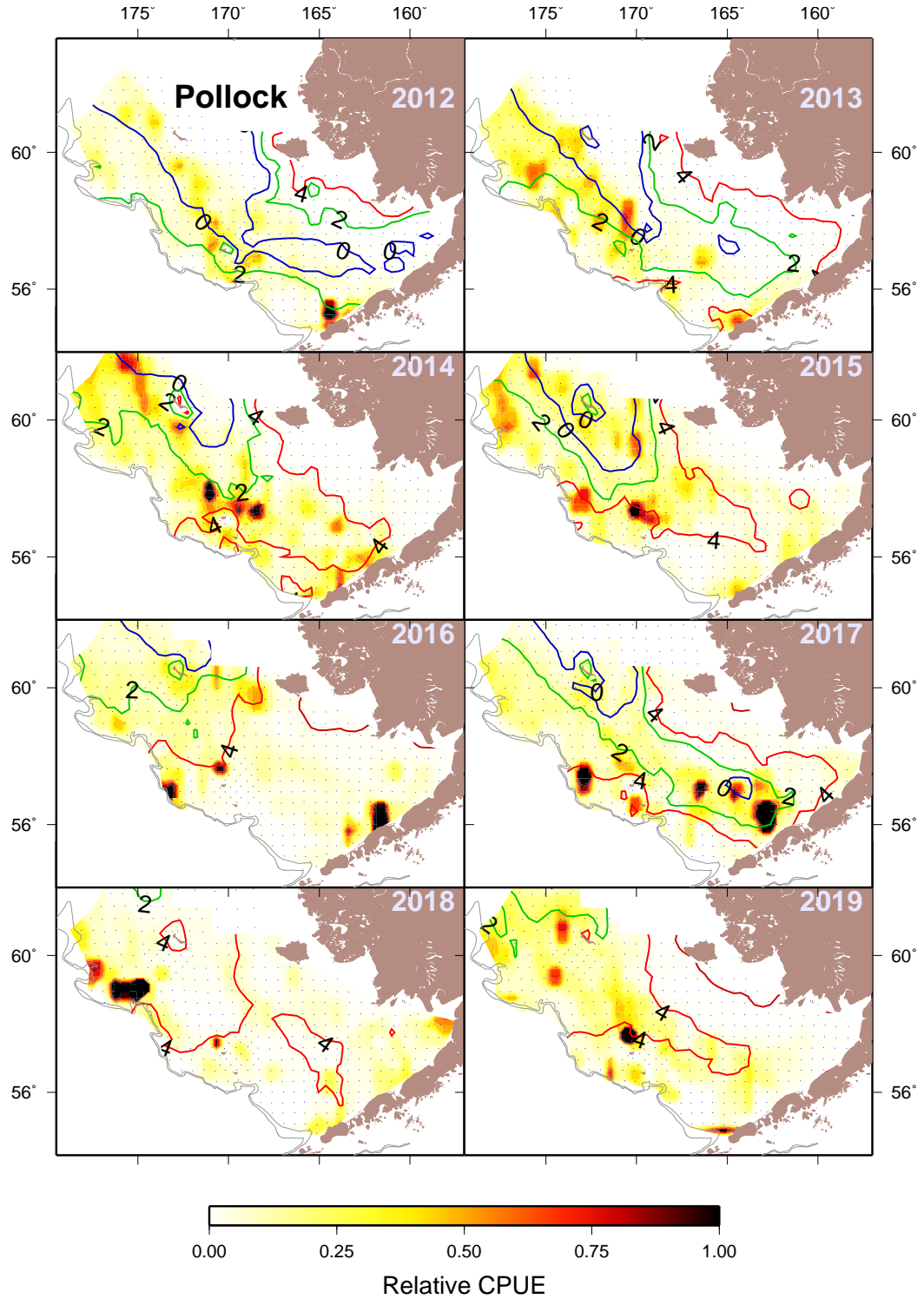


Figure 15: EBS pollock CPUE (shades = relative kg/hectare) and bottom temperature isotherms in degrees C; from the bottom trawl survey data 2011–2019.

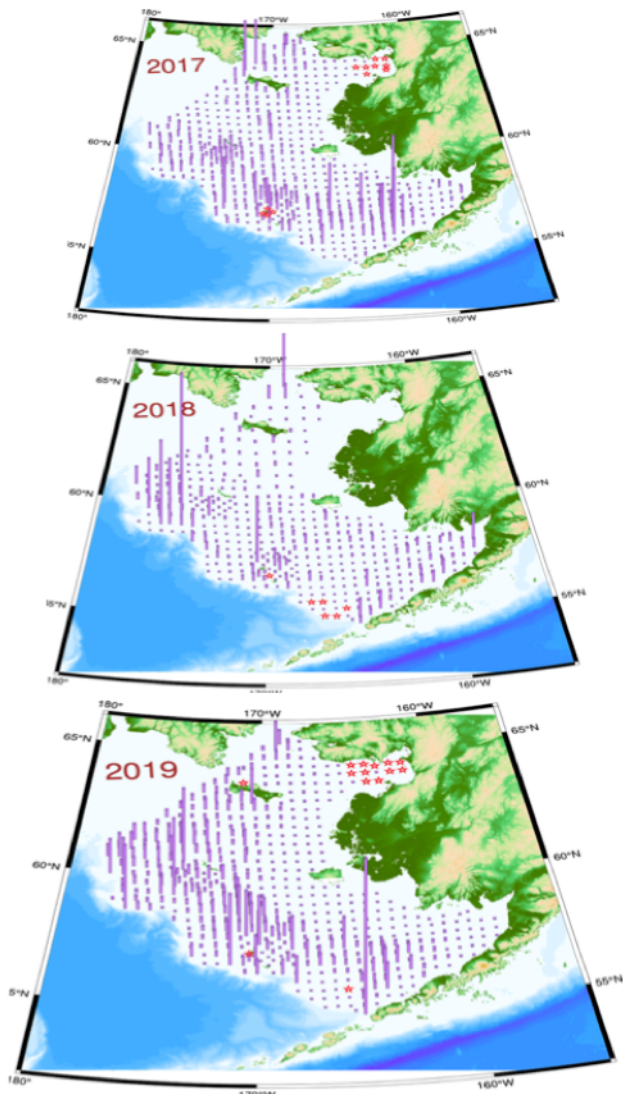


Figure 16: Bottom trawl survey pollock catch in kg per hectare for 2017 - 2019. Height of vertical lines are proportional to station-specific pollock densities by weight (kg per hectare) with constant scales for all years (red stars indicate tows where pollock were absent from the catch).

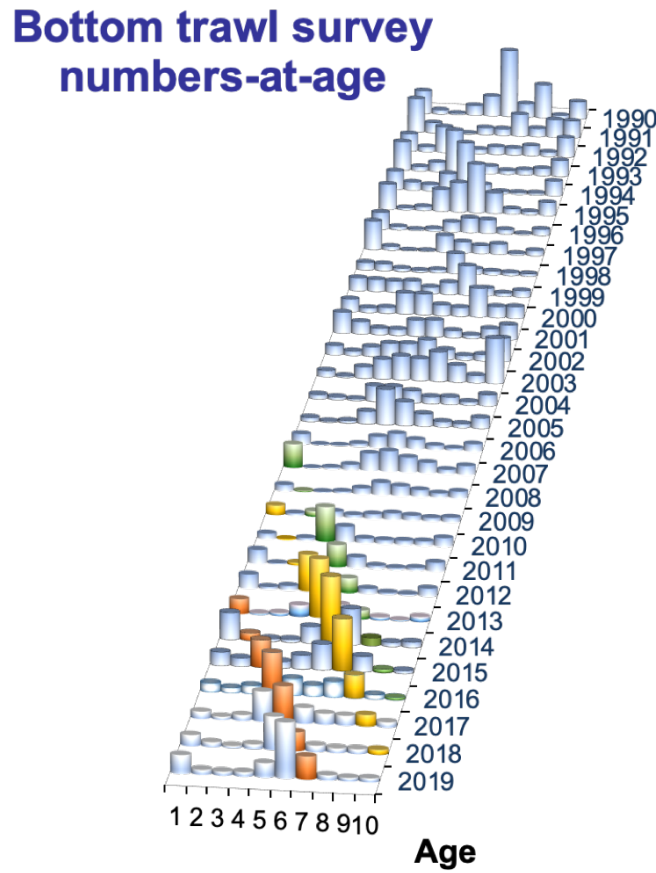


Figure 17: Pollock abundance levels by age and year as estimated directly from the NMFS bottom-trawl surveys (1990–2019). The 2006, 2008, and 2012 year-classes are shaded differently.

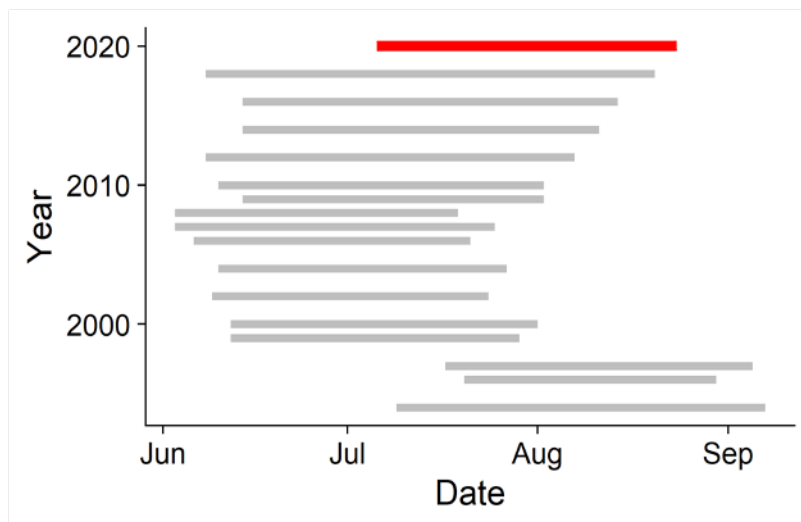


Figure 18: Timing of Acoustic surveys used in the time series. The 2020 USV survey is shown in red.

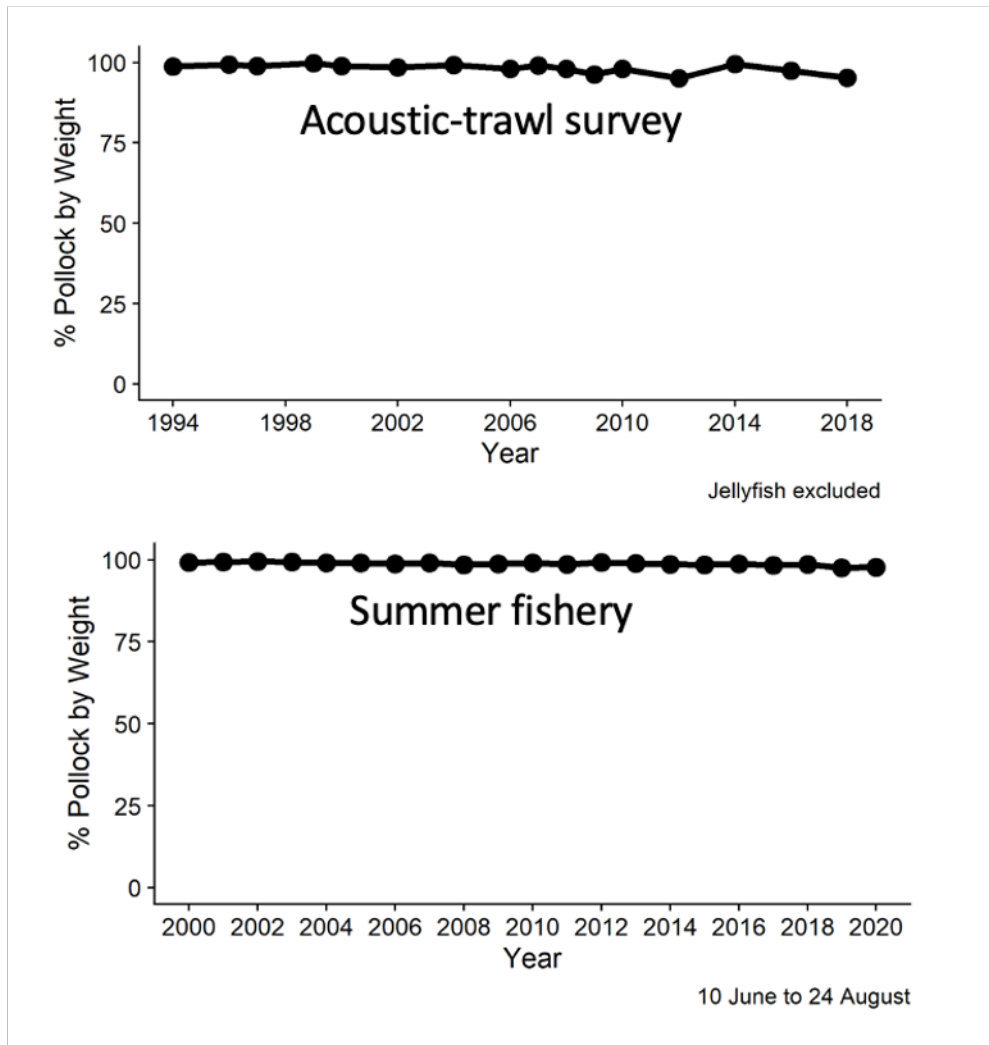


Figure 19: Pollock dominate the catch in historical midwater AT surveys (top panel) and during the summer pollock fishery (bottom panel) in the EBS. Jellyfish, which are very weak acoustic scatterers compared to fishes with a swimbladder have been excluded from the survey catch summaries.

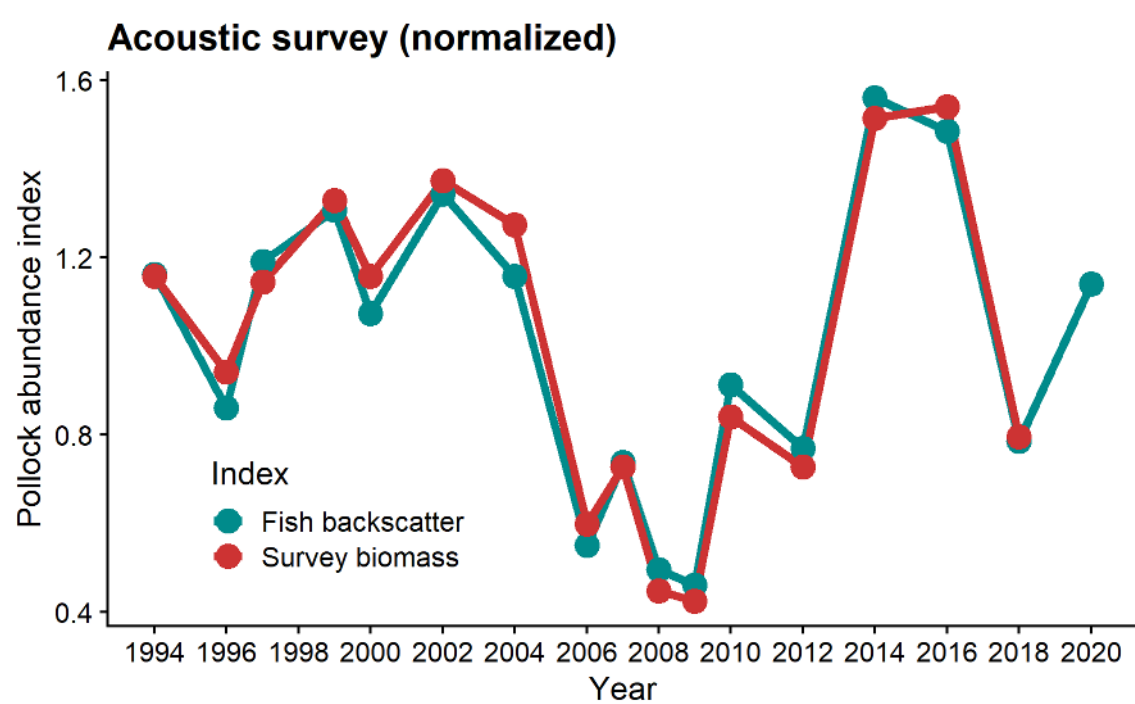


Figure 20: Acoustic backscatter in historical acoustic-trawl surveys compared with the biomass resulting from the survey. Both indices have been normalized to have a mean of 1 over the period 1994-2018 so that they can be directly compared.

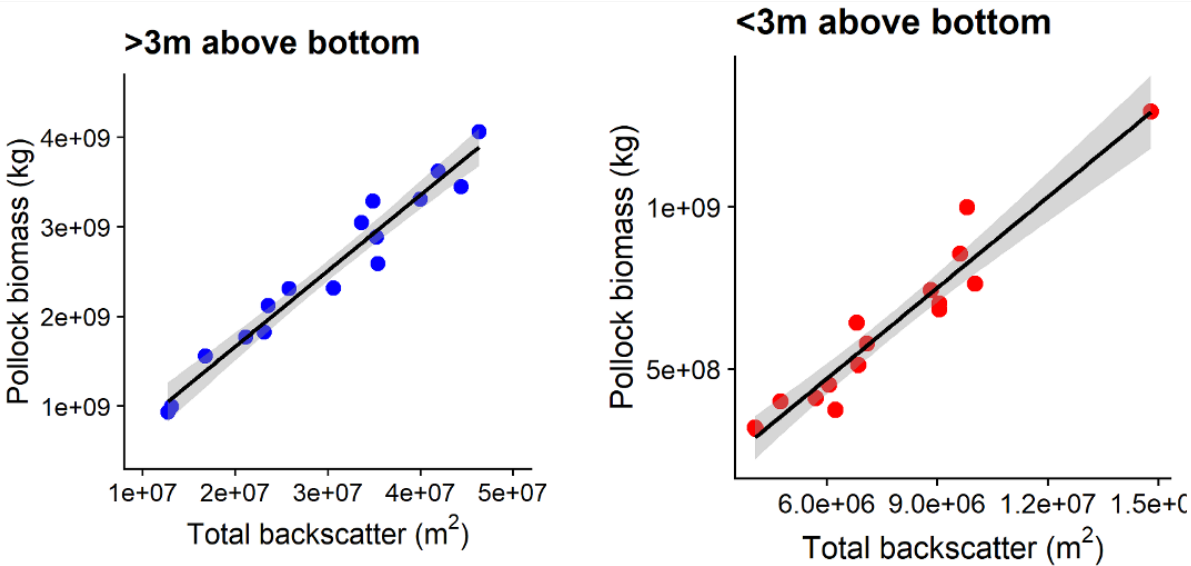


Figure 21: Scatterplots of total backscatter and pollock biomass for acoustic-trawl surveys from 1994-2018. Results for >3m above the seafloor are shown in the left panel and results for the 0.5 to 3m above the seafloor are shown in the right panel.

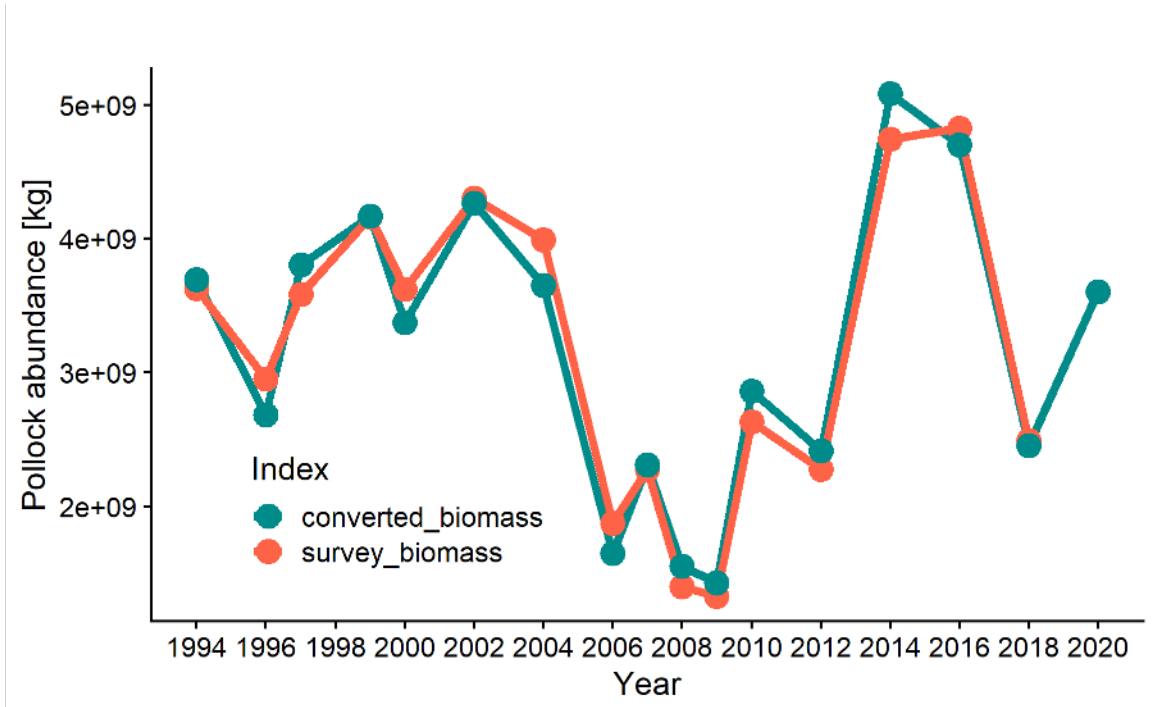


Figure 22: Time series of observed biomass (i.e. ‘survey biomass’) and biomass estimated by dropping all trawl data in that year and predicting survey biomass based on trawl sampling in the other years of the time series (‘converted biomass’). In 2020, no trawling was conducted, and the biomass estimate was predicted based on the average relationships established in previous years (see previous figure). The average discrepancy between the predicted and converted biomass is 5.4% (range 0.1 to 11%).

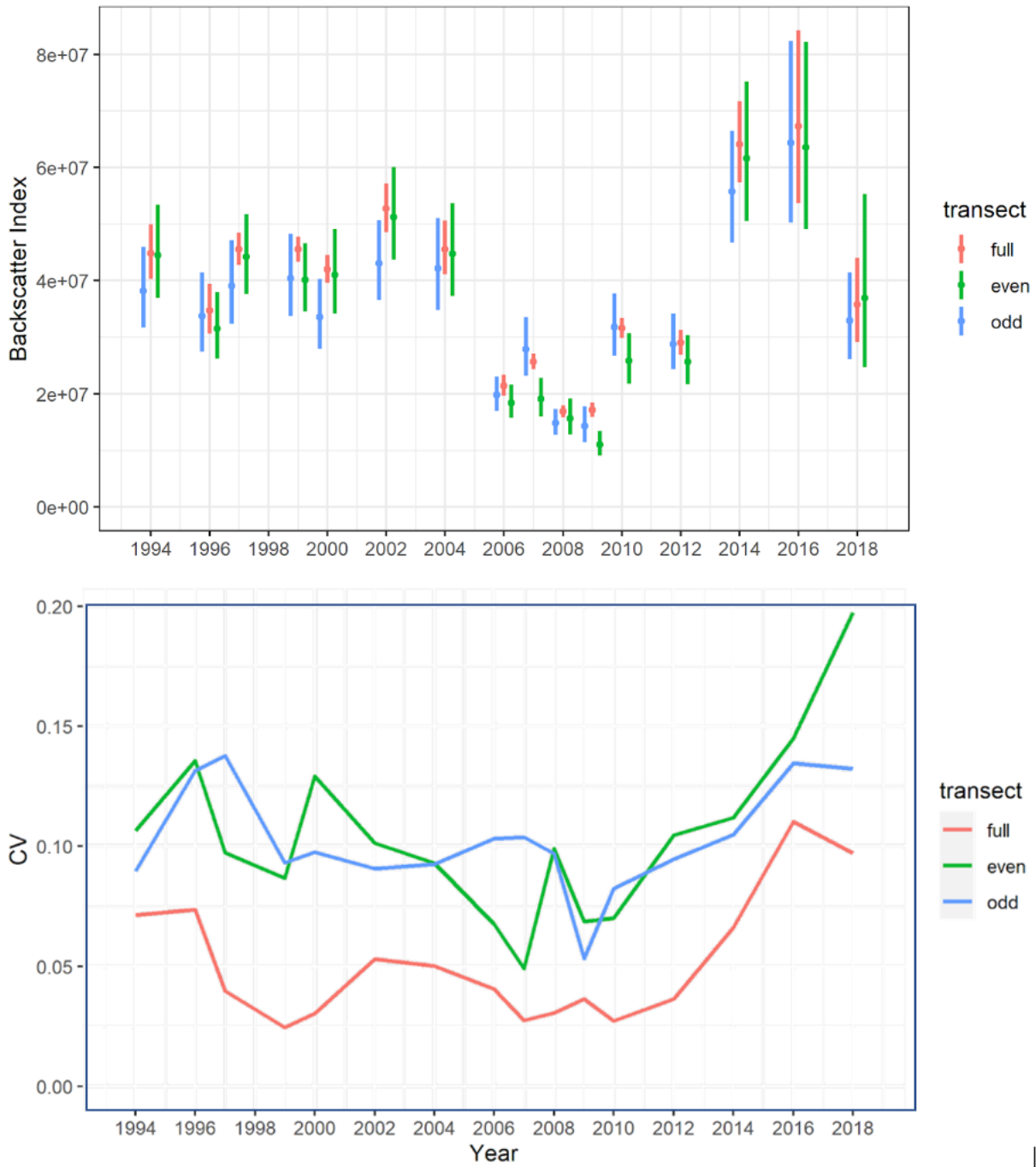


Figure 23: An evaluation of the impact on historical pollock ATS biomass estimates if alternate transects were dropped (and uncertainty increases as depicted by vertical error bars) compared to the actual (full) number of survey transects.

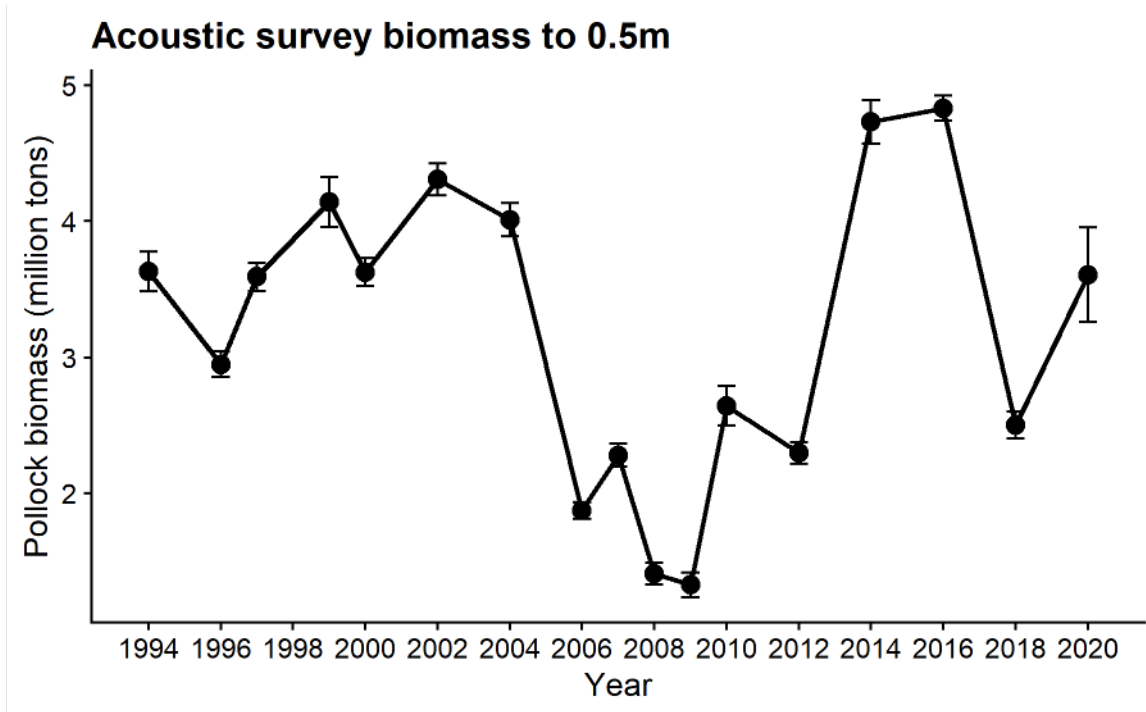


Figure 24: Acoustic-trawl survey pollock biomass time series. Error bars correspond to the relative estimation error (i.e. CV) estimated with a 1-D geostatistical technique. The 2020 survey was conducted with USVs, and has larger errors associated with the estimate that incorporate the effects of reduced sampling effort (i.e. 40 nmi spaced transects rather than 20 nmi transects), and the method used to convert backscatter to biomass conversion.

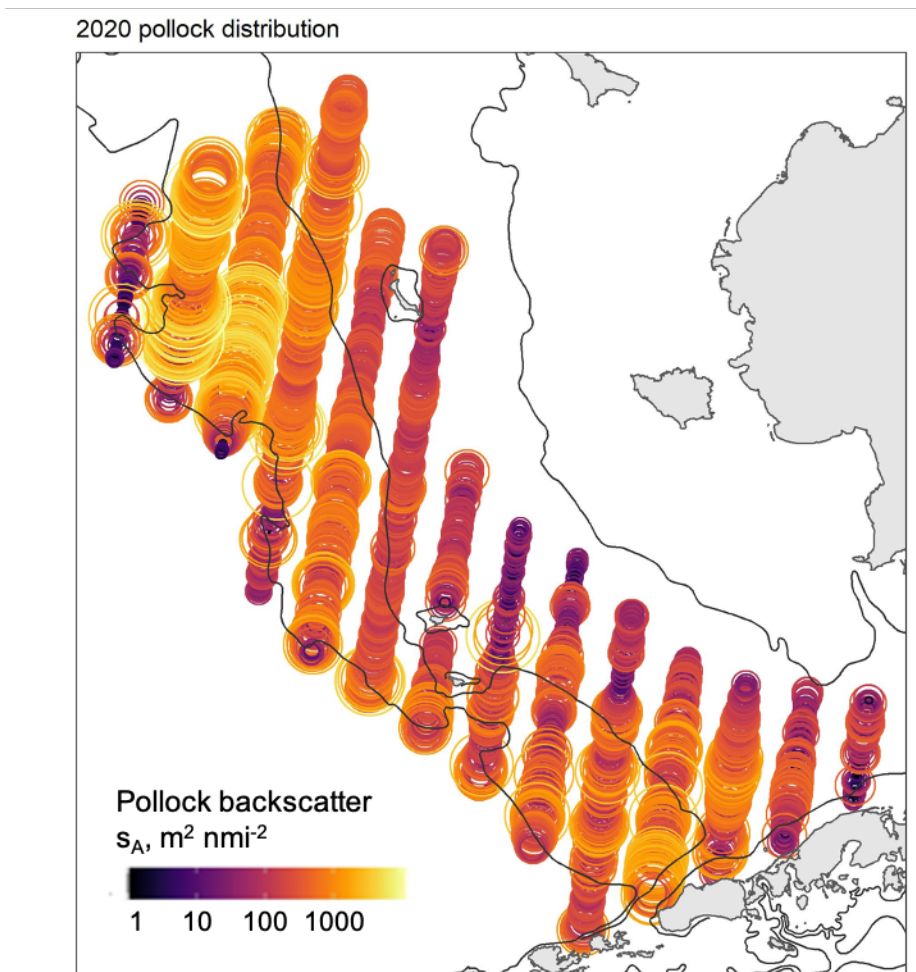


Figure 25: Map of backscatter measurements during the 2020 USV acoustic survey. The size and color of each point represents the mean acoustic backscatter attributed to pollock in a 0.5 nmi transect segment.

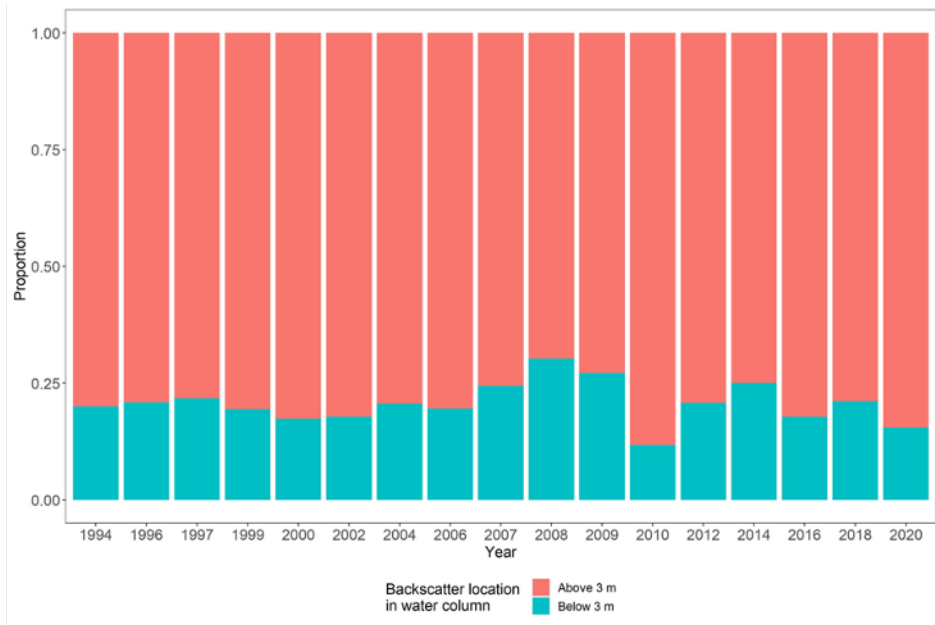


Figure 26: Proportion of pollock backscatter above and below 3m above bottom observed in acoustic-trawl surveys.

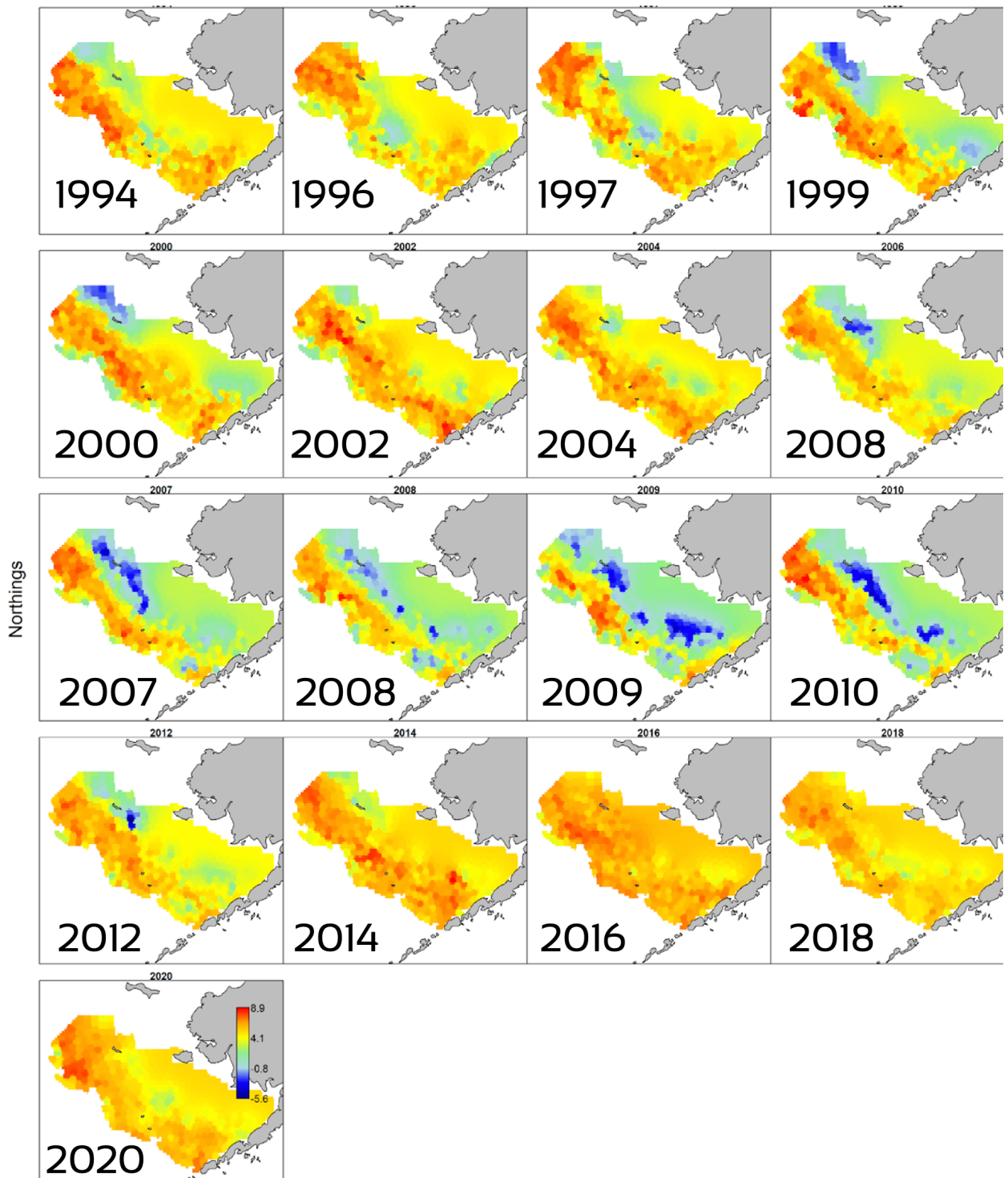


Figure 27: Predicted log-backscatter (arbitrary units) from the VAST model fitted to the AT data, where the 2020 data are from the USV.

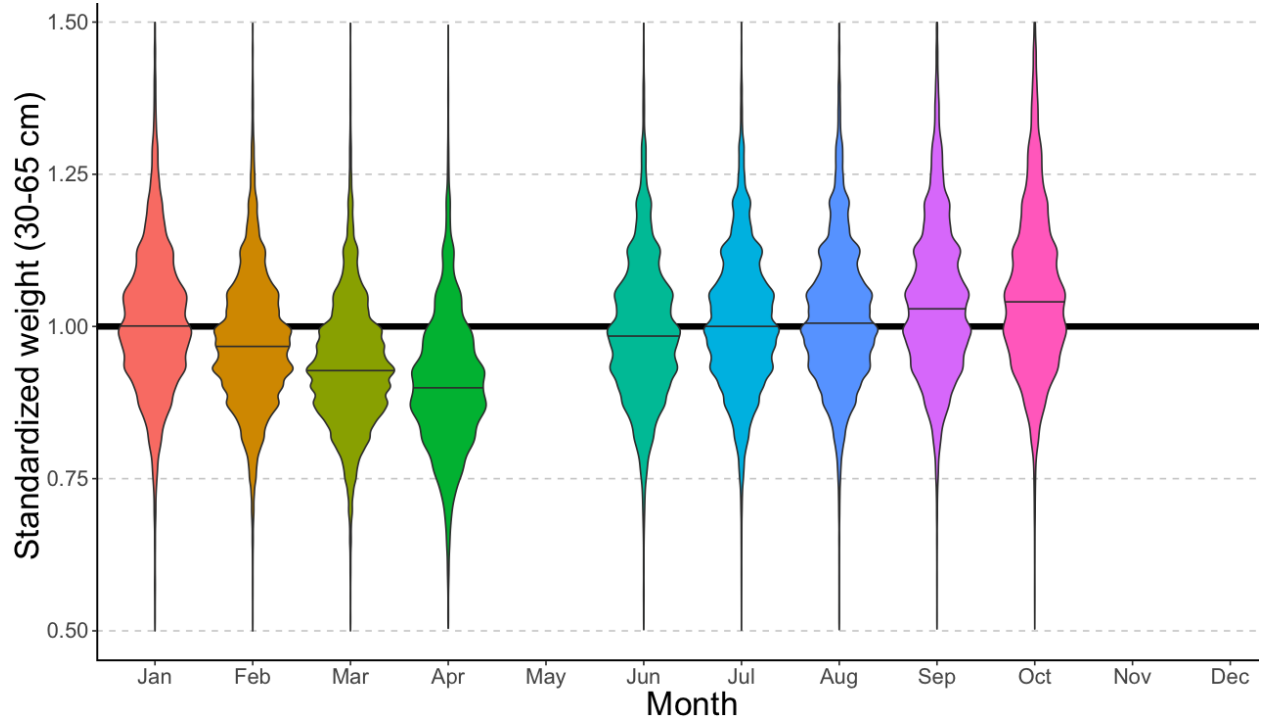


Figure 28: EBS pollock fishery body mass (given length) anomaly (standardized by overall mean body mass at each length) by month based on some over 700 thousand fish measurements from 1991–2019.

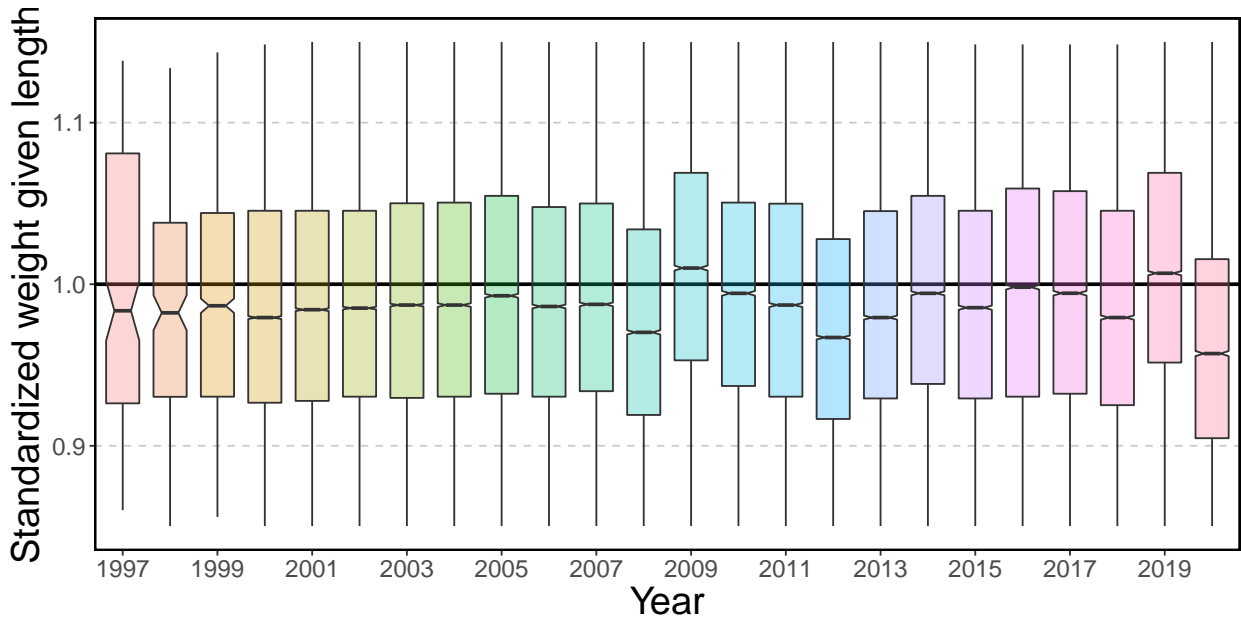


Figure 29: EBS pollock body mass (given length) anomaly (standardized by overall mean body mass at each length) by year, 1991–2020.

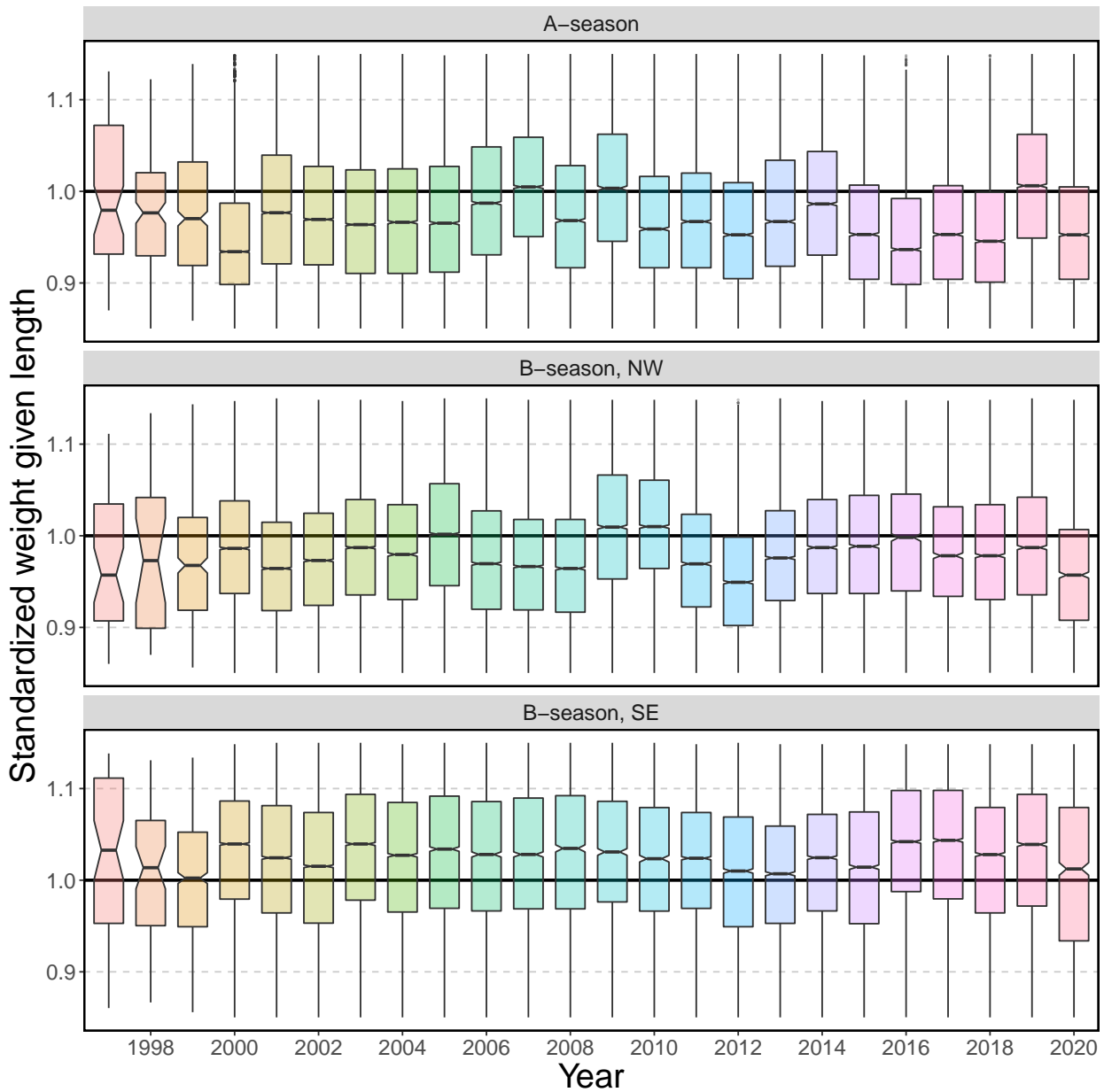


Figure 30: EBS pollock fishery body mass (given length) anomaly (standardized by overall mean body mass at each length) by year and season/area strata, 1991–2020.

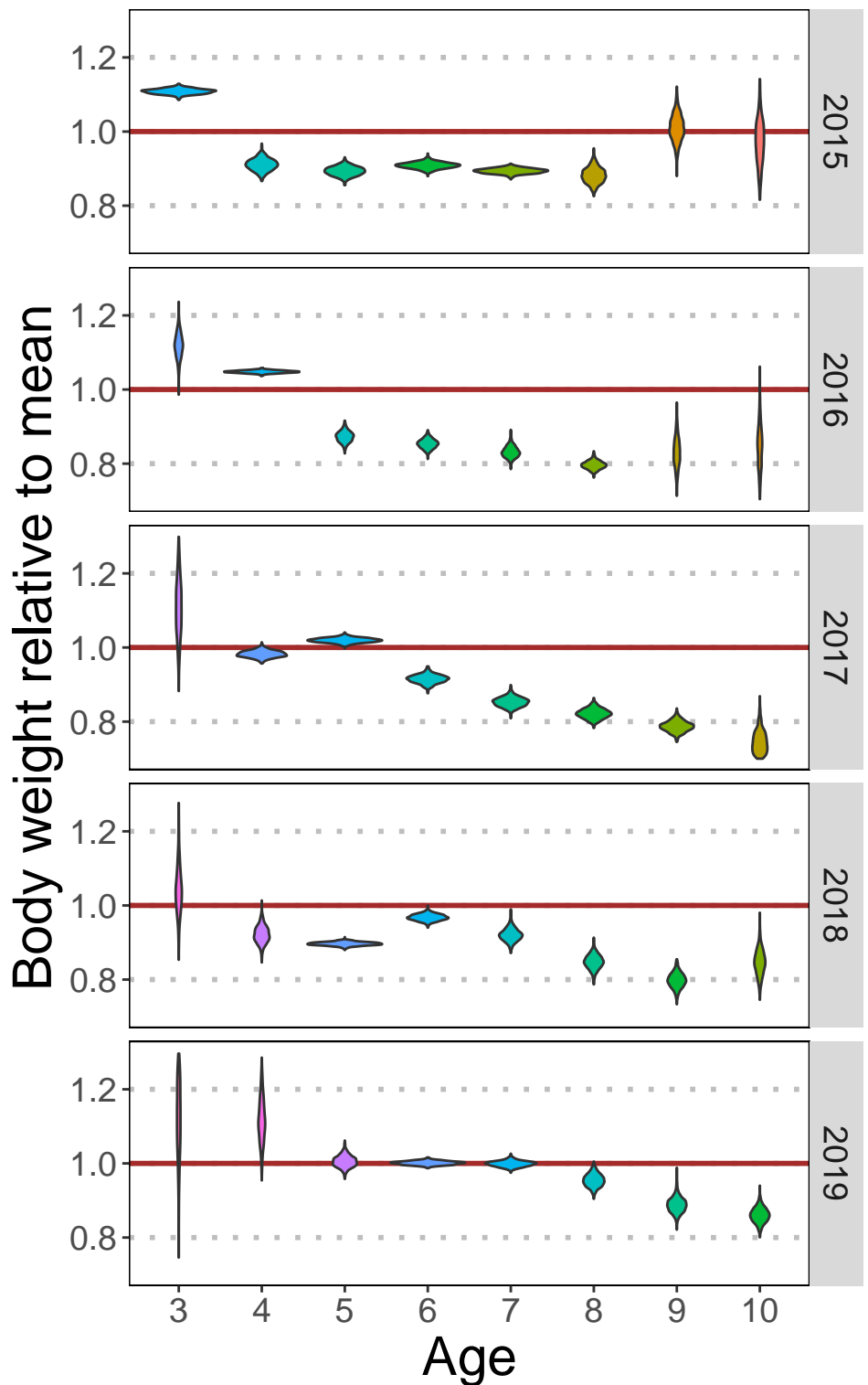


Figure 31: Recent fishery average weight-at-age anomaly (relative to mean) by strata for ages 3–10, 2015–2019. Vertical shape reflects uncertainty in the data (wider shapes being more precise), colors are consistent with cohorts.

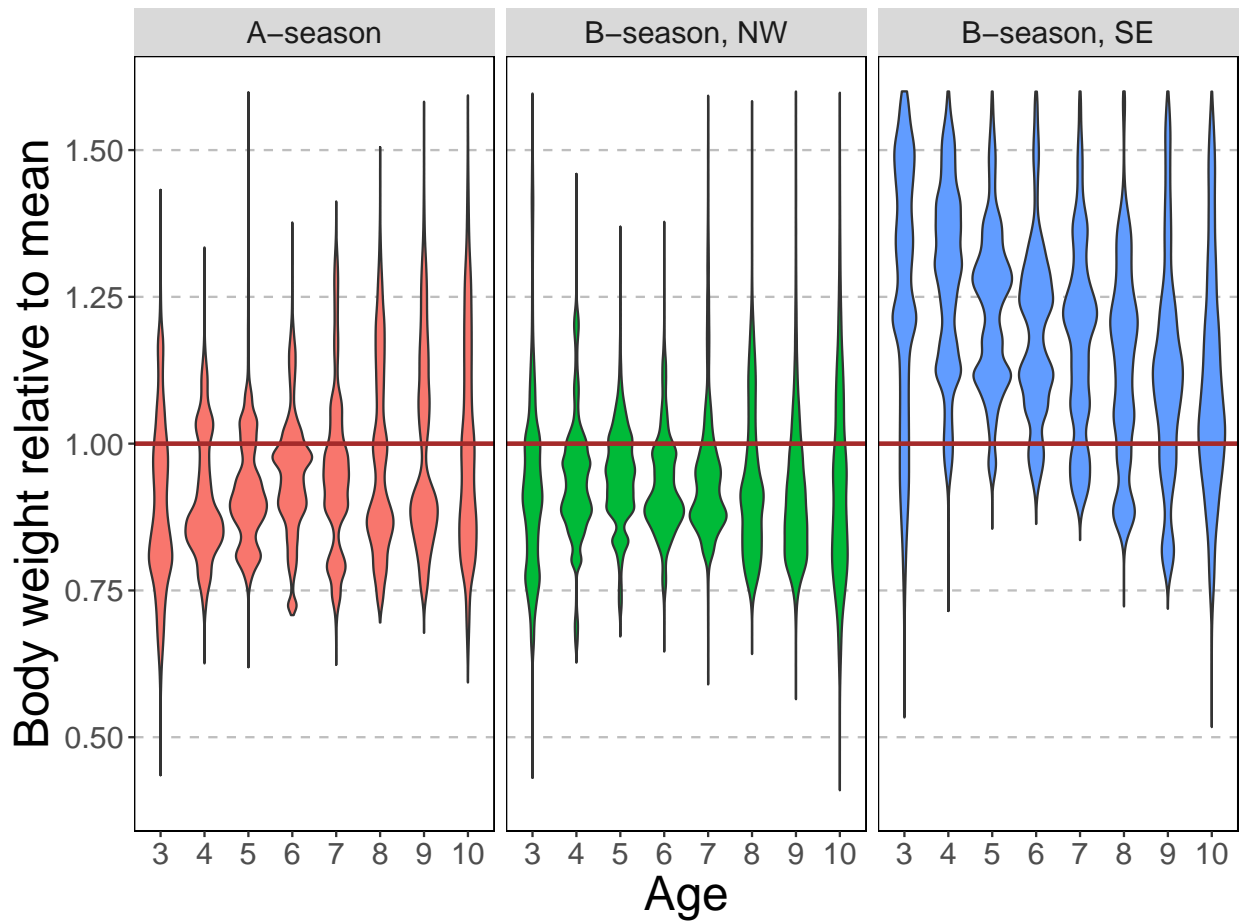


Figure 32: Fishery average weight-at-age anomaly (relative to mean) across strata and combined for all ages (3–10), and available years (1991–2019). Vertical shape reflects uncertainty in the data (wider shapes being more precise), colors are consistent with cohorts.

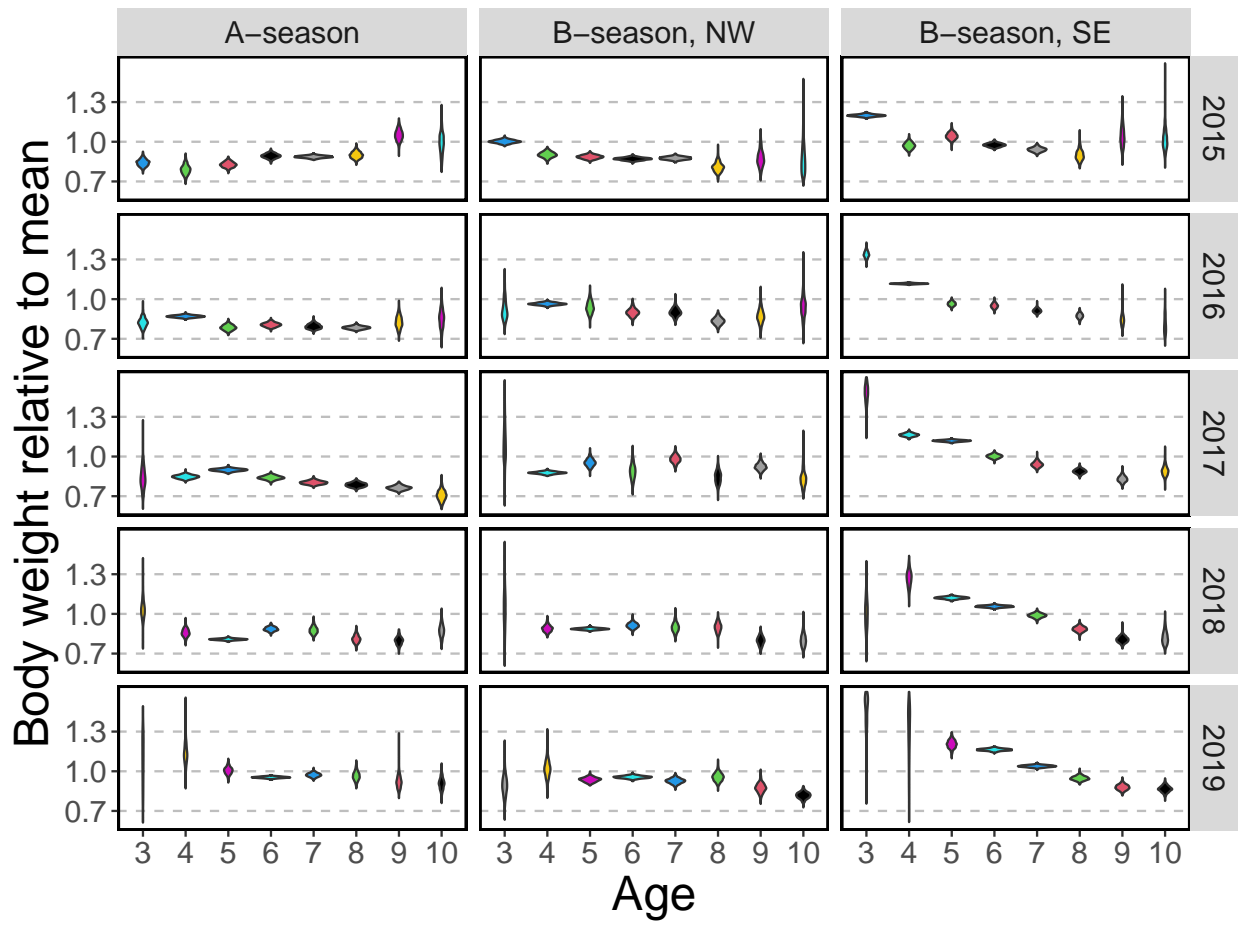


Figure 33: Recent fishery average weight-at-age anomaly (relative to mean) by strata for ages 3–10, 2014–2019. Vertical shape reflects uncertainty in the data (wider shapes being more precise), colors are consistent with cohorts.

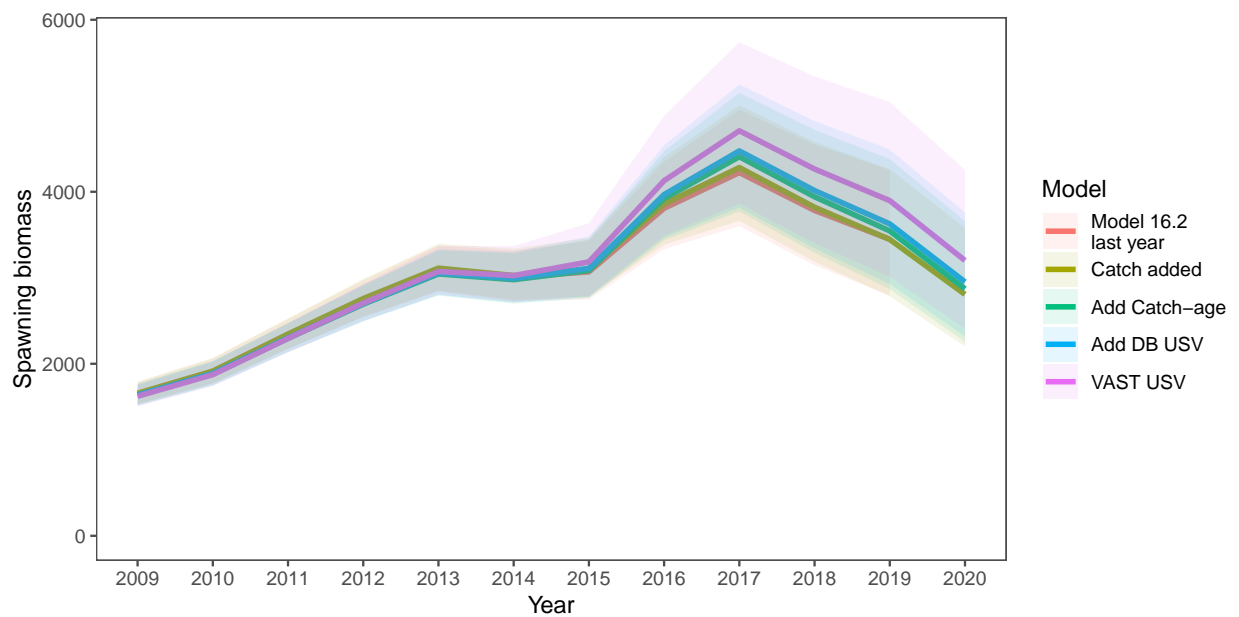


Figure 34: Model runs comparing last year's assessment with the impact of sequentially adding new data (first 2020 catch and 2019 fishery catch-at-age, then the 2020 USV data point, and then replacing that with a VAST treatment of the acoustic survey backscatter).

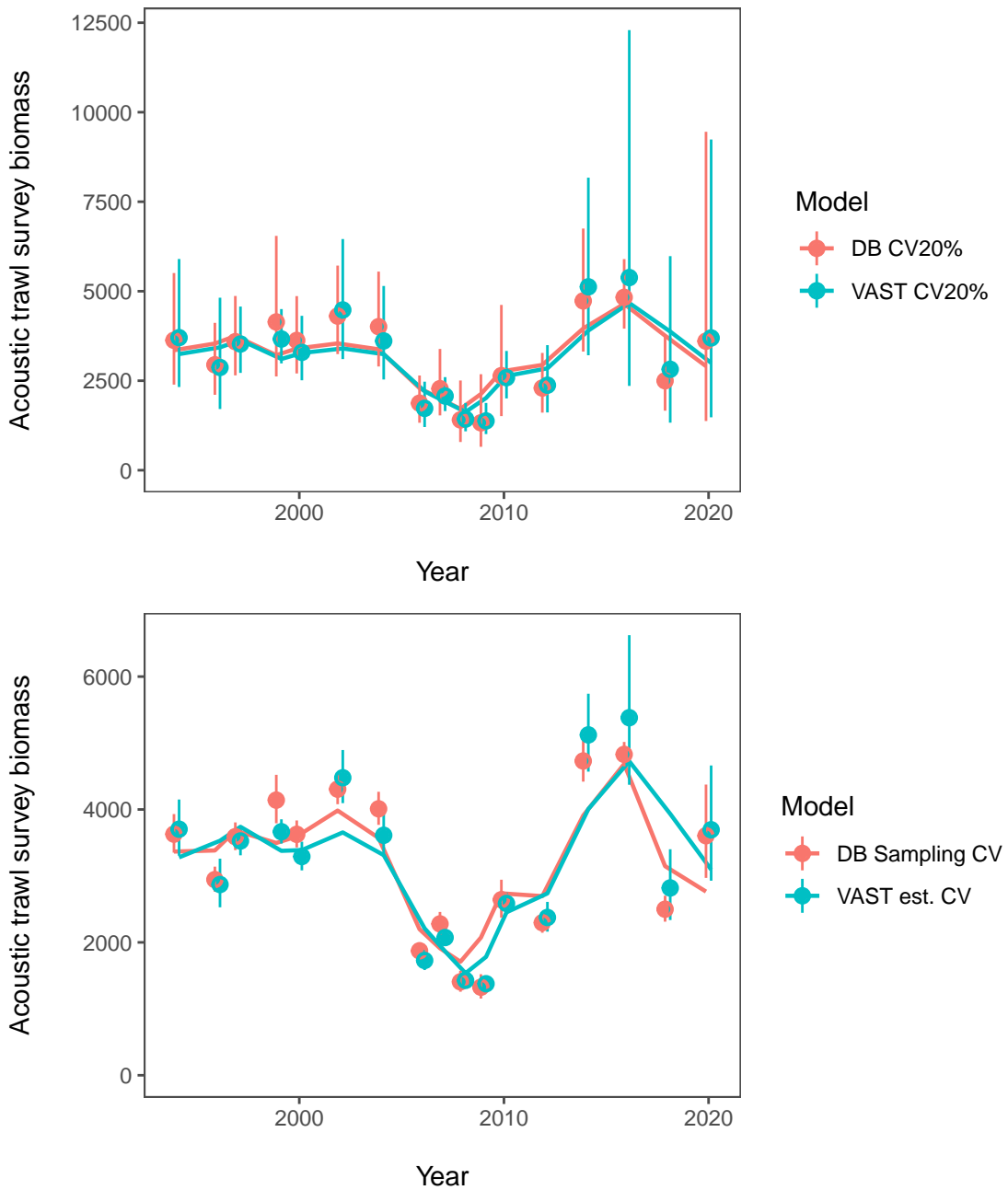


Figure 35: Model fits to different treatment and assumptions about index CPUE for the ATS time series where VAST CV20% and DB CV20% mean that the CVs for the index values between 1994 and 2018 each average 20% for the design-based and VAST treatments, respectively. The other cases use the sampling error and variance estimates arising from the methods.

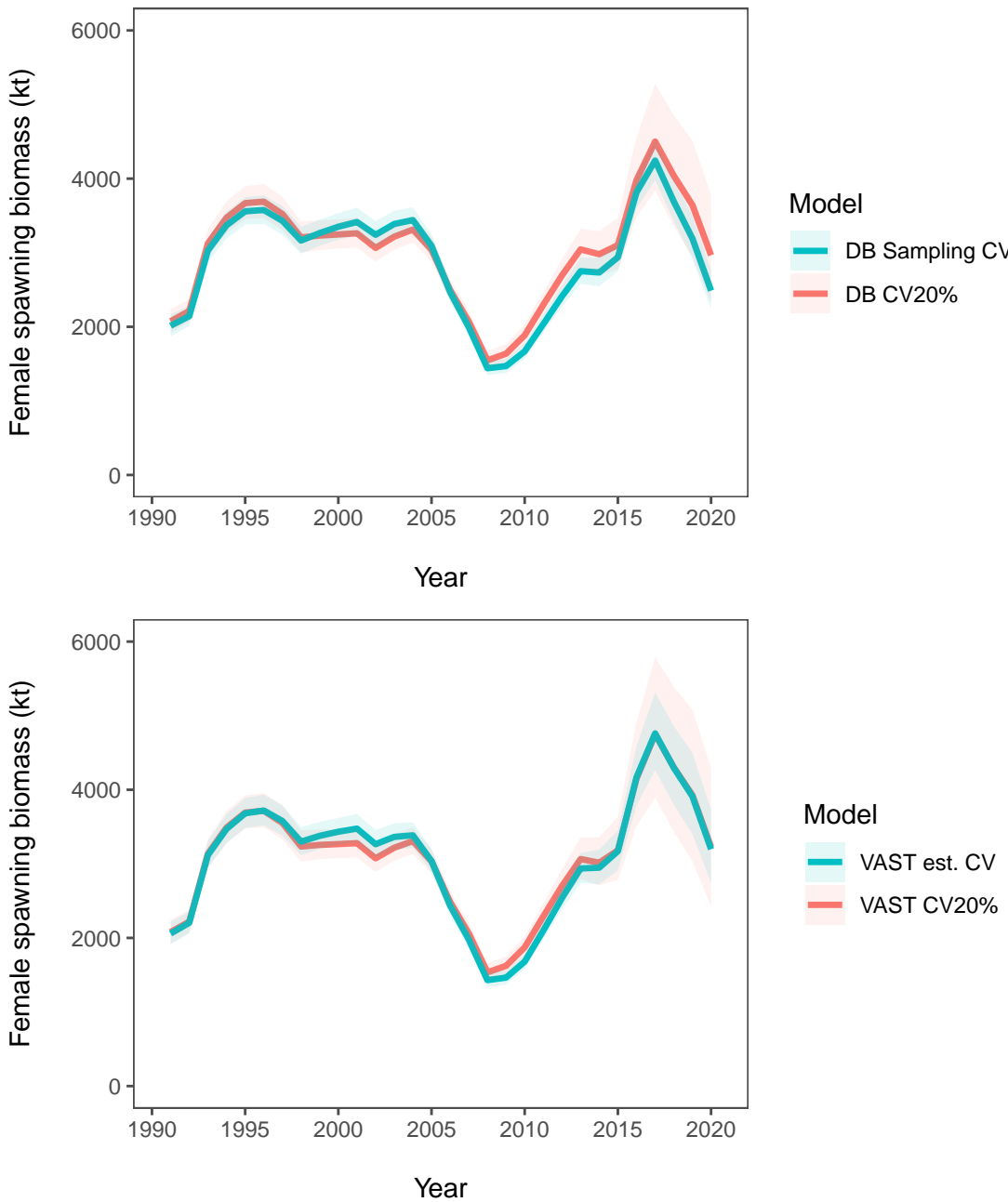


Figure 36: Pollock spawning biomass estimates sensitivity to assumptions about index CPUE for the ATS time series where VAST CV20% and DB CV20% mean that the CVs for the index values between 1994 and 2018 each average 20% for the design-based and VAST treatments, respectively. The other cases use the sampling error and variance estimates arising from the methods.

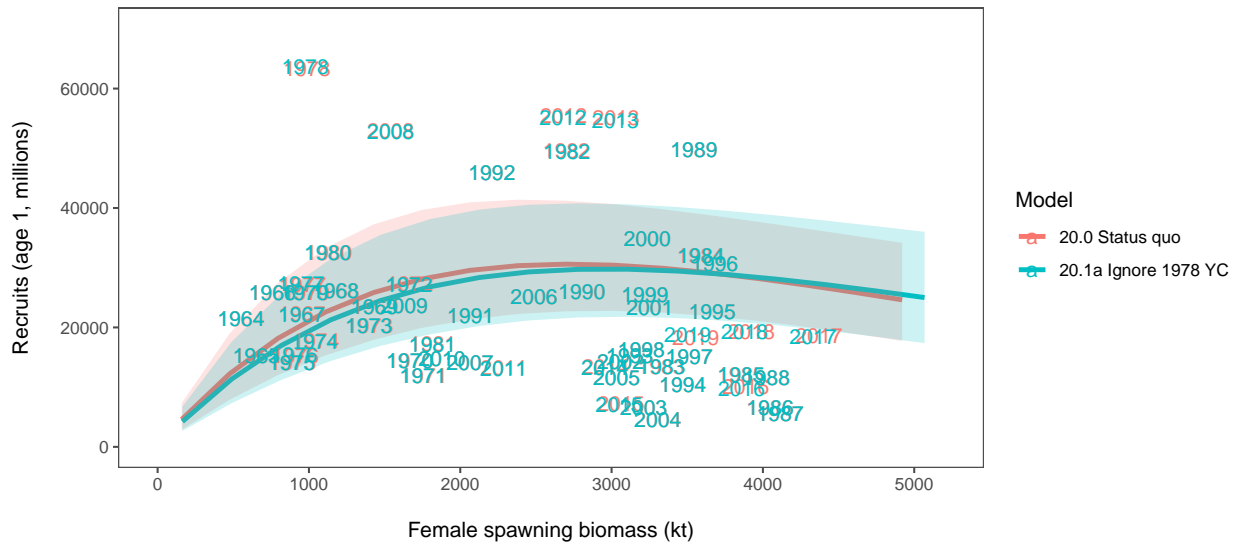


Figure 37: Stock-recruitment estimates (shaded represents uncertainty in SRR) and age-1 EBS pollock estimates labeled by year-classes for Model 20.0 and with the influence of the 1978 year-class removed.

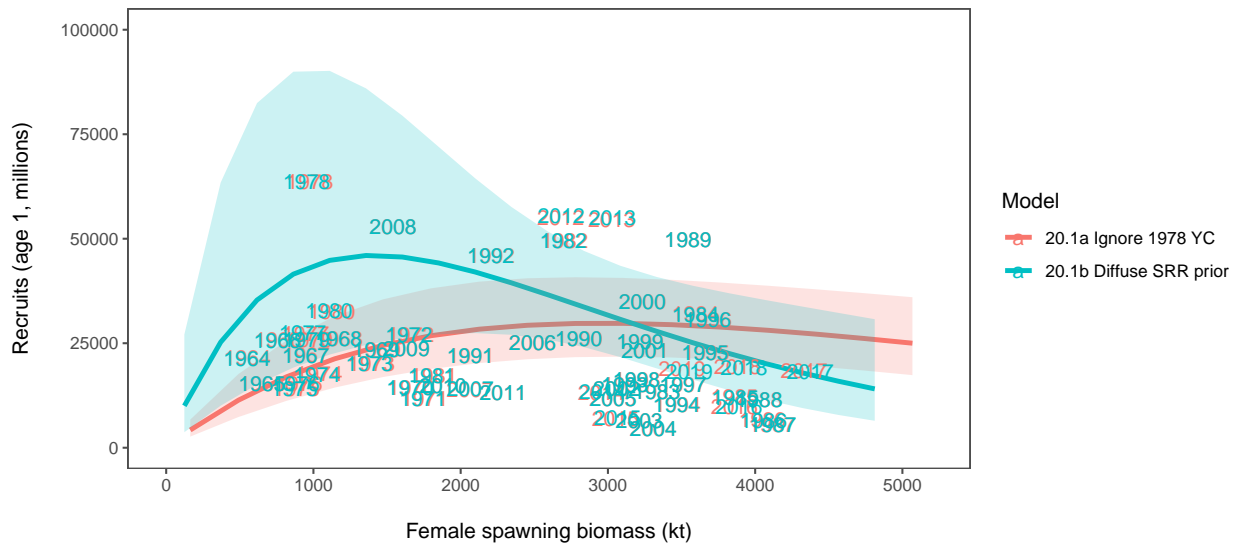


Figure 38: Stock-recruitment estimates (shaded represents uncertainty in SRR) and age-1 EBS pollock estimates labeled by year-classes comparing a result with a diffuse prior on SRR steepness.

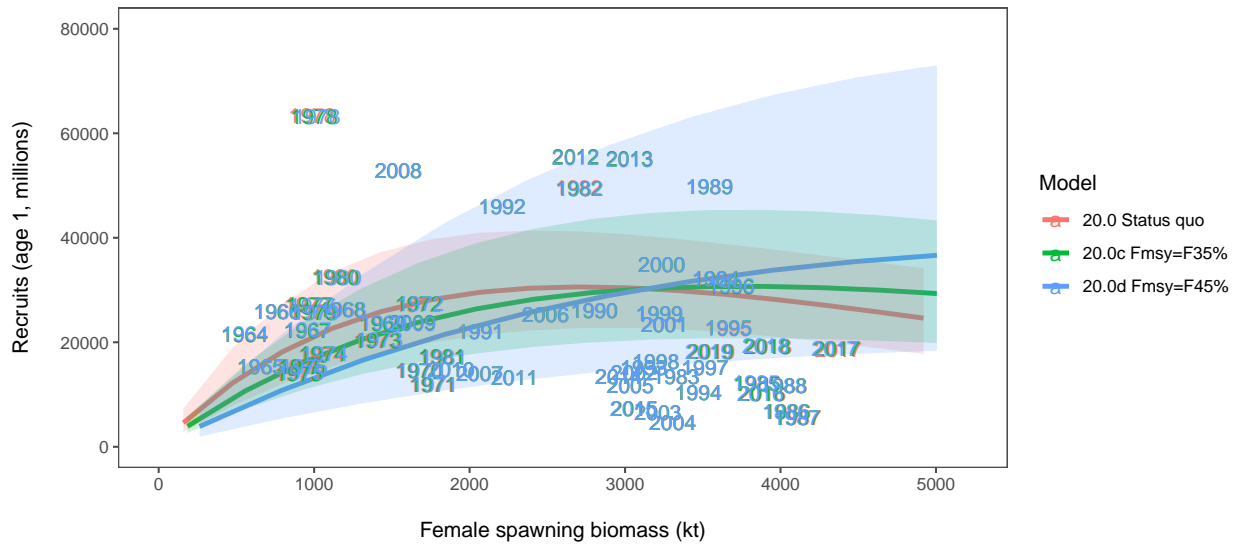


Figure 39: Stock-recruitment estimates (shaded represents uncertainty in SRR) and age-1 EBS pollock estimates labeled by year-classes comparing implied SRR under models conditioned that FMSY equals different SPR rates.

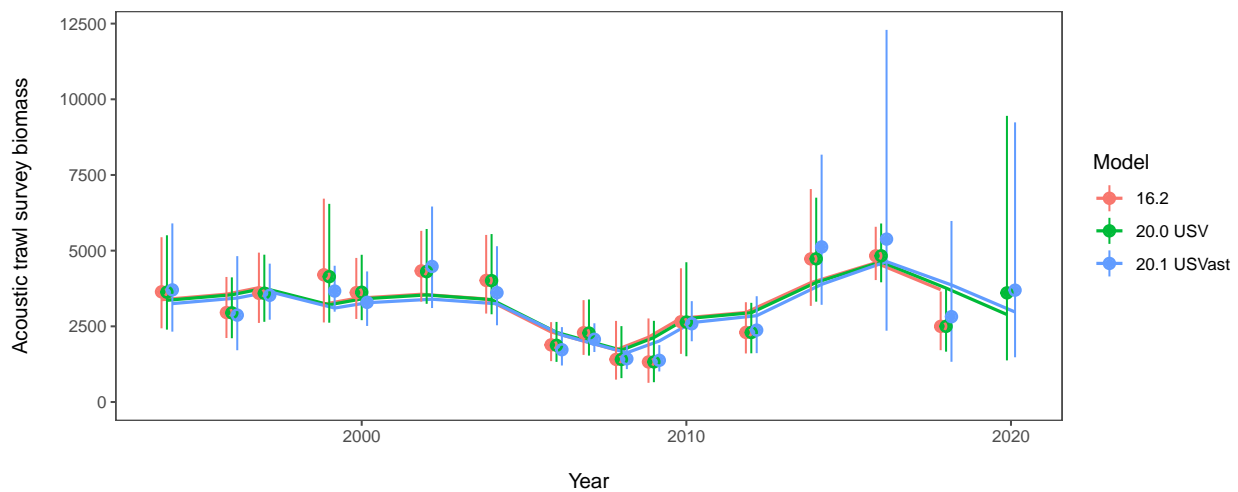


Figure 40: EBS pollock model fit to the alternative ATS biomass indices, 1994–2020.

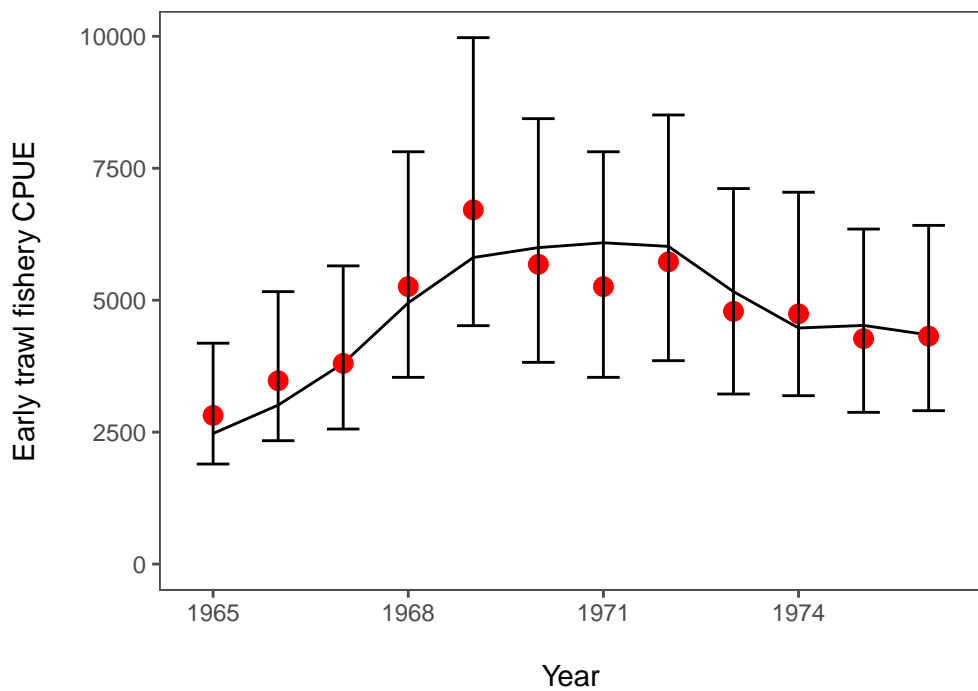


Figure 41: EBS pollock model fits to the Japanese fishery CPUE.

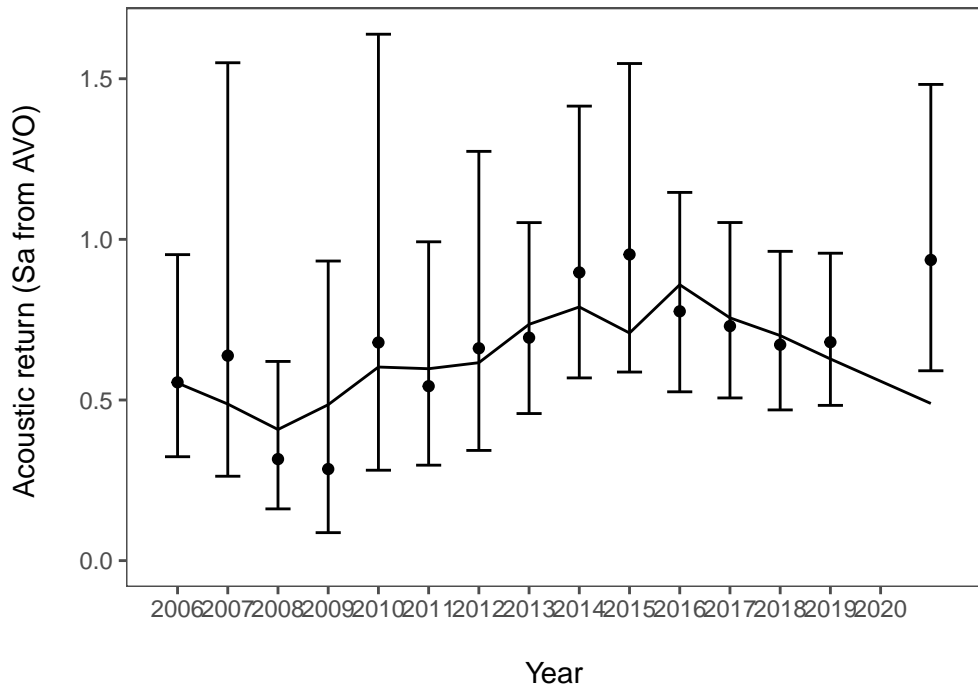


Figure 42: Model results of predicted and observed AVO index. Error bars represent assumed 95% confidence bounds of the input series.

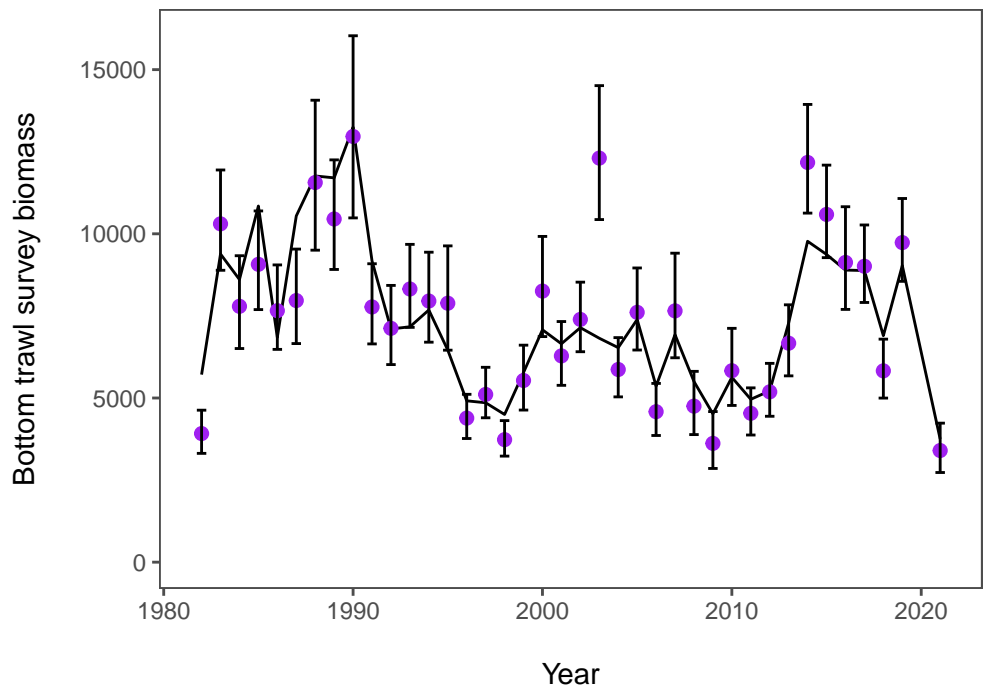


Figure 43: EBS pollock model fit to the BTS survey data (density dependence corrected estimates), 1982–2019. Units are relative biomass.

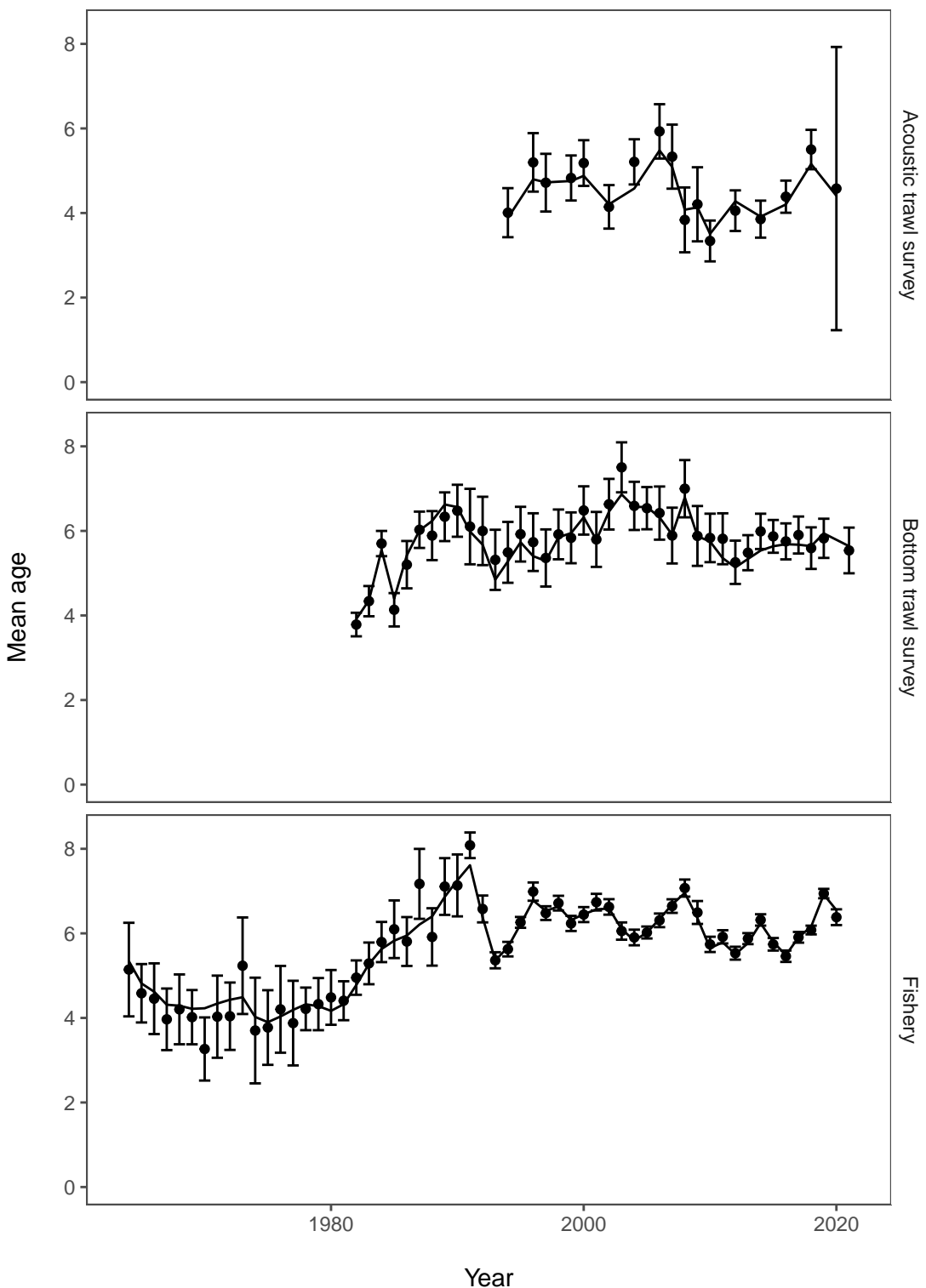


Figure 44: EBS pollock model fits to observed mean age for the Acoustic trawl survey (top), the bottom trawl survey (middle) and fishery (bottom)

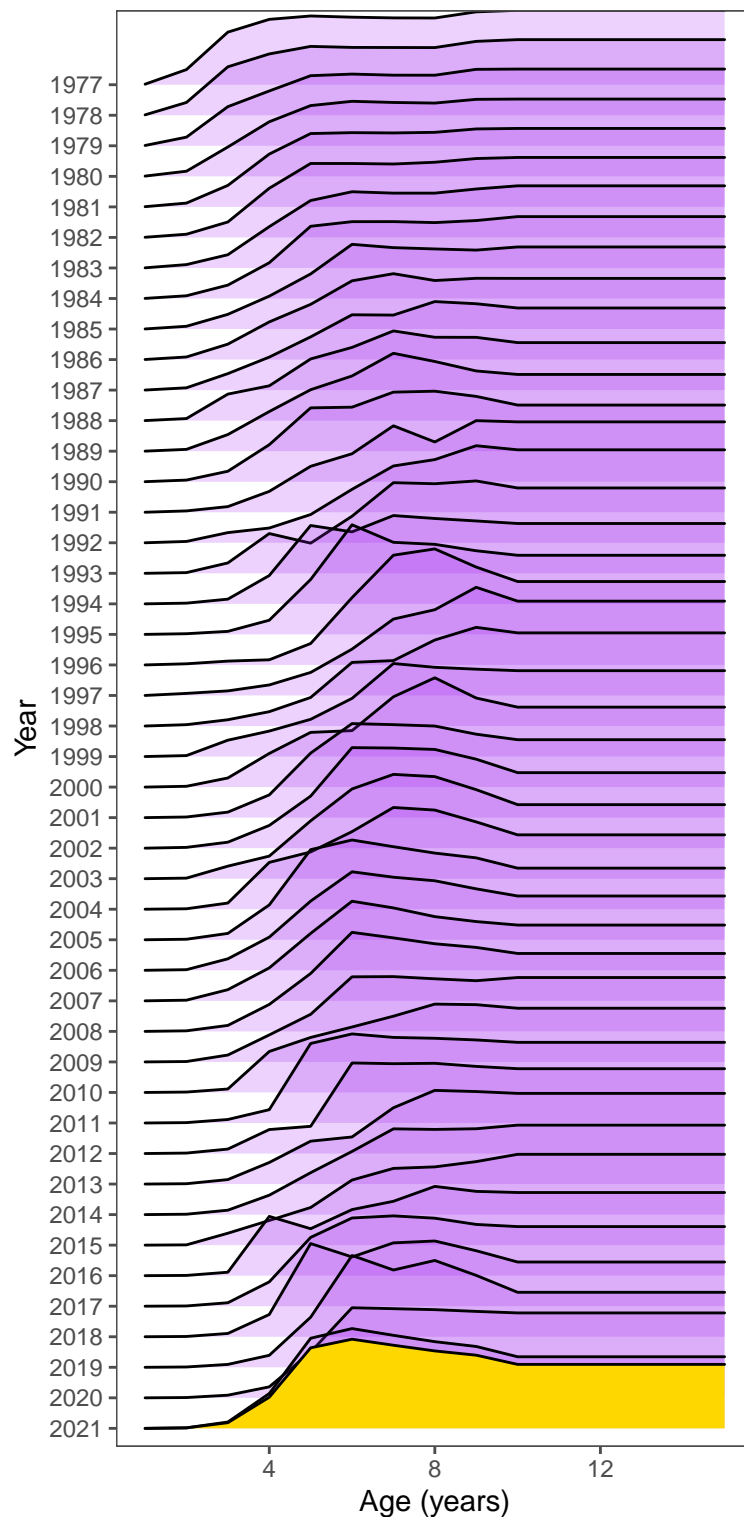


Figure 45: Selectivity at age estimates for the EBS pollock fishery; note that the values for the terminal year is used for ABC and OFL projections.

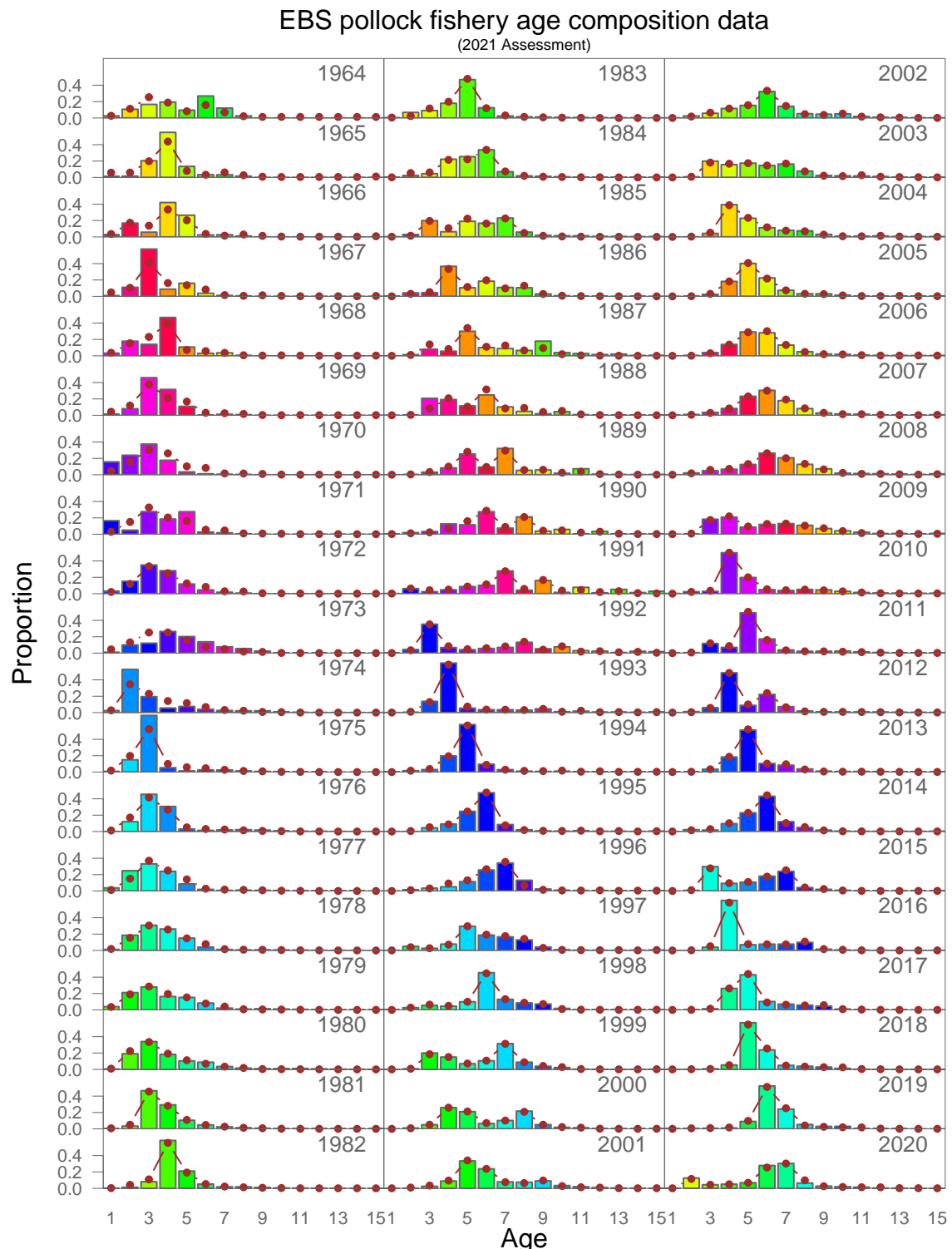


Figure 46: Model fit (dots) to the EBS pollock fishery proportion-at-age data (columns; 1964–2019). The 2019 data are new to this year's assessment. Colors coincide with cohorts progressing through time.

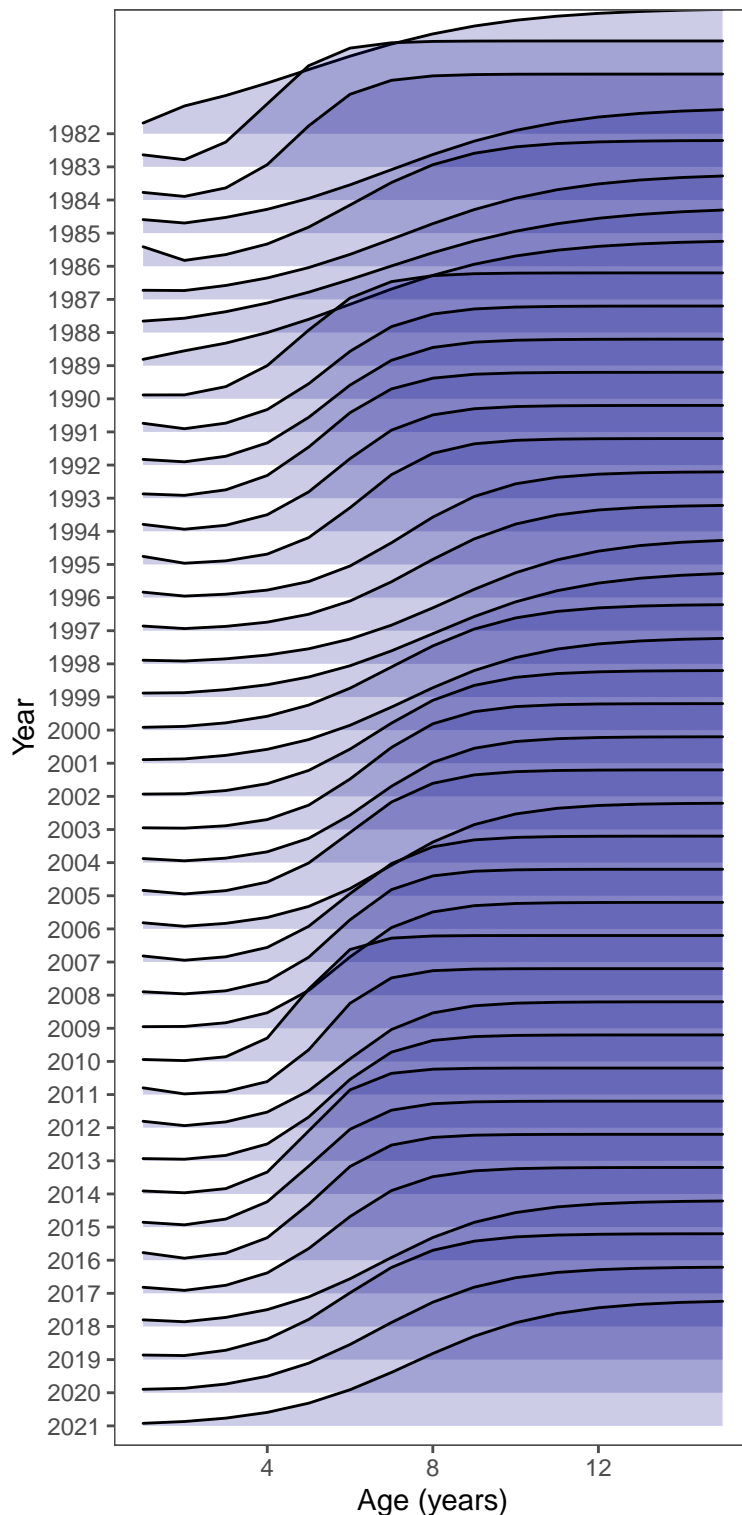


Figure 47: Model estimates of bottom-trawl survey selectivity, 1982–2019.

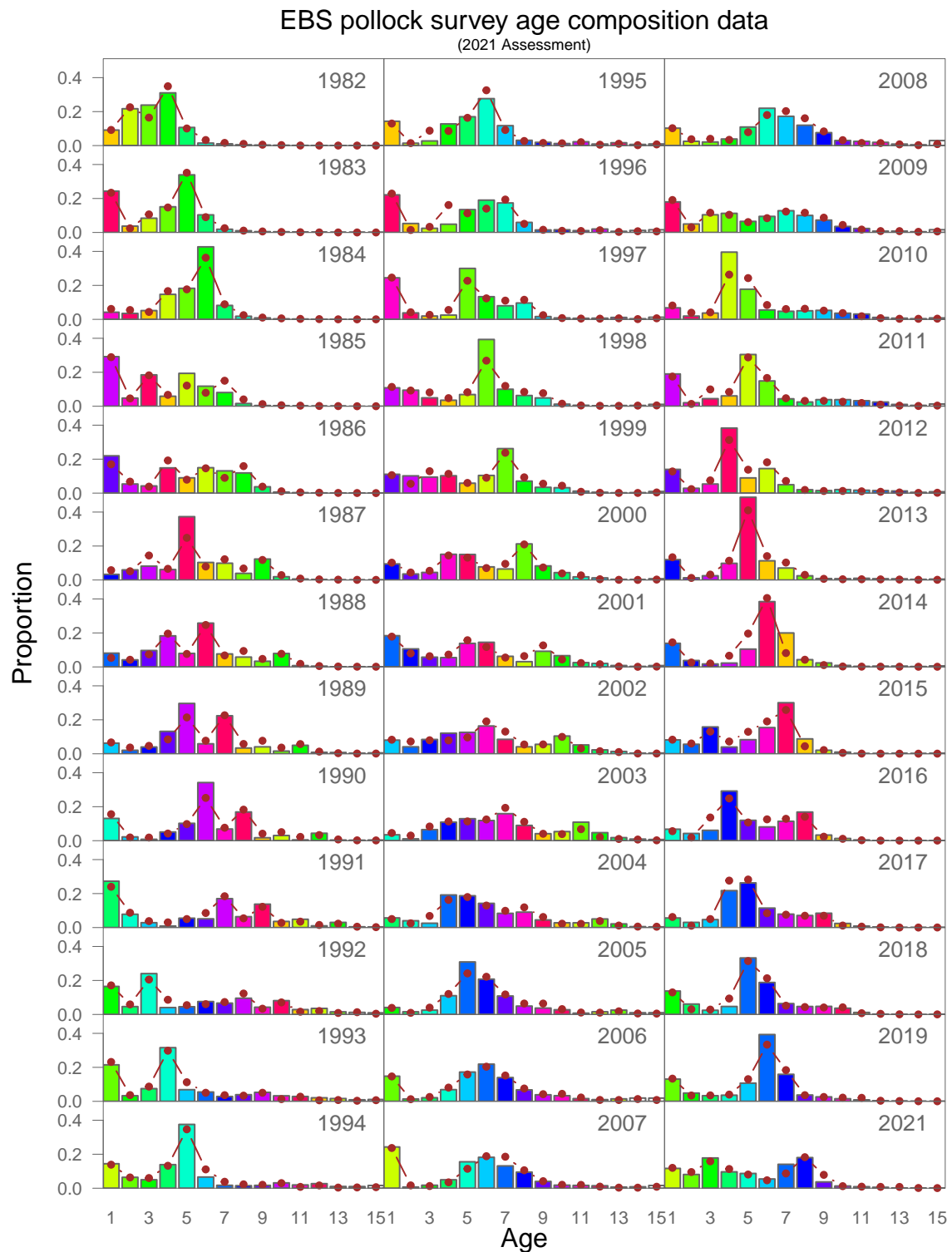


Figure 48: Model fit (dots) to the bottom trawl survey proportion-at-age composition data (columns) for EBS pollock. Colors correspond to cohorts over time.

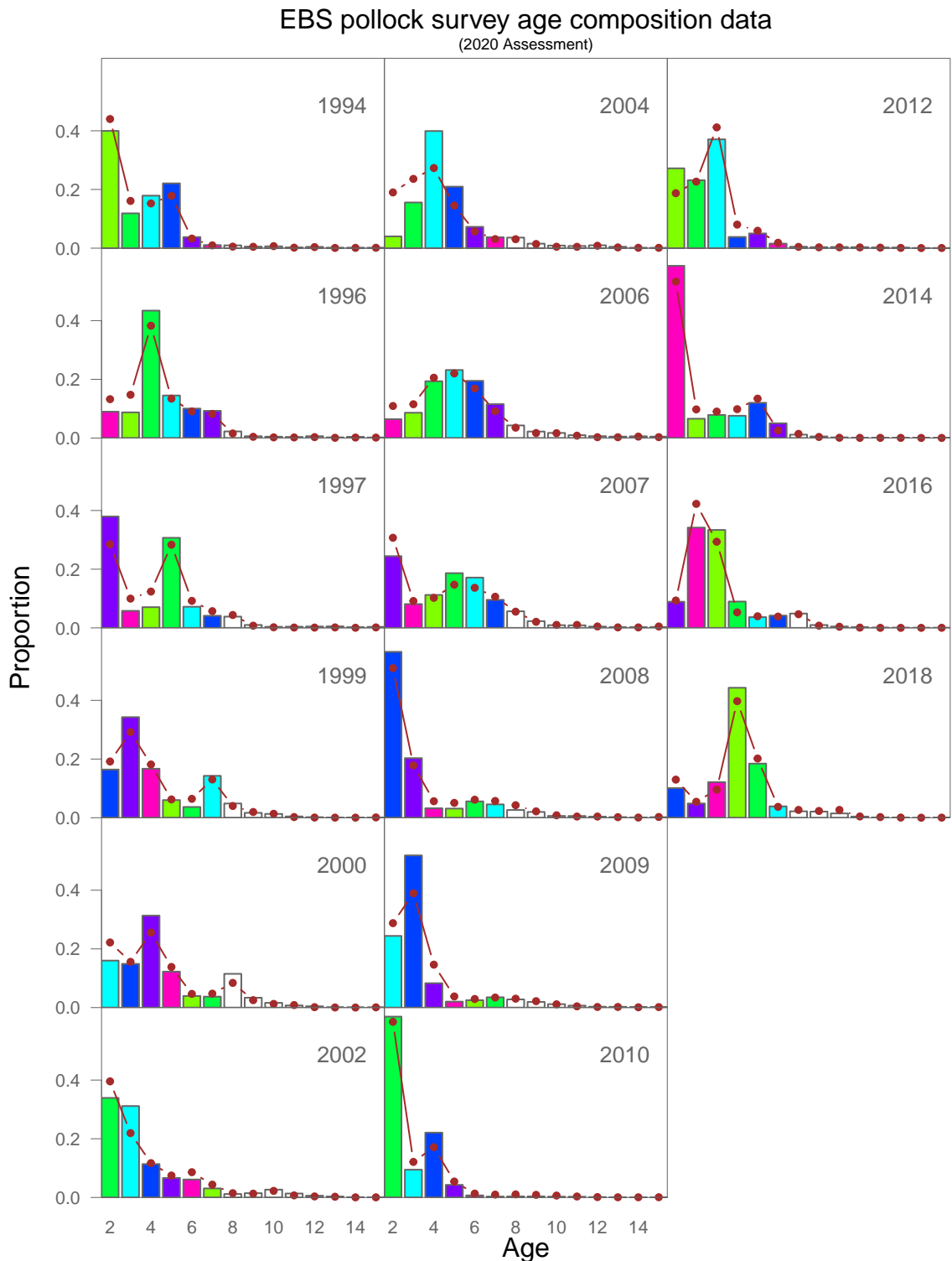


Figure 49: Model fit (dots) to the acoustic-trawl survey proportion-at-age composition data (columns) for EBS pollock. Colors correspond to cohorts over time (for years with consecutive surveys).

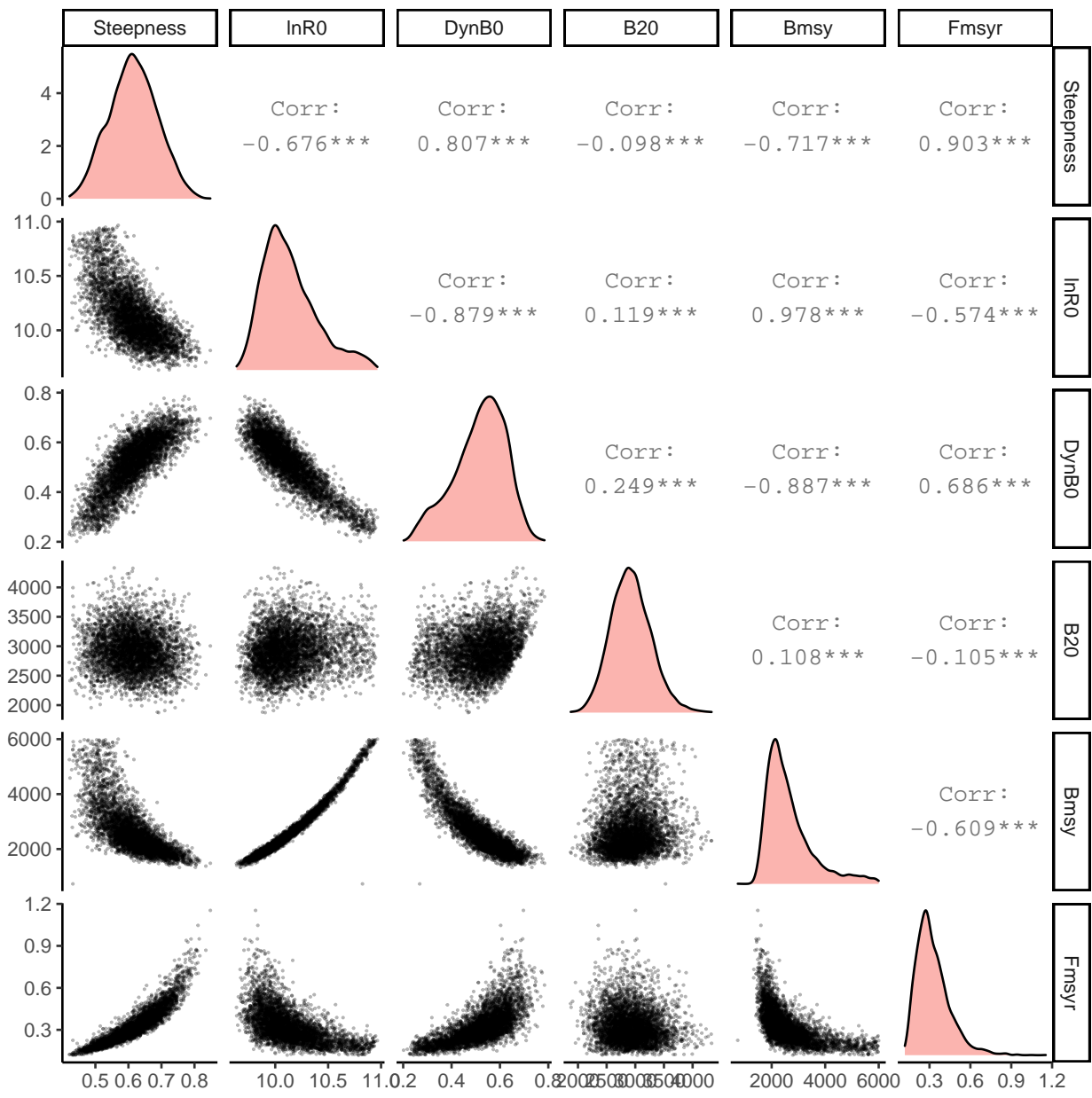


Figure 50: Pairwise plot of selected EBS pollock parameters and output from 3 million MCMC iterations thinned such that 5 thousand draws were saved as an approximation to the multivariate posterior distribution. Note that the figures on the diagonal represent the marginal posterior distributions. Key: lnR0 is the parameter that scales the stock-recruit relationship, B\_Bmsy is estimated  $B_{2018}/B_{MSY}$ , DynB0 is the ratio of spawning biomass estimated for in 2018 over the value estimated that would occur if there had been no fishing, B19 is the spawning biomass in 2019, and B\_Bmean is  $B_{2019}/\bar{B}$ .

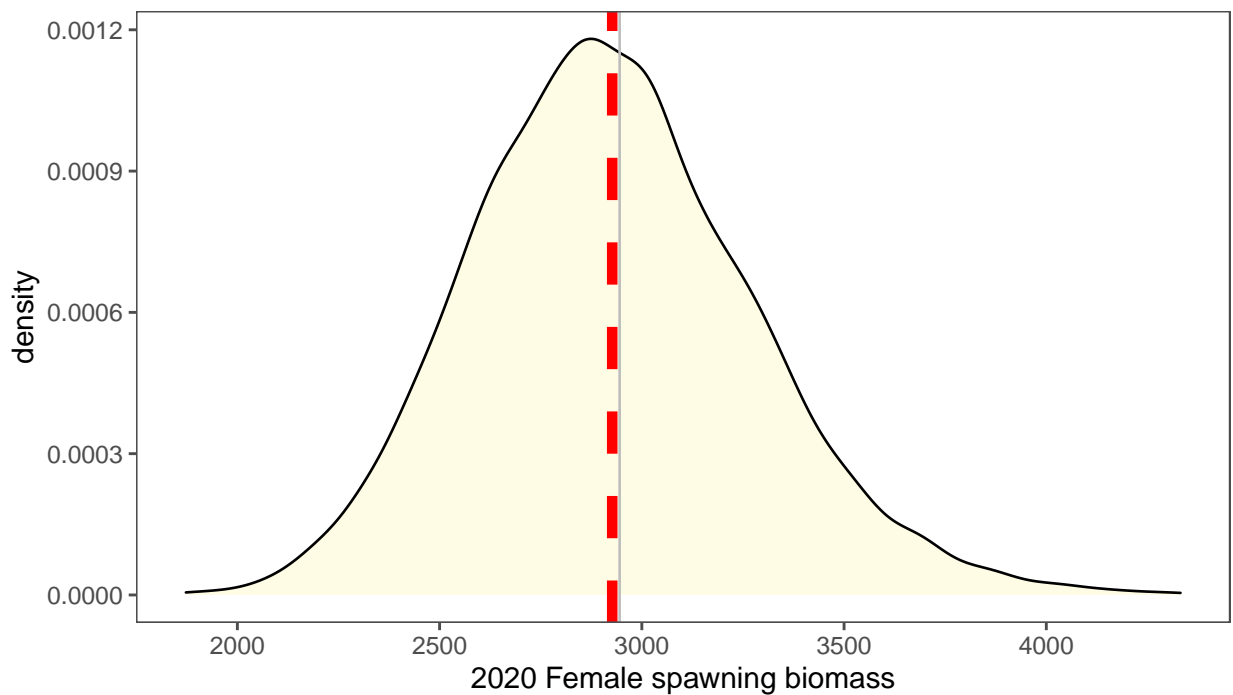


Figure 51: Integrated marginal posterior density (based on MCMC results) for the 2019 EBS pollock female spawning biomass compared to the point estimate (dashed red line). The mean of the posterior is shown in green (under the dashed line).

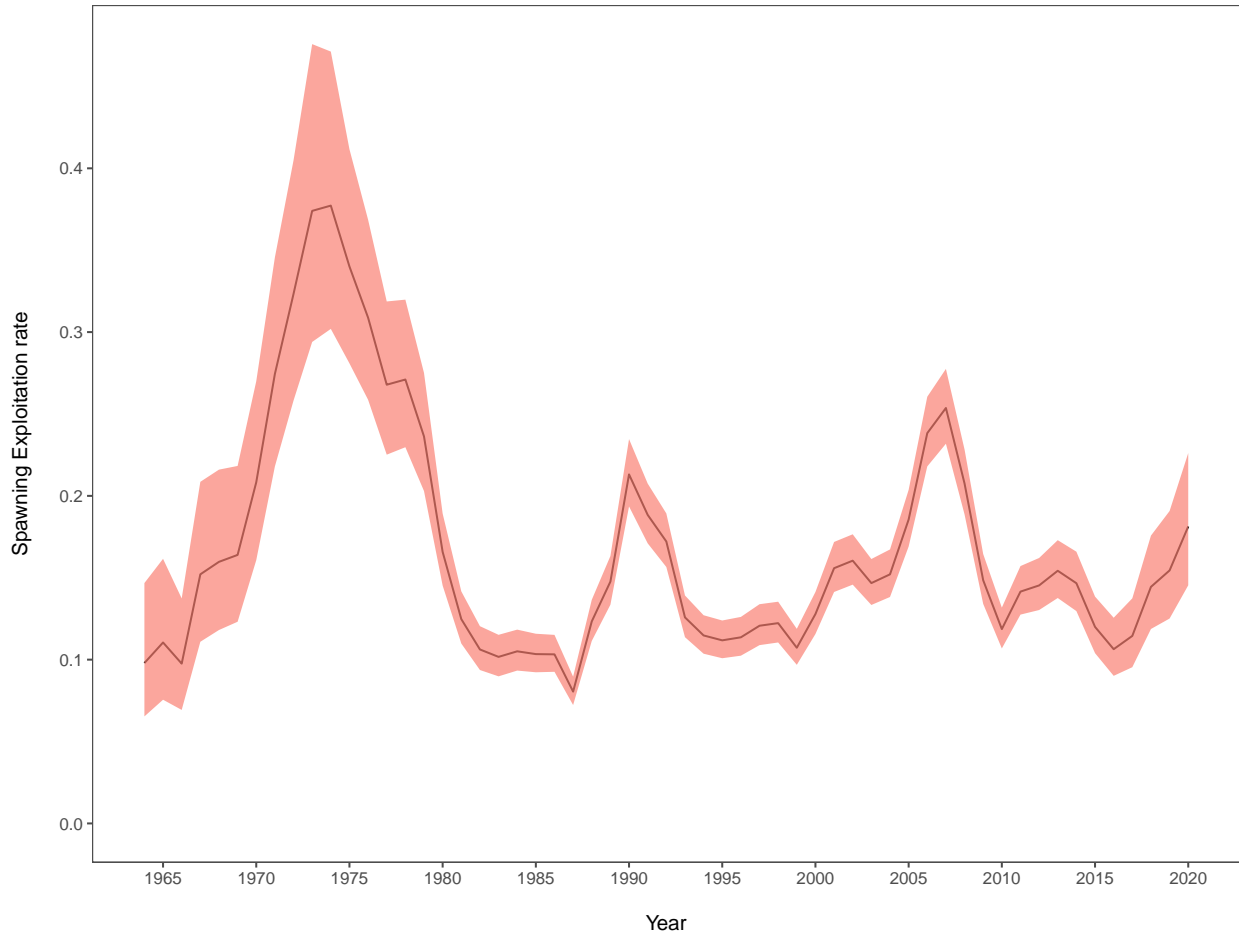


Figure 52: Estimated spawning exploitation rate (defined as the percent removal of egg production in a given spawning year).

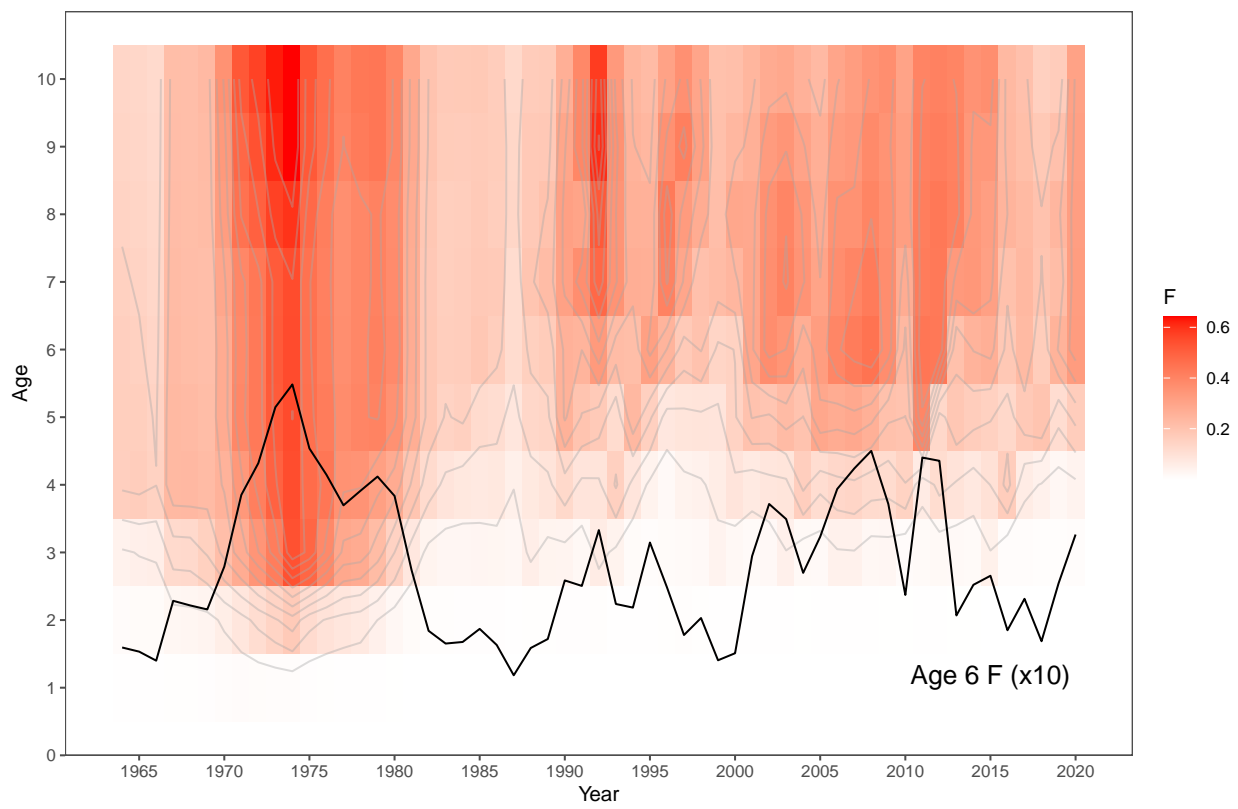


Figure 53: Estimated instantaneous age-specific fishing mortality rates for EBS pollock.

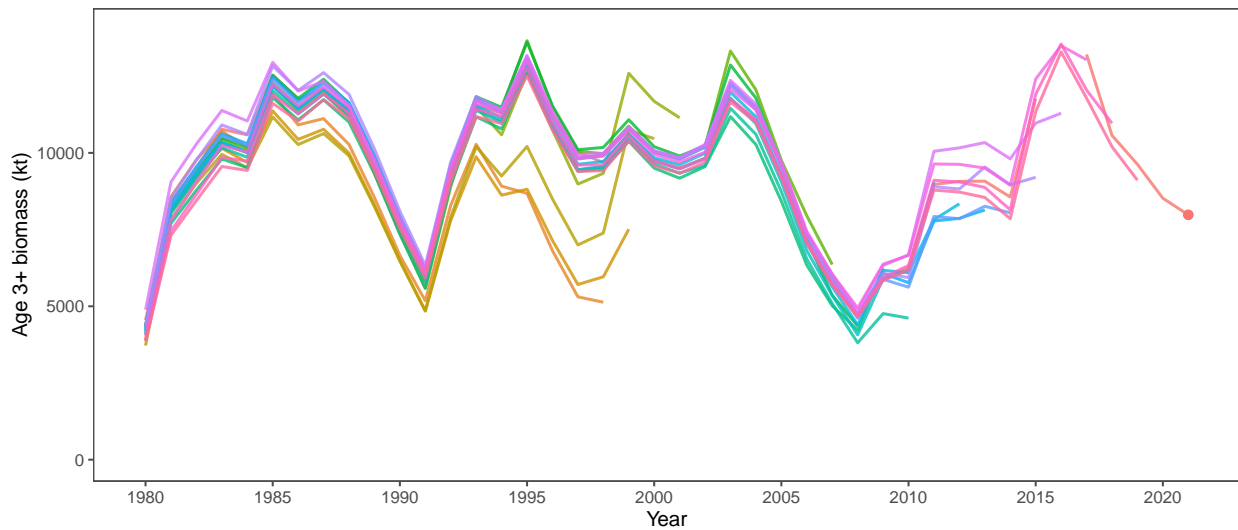


Figure 54: Comparison of the current assessment results with past assessments of begin-year EBS age-3+ pollock biomass.

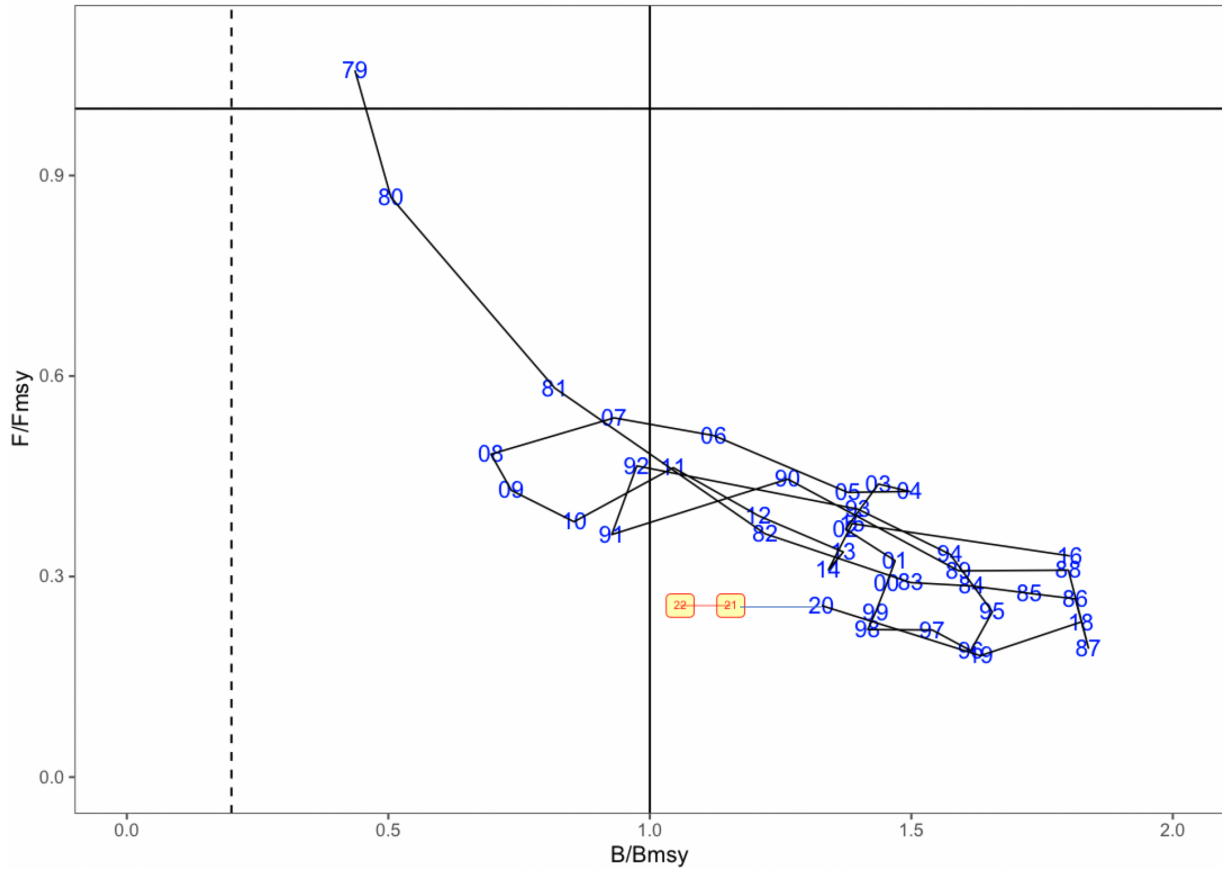


Figure 55: Estimated spawning biomass relative to annually estimated  $F_{\text{MSY}}$  values and fishing mortality rates for EBS pollock. Most recent two years are shaded in yellow

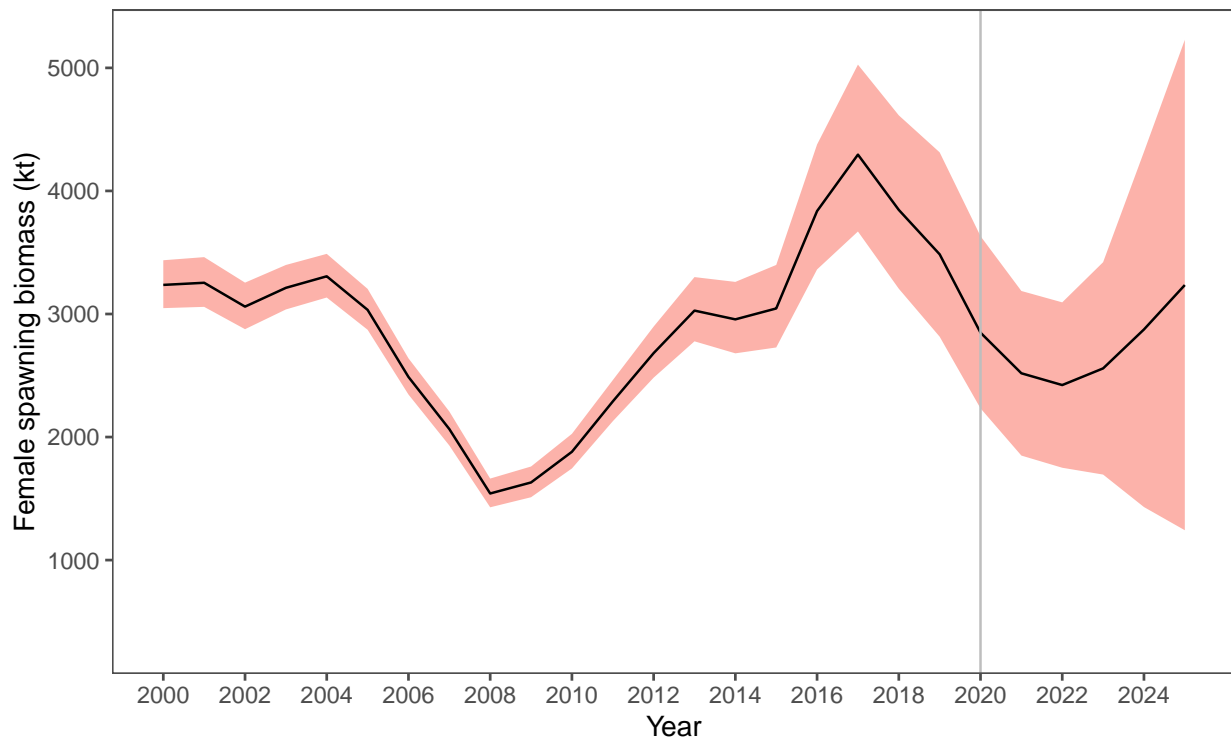


Figure 56: The estimated EBS pollock spawning stock biomass for model 20.0 with projections equal to the estimated fishing mortality from 2020.

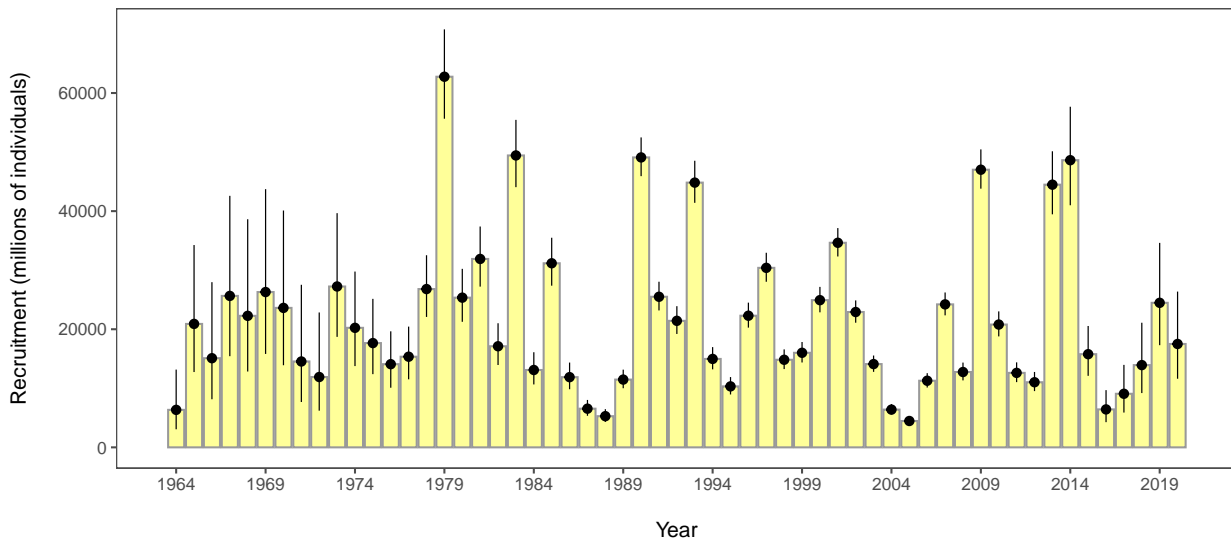


Figure 57: Recruitment estimates (age-1 recruits) for EBS pollock for all years since 1964 (1963–2019 year classes) for Model 20.0. Error bars reflect 90% credible intervals based on model estimates of uncertainty.

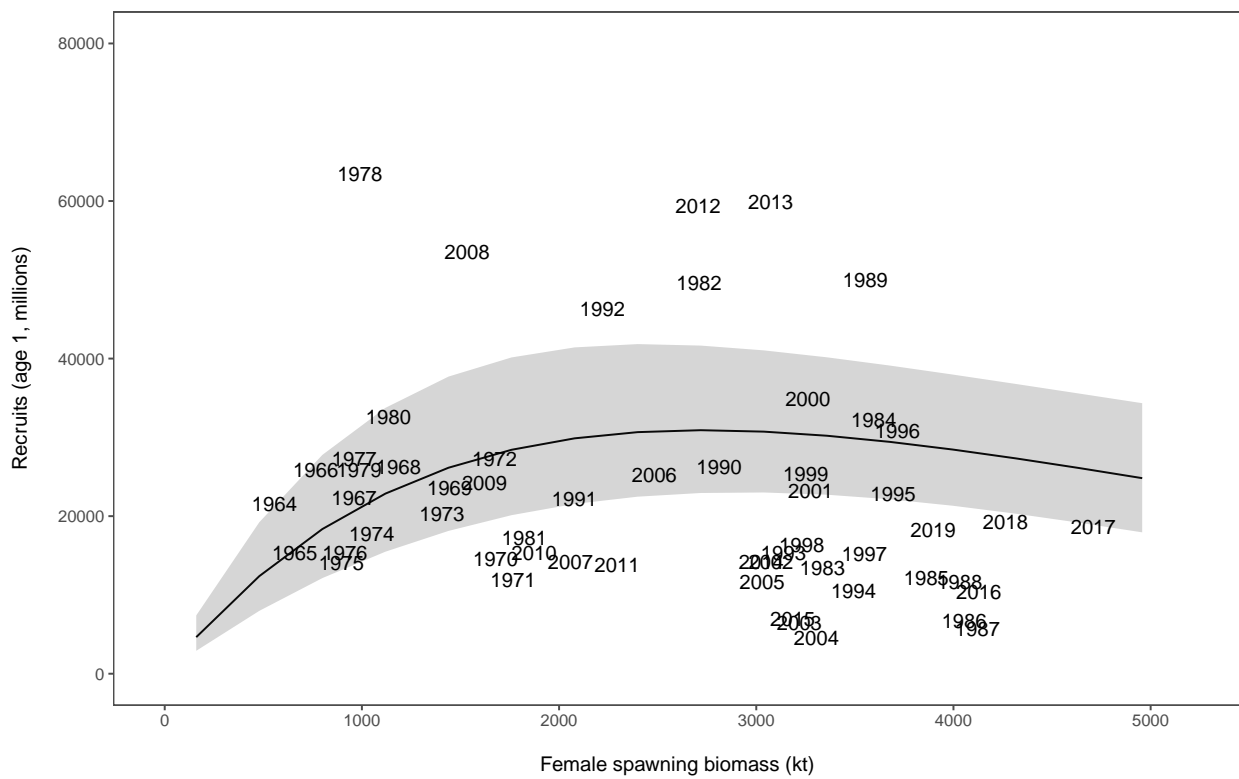


Figure 58: Stock-recruitment estimates (shaded represents structural uncertainty) and age-1 EBS pollock estimates labeled by year-classes

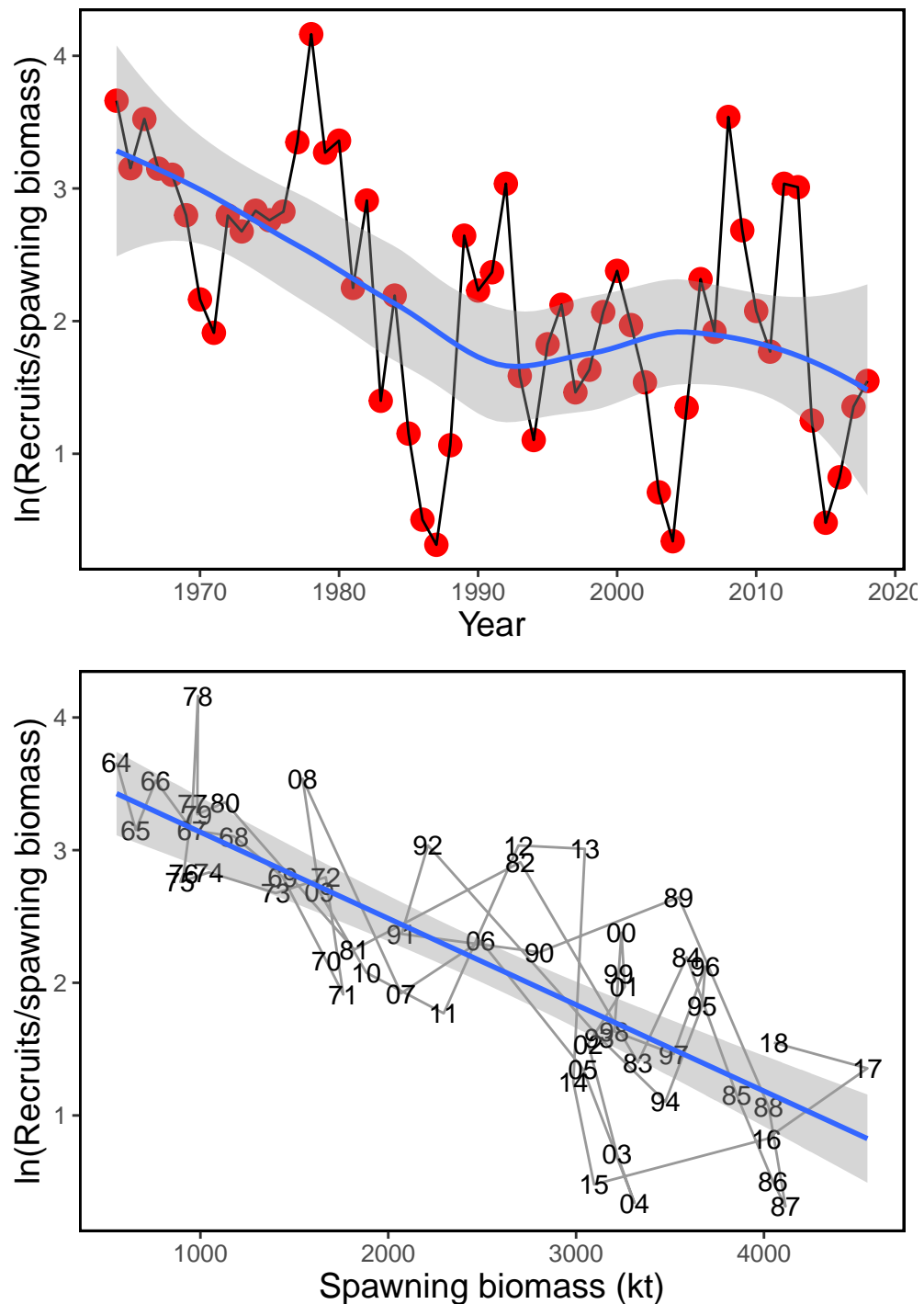


Figure 59: EBS pollock productivity as measured by logged recruits per spawning biomass,  $\log(R/S)$ , as a function of spawning biomass with a linear fit (bottom) and over time, 1964–2018 (top).

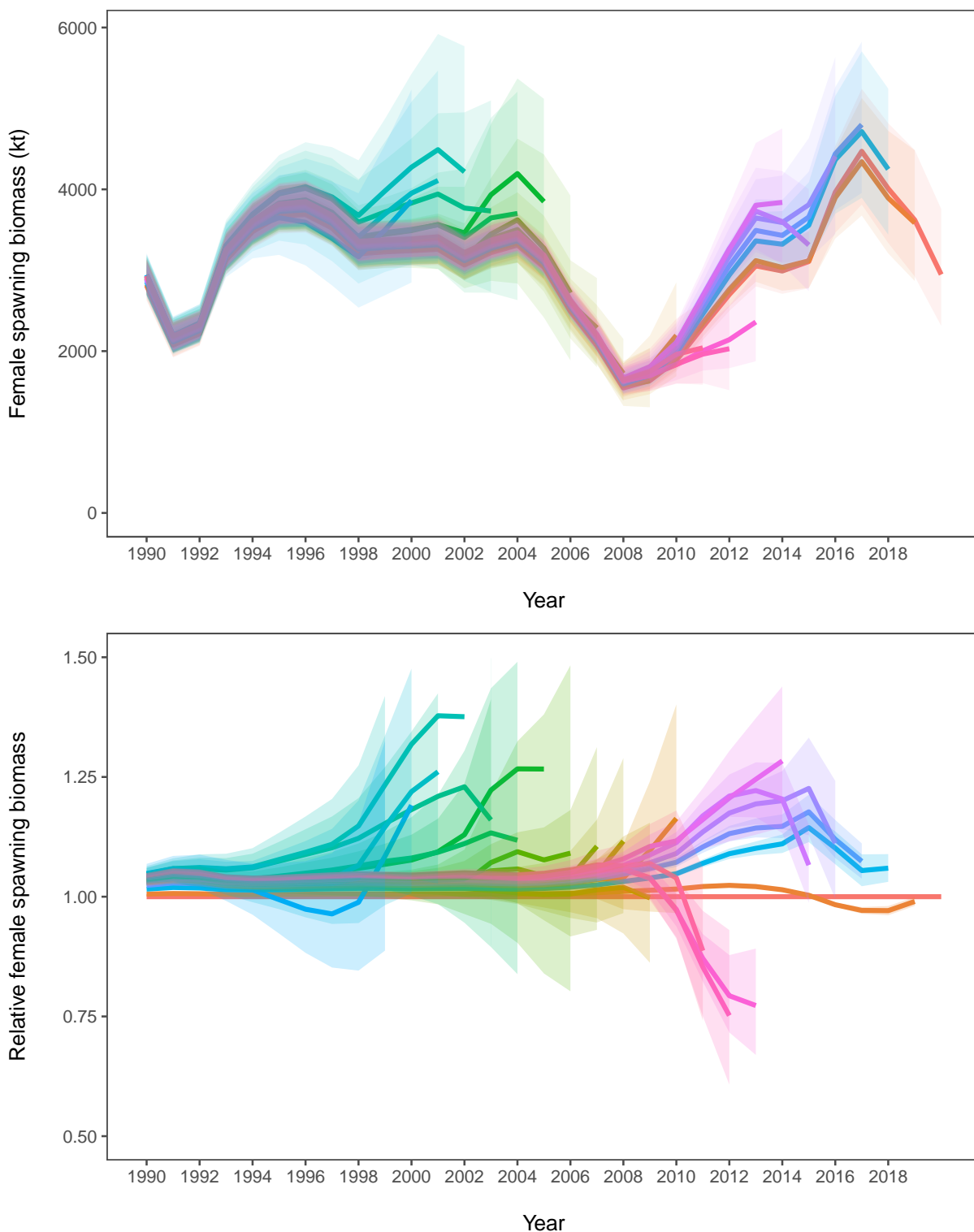


Figure 60: Retrospective patterns for EBS pollock spawning biomass showing the point estimates relative to the terminal year (top panel) and approximate confidence bounds on absolute scale (+2 standard deviations).

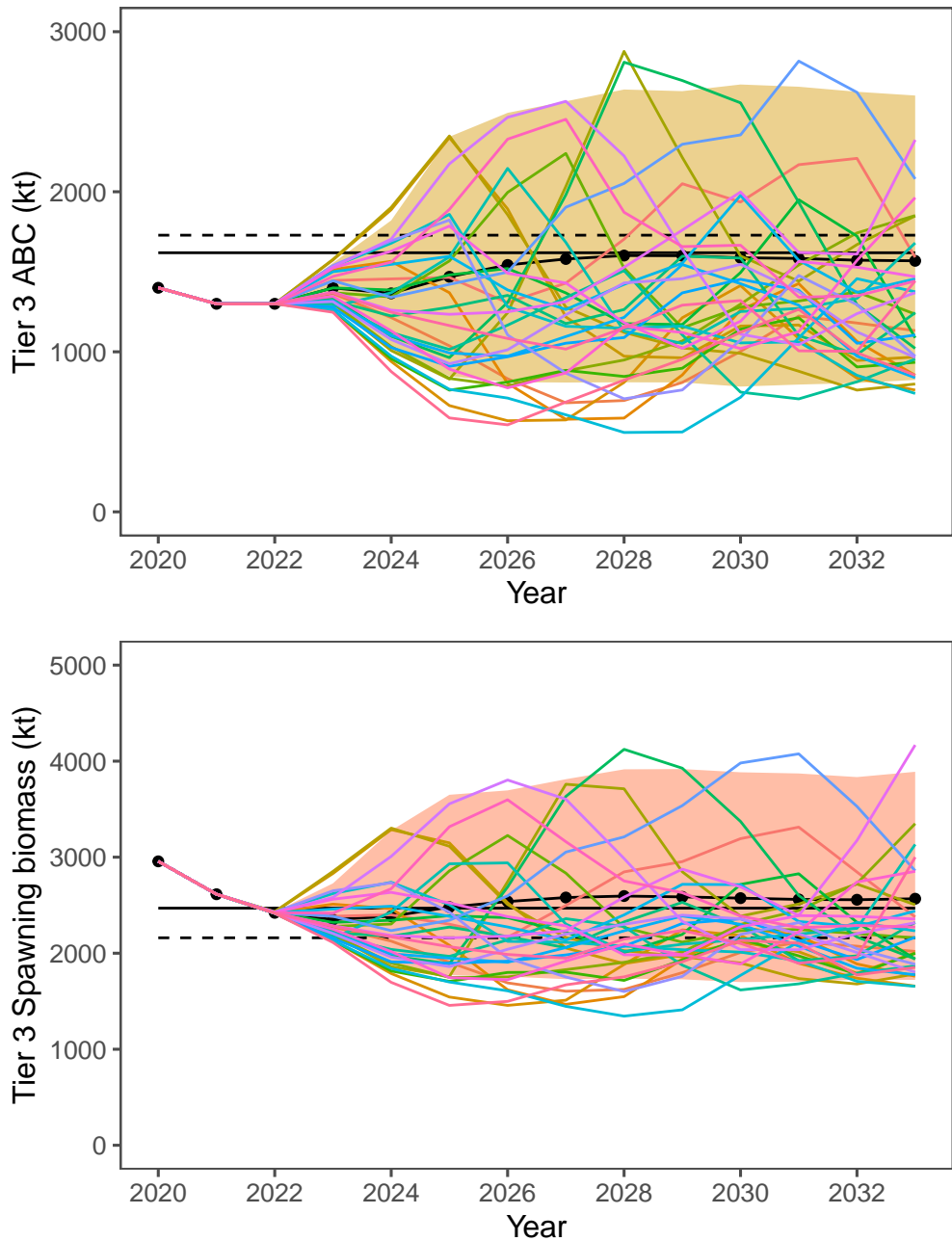


Figure 61: Projected EBS Tier 3 pollock yield (top) and female spawning biomass (bottom) relative to the long-term expected values under  $F_{35\%}$  and  $F_{40\%}$  (horizontal lines).  $B_{40\%}$  is computed from average recruitment from 1978–2017. Future harvest rates follow the guidelines specified under Tier 3 Scenario 1.

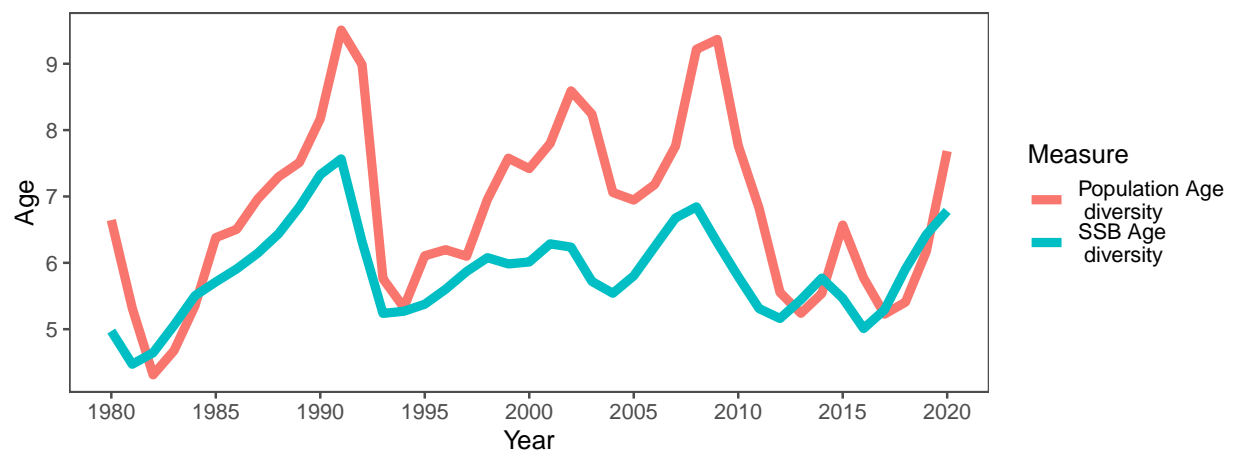


Figure 62: For the mature component of the EBS pollock stock, time series of estimated average age and diversity of ages (using the Shannon-Wiener H statistic), 1980–2018.

## EBS Pollock Model Description

### Dynamics

This assessment is based on a statistical age-structured model with the catch equation and population dynamics model as described in Fournier and Archibald (1982) and elsewhere (e.g., Hilborn and Walters 1992, Schnute and Richards 1995, McAllister and Ianelli 1997). The catch in numbers at age in year  $t$  ( $C_{t,a}$ ) and total catch biomass ( $Y_t$ ) can be described as:

$$C_{t,a} = \frac{F_{t,a}}{Z_{t,a}} (1 - e^{-Z_{t,a}}) N_{t,a}, \quad 1 \leq t \leq T, 1 \leq a \leq A \quad (1)$$

$$N_{t+1,a+1} = N_{t,a-1} e^{-Z_{t,a-1}} \quad 1 \leq t \leq T, 1 \leq a < A \quad (2)$$

$$N_{t+1,A} = N_{t,A-1} e^{-Z_{t,A-1}} + N_{t,A} e^{-Z_{t,A}}, \quad 1 \leq t \leq T \quad (3)$$

$$Z_{t,a} = F_{t,a} + M_{t,a} \quad (4)$$

$$C_{t,.} = \sum_{a=1}^A C_{t,a} \quad (5)$$

$$p_{t,a} = \frac{C_{t,a}}{C_{t,.}} \quad (6)$$

$$Y_t = \sum_{a=1}^A w_{t,a} C_{t,a} \quad (7)$$

$$(8)$$

where

- $T$  is the number of years,
- $A$  is the number of age classes in the population,
- $N_{t,a}$  is the number of fish age  $a$  in year  $t$ ,
- $C_{t,a}$  is the catch of age class  $a$  in year  $t$ ,
- $p_{t,a}$  is the proportion of the total catch in year  $t$ , that is in age class  $a$ ,
- $C_t$  is the total catch in year  $t$ ,
- $w_a$  is the mean body weight (kg) of fish in age class  $a$ ,
- $Y_t$  is the total yield biomass in year  $t$ ,
- $F_{t,a}$  is the instantaneous fishing mortality for age class  $a$ , in year  $t$ ,
- $M_{t,a}$  is the instantaneous natural mortality in year  $t$  for age class  $a$ , and
- $Z_{t,a}$  is the instantaneous total mortality for age class  $a$ , in year  $t$ .

Fishing mortality ( $F_{t,a}$ ) is specified as being semi-separable and non-parametric in form with restrictions on the variability following Butterworth et al. (2003):

$$F_{t,a} = s_{t,a} \mu^f e^{\epsilon_t}, \quad \epsilon_t \sim \mathcal{N}(0, \sigma_E^2) \quad (9)$$

$$s_{t+1,a} = s_{t,a} e^{\gamma_t}, \quad \gamma_t \sim \mathcal{N}(0, \sigma_s^2) \quad (10)$$

where  $s_{t,a}$  is the selectivity for age class  $a$  in year  $t$ , and  $\mu^f$  is the median fishing mortality rate over time.

If the selectivities ( $s_{t,a}$ ) are constant over time then fishing mortality rate decomposes into an age component and a year component. A curvature penalty on the selectivity coefficients using the squared second-differences to provide smoothness between ages.

Bottom-trawl survey selectivity was set to be asymptotic yet retain the properties desired for the characteristics of this gear. Namely, that the function should allow flexibility in selecting age 1 pollock over time. The functional form of this selectivity was:

$$s_{t,a} = \left[ 1 + e^{-\alpha_t a - \beta_t} \right]^{-1}, \quad a > 1 \quad (11)$$

$$s_{t,a} = \mu_s e^{-\delta_t^\mu}, \quad a = 1 \quad (12)$$

$$\alpha_t = \bar{\alpha} e^{\delta_t^\alpha}, \quad (13)$$

$$\beta_t = \bar{\beta} e^{\delta_t^\beta}, \quad (14)$$

where the parameters of the selectivity function follow a random walk process as in Dorn et al. (2000):

$$\delta_t^\mu - \delta_{t+1}^\mu \sim \mathcal{N}(0, \sigma_{\delta^\mu}^2) \quad (15)$$

$$(16)$$

$$\alpha_t^\mu - \alpha_{t+1}^\mu \sim \mathcal{N}(0, \sigma_{\alpha^\mu}^2) \quad (17)$$

$$\beta_t^\mu - \beta_{t+1}^\mu \sim \mathcal{N}(0, \sigma_{\beta^\mu}^2) \quad (18)$$

The parameters to be estimated in this part of the model are thus for t=1982 through to 2020. The variance terms for these process error parameters were specified to be 0.04.

In this assessment, the random-walk deviation penalty was optionally shifted to the changes in log-selectivity. that is, for the BTS estimates, the process error was applied to the logistic parameters as above, but the lognormal penalty was applied to the resulting selectivities-at-age directly. The extent of this variability was evaluated in the context of the impact on age-specific survey catchability/availability and contrasted with an independent estimate of pollock availability to the bottom trawl survey.

$$\ln(s_{t,a}) - \ln(s_{t+1,a}) \sim \mathcal{N}(0, \sigma_{sel}^2) \quad (19)$$

$$(20)$$

In 2008 the AT survey selectivity approach was modified. As an option, the age one pollock observed in this trawl can be treated as an index and are not considered part of the age composition (which then ranges from age 2-15). This was done to improve some interaction with the flexible selectivity smoother that is used for this gear and was compared. Additionally, the annual specification of input observation variance terms was allowed for the AT data.

A diagnostic approach to evaluate input variance specifications (via sample size under multinomial assumptions) was added in the 2018 assessment. This method uses residuals from mean ages together with the concept that the sample variance of mean age (from a given annual data set) varies inversely with input sample size. It can be shown that for a given set of input proportions at age (up to the maximum age  $A$ ) and sample size  $N_t$  for year  $t$ , an adjustment factor  $\nu$  for input

sample size can be computed when compared with the assessment model predicted proportions at age ( $\hat{p}_{ta}$ ) and model predicted mean age ( $\hat{a}_t$ ):

$$\nu = \text{var} \left( r_t^a \sqrt{\frac{N_t}{\kappa_t}} \right)^{-1} \quad (21)$$

$$r_t^a = \bar{a}_t - \hat{a}_t \quad (22)$$

$$\kappa_t = \left[ \sum_a^A \bar{a}_t - \hat{a}_t \right]^{0.5} \quad (23)$$

where  $r_t^a$  is the residual of mean age and

$$\hat{a}_t = \sum_a^A a \hat{p}_{ta} \quad (24)$$

$$\bar{a}_t = \sum_a^A a p_{ta} \quad (25)$$

Based on previous analyses, we used the above relationship as a diagnostic for evaluating input sample sizes by comparing model predicted mean ages with observed mean ages and the implied 95% confidence bands. This method provided support for modifying the frequency of allowing selectivity changes.

### **Recruitment**

In these analyses, recruitment ( $R_t$ ) represents numbers of age-1 individuals modeled as a stochastic function of spawning stock biomass.

$$R_t = f(B_{t-1}) \quad (26)$$

with mature spawning biomass during year  $t$  was defined as:

$$B_t = \sum_{a=1}^A w_{t,a} \phi_a N_{t,a} \quad (27)$$

and,  $\phi_a$  is the proportion of mature females at age  $a$  as shown in the sub-section titled Natural mortality and maturity at age under “Parameters estimated independently” above.

A reparameterized form for the stock-recruitment relationship following Francis (1992) was used. For the optional Beverton-Holt form (the Ricker form presented in Eq. 12 was adopted for this assessment) we have:

$$R_t = \frac{B_{t-1} e^{\varepsilon_t}}{\alpha + \beta B_{t-1}} \quad (28)$$

where

- $R_t$  is recruitment at age 1 in year  $t$ ,
- $B_t$  is the biomass of mature spawning females in year  $t$ ,
- $\varepsilon_t$  is the recruitment anomaly for year  $t$ , ( $\varepsilon_t \sim \mathcal{N}(0, \sigma_R^2)$ )
- $\alpha, \beta$  are stock recruitment parameters.

Values for the stock-recruitment function parameters and are calculated from the values of (the number of 0-year-olds in the absence of exploitation and recruitment variability) and the steepness of the stock-recruit relationship ( $h$ ). The steepness is the fraction of  $R_0$  to be expected (in the absence of recruitment variability) when the mature biomass is reduced to 20% of its pristine level (Francis 1992), so that:

$$\alpha = \tilde{B}_0 \frac{1-h}{4h} \quad (29)$$

$$\beta = \frac{5h-1}{4hR_0} \quad (30)$$

where  $\tilde{B}_0$  is the total egg production (or proxy, e.g., female spawning biomass) in the absence of exploitation (and recruitment variability) expressed as a fraction of  $R_0$ .

Some interpretation and further explanation follows. For steepness equal 0.2, then recruits are a linear function of spawning biomass (implying no surplus production). For steepness equal to 1.0, then recruitment is constant for all levels of spawning stock size. A value of  $h = 0.9$  implies that at 20% of the unfished spawning stock size will result in an expected value of 90% unfished recruitment level. Steepness of 0.7 is a commonly assumed default value for the Beverton-Holt form (e.g., Kimura 1988). The prior distribution for steepness used a beta distribution as in Ianelli et al. (2016). The prior on steepness was specified to be a symmetric form of the Beta distribution with  $\alpha = \beta = 14.93$  implying a prior mean of 0.5 and CV of 12% (implying that there is about a 14% chance that the steepness is greater than 0.6). This conservative prior is consistent with previous years' application and serves to constrain the stock-recruitment curve from favoring steep slopes (uninformative priors result in  $F_{MSY}$  values near an  $F_{SPR}$  of about  $F_{18\%}$  a value considerably higher than the default proxy of  $F_{35\%}$ ). The residual pattern for the post-1977 recruits used in fitting the curve with a more diffuse prior resulted in all estimated recruits being below the curve for stock sizes less than  $B_{MSY}$  (except for the 1978 year class). We believe this to be driven primarily by the apparent negative-slope for recruits relative to stock sizes above  $B_{MSY}$  and as such, provides a potentially unrealistic estimate of productivity at low stock sizes. This prior was elicited from the rationale that residuals should be reasonably balanced throughout the range of spawning stock sizes. Whereas this is somewhat circular (i.e., using data for prior elicitation), the point here is that residual patterns (typically ignored in these types of models) were qualitatively considered.

In model 16.1 (from the 2019 assessment), a Beverton Holt stock recruitment form was implemented using the prior value of 0.67 for steepness and a CV of 0.17. This resulted in beta distribution parameters (for the prior) at  $\alpha = 6.339$  and  $\beta = 4.293$ .

The value of  $\sigma_R$  was set at 1.0 to accommodate additional uncertainty in factors affecting recruitment variability.

To have the critical value for the stock-recruitment function (steepness,  $h$ ) on the same scale for the Ricker model, we begin with the parameterization of Kimura (1990):

$$R_t = \frac{B_{t-1} e^{\alpha(1-B_{t-1}\frac{R_0}{\psi_0})}}{\psi_0} \quad (31)$$

It can be shown that the Ricker parameter  $a$  maps to steepness as:

$$h = \frac{e^\alpha}{e^\alpha + 4} \quad (32)$$

so that the prior used on  $h$  can be implemented in both the Ricker and Beverton-Holt stock-recruitment forms. Here the term  $\psi_0$  represents the equilibrium unfished spawning biomass per-recruit.

### **Diagnostics**

In 2006 a replay feature was added where the time series of recruitment estimates from a particular model is used to compute the subsequent abundance expectation had no fishing occurred. These recruitments are adjusted from the original estimates by the ratio of the expected recruitment given spawning biomass (with and without fishing) and the estimated stock-recruitment curve. I.e., the recruitment under no fishing is modified as:

$$R'_t = \hat{R}_t \frac{f(B'_{t-1})}{f(B_{t-1})}$$

where  $R_t$  is the original recruitment estimate in year  $t$  with  $B'_{t-1}$  and  $B_{t-1}$  representing the stock-recruitment function given spawning biomass under no fishing and under the estimated fishing intensity, respectively.

The assessment model code allows retrospective analyses (e.g., Parma 1993, and Ianelli and Fournier 1998). This was designed to assist in specifying how spawning biomass patterns (and uncertainty) have changed due to new data. The retrospective approach simply uses the current model to evaluate how it may change over time with the addition of new data based on the evolution of data collected over the past several years.

### **Parameter estimation**

The objective function was simply the sum of the negative log-likelihood function and logs of the prior distributions. To fit large numbers of parameters in nonlinear models it is useful to be able to estimate certain parameters in different stages. The ability to estimate stages is also important in using robust likelihood functions since it is often undesirable to use robust objective functions when models are far from a solution. Consequently, in the early stages of estimation we use the following log- likelihood function for the survey and fishery catch at age data (in numbers):

$$nll(i) = n \sum_{t,a} p_{ta} \ln \hat{p}_{ta} \quad (33)$$

$$p_{ta} = \frac{O_{ta}}{\sum_a O_{ta}} \quad \hat{p}_{ta} = \frac{\hat{C}_{ta}}{\sum_a \hat{C}_{ta}} \quad (34)$$

$$\mathbf{C} = \mathbf{CE} \quad (35)$$

$$\mathbf{E} = \begin{matrix} b_{1,1} & b_{1,2} & \dots & b_{1,15} \\ b_{2,1} & b_{2,2} & & b_{2,15} \\ \vdots & & \ddots & \vdots \\ b_{15,1} & b_{15,2} & \dots & b_{15,15} \end{matrix} \quad (36)$$

where  $A$ , and  $T$ , represent the number of age classes and years, respectively,  $n$  is the sample size, and represent the observed and predicted numbers at age in the catch. The elements  $b_{i,j}$  represent

ageing mis-classification proportions are based on independent agreement rates between otolith age readers. For the models presented this year, the option for including aging errors was re-evaluated. Sample size values were revised and are shown in the main document. Strictly speaking, the amount of data collected for this fishery indicates higher values might be warranted. However, the standard multinomial sampling process is not robust to violations of assumptions (Fournier et al. 1990). Consequently, as the model fit approached a solution, we invoke a robust likelihood function which fit proportions at age as:

$$\prod_{a=1}^A \prod_{t=1}^T \left[ \left( \exp \left( -\frac{(p_{ta} - \hat{p}_{ta})^2}{2(\eta_{ta} + 0.1/A) \tau_t^2} \right) + 0.01 \right) \times \frac{1}{\sqrt{2\pi(\eta_{ta} + 0.1/A) \tau_t}} \right] \quad (37)$$

Taking the logarithm we obtain the log-likelihood function for the age composition data:

$$nll(i) = -0.5 \sum_{a=1}^A \sum_{t=1}^T \ln 2\pi (\eta_{ta} + 0.1/A) - \sum_t^T A \ln \tau_t + \sum_{a=1}^A \sum_{t=1}^T \ln \left\{ \exp \left( -\frac{(p_{ta} - \hat{p}_{ta})^2}{(2\eta_{ta} + 0.1/A) \tau_t^2} \right) + 0.01 \right\} \quad (38)$$

where

$$\eta_{ta} = p_{ta}(1 - p_{ta}) \quad (39)$$

$$\text{and} \quad (40)$$

$$\tau_t^2 = 1/n_t \quad (41)$$

which gives the variance for  $p_{ta}$

$$(\eta_{ta} + 0.1/A)\tau_t^2 \quad (42)$$

Completing the estimation in this fashion reduces the model sensitivity to data that would otherwise be considered outliers.

Within the model, predicted survey abundance accounted for within-year mortality since surveys occur during the middle of the year. As in previous years, we assumed that removals by the survey were insignificant (i.e., the mortality of pollock caused by the survey was considered insignificant). Consequently, a set of analogous catchability and selectivity terms were estimated for fitting the survey observations as:

$$\hat{N}_{ta}^s = e^{-0.5Z_{ta}} N_{ta} q_t^s s_{ta}^S \quad (43)$$

where the superscript s indexes the type of survey (AT or BTS). For the option to use the survey predictions in biomass terms instead of just abundance, the above was modified to include observed survey biomass weights-at-age:

$$\hat{N}_{ta}^s = e^{-0.5Z_{ta}} w_{ta} N_{ta} q_t^s s_{ta}^S \quad (44)$$

For the AVO index, the values for selectivity were assumed to be the same as for the AT survey and the mean weights at age over time was also assumed to be equal to the values estimated for the AT survey.

For these analyses we chose to keep survey catchabilities constant over time (though they are estimated separately for the AVO index and for the AT and bottom trawl surveys). The contribution to the negative log-likelihood function (ignoring constants) from the surveys is given by either the lognormal distribution:

$$nll(i) = \sum_t \frac{\ln(u_t^s/\hat{N}_t^s)^2}{2\sigma_{s,t}^2} \quad (45)$$

where  $u_t^s$  is the total (numerical abundance or optionally biomass) estimate with variance  $\sigma_{s,t}$  from survey  $s$  in year  $t$  or optionally, the normal distribution can be selected:

$$nll(i) = \sum_t \frac{(u_t^s - \hat{N}_t^s)^2}{2\sigma_{s,t}^2}. \quad (46)$$

(47)

The AT survey and AVO index is modeled using a lognormal distribution whereas for the BTS survey, a normal distribution was applied.

For model configurations in which the BTS data are corrected for estimated efficiency, a multivariate lognormal distribution was used. For the negative- log likelihood component this was modeled as

$$nll_i = 0.5\mathbf{X}\Sigma^{-1}\mathbf{X}' \quad (48)$$

where  $\mathbf{X}$  is a vector of observed minus model predicted values for this index and  $\Sigma$  is the estimated covariance matrix provided from the method provided in Kotwicki et al. 2014. For the VAST estimates, the supplied covariance matrix was used in the same way.

The contribution to the negative log-likelihood function for the observed total catch biomass ( $C_b^{obs}, \hat{C}_b$ ) by the fishery is given by

$$nll_i = 0.5 \sum_t \frac{\ln(C_b^{obs}/\hat{C}_b)^2}{2\sigma_{C_b,t}^2} \quad (49)$$

where  $\sigma_{C_b,t}$  is pre-specified (set to 0.05) reflecting the accuracy of the overall observed catch in biomass. Similarly, the contribution of prior distributions (in negative log-density) to the log-likelihood function include  $\lambda_\varepsilon \sum_t \varepsilon_t^2 + \lambda_\gamma \sum_{ta} \gamma^2 + \lambda_\delta \sum_t \delta_t^2$  where the size of the  $\lambda$ 's represent prior assumptions about the variances of these random variables. Most of these parameters are associated with year-to- year and age specific deviations in selectivity coefficients. For a presentation of this type of Bayesian approach to modeling errors-in- variables, the reader is referred to Schnute (1994). To facilitate estimating such a large number of parameters, automatic differentiation software extended from Griewank and Corliss (1991) and developed into C++ class libraries was used. This software provided the derivative calculations needed for finding the posterior mode via a quasi-Newton function minimization routine (e.g., Press et al. 1992). The model implementation language (ADModel Builder) gave simple and rapid access to these routines and provided the ability estimate the variance-covariance matrix for all dependent and independent parameters of interest.

### **Uncertainty in mean body mass**

The approach we use to solve for  $F_{MSY}$  and related quantities (e.g.,  $B_{MSY}$   $MSY$ ) within a general integrated model context was shown in Ianelli et al. (2001). In 2007 this was modified to include uncertainty in weight-at-age as an explicit part of the uncertainty for  $F_{MSY}$  calculations. This involved estimating a vector of parameters ( $w_{ta}^{future}$ ) on current (2020) and future mean weights for each age  $i$ ,  $i = (1, 2, \dots, 15)$ , given actual observed mean and variances in weight-at-age over the period 1991-2019. The values of based on available data and (if this option is selected) estimates the parameters subject to the natural constraint:

$$w_{ta}^{future} \sim \mathcal{N}(\bar{w}_a, \sigma_{w_a}^2)$$

Note that this converges to the mean values over the time series of data (no other likelihood component within the model is affected by future mean weights-at-age) while retaining the natural uncertainty that can propagate through estimates of  $F_{MSY}$  uncertainty. This latter point is essentially a requirement of the Tier 1 categorization.

Subsequently, this method was refined to account for current-year survey data and both cohort and year effects. The model for this is:

$$\hat{w}_{ta} = \bar{w}_a e_t^v \quad a = 1, t \geq 1964 \quad (50)$$

$$\hat{w}_{ta} = \hat{w}_{t-1,a-1} + \Delta_a e_t^\psi \quad a > 1, t > 1964 \quad (51)$$

$$\Delta_a = \bar{w}_{a+1} - \bar{w}_a \quad a < A \quad (52)$$

$$\bar{w}_a = \alpha \left\{ L_1 + (L_2 - L_1) \left( \frac{1 - K^{a-1}}{1 - K^{A-1}} \right) \right\}^3 \quad (53)$$

$$(54)$$

where the fixed effects parameters are  $L_1, L_2, K$ , and  $\alpha$  while the random effects parameters are  $v_t$  and  $\psi_t$ .

### **Tier 1 projections**

Tier 1 projections were calculated two ways. First, for 2021 and 2022 ABC and  $OFL$  levels, the harmonic mean  $F_{MSY}$  value was computed and the analogous harvest rate ( $u_{HM}$ ) applied to the estimated geometric mean fishable biomass at  $B_{MSY}$ :

$$ABC_t = B_{GM,t}^f \hat{u}_{HM} \zeta_t \quad (55)$$

$$B_{GM,t}^f = e^{\ln \hat{B}_t^f - 0.5\sigma_{Bf}^2} \quad (56)$$

$$u_{HM,t}^f = e^{\ln \hat{u}_{MSY,t} - 0.5\sigma_{u_{MSY}}^2} \quad (57)$$

$$\zeta_t = \frac{B_t / B_{MSY} - 0.05}{1 - 0.05} \quad B_t < B_{MSY} \quad (58)$$

$$\zeta_t = 1.0 \quad B_t \geq B_{MSY} \quad (59)$$

where  $\hat{B}_t^f$  is the point estimate of the fishable biomass defined (for a given year):  $\sum_a N_{ta} s_{ta} w_{ta}$  with  $N_{ta}$ ,  $s_{ta}$ , and  $w_{ta}$  the estimated population numbers (begin year), selectivity and weights-at-age, respectively.  $B_{MSY}$  and  $B_t$  are the point estimates spawning biomass levels at equilibrium  $F_{MSY}$  and in year  $t$  (at time of spawning). For these projections, catch must be specified (or solved for

if in the current year when  $B_t < B_{MSY}$ ). For longer term projections a form of operating model (as has been presented for the evaluation of  $B_{20\%}$ ) with feedback (via future catch specifications) using the control rule and assessment model would be required.

## Appendix on spatio-temporal analysis of NMFS survey data

### *Overview*

These applications of VAST were configured to model NMFS/AFSC bottom trawl survey (BTS) data and for acoustic backscatter data (next section). For the BTS, the station-specific CPUEs (kg per hectare) for pollock were compiled from 1982-2019. Further details can be found at the [GitHub repo](#) mainpage, wiki, and glossary. The R help files, e.g., `?make_data` for explanation of data inputs, or `?make_settings` for explanation of settings. VAST has involved many publications for developing individual features (see references section below). What follows is intended as a step by step documentation of applying the model to these data.

The software versions of dependent programs used to generate VAST estimates were:

- Microsoft Open R (3.5.3)
- INLA (18.7.12)
- TMB (1.7.18)
- TMBhelper (1.2.0)
- VAST (3.5.2)
- FishStatsUtils (2.7.0)

For the model-based index time series, we used the same VAST model run (and associated results) as the 2019 SAFE. We include additional details regarding model settings here, as requested during the December 2019 SSC meeting.

### *Spatio-temporal treatment of survey data on pollock density*

We fitted records of biomass per unit area from all grid cells and corner stations in the 83-112 bottom trawl survey of the EBS, 1982-2019, as well as 83-112 samples available in the NBS in 1982, 1985, 1988, 1991, 2010, and 2017-2019. NBS samples prior to 2010 did not follow the 30 nautical mile sampling grid that was used in 2010, 2017, and 2019, and the 2018 sampling followed a coarsened grid as well. Assimilating these data therefore required extrapolating into unsampled areas. This extrapolation was assisted by including a spatially varying response to cold-pool extent (Thorson, 2019). This spatially varying response was estimated for both linear predictors of the delta-model, and detailed comparison of results for EBS pollock has showed that it has a small but notable effect (O'Leary et al., 2020). For example, the NBS was not sampled between 2010 and 2017, and the cold-pool extent started to decrease substantially around 2014; therefore including this covariate results in estimates that depart somewhat from a “Brownian bridge” between 2010 and 2017, and instead suggests that densities in the NBS increased progressively after 2014 when cold-pool-extent declined prior to 2017.

Specifically, we used a Poisson-link delta-model (Thorson, 2018) involving two linear predictors, and a gamma distribution for the distribution of positive catch rates. We extrapolated density to the

entire EBS and NBS in each year, using extrapolation-grids that are available within *FishStatsUtils* are used when integrating densities. These extrapolation-grids are defined using 3705 m (2 nmi) X 3705 m (2 nmi) cells; this results in 36,690 extrapolation-grid cells for the eastern Bering Sea and 15,079 in the northern Bering Sea. We used bilinear interpolation to interpolate densities from 250 “knots” to these extrapolation-grid cells; knots were distributed spatially in proportion to the distribution of extrapolation-grid cells (i.e., having an approximately even distribution across space). We estimated “geometric anisotropy” (the tendency for correlations to decline faster in some cardinal directions than others), and including a spatial and spatio-temporal term for both linear predictors. To improve interpolation of density “hotspots” between unsampled years, we specified that the spatio-temporal term was autocorrelated across years (where the magnitude of autocorrelation was estimated as a fixed effect for each linear predictor). However, we did not include any temporal correlation for intercepts, which we treated as fixed effects for each linear predictor and year. Finally, we used epsilon bias-correction to correct for retransformation bias (Thorson and Kristensen, 2016).

### ***Spatio-temporal treatment of survey age composition data***

To date, assessments using spatio-temporal indices have kept age-composition data unchanged (i.e., the estimates were based on the original design-based approach). In 2019 we develop a spatio-temporal approach to obtain age composition estimates (O’leary et al. 2020). The comparison with design-based age composition estimates was similar to the model-based estimates.

### ***Diagnostic plots from BTS work***

#### *Encounter-probability component*

One can check to ensure that observed encounter frequencies for either low or high probability samples are within the 95% predictive interval for predicted encounter probability (Fig. 63). Diagnostics for positive-catch-rate component were evaluated using a standard Q-Q plot. Qualitatively, the fits to pollock data are reasonable (Figures 64 and 65).

#### *Pearson residuals*

Spatially the residual pattern can be evaluated over time. Results for pollock data shows that consistent positive or negative residuals across or within years is limited for the encounter probability component of the model and for the positive catch rate component (Figures 66 and 67, respectively).

#### *Densities and biomass estimates*

Relative densities over time suggests that the biomass of pollock can reflect abundances in the NBS even in years where samples are unavailable (all years except 2010, 2017–2019; (Fig. 68)). Index values and error terms (based on diagonal of covariance matrix over time) are shown in Figure 69

### ***Extending VAST to create estimates from acoustic backscatter data***

We used acoustic backscatter data collected to half meter from the seafloor from RV Oscar Dyson (1994–2018) and the USV in 2020 following the same extrapolation area as for the BTS analyses.

We briefly highlight key differences with the approach as described above. First, the data were acoustic backscatter for each interval summed from half meter from the seafloor to near-surface. VAST assumes the catch inputs are in kg/km<sup>2</sup> so an extra conversion back to backscatter units is required for the acoustic index. The acoustic transects can have unexpected interactions with how the spatial grid is setup, so we used 400 spatial knots but without the bilinear interpolation. The extrapolation region included only the EBS BT footprint (i.e., it did not include the NBS), and was consistent among years in contrast to the design-based AT index whose extent varies by year. We also did not include a cold pool effect, nor any temporal smoothing on the spatiotemporal effects. The diagnostics for the model fit was good (Fig. 70). Relative log densities for the survey years show the biomass of pollock varied spatially with a peak value in 2016 (Fig. 27). Index values and estimation errors from the VAST model covered an constant (and larger) area compared to the design-based approach which covers the transect area. Nonetheless, for the assessment these series are used as trend data which result in quite similar values (Fig. 71).

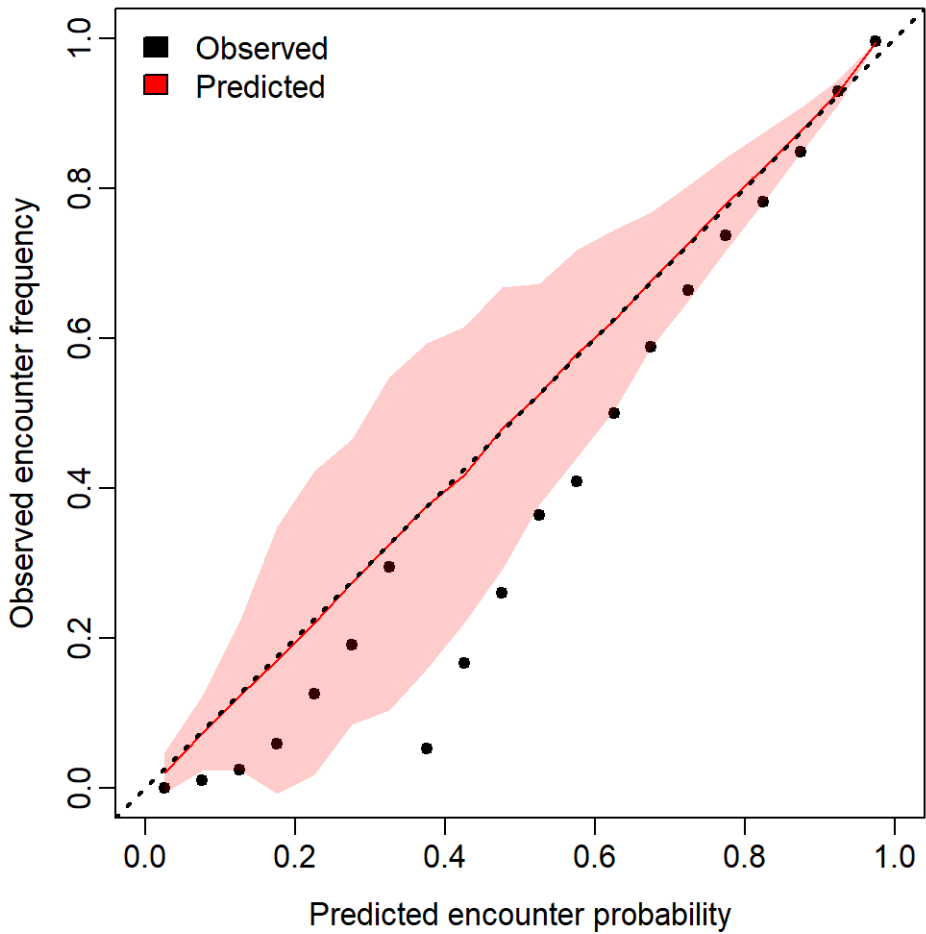


Figure 63: Observed encounter rates and predicted probabilities for pollock in the combined survey area.

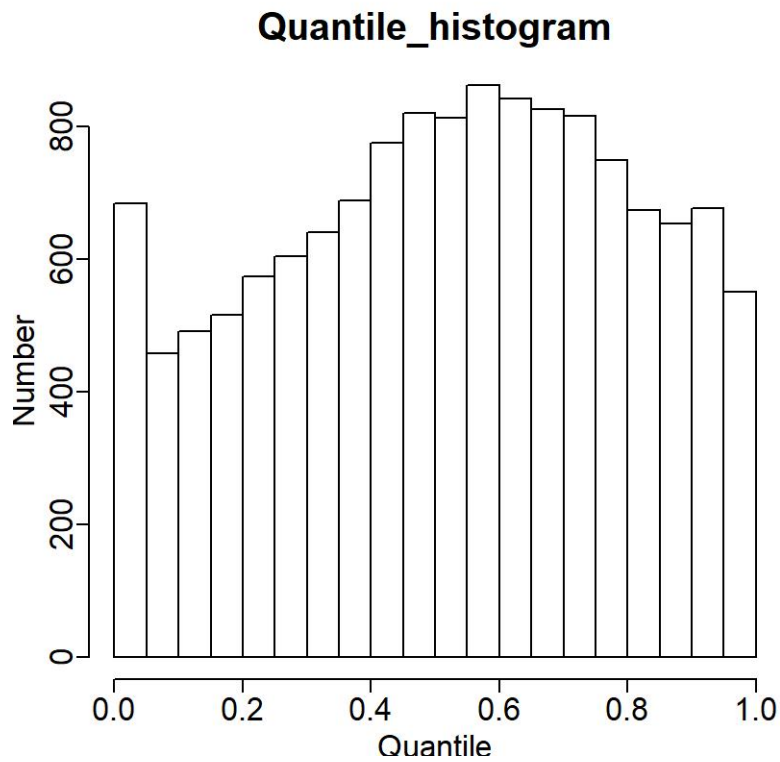


Figure 64: Plot indicating distribution of quantiles for “positive catch rate” component.

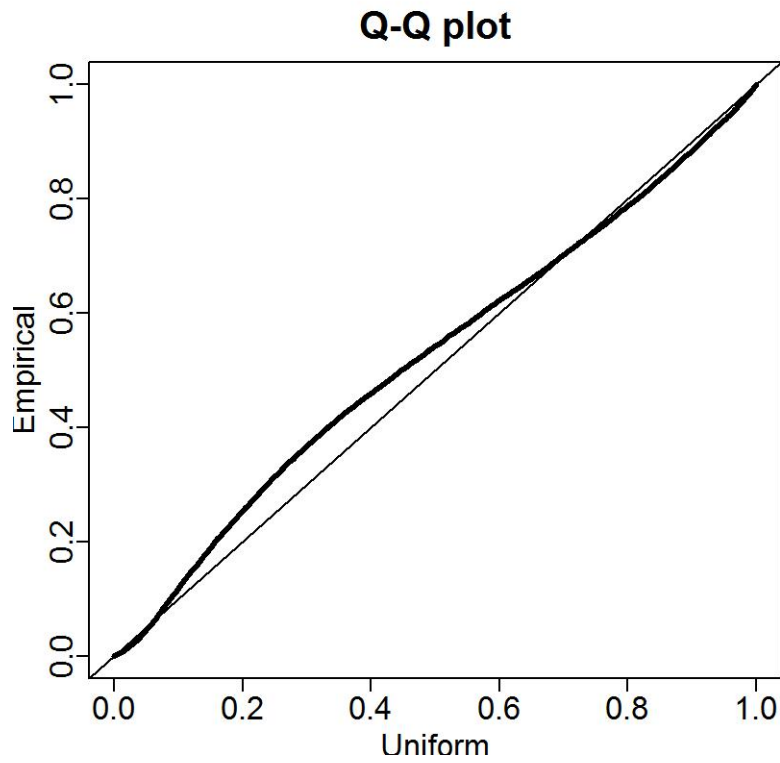


Figure 65: Quantile-quantile plot of residuals for “positive catch rate” component.



Figure 66: Pearson residuals of the encounter probability component for the combined survey area, 1982-2018.



Figure 67: Pearson residuals of the positive catch rate component for the combined survey area, 1982-2018.

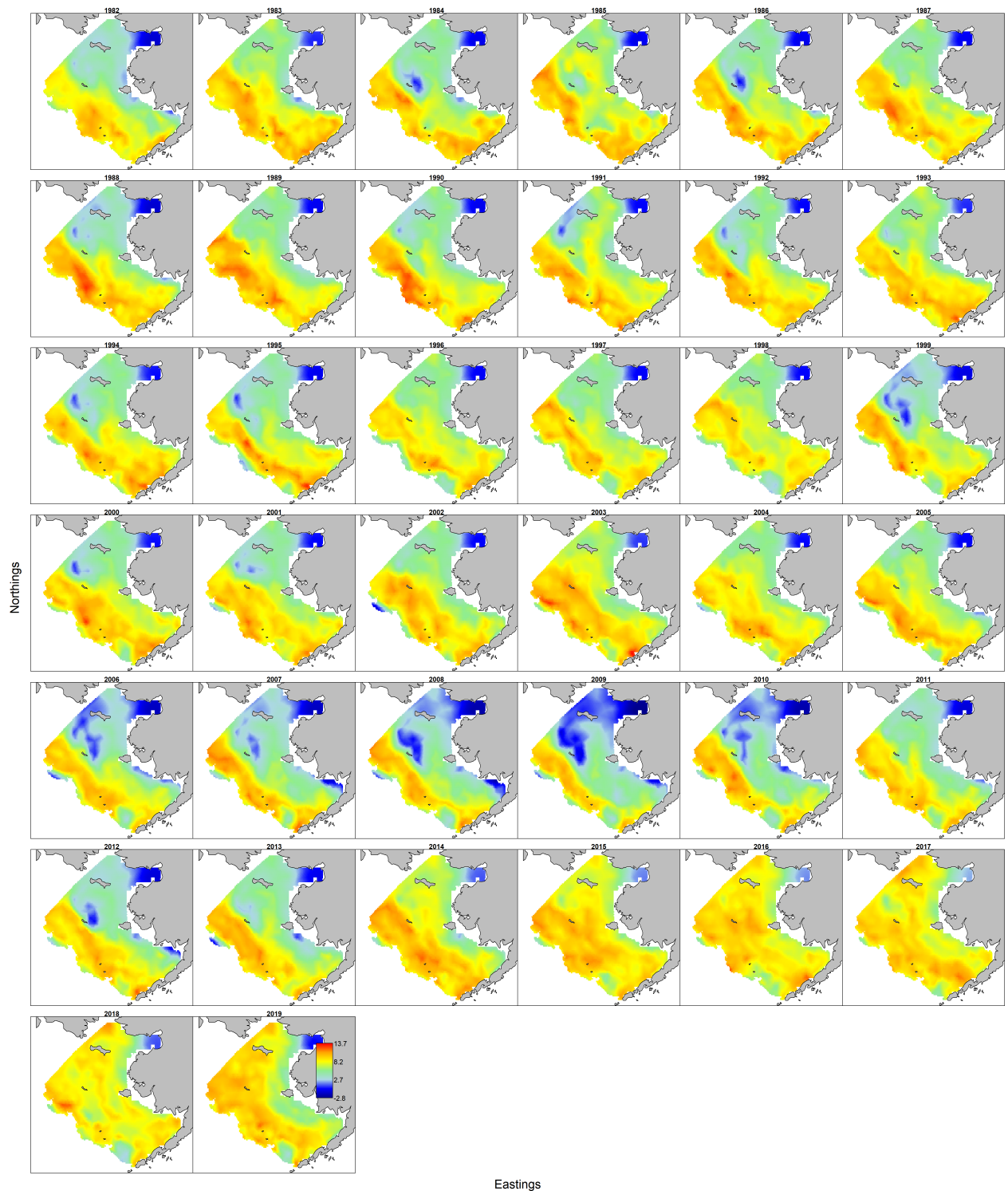


Figure 68: Pollock log density maps of the BTS data using the VAST model approach, 1982-2019.

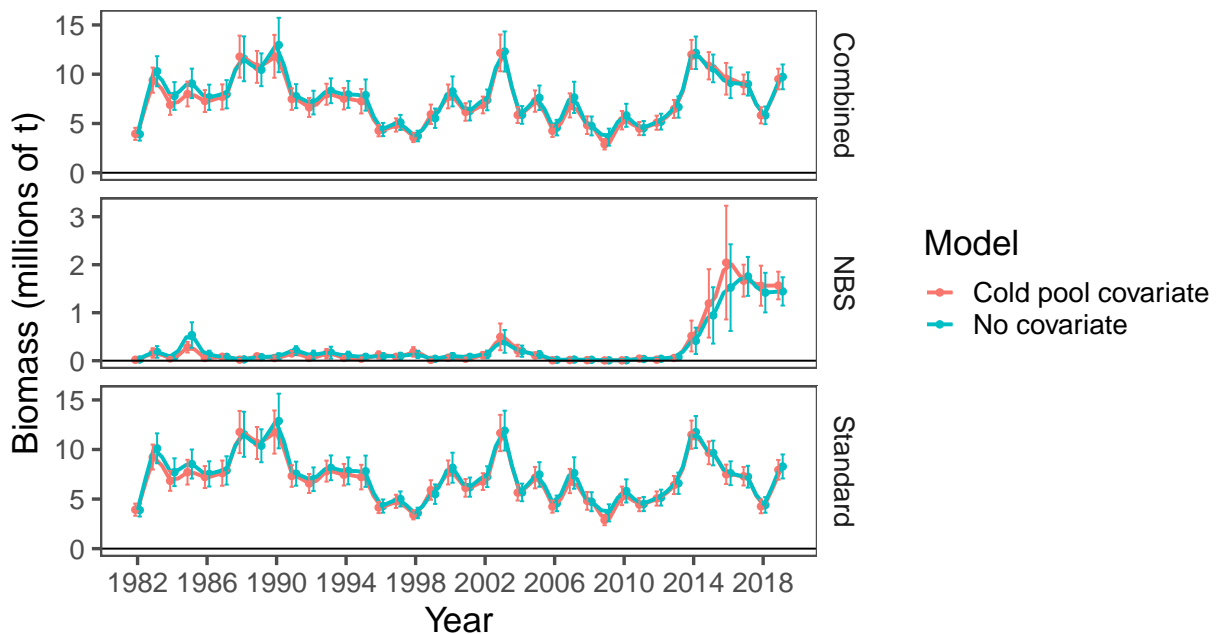


Figure 69: Pollock index values for the standard survey region, the NBS, and combined based on the VAST application to density-dependent corrected CPUE values from the BTS data, 1982–2019. The different lines are smoothed trends for with and without including the cold-pool extent as a covariate.

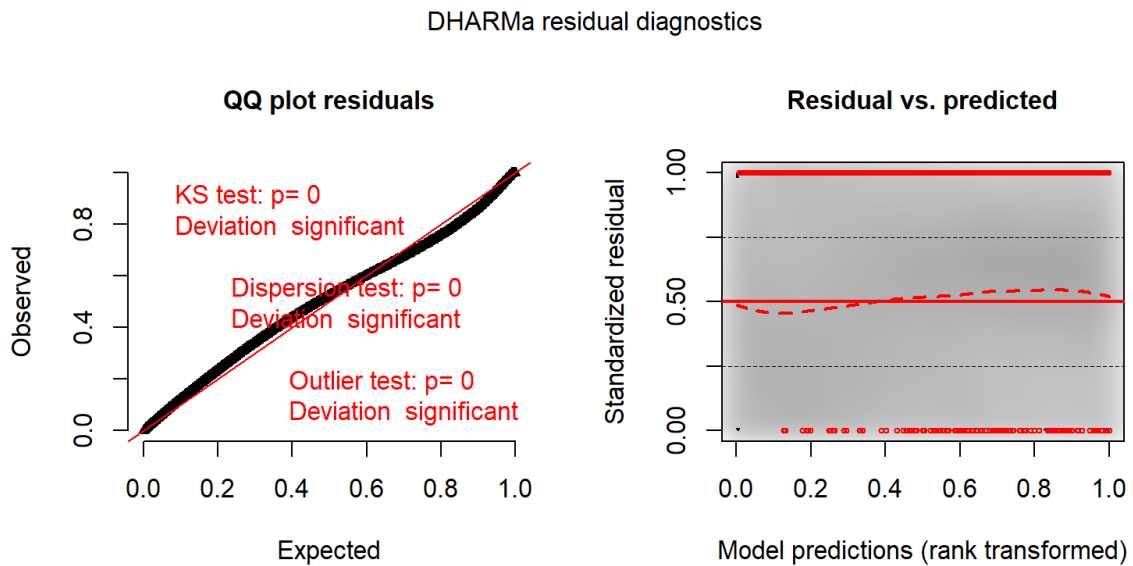


Figure 70: VAST diagnostics for the AT models using simulation residuals based on the DHARMA package.

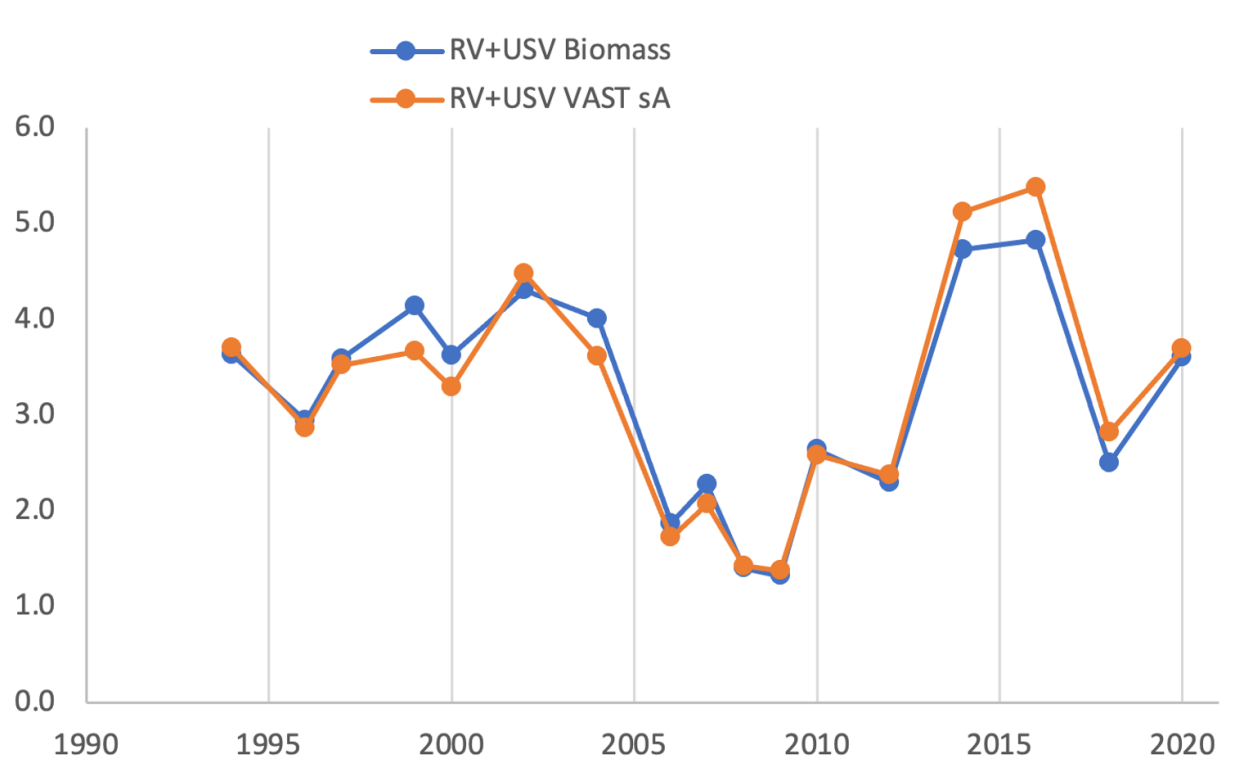


Figure 71: Predicted annual sum of pollock backscatter (RV+USV backscatter as analyzed from the VAST application) compared to the design-based biomass estimates (RV+USV biomass), 1994-2020.

## List of contents, tables and figures

### Contents

#### Executive summary

Summary of changes in assessment inputs . . . . .
Changes in the assessment methods . . . . .
Summary of EBS pollock results . . . . .
Response to SSC and Plan Team comments . . . . .
General comments . . . . .

#### Introduction

General . . . . .
Review of Life History . . . . .
Stock structure . . . . .

#### Fishery

Description of the directed fishery . . . . .
Catch patterns . . . . .
Management measures . . . . .
Economic conditions as of 2019 . . . . .
Pollock fillets . . . . .
Surimi seafood . . . . .
Pollock roe . . . . .
Fish oil . . . . .

#### Data

Fishery . . . . .
Catch . . . . .
Surveys . . . . .
Bottom trawl survey (BTS) . . . . .
Acoustic trawl (AT) surveys . . . . .
Other time series used in the assessment . . . . .
Japanese fishery CPUE index . . . . .
Biomass index from Acoustic-Vessels-of-Opportunity (AVO) . . . . .

#### Analytic approach

General model structure . . . . .
Description of alternative models . . . . .
Tier 1 considerations . . . . .

Input sample size . . . . .
Parameters estimated outside of the assessment model . . . . .
Natural mortality and maturity at age . . . . .
Length and weight-at-age . . . . .
Parameters estimated within the assessment model . . . . .

## Results

Model evaluation . . . . .
Time series results . . . . .
Recruitment . . . . .
Retrospective analysis . . . . .

## Harvest recommendations

Status summary . . . . .
Amendment 56 Reference Points . . . . .
Specification of OFL and Maximum Permissible ABC . . . . .
Standard Harvest Scenarios and Projection Methodology . . . . .
Projections and status determination . . . . .
ABC Recommendation . . . . .
Should the ABC be reduced below the maximum permissible ABC? . . . . .

## Additional ecosystem considerations

Ecosystem effects on the EBS pollock stock . . . . .
EBS pollock fishery effects on the ecosystem . . . . .

## Data gaps and research priorities

## Acknowledgments

## References

## Tables

## Figures

## EBS Pollock Model Description

Dynamics . . . . .
Recruitment . . . . .
Diagnostics . . . . .
Parameter estimation . . . . .
Uncertainty in mean body mass . . . . .
Tier 1 projections . . . . .

## **Appendix on spatio-temporal analysis of NMFS survey data**

Overview . . . . .
Spatio-temporal treatment of survey data on pollock density . . . . .
Spatio-temporal treatment of survey age composition data . . . . .
Diagnostic plots from BTS work . . . . .
Encounter-probability component . . . . .
Pearson residuals . . . . .
Densities and biomass estimates . . . . .
Extending VAST to create estimates from acoustic backscatter data . . . . .

## **List of contents, tables and figures**

### **List of Tables**

- 1 Catch from the Eastern Bering Sea by area, the Aleutian Islands, the Donut Hole, and the Bogoslof Island area, 1979–2020 (2020 values through October 25th 2020). The southeast area refers to the EBS region east of 170W; the Northwest is west of 170W. Note: 1979–1989 data are from Pacfin, 1990–2020 data are from NMFS Alaska Regional Office, and include discards. The 2020 EBS catch estimates are preliminary. . . . .
- 2 Time series of 1964–1976 catch (left) and ABC, TAC, and catch for EBS pollock, 1977–2020 in t. Source: compiled from NMFS Regional office web site and various NPFMC reports. Note that the 2020 value is based on catch reported to October 25th 2020 plus an added component due to bycatch of pollock in other fisheries. . . . .
- 3 Estimates of discarded pollock (t), percent of total (in parentheses) and total catch for the Aleutians, Bogoslof, Northwest and Southeastern Bering Sea, 1991–2020. SE represents the EBS east of 170W, NW is the EBS west of 170W, source: NMFS Blend and catch-accounting system database. 2020 data are preliminary. Note that the higher discard rates in the Aleutian Islands and Bogoslof region reflect the lack of directed pollock fishing. . . . .
- 4 Total EBS shelf pollock catch recorded by observers (rounded to nearest 100 t) by year and season with percentages indicating the proportion of the catch that came from within the Steller sea lion conservation area (SCA), 1998–2019. . . . .
- 5 Highlights of some management measures affecting the pollock fishery. . . . .
- 6 BSAI pollock catch and ex-vessel data showing the total and retained catch (in kt), the number of vessels for all sectors and for trawl catcher vessels including ex-vessel value (million US\$), price (US\$ per pound), and catcher vessel shares. Years covered include the 2010-2014 average, and annual from 2015-2019. . . . .
- 7 BSAI pollock first-wholesale market data including production (kt), value (million US\$), price (US\$ per pound) for all products and then separately for other categories (head and gut, fillet, surimi, and roe production). Years covered include the 2010-2014 average, and annual from 2015-2019. . . . .

- 8 Alaska pollock U.S. trade and global market data showing global production (in kt) and the U.S. and Russian shares followed by U.S. export volumes (kt), values (million US\$), export prices (US\$ per pound), import values (million US\$), and net exports (million US\$). Subsequent rows show the breakout of export shares (of U.S. pollock) by country (Japan, China and Europe) and the share of U.S. export volume and value of fish (i.e., H&G and fillets), and other product categories (surimi and roe). Years covered include the 2010-2014 average, and annual from 2015-2019. . . . .
- 9 BSAI pollock fish oil production index (tons of oil per 100 tons of retained catch); 2010-2014 average, and annual from 2015-2019. . . . .
- 10 Eastern Bering Sea pollock catch at age estimates based on observer data, 1979–2018. Units are in millions of fish. . . . .
- 11 Numbers of pollock NMFS observer samples measured for fishery catch length frequency (by sex and strata), 1977–2019. . . . .
- 12 Number of EBS pollock measured for weight and length by sex and strata as collected by the NMFS observer program, 1977-2019 . . . . .
- 13 Numbers of pollock fishery samples used for age determination estimates by sex and strata, 1977–2019, as sampled by the NMFS observer program. . . . .
- 14 NMFS total pollock research catch by year in t, 1964–2019. . . . .
- 15 Survey biomass estimates (age 1+, t) of Eastern Bering Sea pollock based on design-based area-swept expansion methods from NMFS bottom trawl surveys 1982–2019. .
- 16 Sampling effort for pollock in the EBS from the NMFS bottom trawl survey 1982–2019.
- 17 Bottom-trawl survey estimated numbers *millions* at age used for the stock assessment model. Note that in 1982–84 and 1986 only strata 1–6 were surveyed. Note these estimates are based on design-based procedures. . . . .
- 18 Mean EBS pollock body mass (kg) at age as observed in the summer NMFS bottom trawl survey, 1982–2019. . . . .
- 19 Biomass (age 1+) of Eastern Bering Sea pollock as estimated by surveys 1979–2019 (millions of t). Note that the bottom-trawl survey data only represent biomass from the survey strata (1–6) areas in 1982–1984, and 1986. For all other years the estimates include strata 8–9. DDC indicates the values obtained from the Kotwicki et al. Density-Dependence Correction method and the VAST columns are for the standard survey area including the Northern Bering Sea (NBS) extension. BTS=Bottom trawl survey, DB=Design-based, CPE=cold pool extent, ATS=Acoustic trawl survey.
- 20 Number of (age 1+) hauls and sample sizes for EBS pollock collected by the AT surveys. Sub-headings E and W represent collections east and west of 170W (within the US EEZ) and US represents the US sub-total and RU represents the collections from the Russian side of the surveyed region. . . . .
- 21 Mid-water pollock biomass (near surface down to 0.5m from the bottom) by area as estimated from summer acoustic-trawl surveys on the U.S. EEZ portion of the Bering Sea shelf, 1994–2018 (Honkalehto et al. 2015). CVs for biomass estimates were assumed to average 20 percent with the 1994-2018 inter-annual variability arising from the 1-dimensional variance estimation method. Note the last column reflects biomass index values based on a VAST model application applied to acoustic backscatter was rescaled to have the same mean as the total biomass to 0.5m. . . . .

- 22 AT survey estimates of EBS pollock abundance-at-age (millions), 1979–2018. Age-1s were modeled as a separate index, ages 2+ modeled as proportions at age. . . . .
- 23 An abundance index derived from acoustic data collected opportunistically aboard bottom-trawl survey vessels (AVO index; Honkalehto et al. 2014). Note values in parentheses are the coefficients of variation from using 1-D geostatistical estimates of sampling variability (Petitgas, 1993). See Honkalehto et al. (2011) for the derivation of these estimates. The column “ $CV_{AVO}$ ” was assumed to have a mean value of 0.30 for model fitting purposes (scaling relative to the AT and BTS indices). . . . .
- 24 Pollock sample sizes assumed for the age-composition data likelihoods from the fishery, bottom-trawl survey, and AT surveys, 1964–2020. Note fishery sample size for 1964–1977 was fixed at 10. . . . .
- 25 Mean weight-at-age (kg) estimates from the fishery (1991–2020; plus projections 2021–2022) showing the between-year variability (bottom row). . . . .
- 26 Mean weight-at-age (kg) estimates from the fishery (1991–2020; plus projections 2021–2022) showing the between-year variability (bottom row). . . . .
- 27 Summary of different model results and the stock condition for EBS pollock. Biomass units are thousands of t. . . . .
- 28 Estimates of begin-year age 3 and older biomass (thousands of tons) and coefficients of variation (CV) for the current assessment compared to 2012–2019 assessments for EBS pollock. . . . .
- 29 Estimated billions of EBS pollock at age (columns 2–11) from the current assessment model. . . . .
- 30 Estimated millions of EBS pollock caught at age (columns 2–11) from the current assessment model. . . . .
- 31 Estimated EBS pollock age 3+ biomass, female spawning biomass, and age 1 recruitment for 1964–2020. Biomass units are thousands of t, age-1 recruitment is in millions of pollock. . . . .
- 32 Summary of model results and the stock condition for EBS pollock. Biomass units are thousands of t. . . . .
- 33 Summary results of Tier 1 2021 yield projections for EBS pollock. . . . .
- 34 For the configuration named 20.0a base, Tier 3 projections of EBS pollock catch for the 7 scenarios. . . . .
- 35 For the configuration named 20.0a base, Tier 3 projections of EBS pollock ABC for the 7 scenarios. Note: scenario 2 results for 2021 and 2022 are conditioned on catches in that scenario listed in Table 38). . . . .
- 36 For the configuration named 20.0a base, Tier 3 projections of EBS pollock fishing mortality for the 7 scenarios. . . . .
- 37 For the configuration named 20.0a base, Tier 3 projections of EBS pollock spawning biomass (kt) for the 7 scenarios. . . . .
- 38 For the configuration named 20.0 USV, Tier 3 projections of EBS pollock catch for the 7 scenarios. . . . .
- 39 For the configuration named 20.0 USV, Tier 3 projections of EBS pollock ABC for the 7 scenarios. Note: scenario 2 results for 2021 and 2022 are conditioned on catches in that scenario listed in Table 38). . . . .

- 40 For the configuration named 20.0 USV, Tier 3 projections of EBS pollock fishing mortality for the 7 scenarios. . . . .
- 41 For the configuration named 20.0 USV, Tier 3 projections of EBS pollock spawning biomass (kt) for the 7 scenarios. . . . .
- 42 Bycatch estimates ( $t$ ) of other target species caught in the BSAI directed pollock fishery, 1997–2020 based on then NMFS Alaska Regional Office reports from observers (2020 data are preliminary). . . . .
- 43 Bycatch estimates ( $t$ ) of pollock caught in the other non-pollock EBS directed fisheries, 1997–2020 based on then NMFS Alaska Regional Office reports from observers. . . . .
- 44 Bycatch estimates ( $t$ ) of non-target species caught in the BSAI directed pollock fishery, 2003–2020, based on observer data as processed through the catch accounting system (NMFS Regional Office, Juneau, Alaska). . . . .
- 45 Bycatch estimates of prohibited species caught in the BSAI directed pollock fishery, 1997–2020 based on the AKFIN (NMFS Regional Office) reports from observers. Herring and halibut units are in  $t$ , all others represent numbers of individuals caught. Data for 2020 are preliminary. . . . .
- 46 Ecosystem considerations for BSAI pollock and the pollock fishery. . . . .
- 47 Details and explanation of the decision table factors selected in response to the Plan Team requests (as originally proposed in the 2012 assessment). . . . .
- 48 Outcomes of decision (expressed as chances out of 100) given different 2021 catches (first row, in kt). Note that for the 2018 and later year-classes average values were assumed. Constant  $F$ s based on the 2021 catches were used for subsequent years. . . . .

## List of Figures

- 1 Pollock catch estimates ( $t$ ) from the Eastern Bering Sea by season and region. The A-season is defined as from Jan-May and B-season from June-October. . . . .
- 2 Nominal catch divided by effort (hours towed) for some bycatch species and pollock for the EBS pollock fleet (sectors combined), 2000-2020. . . . .
- 3 Estimate of EBS pollock catch numbers by sex for the A season (January-May) and B seasons (June-October) and total. . . . .
- 4 EBS pollock catch distribution during A-season, 2018–2020. Column height is proportional to total catch. . . . .
- 5 A-season (top) and B-season (bottom) EBS fleet-wide nominal pollock catch (kg) per hour of fishing recorded by NMFS scientific observers along with the catch divided by effort (hours) by season since 2000 (middle panel). . . . .
- 6 Proportion of the annual EBS pollock TAC by month during the A-season, 2000–2020. The higher value observed since 2017 was due to Amendment 110 of the FMP to allow greater flexibility to avoid Chinook salmon. . . . .
- 7 EBS pollock roe production in A and B seasons , 2000-2020. . . . .
- 8 EBS pollock catch distribution during B-season, 2018–2020. Column height is proportional to total catch. Note that directed fishery for pollock generally is finished prior to October; the labels are indicative full-year catches. . . . .
- 9 Estimated mean daily distance between operations, 2000-2020. . . . .

- 10 Pollock fishery data showing the weight-frequency (50 g increments) by year and season. . . . .
- 11 Pollock fishery data showing the weight-frequency (50 g increments) by recent years and weeks of the B-season. . . . .
- 12 EBS pollock fishery estimated catch-at-age data (in number) for 1992–2019. Age 10 represents pollock age 10 and older. The 2012 year-class is shaded in orange. . . . .
- 13 Bottom-trawl survey biomass estimates with error bars representing 1 standard deviation (for design-based and density-dependent correction method) for EBS pollock. . . . .
- 14 Bottom and surface temperatures for the Bering Sea from the NMFS summer bottom-trawl surveys (1982–2019). Dashed lines represent mean values. . . . .
- 15 EBS pollock CPUE (shades = relative kg/hectare) and bottom temperature isotherms in degrees C; from the bottom trawl survey data 2011–2019. . . . .
- 16 Bottom trawl survey pollock catch in kg per hectare for 2017 - 2019. Height of vertical lines are proportional to station-specific pollock densities by weight (kg per hectare) with constant scales for all years (red stars indicate tows where pollock were absent from the catch). . . . .
- 17 Pollock abundance levels by age and year as estimated directly from the NMFS bottom-trawl surveys (1990–2019). The 2006,2008, and 2012 year-classes are shaded differently. . . . .
- 18 Timing of Acoustic surveys used in the time series. The 2020 USV survey is shown in red. . . . .
- 19 Pollock dominate the catch in historical midwater AT surveys (top panel) and during the summer pollock fishery (bottom panel) in the EBS. Jellyfish, which are very weak acoustic scatterers compared to fishes with a swimbladder have been excluded from the survey catch summaries. . . . .
- 20 Acoustic backscatter in historical acoustic-trawl surveys compared with the biomass resulting from the survey. Both indices have been normalized to have a mean of 1 over the period 1994-2018 so that they can be directly compared. . . . .
- 21 Scatterplots of total backscatter and pollock biomass for acoustic-trawl surveys from 1994-2018. Results for >3m above the seafloor are shown in the left panel and results for the 0.5 to 3m above the seafloor are shown in the right panel. . . . .
- 22 Time series of observed biomass (i.e. ‘survey biomass’) and biomass estimated by dropping all trawl data in that year and predicting survey biomass based on trawl sampling in the other years of the time series (‘converted biomass’). In 2020, no trawling was conducted, and the biomass estimate was predicted based on the average relationships established in previous years (see previous figure). The average discrepancy between the predicted and converted biomass is 5.4% (range 0.1 to 11%).
- 23 An evaluation of the impact on historical pollock ATS biomass estimates if alternate transects were dropped (and uncertainty increases as depicted by vertical error bars) compared to the actual (full) number of survey transects. . . . .

- 24 Acoustic-trawl survey pollock biomass time series. Error bars correspond to the relative estimation error (i.e. CV) estimated with a 1-D geostatistical technique. The 2020 survey was conducted with USVs, and has larger errors associated with the estimate that incorporate the effects of reduced sampling effort (i.e. 40 nmi spaced transects rather than 20 nmi transects), and the method used to convert backscatter to biomass conversion. . . . .
- 25 Map of backscatter measurements during the 2020 USV acoustic survey. The size and color of each point represents the mean acoustic backscatter attributed to pollock in a 0.5 nmi transect segment. . . . .
- 26 Proportion of pollock backscatter above and below 3m above bottom observed in acoustic-trawl surveys. . . . .
- 27 Predicted log-backscatter (arbitrary units) from the VAST model fitted to the AT data, where the 2020 data are from the USV. . . . .
- 28 EBS pollock fishery body mass (given length) anomaly (standardized by overall mean body mass at each length) by month based on some over 700 thousand fish measurements from 1991–2019. . . . .
- 29 EBS pollock body mass (given length) anomaly (standardized by overall mean body mass at each length) by year, 1991–2020. . . . .
- 30 EBS pollock fishery body mass (given length) anomaly (standardized by overall mean body mass at each length) by year and season/area strata, 1991–2020. . . . .
- 31 Recent fishery average weight-at-age anomaly (relative to mean) by strata for ages 3–10, 2015–2019. Vertical shape reflects uncertainty in the data (wider shapes being more precise), colors are consistent with cohorts. . . . .
- 32 Fishery average weight-at-age anomaly (relative to mean) across strata and combined for all ages (3–10), and available years (1991–2019). Vertical shape reflects uncertainty in the data (wider shapes being more precise), colors are consistent with cohorts. . . . .
- 33 Recent fishery average weight-at-age anomaly (relative to mean) by strata for ages 3–10, 2014–2019. Vertical shape reflects uncertainty in the data (wider shapes being more precise), colors are consistent with cohorts. . . . .
- 34 Model runs comparing last year's assessment with the impact of sequentially adding new data (first 2020 catch and 2019 fishery catch-at-age, then the 2020 USV data point, and then replacing that with a VAST treatment of the acoustic survey backscatter. . . . .
- 35 Model fits to different treatment and assumptions about index CPUE for the ATS time series where VAST CV20% and DB CV20% mean that the CVs for the index values between 1994 and 2018 each average 20% for the design-based and VAST treatments, respectively. The other cases use the sampling error and variance estimates arising from the methods. . . . .
- 36 Pollock spawning biomass estimates sensitivity to assumptions about index CPUE for the ATS time series where VAST CV20% and DB CV20% mean that the CVs for the index values between 1994 and 2018 each average 20% for the design-based and VAST treatments, respectively. The other cases use the sampling error and variance estimates arising from the methods. . . . .

- 37 Stock-recruitment estimates (shaded represents uncertainty in SRR) and age-1 EBS pollock estimates labeled by year-classes for Model 20.0 and with the influence of the 1978 year-class removed. . . . .
- 38 Stock-recruitment estimates (shaded represents uncertainty in SRR) and age-1 EBS pollock estimates labeled by year-classes comparing a result with a diffuse prior on SRR steepness. . . . .
- 39 Stock-recruitment estimates (shaded represents uncertainty in SRR) and age-1 EBS pollock estimates labeled by year-classes comparing implied SRR under models conditioned that FMSY equals different SPR rates. . . . .
- 40 EBS pollock model fit to the alternative ATS biomass indices, 1994–2020. . . . .
- 41 EBS pollock model fits to the Japanese fishery CPUE. . . . .
- 42 Model results of predicted and observed AVO index. Error bars represent assumed 95% confidence bounds of the input series. . . . .
- 43 EBS pollock model fit to the BTS survey data (density dependence corrected estimates), 1982–2019. Units are relative biomass. . . . .
- 44 EBS pollock model fits to observed mean age for the Acoustic trawl survey (top), the bottom trawl survey (middle) and fishery (bottom) . . . . .
- 45 Selectivity at age estimates for the EBS pollock fishery; note that the values for the terminal year is used for ABC and OFL projections. . . . .
- 46 Model fit (dots) to the EBS pollock fishery proportion-at-age data (columns; 1964–2019). The 2019 data are new to this year’s assessment. Colors coincide with cohorts progressing through time. . . . .
- 47 Model estimates of bottom-trawl survey selectivity, 1982–2019. . . . .
- 48 Model fit (dots) to the bottom trawl survey proportion-at-age composition data (columns) for EBS pollock. Colors correspond to cohorts over time. . . . .
- 49 Model fit (dots) to the acoustic-trawl survey proportion-at-age composition data (columns) for EBS pollock. Colors correspond to cohorts over time (for years with consecutive surveys). . . . .
- 50 Pairwise plot of selected EBS pollock parameters and output from 3 million MCMC iterations thinned such that 5 thousand draws were saved as an approximation to the multivariate posterior distribution. Note that the figures on the diagonal represent the marginal posterior distributions. Key: lnR0 is the parameter that scales the stock-recruit relationship, B\_Bmsy is estimated  $B_{2018}/B_{MSY}$ , DynB0 is the ratio of spawning biomass estimated for in 2018 over the value estimated that would occur if there had been no fishing, B19 is the spawning biomass in 2019, and B\_Bmean is  $B_{2019}/\bar{B}$ . . . . .
- 51 Integrated marginal posterior density (based on MCMC results) for the 2019 EBS pollock female spawning biomass compared to the point estimate (dashed red line). The mean of the posterior is shown in green (under the dashed line). . . . .
- 52 Estimated spawning exploitation rate (defined as the percent removal of egg production in a given spawning year). . . . .
- 53 Estimated instantaneous age-specific fishing mortality rates for EBS pollock. . . . .
- 54 Comparison of the current assessment results with past assessments of begin-year EBS age-3+ pollock biomass. . . . .

- 55 Estimated spawning biomass relative to annually estimated  $F_{MSY}$  values and fishing mortality rates for EBS pollock. Most recent two years are shaded in yellow . . . . .
- 56 The estimated EBS pollock spawning stock biomass for model 20.0 with projections equal to the estimated fishing mortality from 2020. . . . .
- 57 Recruitment estimates (age-1 recruits) for EBS pollock for all years since 1964 (1963–2019 year classes) for Model 20.0. Error bars reflect 90% credible intervals based on model estimates of uncertainty. . . . .
- 58 Stock-recruitment estimates (shaded represents structural uncertainty) and age-1 EBS pollock estimates labeled by year-classes . . . . .
- 59 EBS pollock productivity as measured by logged recruits per spawning biomass,  $\log(R/S)$ , as a function of spawning biomass with a linear fit (bottom) and over time, 1964–2018 (top). . . . .
- 60 Retrospective patterns for EBS pollock spawning biomass showing the point estimates relative to the terminal year (top panel) and approximate confidence bounds on absolute scale (+2 standard deviations). . . . .
- 61 Projected EBS Tier 3 pollock yield (top) and female spawning biomass (bottom) relative to the long-term expected values under  $F_{35\%}$  and  $F_{40\%}$  (horizontal lines).  $B_{40\%}$  is computed from average recruitment from 1978–2017. Future harvest rates follow the guidelines specified under Tier 3 Scenario 1. . . . .
- 62 For the mature component of the EBS pollock stock, time series of estimated average age and diversity of ages (using the Shannon-Wiener H statistic), 1980–2018. . . . .
- 63 Observed encounter rates and predicted probabilities for pollock in the combined survey area. . . . .
- 64 Plot indicating distribution of quantiles for “positive catch rate” component. . . . .
- 65 Quantile-quantile plot of residuals for “positive catch rate” component. . . . .
- 66 Pearson residuals of the encounter probability component for the combined survey area, 1982–2018. . . . .
- 67 Pearson residuals of the positive catch rate component for the combined survey area, 1982–2018. . . . .
- 68 Pollock log density maps of the BTS data using the VAST model approach, 1982–2019. . . . .
- 69 Pollock index values for the standard survey region, the NBS, and combined based on the VAST application to density-dependent corrected CPUE values from the BTS data, 1982–2019. The different lines are smoothed trends for with and without including the cold-pool extent as a covariate. . . . .
- 70 VAST diagnostics for the AT models using simulation residuals based on the DHARMA package. . . . .
- 71 Predicted annual sum of pollock backscatter (RV+USV backscatter as analyzed from the VAST application) compared to the design-based biomass estimates (RV+USV biomass), 1994–2020. . . . .